

**DESIGN AND ANALYSIS OF  
COMMUNICATION PROTOCOLS  
USING QUANTUM RESOURCES**

*Thesis submitted in fulfillment of the requirements for the Degree of*

**DOCTOR OF PHILOSOPHY**

By

**MITALI SISODIA  
ENROLLMENT NO.  
15410006**



Department of Physics and Materials Science and Engineering

**JAYPEE INSTITUTE OF INFORMATION TECHNOLOGY**  
(Declared Deemed to be University U/S 3 of UGC Act)  
A-10, SECTOR-62, NOIDA, INDIA

July, 2019

@ Copyright JAYPEE INSTITUTE OF INFORMATION TECHNOLOGY

(Declared Deemed to be University U/S 3 of UGC Act)

NOIDA, INDIA.

July, 2019

ALL RIGHTS RESERVED

*This thesis is dedicated to my parents and my husband for their constant support and unconditional love. I love you all dearly.*

# TABLE OF CONTENTS

<b>INNER FIRST PAGE</b>	<b>i</b>
<b>TABLE OF CONTENTS</b>	<b>iii</b>
<b>DECLARATION BY THE SCHOLAR</b>	<b>vii</b>
<b>SUPERVISOR’S CERTIFICATE</b>	<b>ix</b>
<b>ACKNOWLEDGEMENT</b>	<b>xi</b>
<b>ABSTRACT</b>	<b>xiii</b>
<b>LIST OF ACRONYMS AND ABBREVIATIONS</b>	<b>xv</b>
<b>LIST OF FIGURES</b>	<b>xvi</b>
<b>LIST OF TABLES</b>	<b>xxi</b>
<b>CHAPTER 1</b>	
<b>INTRODUCTION</b>	<b>1</b>
1.1 What is quantum communication? . . . . .	1
1.2 A chronological history of protocols of quantum communication . . . . .	3
1.2.1 A chronological history of quantum communication protocols of Class 1	3
1.2.2 A chronological history of quantum communication protocols of Class 2	5
1.3 Qubit and measurement basis . . . . .	6
1.4 Various facets of quantum communication schemes of Class 1 . . . . .	8
1.4.1 Quantum teleportation . . . . .	8
1.4.1.1 Entangled orthogonal and nonorthogonal state based quantum teleportation . . . . .	11
1.5 Various facets of quantum communication schemes of Class 2 . . . . .	12
1.5.1 BB84 and other protocols of QKD . . . . .	12
1.5.2 Secure direct quantum communication . . . . .	13
1.5.3 Quantum dialogue (QD) . . . . .	13
1.5.4 Controlled quantum dialogue (CQD) . . . . .	14

1.6	Effect of noise on the protocols of quantum communication . . . . .	14
1.6.1	Amplitude damping noise . . . . .	15
1.6.2	Phase damping noise . . . . .	16
1.6.3	Fidelity as a quantitative measure of the effect of noise . . . . .	16
1.7	Quantum gates and quantum circuits . . . . .	17
1.7.1	Single-qubit quantum gates . . . . .	17
1.7.2	Two-qubit quantum gates . . . . .	20
1.7.3	Other quantum gates . . . . .	22
1.7.4	EPR circuit . . . . .	22
1.7.5	Useful optical components and how to realize quantum gates optically? . . . . .	23
1.8	SQUID-based quantum computer . . . . .	25
1.8.1	IBM QX2 . . . . .	26
1.8.2	IBM QX4 . . . . .	27
1.8.3	Sixteen-qubit IBM quantum computer . . . . .	27
1.9	Basic idea of quantum state tomography (QST) . . . . .	30
1.10	A brief summary of this chapter and the structure of the rest of the thesis . . . . .	31

**CHAPTER 2**

**DESIGN AND EXPERIMENTAL REALIZATION OF AN OPTIMAL SCHEME FOR TELEPORTATION OF AN  $n$ -QUBIT QUANTUM STATE**

**33**

2.1	Introduction . . . . .	33
2.2	Teleportation of an $n$ -qubit state with $m$ unknown coefficients . . . . .	36
2.2.1	Teleportation of state of type $ \psi\rangle = \alpha x_i\rangle + \beta x_j\rangle$ . . . . .	39
2.3	Controlled and bidirectional teleportation with optimal resource . . . . .	39
2.4	Experimental implementation of the proposed efficient QT scheme using IBM's real quantum processor . . . . .	43
2.5	Conclusion . . . . .	47

**CHAPTER 3**

**QUANTUM TELEPORTATION OF AN EIGHT-QUBIT STATE USING OPTIMAL QUANTUM RESOURCES**

**49**

3.1	Introduction . . . . .	49
3.2	Complete teleportation process . . . . .	51
3.3	Concluding remark . . . . .	52

**CHAPTER 4**

**TELEPORTATION OF A QUBIT USING ENTANGLED NONORTHOGONAL STATES: A COMPARATIVE STUDY**

**53**

4.1	Introduction . . . . .	53
-----	------------------------	----

4.2	Entangled nonorthogonal states . . . . .	54
4.3	Teleportation using entangled nonorthogonal state . . . . .	57
4.4	Effect of noise on average fidelity . . . . .	64
4.5	Conclusion . . . . .	71

**CHAPTER 5**

**EXPERIMENTAL REALIZATION OF NONDESTRUCTIVE DISCRIMINATION OF BELL STATES USING A FIVE-QUBIT QUANTUM COMPUTER 73**

5.1	Introduction . . . . .	73
5.2	Quantum circuits and method used for nondestructive discrimination of Bell states . . . . .	75
5.3	Results . . . . .	81
5.4	Conclusion . . . . .	93

**CHAPTER 6**

**OPTICAL DESIGNS FOR THE REALIZATION OF A SET OF SCHEMES FOR QUANTUM CRYPTOGRAPHY 96**

6.1	Introduction . . . . .	96
6.2	Quantum cryptographic protocols . . . . .	98
6.2.1	Controlled quantum dialogue . . . . .	99
6.2.1.1	CQD with single photons . . . . .	99
6.2.1.2	Kak’s three-stage scheme inspired five-stage scheme of CQD with single photons . . . . .	102
6.2.1.3	CQD protocol with entangled photons . . . . .	105
6.2.2	Controlled direct secure quantum communication . . . . .	108
6.2.2.1	CDSQC with single photons . . . . .	109
6.2.2.2	CDSQC with entangled photons . . . . .	109
6.2.2.3	CDSQC with entanglement swapping . . . . .	109
6.2.3	Quantum Dialogue . . . . .	111
6.2.3.1	QD with single photons . . . . .	112
6.2.4	Quantum secure direct communication/Direct secure quantum communication . . . . .	113
6.2.5	Quantum key agreement . . . . .	113
6.2.6	Quantum key distribution . . . . .	113
6.3	Conclusions . . . . .	114

**CHAPTER 7**

**CONCLUSIONS AND SCOPE FOR FUTURE WORK 115**

7.1	Conclusions and a brief summary of the work . . . . .	115
-----	---	-----

7.2	Limitations of the present work and scope for future work . . . . .	120
<b>REFERENCES</b>		<b>120</b>
<b>LIST OF PUBLICATIONS DURING Ph.D. THESIS WORK</b>		<b>147</b>

## DECLARATION BY THE SCHOLAR

I hereby declare that the work reported in the Ph.D. thesis entitled “**Design and Analysis of Communication Protocols Using Quantum Resources**” submitted at **Jaypee Institute of Information Technology, Noida, India**, is an authentic record of my work carried out under the supervision of **Prof. Anirban Pathak**. I have not submitted this work elsewhere for any other degree or diploma. I am fully responsible for the contents of my Ph.D. Thesis.

(Signature of the Scholar)

(Mitali Sisodia)

Department of Physics and Materials Science and Engineering

Jaypee Institute of Information Technology, Noida, India

Date:





## **SUPERVISOR'S CERTIFICATE**

This is to certify that the work reported in the Ph.D. thesis entitled “**Design and Analysis of Communication Protocols Using Quantum Resources**” submitted by **Mitali Sisodia** at **Jaypee Institute of Information Technology, Noida, India**, is a bonafide record of her original work carried out under my supervision. This work has not been submitted elsewhere for any other degree or diploma.

(Signature of Supervisor)

(Prof. Anirban Pathak)

Department of Physics and Materials Science and Engineering

Jaypee Institute of Information Technology, Noida, India

Date:



## ACKNOWLEDGEMENT

Completion of this doctoral dissertation has been a truly life-changing experience for me and it would not have been possible to do without the support and guidance that I received from many people. Now, I got a chance to express thanks from my heart through this acknowledgment.

First and foremost, I would like to start with the person who made the biggest difference in my life, my mentor, my guide, my supervisor Prof. Anirban Pathak. I would like to extend my sincere gratitude to him for the continuous support of my doctoral research and introducing me to this exciting field of science and for his dedicated help, advice, inspiration, encouragement and continuous support, throughout my Ph.D. Without his guidance and constant feedback this Ph.D. would not have been achievable. I have learnt extensively from him, including how to raise new possibilities, how to regard an old question from a new perspective, how to approach a problem by systematic thinking, data-driven decision making and exploiting serendipity. I would like to say- *As you walk with the GURU, you walk in the LIGHT of existence, away from the darkness of IGNORANCE, you leave behind all the problems of your life, and move towards the peak experiences of life.*

I wish to respectfully express my gratitude to Dr. Papia Chowdhury for all her kind support and affections. Prof. D. K. Rai for their timely support provided in successful completion of the thesis work. My DPMC members Prof. S.P. Purohit and Prof. B. P. Chamola for their fruitful suggestions during end semester Ph.D. presentations and all faculty members of the Department of Physics and Materials Science and Engineering for their valuable suggestions during my studies.

Further, my heartfelt thanks to my super seniors Dr. Amit Verma, Dr. Anindita Banerjee for their kind supports. My heartfelt and special thanks to my senior who is my inspiration Dr. Chitra Shukla for all her kind and continuous support, encouragement, discussions over the phone and chat regarding research work. I always feel free to discuss the work and share many other things any time with her. Actually, I feel very happy and friendly with her and I love talking to her very much. During my end semester presentations, I always called her and asked many queries, after my presentations, she used to call me back and ask- hey Mitali, how was your presentation? thank you Chitra Mam for everything. Further, a special thanks to my senior Dr. Kishore Thapliyal, who has played a very important role in my Ph.D. duration. I really thank to him for his great help, encouragement, continuous support, guidance, cooperation and motivation which have always kept me going ahead. I owe a lot of gratitude to him for always being there for me and I feel privileged to be associated with a person like him during my research life,

thanks for everything Kishore Sir, professionally, you are “perfection personified”. I am also thankful to Dr. Abhishek Shukla for helping me doing work on the IBM quantum computer, Dr. Nasir Alam for helping me to clear the basic concepts of physics and Dr. Meenakshi Rana for helping me each and every stage of Ph.D. and my of my personal life, too.

I would also like to thank to my seniors, juniors, friends Dr. Vikram Verma, Dr. Rishi Dutt Sharma, Dr. Animesh, Ashwin Saxena, Priya Malpani (near and dear friend), Kathakali Mandal, Vikas Deep, Ankit Pandey, Vinne Malik for listening, advising, and supporting me through this entire process, other research scholars and all the technical staff Mr. T. K. Mishra, Mr. Kailash Chandra and Mr. Munish Verma of Materials Science Laboratory, IIIT Noida, for their timely support, kind help and cooperation during the smooth conduction of B. Tech. Labs. I am indebted to the Jaypee Institute of Information technology, Noida for providing me teaching assistantship during Ph.D. work.

I cannot forget to mention the name of my Bhaiya (Dr. Manoj Kumar Chauhan), bhabi (Mrs. Rama Chauhan) and their kids (Nonu and Pihu) for their support and lots of love.

It is my fortune to gratefully acknowledge the support of my family members, respected parents who are my God, Mummy (Mrs. Saroj Sisodia), Papa (Mr. Ashok Kumar Sisodia) for showing faith in me and giving me liberty to choose what I desired, Sister (Neha Sisodia), Brother (Vipul Kumar Sisodia) for their selfless love. Words are short to express my deep sense of gratitude towards my in-laws, Mother-in-law (Mrs. Renu Rajput), Father-in-law (Mr. Akhilesh Rajput) and Brother-in-law (Priyanshu Rajput) who gave me the love, strength, blessings and patience to work through all these years so that today I can stand proud with my head held high.

Finally, my special acknowledgment goes to a special person who mean world to me, my better half my husband (Mr. Sudhanshu Rajput) for his unconditional love, eternal and moral support and understanding of my goals and aspirations. He was always around at times, I thought that it is impossible to continue, he helped me to keep things in perspective. These past several years have not been an easy ride, both academically and personally. I truly thank Sudhanshu for sticking by my side, even when I was irritable and depressed. Thank you for all the little things you have done for me. Thanks for listening to me always at late nights and really sorry for the sleepless nights. I consider myself the luckiest in the world to have such a supportive husband, standing behind me with his love and support.

(Mitali Sisodia)

## ABSTRACT

This thesis is focused on the design and analysis of quantum communication protocols. Several schemes for quantum communication have been introduced in the recent past. For example, quantum teleportation, dense coding, quantum key distribution, quantum secure direct communication, etc., have been rigorously studied in the last 2-3 decades. Specifically, a specific attention of the present thesis is to study the quantum teleportation schemes with entangled orthogonal and nonorthogonal states and their experimental realization, but not limited to it. We have also studied some aspects of quantum cryptography. The present thesis contains 7 chapters. In Chapter 1, we have introduced about the basic concepts related to quantum communication schemes with a specific attention on quantum teleportation and quantum cryptography and some specific examples of the quantum communication schemes, which are rigorously studied in the next chapter of this thesis. Chapters 2-4 are dedicated to the quantum teleportation schemes using different type of quantum resources (entangled orthogonal state and entangled nonorthogonal state) and their experimental realization using superconductivity-based IBM quantum computer. In these chapters, we have shown a perfect teleportation of multi-qubit quantum states can be done using an optimal amount of quantum resources and also shown a proof-of-principle experimental realization of our optimal quantum teleportation scheme using IBMQX2 processor of five-qubit IBM quantum computer. We have also proved that which quasi-Bell state (Bell-type entangled nonorthogonal states) as a quantum channel is perfect for the teleportation scheme in the absence and presence of noise. In Chapter 5, we have reported an experimental realization of a scheme for nondestructive Bell state discrimination using the newest popular experimental platform, i.e., superconductivity-based five-qubit IBM quantum computer, which is recently placed in the cloud in 2016 and easily available free of cost through the internet. In Chapter 6, optical circuits for a set of quantum cryptographic schemes have been designed using available optical elements, like a laser, beam splitter, polarizing beam splitter, half wave plate. Finally, the thesis work is concluded in Chapter 7 with a brief discussion on the limitations of the present work and the scope for future work.



## LIST OF ACRONYMS & ABBREVIATIONS

AD	Amplitude Damping
BB84	Bennett and Brassard 1984
BST	Bidirectional State Teleportation
BS	Beam Splitter
CDSQC	Controlled Deterministic Secure Quantum Communication
CNOT	Controlled-NOT
CQD	Controlled Quantum Dialogue
DSQC	Deterministic Secure Quantum Communication
EPR	Einstein-Podolsky-Rosen
GHZ	Greenberger-Horne-Zeilinger
HWP	Half Wave Plate
IBM	International Business Machine
MFI	Minimum Fidelity
MASFI	Minimum Assured Fidelity
MAVFI	Minimum Average Fidelity
MDI	Measurement-Device-Independent
NMR	Nuclear Magnetic Resonance
OD	Optical Delay
OS	Optical Switch
PBS	Polarizing Beam Splitter
PC	Polarization Controller
PD	Phase Damping
PM	Polarizing Modulator
QD	Quantum Dialogue
QT	Quantum Teleportation
QIS	Quantum Information Splitting
QKD	Quantum Key Distribution
QSDC	Quantum Secure Direct Communication
QST	Quantum State Tomography
SQUID	Superconducting Quantum Interference Device
SPDC	Spontaneous Parametric Down Conversion



## LIST OF FIGURES

1.1	Standard quantum teleportation circuit. CC stands for classical communication. The quantum gates shown here are described in Section 1.7. . . . .	10
1.2	General circuit representation of an arbitrary single-qubit gate $U$ which is essentially reversible (i.e., existence of $U$ implies the existence of $U^{-1}$ ). . . . .	18
1.3	Circuit representation of a CNOT gate. . . . .	21
1.4	(a) Symbolic representation of a SWAP gate (b) how to realize a SWAP gate using three CNOT gates. . . . .	22
1.5	Diagram for a quantum circuit. This particular circuit is known as EPR circuit. It transforms a separable input states to a Bell state as shown. Different inputs (e.g., $ 01\rangle,  10\rangle,  11\rangle$ ) will generate different Bell states. . . . .	23
1.6	Schematic diagrams of optical elements. (a) optically realization of qubit. (b) PBS, which transmits horizontally polarized photon and reflects vertically polarized photon. (c) entanglement generation through the SPDC process (d) A heralded single photon from the SPDC process. . . . .	25
1.7	Figures (a) and (b) are the old and new versions of IBM QX2 processor. . . . .	27
1.8	The architecture used in IBM five-qubit quantum computer. The upper trace in the figure helps in control and read out. The left arm is used for input, and the right arm is used for output. The lower trace is the chip layout, in which five-qubits are positioned. A dedicated coplanar waveguide resonator is used to control and read-out the individual qubits, transmission lines for the purpose are shown in dark color. The coupling between two qubits can be realized via coupled microwave resonator shown by white lines. . . . .	28
1.9	Figures (a) and (b) are depicting chip layout and the topology of the old and new versions of IBM QX4 processor. . . . .	29
1.10	Chip layout and qubit topology of IBM QX5 quantum processor. . . . .	30
2.1	The circuit designed for generalized quantum teleportation of an $n$ -qubit quantum states with $m$ unknown coefficients. Here, $m' = \lceil \log_2 m \rceil$ is the number of Bell states. $U_i$ is the unitary operation applied by Bob and BM stands for Bell measurement. . . . .	38

2.2	As an explicit example, a quantum circuit (which uses a single Bell state as quantum channel) for the the teleportation of an $n$ -qubit quantum state having two unknown coefficients is shown. . . . .	42
2.3	Teleportation circuit used for the teleportation of two-qubit unknown quantum state $(\alpha( 00\rangle +  11\rangle) + \beta( 01\rangle -  10\rangle))$ using single Bell state as a quantum channel. This circuit which is implemented using five-qubit IBM quantum computer, is divided into four parts. In (A) part state preparation is done, where an EPR channel and a quantum state $ \psi\rangle$ with $ \alpha ^2 = 0.375$ and $ \beta ^2 = 0.125$ are prepared. In (B) the decomposition of the unitary operation $U$ which transforms $(\alpha( 00\rangle +  11\rangle) + \beta( 01\rangle -  10\rangle))$ to $(\alpha 00\rangle + \beta 10\rangle)$ in the computational basis is shown. In (C) teleportation of a single-qubit state is realized, and In (D) $ \psi\rangle$ is reconstructed from the teleported single-qubit state by applying $U^\dagger$ followed by projective measurement. . . . .	44
2.4	Graphical representation of real (Re) and imaginary (Im) parts of the density matrices of (a) the theoretical state $\alpha( 00\rangle +  11\rangle) + \beta( 01\rangle -  10\rangle)$ , (b) the experimentally prepared state, and (c) the reconstructed state after teleportation. . . . .	46
3.1	Teleportation circuit for the teleportation of an eight-qubit unknown quantum state (i.e., the state described by Eq. (3.1) using two Bell states (optimal amount of quantum resource). Here, BM and CC stand for Bell measurement and classical communication, respectively. $U_i$ is the unitary operation required to reconstruct the quantum state we wish to teleport. . . . .	51
4.1	The dependence of the average fidelity on nonorthogonality parameters $(r, \theta)$ is illustrated via 2D and 3D plots. Plots (a), (b) and (c) are showing the variation of $F$ with $r$ for $\theta = 0, \frac{\pi}{4},$ and $\frac{\pi}{2}$ , respectively and in these plots the horizontal dotted black line corresponds to classical fidelity. Similarly, (d) shows the variation of $F$ in 3D for both $\psi_+$ and $\psi_-$ in light (yellow) and dark (blue) colored surface plots, respectively. The same fact is illustrated using contour plots for both of these cases in (e) and (f). Note that the quantity plotted in this and the following figures is $F_{ave}$ , which is mentioned as $F$ in the $y$ -axis. . . . .	62

4.2	The dependence of the average fidelity on the number of qubits exposed to AD channels is illustrated for $r = \frac{1}{2}$ and $\theta = \frac{\pi}{3}$ . The choice of the initial Bell states in each case is mentioned in plot legends, where the superscript B, AB, and All corresponds to the cases when only Bob's, both Alice's and Bob's, and all three qubits were subjected to the noisy channel. The same notation is adopted in the following figures. Amplitude damping noise effect on Bob's, both Alice's and Bob's, and all three qubits (superscript B, AB, and All is mentioned in the following figures) is shown with the variation of the average fidelity ( $F_{AD}$ ) with noise parameter ( $\eta$ ) for the specific values of nonorthogonality parameters $r = \frac{1}{2}$ and $\theta = \frac{\pi}{3}$ . . . . .	67
4.3	The effect of phase damping noise is shown for all the quasi-Bell states through the variation of the average fidelity for the specific values of $r = \frac{1}{2}$ and $\theta = \frac{\pi}{3}$ . . . . .	68
4.4	The variation of average fidelity is illustrated for all the possible cases by considering each quasi-Bell state as quantum channel. Average fidelity is plotted for AD ((a)-(c)) and PD ((d)-(f)) channels with $r = \frac{1}{2}$ and $\theta = \frac{\pi}{3}$ . . . . .	69
5.1	The circuit for nondestructive discrimination of all the four Bell states. (a) A four-qubit circuit with two system-qubits (used for Bell-state preparation) and two ancilla-qubits (subsequently used for phase detection (left block) and parity detection (right block)). Here, (b) and (c) are the divided part of (a), whereas, (b) is the phase checking circuit and (c) is the parity checking circuit. . . . .	77
5.2	Experimental implementation of parity and phase checking circuits using five-qubit IBM quantum computer for the Bell state $ \psi^-\rangle$ . Qubits q[0], q[1] are system-qubits, and q[2] mimics ancilla-qubits. Here, (a) and (b) correspond to the parity and phase checking circuits, respectively. In (a) and (b), the left block prepares desired Bell states, the middle block corresponds to a parity and phase checking circuit, respectively and the right block is used for reverse EPR circuit. . . . .	78
5.3	Experimentally implementable (a) parity and (b) phase checking circuits on IBM QX2 followed by tomography block (involves measurement in different basis). Here, configuration implements measurement in X- basis is shown. . . . .	78
5.4	Reconstructed Bell states on Bell-state-ancilla composite system corresponding to ideal states (a) $ \psi^+0\rangle$ , (b) $ \psi^-0\rangle$ , (c) $ \phi^+0\rangle$ , (d) and $ \phi^-0\rangle$ . In each plot, the states $ 000\rangle$ , $ 001\rangle$ , $ 010\rangle$ , $ 011\rangle$ , $ 100\rangle$ , $ 101\rangle$ , $ 110\rangle$ and $ 111\rangle$ are labeled as 1–8 consecutively in X and Y axis. . . . .	85
5.5	Experimental results obtained by implementing the circuits shown in Figure 5.2. Measurement results after implementing phase checking and parity checking circuits are shown in (a)-(d) and (e)-(h), respectively. . . . .	86

5.6	Reconstructed density matrices of various states of Bell-state-ancilla composite system obtained after the implementation of phase and parity checking circuits shown in Figure 5.3. The first column (a)-(d) illustrates the density matrices corresponding to ideal quantum states $ \psi^+0\rangle$ , $ \psi^-1\rangle$ , $ \phi^+0\rangle$ , and $ \phi^-1\rangle$ , respectively. The density matrices in the second column correspond to ideal states (e)-(h) $ \psi^+0\rangle$ , $ \psi^-0\rangle$ , $ \phi^+1\rangle$ , and $ \phi^-1\rangle$ , respectively. . . . .	94
5.7	(a) For the Bell state $ \psi^+\rangle$ , actual implementation of the combined (phase and parity checking) four-qubit quantum circuit shown in Figure 5.1 a using five-qubit IBM quantum computer. (b) To circumvent the constraints of IBM quantum computer, the implemented circuit utilizes this circuit identity. (c) Probability of various measurement outcomes obtained in actual quantum computer after running the circuit 8192 times. (d) Simulated outcome after running the circuit on IBM simulator. This outcome coincides exactly with the expected theoretical value, but the experimental outcome shown in (c) is found to deviate considerably from it. . . . .	95
6.1	Schematic diagram for CQD scheme based on polarization qubit. Four lasers are used to prepare the polarization states of photons. In the proposed optical design, BS stands for symmetric (50:50) beam splitter , PBS is polarizing BS, M is mirror, AM is amplitude modulator, PhM is phase modulator, QRNG is quantum random number generator, PC is polarization controller, HWP is half wave plate, OD is optical delay, PM is polarization modulator, OS is optical switch, $D_i$ represents the detector; whereas $D_H$ and $D_V$ correspond to detectors used for measurements in horizontal and vertical basis and similarly $D_+$ and $D_-$ correspond to measurements in the diagonal basis; and CC is classical communication. . . . .	100
6.2	A proposed optical implementation using polarization qubit of the CQD scheme inspired from the three stage scheme. Laser is used to prepare the photons. In the all lab's, $PM_{A,B,C}$ is polarization modulator used to implement a rotation operator, and $PM'_{A,B,C}$ performs corresponding inverse rotation operator. . . . .	104
6.3	Optical design of the CQD scheme with a complete Bell state measurement (BSM). In Charlie's lab Cr is a nonlinear crystal which is used to generate the entangled photon. Sum frequency generation (SFG) type-I and type-II are nonlinear interactions, which are used to perform the BSM. DBS is dichroic BS and PP1 and PP2 are $45^\circ$ projector. Attenuator (Att) is used to control the intensity of light so that a single Bell pair can be generated. This can also be controlled by changing the pump power. BSM is shown in the box. . . . .	106
6.4	Schematic optical design of controlled direct secure quantum communication with entanglement swapping. . . . .	110

6.5 The proposed optical diagram using linear optics of the QD scheme which is based on single photons. . . . . 112

## LIST OF TABLES

1.1	Table of Alice’s measurement results and Bob’s appropriate choices of Pauli gates to reconstruct the unknown state $(\alpha 0\rangle + \beta 1\rangle)$ . . . . .	11
1.2	Details about experimental parameters used in IBM quantum computer architecture which are available on the website. The first column is qubit index $q$ in IBM quantum computer. The second column shows resonance frequencies $\omega^R$ of corresponding read-out resonators. The qubit frequencies $\omega$ are given in the third column. Anharmonicity $\delta$ , a measure of information leakage out of the computational space, is the difference between two subsequent transition frequencies. Also, $\chi$ and $\kappa$ given in the fifth and sixth columns are qubit-cavity coupling strengths and coupling of the cavity to the environment for corresponding qubits. . . . .	28
1.3	Details about experimental parameters used in IBM quantum computer architecture which are available on the website. The first row and the first column shows qubit index $q[i]$ . Entries of the matrix are the couplings between corresponding qubits. Last two columns depict values of longitudinal relaxation time (T1) and transverse relaxation time (T2). used in IBM quantum computer. Rest of the entries in this table have the same meaning as was described in the the previous table. . . . .	29
2.1	Unitary applied by Bob to reconstruct the quantum state for QT. In the table, SMO is the sender’s measurement outcome. . . . .	38
2.2	A list of quantum states and the quantum resources used to teleport them. The number of qubits in the unknown quantum states, the unknown quantum state (i.e., the state to be teleported) and the resources used to teleport them are mentioned in the first, second and third column, respectively. Here, CS stands for cluster state and $a_i$ represents the binary value of decimal number $i$ expanded up to $k$ digits. Corresponding minimum resources used to teleport that states are given in the forth column. The unitary required to decrease the number of entangled qubits to be used as quantum channel is given in the last column. . . .	40

4.1	Bell states and the corresponding quasi-Bell states. The table shows that the quasi-Bell states can be expressed in orthogonal basis and it introduces the notation used in this chapter. Here, $ \psi^\pm\rangle = \frac{1}{\sqrt{2}}( 00\rangle \pm  11\rangle)$ $ \phi^\pm\rangle = \frac{1}{\sqrt{2}}( 01\rangle \pm  10\rangle)$ , $\eta = \frac{2re^{i\theta}}{\sqrt{2(1+r^2)}}$ , $\varepsilon = \sqrt{\frac{1-r^2}{2(1+r^2)}}$ , $k_\pm = \frac{1\pm r^2 e^{2i\theta}}{\sqrt{2(1\pm r^2 \cos 2\theta)}}$ , $l_\pm = \frac{(\sqrt{1-r^2})re^{i\theta}}{\sqrt{2(1\pm r^2 \cos 2\theta)}}$ , $m_\pm = \frac{1-r^2}{\sqrt{2(1\pm r^2 \cos 2\theta)}}$ , $N_\pm = [2(1 \pm  \langle a b\rangle ^2)]^{-\frac{1}{2}}$ , and $M_\pm = \frac{1}{\sqrt{2(1\pm r^2 \cos 2\theta)}}$ represent the normalization constant. . . . .	56
4.2	The selection of the best and worst quasi-Bell state to be used as a quantum channel for quantum teleportation depends on the value of decoherence rate. A specific case ( $r = \frac{1}{2}$ and $\theta = \frac{\pi}{3}$ ) is shown here for both AD and PD channels. The results observed for PD channel are mentioned in brackets with corresponding results for AD channel without bracket. The same notation is used in the next table, too. . . . .	70
4.3	Even in the presence of noise, different choices of quasi-Bell states (as quantum teleportation channel) may yield fidelity higher than the maximum achievable classical fidelity in the noiseless situation ( $\frac{2}{3}$ ). Here, a specific case for $r = \frac{1}{2}$ and $\theta = \frac{\pi}{3}$ over both AD and PD channels is shown. . . . .	71
5.1	Expected outcomes after parity and phase checking circuit for ancilla-Bell-state combined system for all Bell states. Expected obtained results of ancilla qubits in the same cases are also given. Column 1 illustrates Bell states to be examined. In Column 2, states of the Bell-state-ancilla composite system is shown. Outcomes of measurements on ancilla for two cases is shown in Columns 3 and 4 and outcomes of measuring composite states in the computational basis is shown in Columns 5 and 6 (from left to right). . . . .	80

# CHAPTER 1

## INTRODUCTION

### 1.1 What is quantum communication?

Communication is the act of conveying an intended message to another party through the use of mutually understood signs and rules. Effective communication has played a pivotal role in the development of civilization, and often the ability to communicate effectively distinguishes the human being from the other living species. With time, we have learned many techniques of communication, and our dependence on the communication schemes have increased. In fact, in a modern society communication plays a crucial role, and our dependence on the communication technologies is increasing continuously with the rapid development and enhanced uses of e-banking, mobile phones, internet, IoT, etc. Motivated by this fact, the present thesis is focused on a set of modern techniques of communication.

On the basis of the nature of the physical resources used, this important aspect of modern life (communication) can be broadly categorized into two classes: (1) classical communication and (2) quantum communication. Classical communication includes, all the traditional modes of communication, like internet, mobile, post, where classical resources are used to perform the communication tasks. In contrast, when nonclassical features of quantum mechanics (e.g., non-locality or noncommutativity) and/or nonclassical states like entangled states or squeezed states are used to perform a communication task, it is referred to as quantum communication. This thesis is focused on some aspects of quantum communication schemes which are not possible in the classical domain. Some of the communication schemes studied here require security, whereas others don't. Specifically, in what follows, we study schemes for quantum teleportation and its variants where security is not required and schemes related quantum cryptography where security of the scheme is the primary concern.

In classical communication, the security of the transferred information is not unconditional. As the security of the communicated information in every public key cryptography system is ensured via the computational complexity of the task used for creating a key which is used for encryption of the message. In contrast, in quantum communication, it is possible to attain the



unconditional security as the security of the schemes for quantum cryptography are independent of computational complexity of a task and is obtained using the laws of nature. In addition, there exist a few quantum communication tasks such as teleportation and dense coding, which can be realized only in the quantum domain. These communication tasks (teleportation, dense coding and most of their variants) do not require security, but they may be used as primitives for secure quantum communication.

In this thesis, we have worked on both types of quantum communication schemes (i.e., quantum teleportation and quantum cryptography), but with a greater stress on quantum teleportation. From last 3-4 decades, several cryptographic and non-cryptographic quantum communication tasks have been studied rigorously. Historically, the journey of quantum communication formally began with the publication of the pioneering work of S. Wiesner [1] in 1983<sup>1</sup>. In the next year (i.e., in 1984), Bennett and Brassard [3] proposed the first ever protocol of quantum key distribution (QKD). This pioneering work which is now known as BB84 protocol, changed the entire notion of cryptographic security. The security of this protocol was based on our inability to perform simultaneous measurements in two nonorthogonal bases (non-commutativity), and the protocol in its original form was described using the polarization states of single photons. Later in 1991, Ekert introduced another interesting protocol of QKD, which is now known as E91 protocol [4]. In contrast to single particle states based BB84 protocol, E91 protocol used the properties of entangled states. This was probably the first occasion when entanglement was used for quantum communication. Soon, it was realized that entanglement is one of the most important resources for quantum communication, as in 1992 and 1993, the concept of dense coding [5], and teleportation [6] were introduced, respectively, and entanglement was found to be essential (may not be sufficient) for both of these communication schemes having no classical analogue. Later, a stronger version of entanglement (Bell nonlocality) has been found to be essential for device independent quantum cryptography [7]. Among these nonclassical schemes of communication, teleportation can be viewed as one of the most important schemes of quantum communication. It deserves special attention, as a large number of other quantum communication schemes can be viewed as variants of teleportation. For example, quantum information splitting (QIS) [8, 9], hierarchical QIS [10, 11], quantum secret sharing (QSS) [12], quantum cryptography based on entanglement swapping [13], remote state preparation [14, 15] may be viewed as variants of teleportation.

The first quantum teleportation scheme was introduced by Bennett et al., in 1993 [6]. This scheme was designed for the transmission of an unknown quantum state (a qubit) from Alice (sender) to Bob (receiver) using two bits of classical communication and a pre-shared maximally entangled state (see Section 1.4.1 for details). Dense coding (or super dense coding) is a closely related scheme for quantum communication, where two classical bits of information is

---

<sup>1</sup>A version of this paper was prepared and communicated in 1970, but it was not accepted for publication at that time (for detail see [2]).

transferred by using a single-qubit and prior shared entanglement. Bennett et al., introduced this scheme in 1992 [5]. After these pioneering works, several quantum communication schemes have been proposed [8–13, 15–136] which can be classified into following two classes.

**Class 1:** Quantum communication protocols without security: where security is not relevant (e.g., dense coding, teleportation and its variants).

**Class 2:** Quantum communication protocols with security: where security is relevant. All schemes of secure quantum communication, including the protocols for QKD and secure direct quantum communication belong to this class.

In the following section, we have briefly discussed the history of protocols of quantum communication belonging to the above classes with a focus on the schemes which are relevant for this thesis.

## 1.2 A chronological history of protocols of quantum communication

In this section, we aim to discuss the historical development of quantum communication schemes belonging to both the classes mentioned above<sup>2</sup>. To begin with, we discuss the schemes belonging to Class 1. However, we have given more stress to the schemes that can be viewed as variants of teleportation in comparison to the schemes of dense coding as this thesis is focused on teleportation.

### 1.2.1 A chronological history of quantum communication protocols of Class 1

**1992:** In 1992, the concept of dense coding was proposed by Charles H Bennett and Stephen J Wiesner [5]. This scheme allowed Alice to send 2 bits of classical information to Bob by sending only one qubit provided they already share an entangled state. This was exciting as the communication capacity of this scheme was higher than the maximum possible classical value (as maximum information that can be communicated classically by sending a particle in one bit).

**1993:** In 1993, Charles H Bennett et al., proposed the first quantum teleportation scheme [6], which does not have any classical analogue. This was an exciting development as in this scheme (to be elaborated in Section 1.4.1) the quantum state to be teleported does not

---

<sup>2</sup>As the existing literature is huge, some important works on quantum communication may be excluded by us. Any such omission is unintentional.

travel through the channel, and at the end of the scheme all information about the state is lost at the sender's end and the quantum state is obtained at the receiver's end.

- 1997:** Dik Bouwmeester et al., presented the first experimental demonstration of the quantum teleportation scheme [137] using entangled photons generated by type II spontaneous parametric down-conversion (SPDC) process.
- 1998:** Anders Karlsson and Mohamed Bourennane proposed the first scheme for QIS or controlled quantum teleportation scheme [46], where a sender teleports an unknown quantum state to two receivers. Due to no-cloning theorem only one of them can reproduce the state with the help of other receiver who may be treated as a controller.
- 2000:** Arun K Pati proposed the first scheme of remote state preparation, which can be viewed as a scheme for QT of a known quantum state [14]. After that, several experimental realizations of remote state preparation have been reported.
- 2001:** Susana F Huelga et al., [42] proposed a first scheme for bidirectional (sender  $\iff$  receiver) quantum teleportation or bidirectional state teleportation (BST).
- 2004:** Various facets of teleportation have been experimentally demonstrated. For example, a proof of principle experimental realizations of a scheme for quantum information splitting was reported by Zhi Zhao et al., by preparing a five-qubit entangled state of photon [130], MD Barretti et al., demonstrated teleportation of massive particle (atomic) qubits using ( $^9\text{Be}^+$ ) ions confined in an ion trap [138] and Yun-Feng Huang et al., performed experimental teleportation of a CNOT gate [139].
- 2005:** Gustavo Rigolin proposed a scheme [76] for QT of an arbitrary two-qubit state and shown that all the multi-qubit states can be teleported using Bell states.
- 2006:** Qiang Zhang et al., [125] experimentally realized the quantum teleportation of a two-qubit composite system.
- 2010:** The 16 kilometer free space QT was achieved by Xian-Min Jin et al., in China [140].
- 2011:** In 2011, Anirban Pathak and Anindita Banerjee proposed an efficient and economical (as far as the amount of quantum resource requirement is concerned) scheme for the perfect quantum teleportation and controlled quantum teleportation [9].
- 2012:** Xiao-Song Ma et al., reported QT over 143 kilometers between the Canary Islands of La Palma and Tenerife [57] using optical fiber, and Juan Yin et al., also reported the free space QT and entanglement distribution over 100 kilometers in China [121].

**2012:** Above mentioned QT schemes were based on orthogonal-state-based entangled channels. To the best of our knowledge the first nonorthogonal-state-based QT scheme was proposed by Satyabrata Adhikari et al. [141].

**2005-16:** Various interesting schemes of QT (two party and three party scheme) have been reported. Here, we may mention a few of them, such as protocols designed by Zhuo-Liang Cao and Wei Song in 2005 [16], Li Da-Chuang and Cao Zhuo-Liang in 2007 [23], Li Song-Song et al., in 2008 [90], Chia-Wei Tsai and Tzonelih Hwang in 2010 [98], Yuan-hua Li et al., in 2016 [51]. Authors of all these works used costly (in terms of preparation and maintenance) quantum resources (multi-qubit state) to teleport unknown quantum state.

**2017:** In 2017, we proposed a general scheme of QT with a reduced amount of quantum resources [85] and their experimental realization. We have also proposed a nonorthogonal-state-based QT scheme [84].

**2018:** Many people are found to propose QT schemes with higher amount of quantum resource even after the introduction of our optimal scheme in 2017. So, in 2018, we have written a specific comment [86] to specifically show how our optimal scheme can be realized in a particular case.

## **1.2.2 A chronological history of quantum communication protocols of Class 2**

**1983:** Stephen Wiesner [1] published a paper entitled, “Conjugate coding” which inherently contained many concepts of secure quantum communication. The formal journey of quantum cryptography began with this paper.

**1984:** First protocol for QKD was proposed by Charles H Bennett and G Brassard [3]. The protocol is now known as BB84 protocol. This protocol requires four states.

**1991:** Artur K Ekert proposed a QKD protocol, which was based on Bell’s theorem [4]. Six states were used in this protocol.

**1992:** Charles H Bennett proposed a new protocol to establish that two states selected from two nonorthogonal bases would be sufficient for QKD [142]. The protocol is now known as B92 protocol.

**2002:** The popular Ping-pong (PP) protocol for quantum secure direct communication (QSDC) introduced by Kim Boström and Timo Felbinger [143].

**2004:** The first scheme for bidirectional secure quantum communication, i.e., a scheme for quantum dialogue (QD) introduced by Ba An Nguyen [65] in 2004.

**2005:** Marco Lucamarini and Stefano Mancini presented a protocol, which is known as LM05 scheme [144]. This is a PP- type protocol which can be realized using single photon states, i.e., without using entanglement.

**2009:** Tae-Gon Noh proposed a counterfactual protocol for QKD [145]. The protocol is now known as N09 protocol. This protocol is recently tested experimentally [146–148], it’s also interesting because it motivated researchers to introduce many counterfactual schemes of secure quantum communication.

**2006-2018:** Several quantum cryptographic protocols have been reported and a few of them have been realized experimentally [118, 149–154]. During this period, many other facets of QKD have also been explored. For example, the notion of semi-quantum key distribution [155, 156], counterfactual key distribution [157, 158], device independent QKD [159–161], semi-device independent QKD and measurement device independent QKD have also been evolved and gradually matured (for a review see [162]). Here, it would be interesting to note that in a semi-quantum scheme, the end user can be classical, and in a device independent scheme a completely secure key distribution is possible even when the devices used are faulty. However, to achieve complete device independence, we would generally require 100% efficient photon-detector, which is not achievable at the moment. In contrast, measurement device independent schemes allow one to distribute secure key when only the measurement devices are faulty. The realization of this state of art scheme of QKD requires Bell nonlocal state, but it’s realized that one-way device independence (measurement device independence can be realized using steering). Further, schemes of secure direct communication have been realized in the laboratories [151, 163]. In this decade, exciting works have been done in many facets of cryptography beyond QKD and secure direct quantum communication. In particular, many protocols of quantum voting [164–171], quantum auction [172–176], quantum e-commerce, etc. have been studied in detail. Finally, various commercial products for performing QKD have been launched and marketed [177, 178], some of them have also been successfully used in providing information security to mega events like 2010 Soccer World Cup. Any discussion on this topic would remain incomplete without a mention of the recent successful satellite-based experimental quantum communication [152] between China and Austria [153].

### 1.3 Qubit and measurement basis

Before introducing quantum communication schemes, we would like to introduce here the basic building block of quantum information processing which is known as a “qubit”. A qubit can be viewed as a quantum analogue of a bit. As we know, classical information is measured in bit, which is either in the state 0 or in 1, similarly quantum information is represented by qubit,

which is allowed to exist simultaneously in the states 0 and 1. These states or vectors are denoted as  $|0\rangle = \begin{pmatrix} 1 \\ 0 \end{pmatrix}$  and  $|1\rangle = \begin{pmatrix} 0 \\ 1 \end{pmatrix}$ , which are written in the Dirac's notation or bra-ket notation. In this notation,  $|0\rangle$  and  $|1\rangle$  are pronounced as *ket0* and *ket1*, respectively. Transpose conjugate of a state vector described as  $|\psi\rangle$  is described as  $\langle\psi|$  and is pronounced as *bra  $\psi$* . Thus, the state vectors are usually described as a column matrix representing  $|\psi\rangle$ , whereas  $\langle\psi|$  is described by a row matrix. Now, a qubit is represented by a state vector  $|\psi\rangle = \alpha|0\rangle + \beta|1\rangle$ , where  $\alpha$  and  $\beta$  are the probability amplitudes and complex numbers, which satisfies the condition  $|\alpha|^2 + |\beta|^2 = 1$ .  $|\alpha|^2$  and  $|\beta|^2$  are the probabilities of obtaining the qubit in the state  $|0\rangle$  and  $|1\rangle$ , respectively on performing a measurement in the computational basis [2, 179]. The last statement and the fact that a quantum state collapses to a basis state on performing a measurement in a particular basis will be further clarified in the following paragraphs, but before we do so, we need to elaborate on the basis sets used in this work.

A set of vectors is  $\{|v_1\rangle, |v_2\rangle, |v_3\rangle, \dots, |v_n\rangle\}$ . If the elements of this set are linearly independent (condition of linear independence of a set of vectors is  $\sum_{i=1}^n a_i |v_i\rangle = 0$  iff all  $a_i = 0$ ) to each other, satisfy the condition of orthogonality  $\langle v_i | v_j \rangle = \delta_{ij}$  and show a completeness relation given by  $\sum_{i=1}^n |v_i\rangle \langle v_i| = 1$ , then the set is known as a basis set. In this thesis, we have mostly used three basis sets- computational basis, diagonal basis and Bell basis. These basis sets can be defined as follows

Computational basis:  $\{|0\rangle, |1\rangle\}$ .

In the context of quantum communication the basis elements (states to which an arbitrary quantum state is projected on measurement) are usually viewed as horizontal ( $|0\rangle$ ) and vertical ( $|1\rangle$ ) polarization states of photon. In two-qubit scenario computational basis refers to  $\{|00\rangle, |01\rangle, |10\rangle, |11\rangle\}$ . Similarly, we can easily extend it to multi-qubit scenario as one can write a multi-qubit state as tensor product of states of individual qubits. In general, in this basis set, basis elements are not expressed in a superposition

Diagonal basis:  $\left\{ |+\rangle = \frac{|0\rangle + |1\rangle}{\sqrt{2}}, |-\rangle = \frac{|0\rangle - |1\rangle}{\sqrt{2}} \right\}$ .

In QKD, we usually view  $|+\rangle$  as a photon polarized at  $45^\circ$  w.r.t. horizontal direction and  $|-\rangle$  as a photon polarized at  $135^\circ$  w.r.t. horizontal direction.

Bell basis:  $\left\{ |\psi^+\rangle = \frac{|00\rangle + |11\rangle}{\sqrt{2}}, |\psi^-\rangle = \frac{|00\rangle - |11\rangle}{\sqrt{2}}, |\phi^+\rangle = \frac{|01\rangle + |10\rangle}{\sqrt{2}}, |\phi^-\rangle = \frac{|01\rangle - |10\rangle}{\sqrt{2}} \right\}$ .

Here, the basis elements are maximally entangled and these are known as Bell states.

## 1.4 Various facets of quantum communication schemes of Class 1

The pioneering work of Bennett et al., on QT drew considerable attention of the quantum communication community since its introduction in 1993 [6]. As a consequence, a large number of modified QT schemes have been proposed. To elucidate on this point, we may mention a few schemes of quantum communication tasks, which can be viewed as modified schemes for QT. This set of quantum communication tasks includes—remote state preparation [14], controlled quantum teleportation [9, 46], or equivalently quantum information splitting, [12, 67] bidirectional quantum teleportation [42], bidirectional controlled quantum teleportation [81, 94, 95], quantum secret sharing [12], hierarchical quantum secret sharing [11, 180], and many more. The interconnection among these variants of QT can be understood easily if we note that QT of a known state (i.e., when the probability amplitudes (coefficients) of the state to be teleported are known to the sender (usually referred to as Alice) but not to the receiver (usually referred to as Bob)) is called remote state preparation, whereas simultaneous QT of a quantum state each by Alice and Bob is known as bidirectional state teleportation. Similarly, controlled teleportation and bidirectional controlled state teleportation schemes are controlled variants of QT and bidirectional state teleportation schemes, where a third party (Charlie) supervises the whole proceeding by preparing a quantum channel to be used for the task and withholding part of the useful information. In other words, in controlled teleportation (bidirectional controlled state teleportation), Alice and Bob can execute a scheme for QT (bidirectional state teleportation) if Charlie allows them to do so.

Many of the above-mentioned schemes have very interesting applications (for details see Ref. [2]). For example, we may mention that every scheme of BST can be used to design quantum remote control [42]. It is also worth noting here that although teleportation (and most of its variants) in its original form is not a secure communication scheme, it can be used as a primitive for secure quantum communication. As a major part of this thesis is focused around quantum teleportation and its modified version, in the following section, we will briefly describe the concept of QT.

### 1.4.1 Quantum teleportation

Teleportation is a quantum task and it can be achieved only by using a shared entangled state as a quantum channel and some classical communication. The standard quantum teleportation scheme uses a Bell state as quantum channel [6]. The basic idea of the original quantum teleportation scheme was to teleport an unknown single-qubit quantum state  $|\psi\rangle = \alpha|0\rangle + \beta|1\rangle$  from Alice (sender) to spatially separated Bob (receiver) by using 2 bits of classical communication using a shared entangled state (Bell state). After the pioneering work of Bennett et al.,

a large number of quantum teleportation schemes and their modifications have been reported by using Bell state, GHZ state, and other multi-partite entangled states as a quantum channel [16, 23, 38, 50–52, 63, 64, 67, 90, 93, 98, 104, 123]. Several experimental realizations of quantum teleportation schemes have also been reported ([57, 121, 125, 130, 137–140] and references therein).

All these schemes and their modified version may be classified into two classes- (1) Perfect teleportation- where an unknown quantum state is transmitted with unit fidelity. A perfect teleportation scheme is also called deterministic if the success rate of the teleportation scheme is found to be unity, such a deterministic perfect teleportation scheme requires a maximally entangled state as a quantum channel. (2) Probabilistic teleportation- After the Bennett et al.'s scheme, it was shown that the teleportation is possible with unit fidelity even when a non-maximally entangled state is used as a quantum channel. In that case, the success rate of teleportation will not be unity such a scheme of teleportation is referred to as probabilistic teleportation scheme. In what follows, we briefly describe the original scheme of Bennett et al., as an example of deterministic perfect teleportation scheme.

**Deterministic perfect teleportation:** A standard quantum circuit for deterministic perfect teleportation is shown in Figure 1.1. According to this figure, initially Alice and Bob share a maximally entangled Bell state  $|\psi^+\rangle = \frac{1}{\sqrt{2}}(|00\rangle + |11\rangle)$  of which the first qubit is with Alice and the second qubit is with Bob. In the left most block of the circuit shown in Figure 1.1, this Bell state is created from the separable states  $(|0\rangle \otimes |0\rangle)$  by applying a Hadamard gate<sup>3</sup> on the first qubit followed by a CNOT gate (EPR circuit) which uses the first qubit as the control qubit and the second qubit as the target qubit. In the second box from left, a reverse EPR circuit is shown. It helps Alice to entangled the state to be teleported using the shared entangled state as follows. First Alice combines her unknown quantum state  $|\psi\rangle = \alpha|0\rangle + \beta|1\rangle$  to be teleported with her shared entangled qubit. The combined state is

$$\begin{aligned} |\psi\rangle_{combined} &= |\psi\rangle \otimes |\psi^+\rangle \\ &= (\alpha|0\rangle + \beta|1\rangle)_A \otimes \frac{1}{\sqrt{2}}(|00\rangle + |11\rangle)_{AB} . \\ &= \left( \alpha \frac{(|000\rangle + |011\rangle)}{\sqrt{2}} + \beta \frac{(|100\rangle + |111\rangle)}{\sqrt{2}} \right)_{AAB} \end{aligned}$$

Then she applies a CNOT gate on the first two qubits (indexed as AA) available with her. Where the first A corresponds to a control qubit and the second A corresponds to a target qubit. This operation transforms the combined state  $|\psi\rangle_{combined}$  to  $|\psi\rangle_1$

$$|\psi\rangle_1 = \left( \alpha \frac{(|000\rangle + |011\rangle)}{\sqrt{2}} + \beta \frac{(|110\rangle + |101\rangle)}{\sqrt{2}} \right)_{AAB} .$$

---

<sup>3</sup>All quantum gates are explained in detail in Section 1.7 .



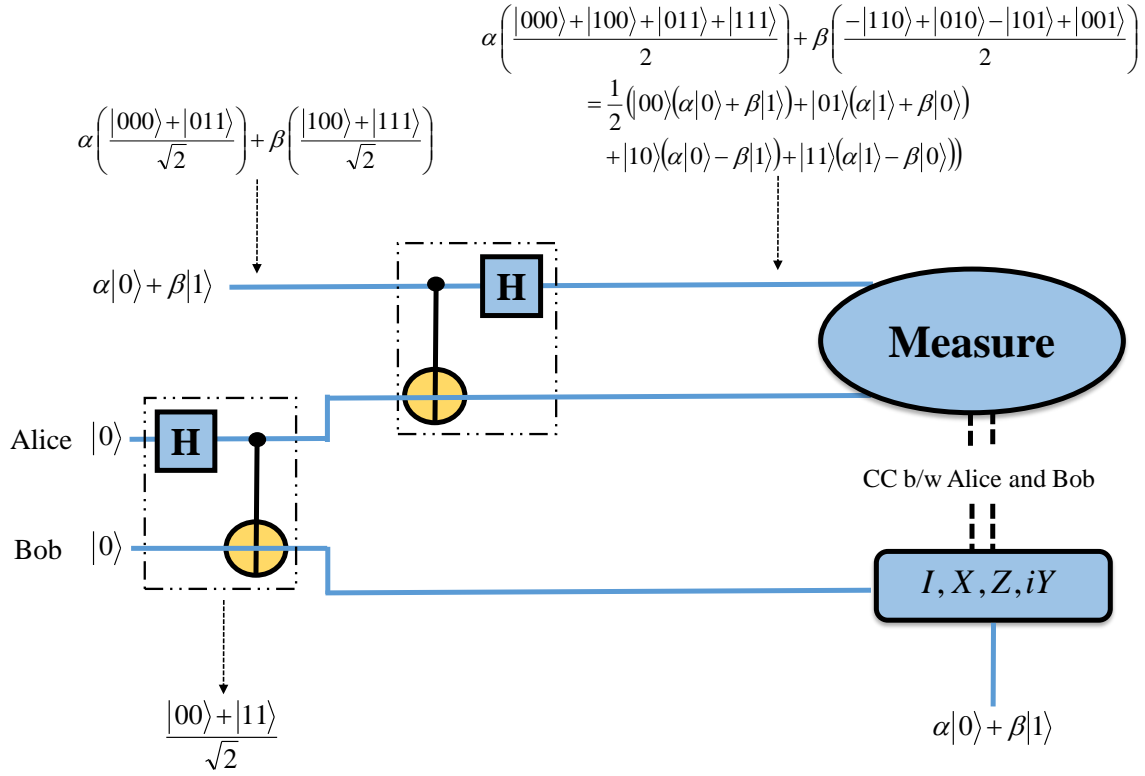


**Figure 1.1:** Standard quantum teleportation circuit. CC stands for classical communication. The quantum gates shown here are described in Section 1.7.

After that Alice applies Hadamard operation on the first qubit to yield

$$\begin{aligned} |\psi\rangle_2 &= \left( \alpha \frac{|(0)+|1\rangle}{\sqrt{2}} \frac{|(00)+|11\rangle}{\sqrt{2}} + \beta \frac{|(0)-|1\rangle}{\sqrt{2}} \frac{|(10)+|01\rangle}{\sqrt{2}} \right)_{AAB} \\ &= \frac{1}{2} (|00\rangle (\alpha|0\rangle + \beta|1\rangle) + |01\rangle (\alpha|1\rangle + \beta|0\rangle) \\ &\quad + |10\rangle (\alpha|0\rangle - \beta|1\rangle) + |11\rangle (\alpha|1\rangle - \beta|0\rangle))_{AAB} \end{aligned}$$

Subsequently, Alice measures her both qubits  $AA$  in computational basis  $\{|00\rangle, |01\rangle, |10\rangle, |11\rangle\}$ . Subsequently, she sends her measurement result to Bob by classical communication. At the end of Bob, he applies unitary operation on his qubit to reconstruct the unknown quantum state. Pauli operation applied by Bob depends on the classical communication of Alice as shown in Table 1.1. In all cases Bob reconstructs  $\alpha|0\rangle + \beta|1\rangle$ . Thus, the perfect teleportation task is accomplished with unit fidelity. It may be noted that the teleportation scheme described above is a scheme for teleportation of an unknown single-qubit quantum state using a Bell state. Extending this idea, in Chapters 2 and 3, we will present a scheme for the teleportation of the multi-qubit unknown quantum states using minimal number of Bell states.

**Table 1.1:** Table of Alice’s measurement results and Bob’s appropriate choices of Pauli gates to reconstruct the unknown state  $(\alpha|0\rangle + \beta|1\rangle)$ .

Alice measures	State of Bob’s qubit	Bob’s operation	Bob’s state after operation
00	$\alpha 0\rangle + \beta 1\rangle$	$I$	$\alpha 0\rangle + \beta 1\rangle$
01	$\alpha 0\rangle - \beta 1\rangle$	$Z$	$\alpha 0\rangle + \beta 1\rangle$
10	$\alpha 1\rangle + \beta 0\rangle$	$X$	$\alpha 0\rangle + \beta 1\rangle$
11	$\alpha 1\rangle - \beta 0\rangle$	$iY$	$\alpha 0\rangle + \beta 1\rangle$

#### 1.4.1.1 Entangled orthogonal and nonorthogonal state based quantum teleportation

Usually, standard entangled states, which are inseparable states of orthogonal states, are used to implement teleportation based schemes. However, entangled nonorthogonal states do exist, and they may be used to implement some of these teleportation-based protocols [141]. Specifically, entangled coherent states [71, 73, 100, 181–186] and Schrödinger cat states prepared using  $SU(2)$  coherent states [187] are the typical examples of entangled nonorthogonal states. Such a state was first introduced by Sanders in 1992 [181].

Since then several investigations have been performed on the properties and applications of the entangled nonorthogonal states. The investigations have yielded a handful of interesting results. To be precise, in Ref. [188], Prakash et al., have provided an interesting scheme for entanglement swapping for a pair of entangled coherent states; subsequently, they investigated the effect of noise on the teleportation fidelity obtained in their scheme [189], and Dong et al., [190] showed that this type of entanglement swapping schemes can be used to construct a scheme for continuous variable quantum key distribution (QKD); the work of Hirota et al., [191] has established that entangled coherent states, which constitute one of the most popular examples of the entangled nonorthogonal states, are more robust against decoherence due to photon absorption in comparison to the conventional bi-photon Bell states; another variant of entangled nonorthogonal states known as squeezed quasi-Bell state has recently been found to be very useful for quantum phase estimation [192]; in [141], Adhikari et al., have investigated the merits and demerits of an entangled nonorthogonal state-based teleportation scheme analogous to the standard teleportation scheme. In brief, these interesting works have established that most of the quantum computing and communication tasks that can be performed using usual entangled states of orthogonal states can also be performed using entangled nonorthogonal states. Interestingly, nonorthogonal-based QT scheme will be discuss in Chapter 4.

## 1.5 Various facets of quantum communication schemes of Class 2

It is well known that all the classical cryptographic protocols are secure under some assumptions related to the complexity of a computational task, and consequently security of classical schemes are conditional. In contrast, secure communication is possible in the quantum domain without any such assumption. So most of the quantum cryptographic protocols or secure quantum communication protocols are unconditionally secure, which is never achievable in the classical regime. We have already mentioned that in 1984, Bennett and Brassard [3] introduced the first QKD protocol, which is now known as BB84 protocol. This unconditionally secure quantum key can be used for encryption in one-time pad [193]. This pioneering work was followed by several new different protocols for QKD and other tasks related to secure quantum communication (see [4, 142, 162, 194] and references therein). Most of these protocols have not yet been realized experimentally. The protocols which have not yet been reported experimentally, require some modifications for the realizations using the existing technology. Such a possibility is discussed in the present thesis. This section aims to introduce a few protocols of secure quantum communication that are relevant to the present thesis. Such protocols are briefly discussed below.

### 1.5.1 BB84 and other protocols of QKD

Detailed description of BB84 and other protocols of QKD and their inter-relations can be found in Chapter 8 of Ref. [2] and in the other text books, so we are not going to provide detailed description of any scheme here. We just wish to note that in contrast to classical schemes of secure communication (where the security arises from the complexity of a computational task), in QKD the security arises from the fundamental laws of physics. In BB84 protocol, initially, Alice prepares a random sequence of quantum states  $\{|0\rangle, |1\rangle, |+\rangle, |-\rangle\}$  or equivalently a random sequence of single photon states prepared in horizontal, vertical,  $45^\circ$ , and  $135^\circ$  polarized states. After receiving the sequence, Bob measures each qubit randomly using  $\{|0\rangle, |1\rangle\}$  basis or  $\{|+\rangle, |-\rangle\}$  basis and subsequently announces which qubit is measured by him in which basis. Alice checks in which cases the basis used for preparing the state coincides with the basis used by Bob to measure the states. She informs Bobs to keep those cases and discard the rest. In all these cases, in absence of Eve the Bob's measurement should reveal the same state as was prepared by Alice. To check that they compare half of these cases, to check the presence of Eve (an authorized party who wishes obtain the key). In the absence of Eve they use rest of the bits as key by considering  $|0\rangle$  and  $|+\rangle$  as 0 and  $|1\rangle$  and  $|-\rangle$  as 1.

Here, it's important to note that as Eve does not know which qubit is prepared in which basis, she cannot perform a measurement without disturbing the state of the qubit. So her

efforts to obtain information by performing any type of measurement leaves detectable trace which is revealed in the comparison step performed by Alice and Bob. This primarily happens because of Eve's inability to perform simultaneous measurement in two nonorthogonal bases (i.e., in  $\{|0\rangle, |1\rangle\}$  basis or  $\{|+\rangle, |-\rangle\}$  basis). Further, no-cloning theorem states that an unknown quantum state cannot be copied perfectly. As a consequence, Eve cannot keep a copy of the transmitted qubit and perform measurement using appropriate basis at a later time when Bob discloses the basis used by him to measure a particular qubit. Thus, we can clearly see that the security arises from noncommutativity (our inability to perform simultaneous measurement in two or more nonorthogonal bases) and noncloning principle, and it does not depend on the complexity of a computational task. This is why schemes of quantum cryptography in general and schemes of QKD in particular are considered as unconditionally secure.

In the above, we have elaborated what kind of laws of physics lead to the security of QKD in view of BB84 protocol. After this pioneering work many other schemes of QKD have been proposed. Some of them (e.g., [142]) use nonorthogonal states and thus the same principle as described above.

However, there exist various orthogonal states based schemes, too (e.g., [194]). Here, we would not elaborate on the working of these schemes as they are not used in this work.

## 1.5.2 Secure direct quantum communication

Most of the initial proposals on quantum cryptography were limited to QKD [3, 4, 142, 194]. Later on, it was observed that secure quantum communication is possible without prior generation of key. In other words, it is possible to design schemes of direct secure quantum communication circumventing prior distributed key. In last two decades, many schemes for secure direct quantum communication have been proposed. All the schemes of secure direct quantum communication can be classified into two categories [195]: (1) deterministic secure quantum communication scheme (DSQC), (2) quantum secure direct communication scheme (QSDC) [143, 144, 200]. In DSQC protocol, Alice needs to send some classical information (at least 1 bit for each qubit) to Bob, who can't decode the information encoded by Alice in the absence of this classical information. In QSDC, no such classical information is required for decoding.

## 1.5.3 Quantum dialogue (QD)

In all protocols of QSDC and DSQC ([114, 143, 144, 195–199, 201] and references therein), a secret message is transmitted from Alice (sender) to Bob (receiver). Thus, these schemes are one way (unidirectional) schemes for communication. In other words, Alice and Bob cannot

exchange their messages to each other at the same time. Of course they can use two independent QSDC or DSQC schemes to do that. However, that would not be considered as simultaneous communication. Keeping this in mind, a notion of two-way communication using Bell states was proposed by Ba An [65] in 2004. The two-way communication scheme which allows both Alice and Bob to simultaneously send message to each other in a secure manner is referred to as quantum dialogue (QD). A very important feature of this scheme is that in this scheme information encoded by Alice and Bob simultaneously exists in the channel. Almost immediately after Ba An's work, in 2005, Man et al., [202] found that Ba An's original protocol for QD is not secure against intercept-resend attack and he proposed a modified scheme. However, eventually, it was found that there were some issues with Man et al.'s scheme, too. Finally, in 2005, Ba An proposed an improved version of his original QD protocol and addressed all the issues raised until then [203]. After this work of Ba An, several protocols of QD have been reported [82, 106, 204–206]. The reason behind the interest on QD is obvious, as ability to perform QD ensure the ability to perform QSDC/DSQC and QKD. This point will be further elaborated in the next section.

#### **1.5.4 Controlled quantum dialogue (CQD)**

Controlled QD corresponds to a novel scheme for bidirectional secure quantum communication which is essentially a scheme for QD controlled by a controller or a supervisor. It is a three party scheme involving sender (Alice), receiver (Bob) and supervisor (Charlie). In this two way communication scheme, Alice and Bob can execute a scheme for QD provided the controller Charlie allows them to do so. This scheme is interesting for various reasons. Firstly, ability to perform CQD ensures the ability to perform QD. In term if one can perform two way direct communication he can also perform one way direct communication (we may assume that Alice encodes a message, but Bob always encodes zero). Now ability to communicate a message in a secure manner implies the ability to distribute a key in a secure manner. Thus, if we can do CQD, we can do QD, DSQC, QKD, CDSQC, etc.

## **1.6 Effect of noise on the protocols of quantum communication**

We have already introduced various quantum communication schemes. Now in this section, we will discuss the effect of noise on these quantum communication schemes. Generally, dynamics of a system can be defined as unitary evolution neglecting the effect of surrounding on it, which is also called closed system description. In contrast, considering the effect due to ambient environment, the system dynamics cannot always be described by a unitary evolution studied as open quantum system. In open quantum systems, a pure state can evolve into a mixed state.

The effect of environment on the system can be studied by describing unitary dynamics of the composite system-environment state. Let's consider initial state of the system and environment as  $\rho_s$  and  $\rho_R$  and consider evolution of the state of the composite system, i.e.,  $\rho = \rho_s \otimes \rho_R$ , under unitary  $U$  as

$$\rho(t) = U(\rho_s \otimes \rho_R)U^\dagger. \quad (1.1)$$

The system evolution can be obtained by tracing over the reservoir (environment) state as  $\rho_s(t) = Tr_R \{\rho(t)\}$ . For the sake of simplicity, we can assume environment to be in the pure state, say  $|e_i\rangle$ . Then Eq. (1.1) can be rewritten as

$$\varepsilon(\rho_s) = Tr_R \left\{ U(\rho_s \otimes |e_i\rangle\langle e_i|)U^\dagger \right\}. \quad (1.2)$$

Here,  $\varepsilon$  is a completely positive and trace preserving dynamical map, completely positive and trace preserving conditions are imposed by the density matrix definition employing positivity and unit trace condition. Here, we will briefly discuss a representation in which the effect of environment on the system can be encapsulated nicely as completely positive and trace preserving dynamical map. The representation is known as operator sum representation or Kraus operator representation. The system state from the above equation can be derived by tracing out the environment in basis  $|e_k\rangle$  thus Eq. (1.2) becomes

$$\varepsilon(\rho_s) = Tr_R \left\{ U(\rho_s \otimes |e_i\rangle\langle e_i|)U^\dagger \right\} = \sum_k \langle e_k | U(\rho_s \otimes |e_i\rangle\langle e_i|)U^\dagger | e_k \rangle = \sum_k E_k \rho_s E_k^\dagger. \quad (1.3)$$

The equation in the last row elucidate mathematical statement of operator sum representation and  $E_k$  are known as Kraus operator which satisfy a completeness relation  $\sum_i E_k E_k^\dagger = I$ .

There are various types of noise which have been well established in the past [207–209].

In this thesis, we have mainly studied two types of Markovian noise, amplitude damping (AD) noise and phase damping (PD) noise. These two types of noise are briefly described below.

### 1.6.1 Amplitude damping noise

A large number of investigations considering different noise models have been performed recently. The amplitude damping (AD) noise model is one the most important noise models that have been studied recently. This noise model has been rigorously studied in the recent past ([79, 207, 210–216] and references therein) because of the fact that it can mimic (simulate) the dissipative interaction between a quantum system and a vacuum bath.

The Kraus operators for AD noise are [209]

$$E_0 = |0\rangle\langle 0| + \sqrt{1-\eta}|1\rangle\langle 1|, \quad E_1 = \sqrt{\eta}|0\rangle\langle 1|. \quad (1.4)$$

where  $\eta$  ( $0 \leq \eta \leq 1$ ) is the decoherence rate for the AD channel, which determines the effect of the noisy channel on the quantum system.

### 1.6.2 Phase damping noise

The phase damping (PD) noise involves information loss about relative phases in a quantum state. The PD noise model is characterized by the following Kraus operators.

$$E_0 = |0\rangle\langle 0| + \sqrt{1-\eta}|1\rangle\langle 1|, \quad E_1 = \sqrt{\eta}|1\rangle\langle 1|. \quad (1.5)$$

For PD noise,  $\eta$  ( $0 \leq \eta \leq 1$ ) is the decoherence rate, which describes the probability of error due to PD channel.

### 1.6.3 Fidelity as a quantitative measure of the effect of noise

The concept of fidelity is a basic ingredient in quantum communication scheme. Let us consider  $\rho^1 = |\psi_1\rangle\langle\psi_1|$  and  $\rho^2 = |\psi_2\rangle\langle\psi_2|$  are the two quantum states on a finite dimensional Hilbert space, and we want to know the closeness of these quantum states. So, one measure of distinguishability or closeness between two quantum states is known as the fidelity. In other words, fidelity is used to describe the closeness between two quantum states ( $\rho^1$  and  $\rho^2$ ).

Given two states  $\rho^1$  and  $\rho^2$ , generally the fidelity is defined as the quantity<sup>4</sup>

$$F(\rho^1, \rho^2) = \text{Tr}[\sqrt{\sqrt{\rho^1}\rho^2\sqrt{\rho^1}}]. \quad (1.6)$$

There are some special cases where we can acquire more useful and easily understood expressions of fidelity. For simplicity, here we consider two pure states. In this particular case, we may consider  $\rho^1 = |\psi_1\rangle\langle\psi_1|$  and  $\rho^2 = |\psi_2\rangle\langle\psi_2|$  are both pure states for which  $(\rho^i)^2 = \rho^i$ . Consequently,  $F(|\psi_1\rangle, \rho^2) = \text{Tr}[\sqrt{\sqrt{\rho^1}\rho^2\sqrt{\rho^1}}] = \text{Tr}[\sqrt{|\psi_1\rangle\langle\psi_1|\rho^2|\psi_1\rangle\langle\psi_1|}] = \sqrt{\langle\psi_1|\rho^2|\psi_1\rangle}$ . In another case,

$$F(|\psi_1\rangle, |\psi_2\rangle) = \text{Tr}[\sqrt{\sqrt{\rho^1}\rho^2\sqrt{\rho^1}}] = \text{Tr}[\sqrt{|\psi_1\rangle\langle\psi_1|\psi_2\rangle\langle\psi_2|\psi_1\rangle\langle\psi_1|}] = |\langle\psi_2|\psi_1\rangle|.$$

There are a few general properties of fidelity.

---

<sup>4</sup>In some literature for example Ref [217], the formula of fidelity  $\left(\text{Tr}[\sqrt{\sqrt{\rho^1}\rho^2\sqrt{\rho^1}}]\right)^2$  has been used. Both definitions yield the same physical meaning.

(i) The first is that fidelity ranges between  $0 \leq F(\rho^1, \rho^2) \leq 1$ , with unity iff  $\rho^1 = \rho^2$  and 0 if there is no overlap whatsoever.

(ii)  $F(\rho^1, \rho^2) = F(\rho^2, \rho^1)$ .

(iii) Fidelity is invariant under unitary transformations  $F(U\rho^1U^\dagger, U\rho^2U^\dagger) = F(\rho^2, \rho^1)$ .

We can also see fidelity as a quantitative measure of the effect of noise. For example, a pure quantum state is  $|\psi\rangle$  (initial state) so the density matrix of this initial state is  $\rho = |\psi\rangle\langle\psi|$ . Now, if the pure state interacts with the environment which converts it into mixed state  $\rho' = \sum p_i |\psi_i\rangle\langle\psi_i|$  ( $p_i$  is the probability with  $\sum p_i = 1$ ). To quantify how much the state is affected due to noise, we calculate fidelity between the initial state and noise affected state by using above formula 1.6.

## 1.7 Quantum gates and quantum circuits

Except NOT and Identity gates, all the other conventional classical gates, such as AND, OR, NOR, NAND are irreversible ( $\rightarrow$ ), in the sense that we cannot uniquely obtain the input state from the output state. During operation of each of the above mentioned irreversible gates, one bit of information is erased as these gates always map a 2-bit input state into a 1-bit output state. It was Landauer's pioneering work [218], which led to the observation that erasure of a bit involves a loss of energy amounting at least  $kT \log 2$ , and such an energy loss due to logical operation can be circumvented by using reversible logic gates. It's technically possible to make classical reversible gates. However, they are not of much interest as they cannot be used to perform any task that cannot be performed by the irreversible circuits. In contrast, all the quantum gates are reversible ( $\leftrightarrow$ ) in nature, implying that we can uniquely reconstruct the input states from the output states (bijective mapping). Here, it may be noted that all the quantum gates are reversible, but all the reversible gates are not referred to as the quantum gates. Usually, quantum gates are called just quantum gates and classical reversible gates are referred to as reversible gates. In what follows, we will also follow the same convention. Basically, a quantum gate or a quantum logic gate corresponds to a unitary operation that maps a quantum state into another quantum state in a unique manner. The map is always bijective as expected. In matrix notation, an  $N$  qubit quantum gate is represented by  $2^N \times 2^N$  matrix. In what follows, we will discuss important single-qubit and two-qubit gates and their combinations, which lead to quantum circuit. Some quantum gates, which are not used in this thesis will also be summarized. To begin with, in the next section, we will introduce some single-qubit gates.

### 1.7.1 Single-qubit quantum gates

The vector representation of a single-qubit is  $\begin{pmatrix} \alpha \\ \beta \end{pmatrix}$  and a single-qubit quantum gate is represented by a  $2 \times 2$  matrix. Single-qubit gate is a unitary operator  $U$ , which transforms a single-



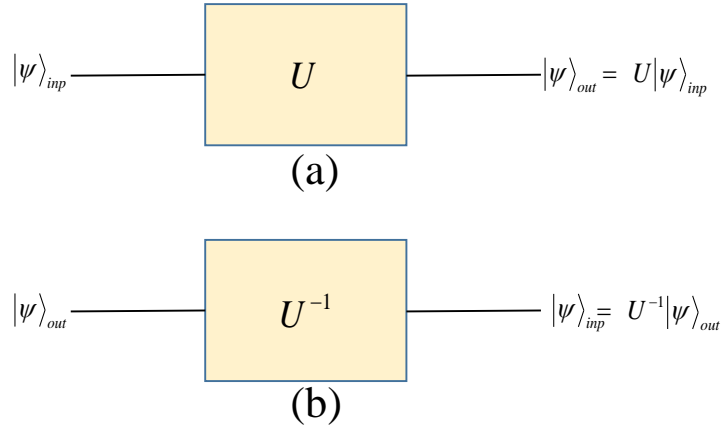


**Figure 1.2:** General circuit representation of an arbitrary single-qubit gate  $U$  which is essentially reversible (i.e., existence of  $U$  implies the existence of  $U^{-1}$ ).

qubit state  $|\psi\rangle_{inp}$  to another single-qubit state  $|\psi\rangle_{out} = U|\psi\rangle_{inp}$ . Further, the existence of  $U$  ensures the existence of  $U^{-1}$ . Thus the feasibility of the inverse operation  $U^{-1}|\psi\rangle_{out} = |\psi\rangle_{inp}$  (see Figure 1.2). In this section, single-qubit gates are introduced.

**1. Pauli-X gate or NOT gate:** The matrix representation of unitary operator  $X$  gate is

$$X = \begin{pmatrix} 0 & 1 \\ 1 & 0 \end{pmatrix}.$$

Operation of  $X$  gate can be described by the following input-output maps.

$$X|0\rangle = |1\rangle, \quad X|1\rangle = |0\rangle,$$

$$X(\alpha|0\rangle + \beta|1\rangle) = (\alpha|1\rangle + \beta|0\rangle).$$

**2. Pauli-Z gate:**  $Z$  gate is represented in matrix form as follows

$$Z = \begin{pmatrix} 0 & 1 \\ -1 & 0 \end{pmatrix}.$$

It is easy to see that  $Z$  gate transforms the single-qubit state as

$$Z|0\rangle = |0\rangle, \quad Z|1\rangle = -|1\rangle,$$

$$Z(\alpha|0\rangle + \beta|1\rangle) = (\alpha|0\rangle - \beta|1\rangle).$$

Thus,  $Z$  gate just flips the phase. So, it is also known as phase flip operator as well as  $\sigma_z$ .

**3. Pauli-Y gate:** Similarly, the matrix representation of  $Y$  gate or  $\sigma_y$  is

$$Y = \begin{pmatrix} 0 & -i \\ i & 0 \end{pmatrix}.$$

It will transform the single-qubit states as

$$Y|0\rangle = |1\rangle, \quad Y|1\rangle = |0\rangle,$$

$$Y(\alpha|0\rangle + \beta|1\rangle) = (\alpha|1\rangle - \beta|0\rangle).$$

$Y$  gate is the combination of  $X$  gate and  $Z$  gate. It is a bit flip and phase flip operator.

**4. Hadamard gate:** The other single-qubit gate is Hadamard gate ( $H$ ), which is represented by a matrix

$$H = \frac{1}{\sqrt{2}} \begin{pmatrix} 1 & 1 \\ 1 & -1 \end{pmatrix}.$$

The Hadamard transformations is defined by

$$H|0\rangle = \frac{1}{\sqrt{2}}(|0\rangle + |1\rangle),$$

$$H|1\rangle = \frac{1}{\sqrt{2}}(|0\rangle - |1\rangle).$$

**5. Phase gate:** We can represent the phase gate by a matrix form is

$$P = \begin{pmatrix} 1 & 0 \\ 0 & e^{i\theta} \end{pmatrix}.$$

Since  $\theta$  can have infinitely many values, but here we are taking two values of  $\theta$ . For  $\theta = \frac{\pi}{2}$ , we obtain  $S$  gate described as

$$S = P\left(\frac{\pi}{2}\right) = \begin{pmatrix} 1 & 0 \\ 0 & i \end{pmatrix}.$$

It is usually referred to as  $S$  gate, and it maps

$$S|0\rangle = |0\rangle, S|1\rangle = i|1\rangle.$$

If  $\theta = \frac{\pi}{4}$ , then we obtain a  $T$  gate which is described in matrix form as

$$T = P\left(\frac{\pi}{4}\right) = \begin{pmatrix} 1 & 0 \\ 0 & \frac{1}{\sqrt{2}}(1+i) \end{pmatrix}.$$

It may be noted that  $P$  gate is not self-inverse in general.

## 1.7.2 Two-qubit quantum gates

A two-qubit state is represented by the column matrix  $\begin{pmatrix} \alpha \\ \beta \\ \gamma \\ \delta \end{pmatrix}$  and a two-qubit quantum gate

is represented by a  $2^2 \times 2^2 = 4 \times 4$  matrix. Now, when a two-qubit quantum gate acts on a two-qubit state it maps the input state into another two-qubit output state in a well-defined manner which characterizes that particular gate.

**1 Controlled-NOT gate-** Controlled NOT gate, i.e., CNOT gate, which is represented by in a matrix form as,

$$\text{CNOT} = \begin{pmatrix} 1 & 0 & 0 & 0 \\ 0 & 1 & 0 & 0 \\ 0 & 0 & 0 & 1 \\ 0 & 0 & 1 & 0 \end{pmatrix},$$

and the bra-ket notation of CNOT gate is

$$\text{CNOT} = |00\rangle\langle 00| + |01\rangle\langle 01| + |11\rangle\langle 10| + |10\rangle\langle 11|.$$

This gate is a two-qubit gate, in which first qubit is control and second qubit is target as shown

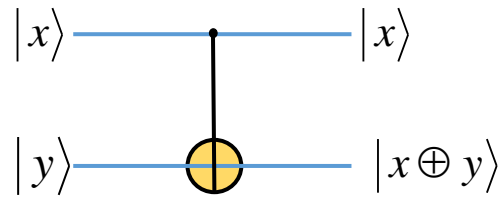


**Figure 1.3:** Circuit representation of a CNOT gate.

in Figure 1.3. According to the figure, if the first qubit as control qubit is  $|0\rangle$  then target will not be flip if control qubit is  $|1\rangle$  then target will be flip. So, the CNOT mapping is

$$\begin{aligned} |00\rangle &\rightarrow |00\rangle \\ |01\rangle &\rightarrow |01\rangle \\ |10\rangle &\rightarrow |11\rangle \\ |11\rangle &\rightarrow |10\rangle \end{aligned} .$$

**2 SWAP gate:** Another two-qubit gate is SWAP gate. The matrix of SWAP gate is

$$\text{SWAP} = \begin{pmatrix} 1 & 0 & 0 & 0 \\ 0 & 0 & 1 & 0 \\ 0 & 1 & 0 & 0 \\ 0 & 0 & 0 & 1 \end{pmatrix},$$

and the same can be expressed in bra-ket notation as

$$\text{SWAP} = |00\rangle\langle 00| + |10\rangle\langle 01| + |01\rangle\langle 10| + |11\rangle\langle 11|.$$

A SWAP gate maps a two-qubit state  $|ab\rangle$  to  $|ba\rangle$ . Specifically, it maps

$$\begin{aligned} |00\rangle &\rightarrow |00\rangle \\ |01\rangle &\rightarrow |10\rangle \\ |10\rangle &\rightarrow |01\rangle \\ |11\rangle &\rightarrow |11\rangle \end{aligned} .$$

A SWAP gate can be constructed by using three CNOT gates as shown in Figure 1.4.

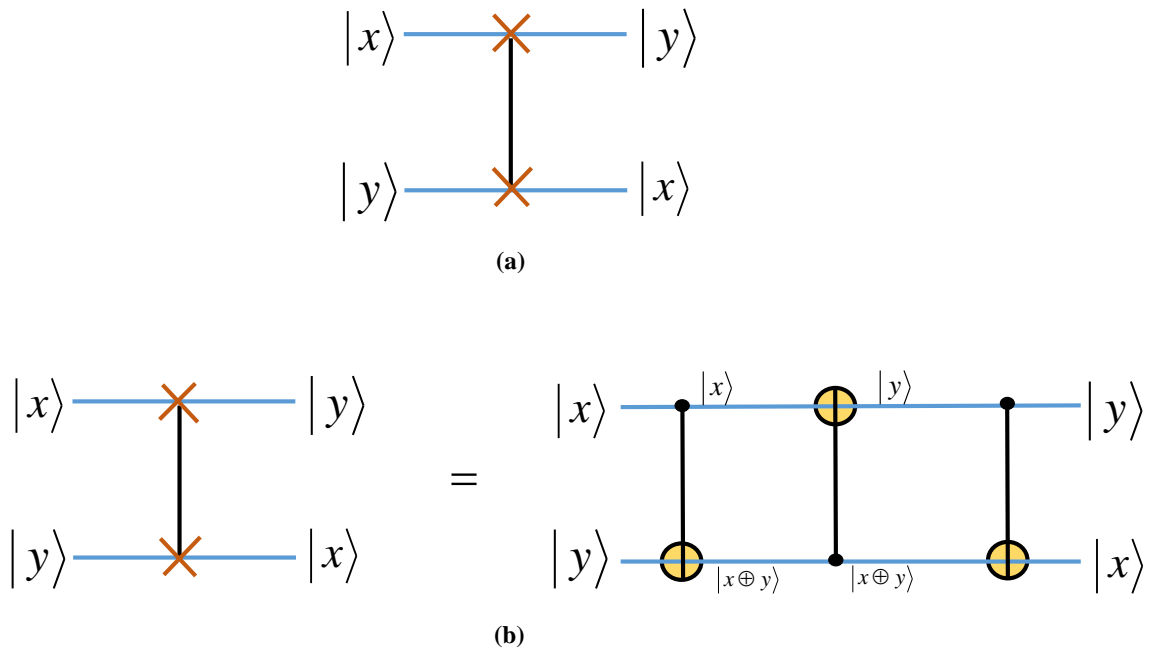


**Figure 1.4:** (a) Symbolic representation of a SWAP gate (b) how to realize a SWAP gate using three CNOT gates.

### 1.7.3 Other quantum gates

Here, we would like to briefly mention about a few other quantum gates which are often used. One such single qubit gate is a square-root of NOT gate ( $\sqrt{\text{NOT}}$ ) which can be represented by the following matrix  $\frac{1}{2} \begin{pmatrix} 1+i & 1-i \\ 1-i & 1+i \end{pmatrix}$ . It's action and the origin of the name can be visualized easily if we note that  $\sqrt{\text{NOT}}\sqrt{\text{NOT}}|0\rangle = |1\rangle$  and  $\sqrt{\text{NOT}}\sqrt{\text{NOT}}|1\rangle = |0\rangle$ . A controlled version of this gate is also often used as a two-qubit gate. In fact, in the domain of classical reversible circuits, this gate plays a crucial role. Finally, there are 2 three-qubit gates which (or their decomposition into single-qubit and two-qubit gates) are often used. These gates are referred to as Toffoli and Fredkin gates and they may be viewed as CCNOT and CSWAP gates, respectively. In the Toffoli gate (first two qubits are control and the third qubit is target), if first two qubits are found to be in state  $|1\rangle$  then only the target (third qubit) flips, nothing happens otherwise. Similarly, in a Fredkin gate, if first qubit is found to be at state  $|1\rangle$  then a SWAP operation is performed between second and third qubits, and nothing happens otherwise.

### 1.7.4 EPR circuit

EPR circuit is the combination of single-qubit and two-qubit quantum gate, i.e., Hadamard gate followed by CNOT gate, which generate the maximally entangled state (see the circuit

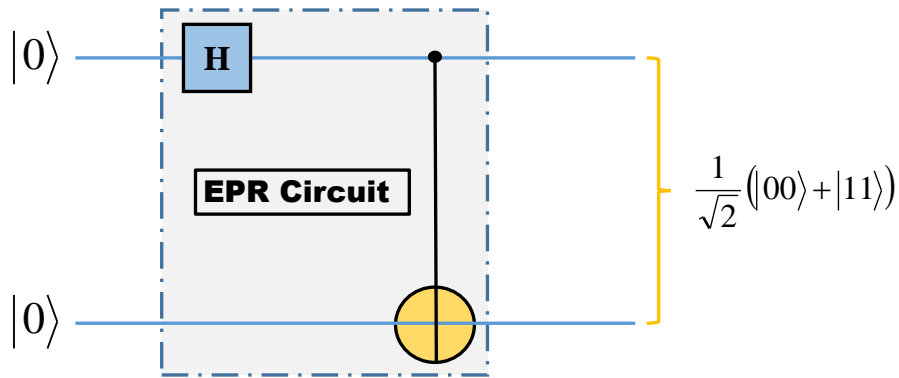


**Figure 1.5:** Diagram for a quantum circuit. This particular circuit is known as EPR circuit. It transforms a separable input states to a Bell state as shown. Different inputs (e.g.,  $|01\rangle, |10\rangle, |11\rangle$ ) will generate different Bell states.

shown in Figure 1.5). The mathematical operation of this circuit is  $\text{CNOT}(\text{H} \otimes \text{I})|00\rangle$ . We start with two separable states  $|00\rangle$ . Now, first of all H applied on the first qubit and  $I$  on second qubit then the state maps into  $\frac{1}{\sqrt{2}}(|00\rangle + |10\rangle)$ . Subsequently, two-qubit gate CNOT operates on it, where the first qubit works as control qubit and the second qubit works as target qubit. According to the CNOT gate, second qubit will be flip when first qubit is  $|1\rangle$ . Now, the state is,  $\text{CNOT}\left(\frac{1}{\sqrt{2}}(|00\rangle + |10\rangle)\right) = \frac{1}{\sqrt{2}}(|00\rangle + |11\rangle)$ , which is a maximally entangled state.

### 1.7.5 Useful optical components and how to realize quantum gates optically?

In Chapter 6, we wish to present some optical setups, which can be used to realize various schemes for secure quantum communication. As a background to that here we plan to discuss how to realize a qubit optically and how to use basic optical elements as quantum gates. In Figure 1.6 (a), we use an attenuated laser (approximate single photon source) to generated the single photons which incident on the symmetric beam splitter. As we know the basic concept of symmetric (50:50) BS that transmits half of the incident light and reflects rest half. Thus, when a single photon is incident on a (50:50) BS then with half probability the photon would be found on the transmitted path say  $|0\rangle$  and with half probability it would be found on the reflected path say  $|1\rangle$ . This happens after measurement. Prior to that the photon simultaneously exists in both paths as shown in Figure 1.6 (a). Then a single photon emerges in a superposition state of the photon  $\alpha|0\rangle + \beta|1\rangle$ , for a (50:50) BS we obtain  $|\alpha|^2 = |\beta|^2 = \frac{1}{2}$ , where  $|\alpha|^2$  and  $|\beta|^2$  are the probabilities of getting the photon on transmitted and reflected path.

In the above, a photonic qubit is introduced using their position (path). A photonic qubit can

also be defined using other degrees of freedom of the photon (say orbital angular momentum or polarization state). In this thesis, we will primarily deal with the polarization based photonic qubits, where a single photon having arbitrary linear polarization can be viewed to be in the state  $|\psi\rangle = \alpha|H\rangle + \beta|V\rangle$ . If this photon is made to incident on a PBS (see Figure 1.6 (b)), it will reflect with the probability  $|\beta|^2$ , and transmit with the probability  $|\alpha|^2$ . Thus, in other words, if this qubit is measured in  $\{|H\rangle, |V\rangle\}$  by applying two single photon detectors at the two output ports of the PBS, then the qubit will be found in the state  $|H\rangle$  with probability  $|\alpha|^2$  and in the state  $|V\rangle$  with probability  $|\beta|^2$ .

Similarly, quantum gates can be realized by using optical elements. There are two types of optical elements linear and non-linear. Beam splitter (BS), half wave plate (HWP), etc., are linear optical elements and down converters are non-linear optical elements. Each optical element is represented by a square matrix, i.e., Jones matrix. The Jones matrix of HWP with fast axis at an angle  $\theta$  with respect to horizontal is  $\begin{pmatrix} \cos 2\theta & \sin 2\theta \\ \sin 2\theta & -\cos 2\theta \end{pmatrix}$ , if  $2\theta = 90^\circ$  then the matrix of HWP will be  $\begin{pmatrix} 0 & 1 \\ 1 & 0 \end{pmatrix}$  and it would convert the horizontally polarized photon ( $|H\rangle$ ) into vertically polarized photon ( $|V\rangle$ ) and vice versa. Consequently, a  $\text{HWP}_{(2\theta=90^\circ)}$  would work as a quantum NOT gate for the qubits based on polarization states of a single photon. If  $2\theta = 45^\circ$ , then the matrix of HWP would become  $\frac{1}{\sqrt{2}} \begin{pmatrix} 1 & 1 \\ 1 & -1 \end{pmatrix}$  and it would transform the basis states as  $\text{HWP}_{(2\theta=45^\circ)}|H\rangle = \frac{1}{\sqrt{2}}(|H\rangle + |V\rangle)$  and  $\text{HWP}_{(2\theta=45^\circ)}|V\rangle = \frac{1}{\sqrt{2}}(|H\rangle - |V\rangle)$ . Thus, in this case HWP would work as a Hadamard gate. Another optical element of particular use is polarizing BS (PBS) which always transmits the horizontally polarized light and reflects the vertically polarized light as shown in Figure 1.6 (b). In Chapter 6, we will show that these optical components play a crucial role in the experimental realization of the schemes of secure quantum communication.

Further, we know that entangled states play a very important role in quantum communication schemes. To optically generate entangled states we need an interaction between photons which is possible only by using nonlinear optical components. In this thesis, we have proposed to use a nonlinear optical process called spontaneous parametric down conversion (SPDC) to generate the entangled photons. SPDC process is a second order nonlinear optical process in which a high frequency photon (pump) gets converted into two correlated photons (signal and idler)<sup>5</sup> of lower frequencies simultaneously in accordance with the laws of conservation of momentum and energy<sup>6</sup> after passing through the nonlinear crystal, like barium borate as shown in Figure 1.6 (c). Now, if we put a detector on the signal photon's path and get it to click, that means photon will exist on the idler's path. Thus, the detection of one photon heralds the

---

<sup>5</sup>The photons are correlated in momentum, frequency and polarization.

<sup>6</sup>The combined energy and momentum of the generated photons is equal to the energy and momentum of the incident photon.

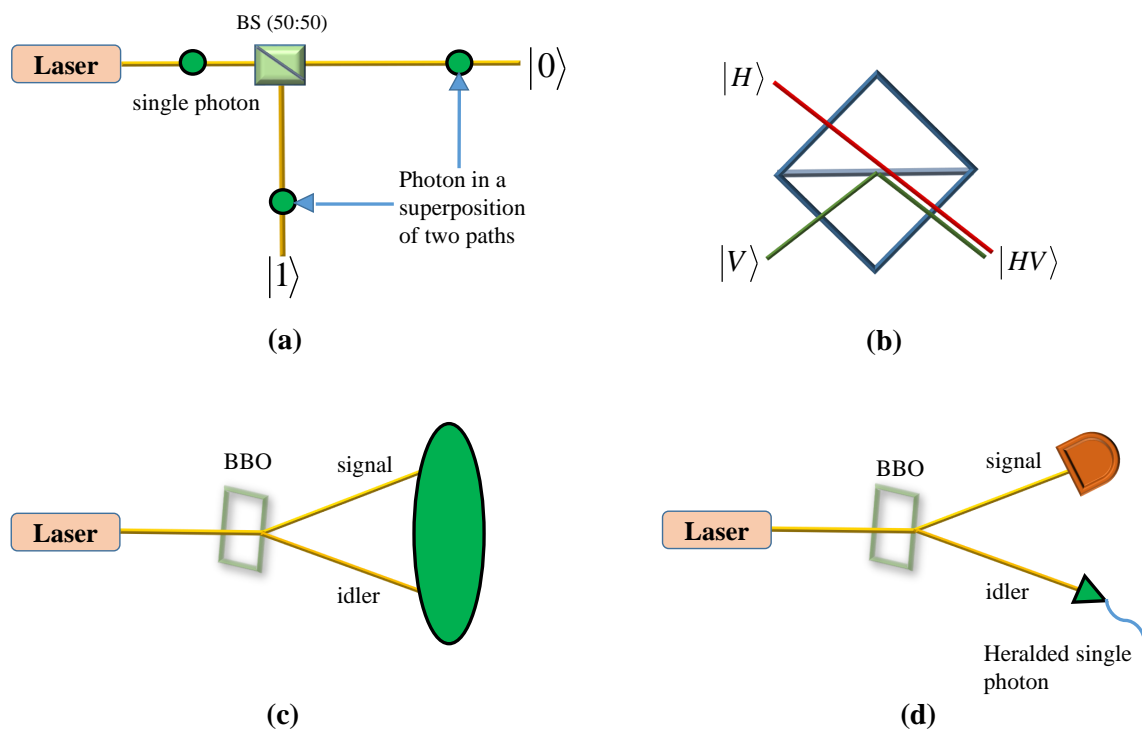


**Figure 1.6:** Schematic diagrams of optical elements. (a) optically realization of qubit. (b) PBS, which transmits horizontally polarized photon and reflects vertically polarized photon. (c) entanglement generation through the SPDC process (d) A heralded single photon from the SPDC process.

production of the other. This is how through the SPDC process and heralding a single photon source can be created for the use in designing experimentally feasible schemes of quantum cryptography. Such schemes will be discussed in Chapter 6.

## 1.8 SQUID-based quantum computer

Quantum information processing can be done using various experimental platforms, such as experimental architecture based on NMR, ion-trap, silicon, Nitrogen-vacancy center. These experimental facilities are not easily available to all the researchers. Only a few researchers had adequate access to such quantum computing facilities. Surprisingly, in 2016, the scenario has been changed considerably after the introduction of a set of SQUID-based quantum computers by IBM as these computers were placed on cloud and free access to these computers were given to every researcher and students. This experimental platform has attracted the attention of the entire quantum information community because everyone can access it freely and easily through IBM Quantum Experience. More specifically, IBM has designed several, five-qubit, sixteen-qubit and twenty-qubit quantum computers. Interestingly, several quantum communi-



cation tasks [58, 219–234] have already been verified and tested by using these SQUID-based quantum computers<sup>7</sup>. The first IBM quantum computer was made-up of five superconducting transmon qubits. There are two processors of five-qubit quantum computer (i.e., IBM QX2 see Figure 1.7 and IBMQX4 see Figure 1.9), one quantum computer (IBM QX5) of sixteen-qubit see Figure 1.10 and one processor (QS1\_1) of twenty-qubit IBM computer. In all the IBM processors, gates from the Clifford+T gate library can be implemented directly. Single-qubit gates can be applied anywhere on the qubit lines. However, application of two-qubit gate (CNOT) is given by the architecture as shown in Figures 1.7, 1.9 and 1.10. In this thesis work, we have extensively used IBM QX2 processor (old version) of five-qubit SQUID-based quantum computer to realize quantum communication schemes experimentally.

Keeping the above in mind in this section, we will discuss the technical aspects of the old version of the IBM QX2 processor of five-qubit IBM quantum computer with focus on the architecture of the computer, nature of the qubits realized in it and their manipulation, and readout. In the subsections, we will briefly discuss IBM QX4 and IBM QX5, too.

### 1.8.1 IBM QX2

IBM QX2 is one of the processors of five-qubit quantum computer placed in cloud by IBM. This processor has two versions. In Figures 1.7 (a) and (b) the topology and schematic diagram of the processor is shown for the old version and new version of IBM QX2, respectively. These two versions are different in the sense that their topology is different which implies that the CNOT gates that can be implemented directly in a particular version is different from the other version.

Specifically, the allowed CNOT operations for the old version are  $q[0] \rightarrow q[1]$ ,  $q[0] \rightarrow q[2]$ ,  $q[4] \rightarrow q[2]$ ,  $q[3] \rightarrow q[2]$ ,  $q[3] \rightarrow q[4]$ ,  $q[1] \rightarrow q[2]$  and for new version are  $q[0] \rightarrow q[1]$ ,  $q[0] \rightarrow q[2]$ ,  $q[4] \rightarrow q[2]$ ,  $q[4] \rightarrow q[3]$ ,  $q[3] \rightarrow q[2]$ ,  $q[1] \rightarrow q[2]$ . Here  $q[i] \rightarrow q[j]$  means  $q[i]$  is the control bit and  $q[j]$  is the target bit.

In general, there are several types of superconducting qubits that can be used for realizing quantum information tasks. In the IBM quantum processors, the qubits used are transmon qubits, which are charged qubits designed to reduce the charge noise [237]. The arrangement of five superconducting qubits ( $q[0]$ ,  $q[1]$ ,  $q[2]$ ,  $q[3]$ ,  $q[4]$ ) and their control mechanism as provided in IBM quantum experience website [235] including chip layout, is shown in Figure 1.8. Each qubit can be controlled and read out by a dedicated coplanar waveguide resonator, shown in the figure by black transmission lines. Also, the qubit-qubit coupling realized by coplanar microwave resonator and is shown by white transmission lines. These coplanar wave guides have also been used for read out purpose. It is evident from the qubit topology, as given in [235] that qubits  $q[0]$ ,  $q[1]$  and  $q[2]$  are interconnected, but only qubit  $q[2]$  is connected to qubits

---

<sup>7</sup>Interested readers may find a detailed user guide on how to use this superconducting-based quantum computer at [235], and a lucid explanation of the working principle of a IBM quantum computer in Ref. [236]

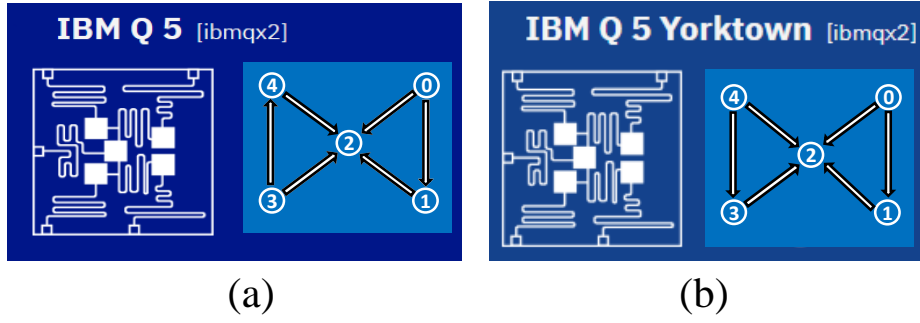


**Figure 1.7:** Figures (a) and (b) are the old and new versions of IBM QX2 processor.

q[3] and q[4], in addition qubits q[3] and q[4] are also interconnected. Such a topological set-up limits the applicability of two-qubit gates between the possible pairs. Details about experimental parameters, obtained from the IBM quantum experience website [238] are given in Table 1.2. Two relaxation time scales namely, longitudinal relaxation time ( $T_1$ ) and transverse relaxation time ( $T_2$ ) for qubits (q[0], q[1], q[2], q[3], q[4]) are given in another Table 1.3 as well as the coupling strengths between pair of connected qubits are provided through the crosstalk matrix (see Table 1.3).

### 1.8.2 IBM QX4

IBM QX4 is another type of five-qubit IBM quantum computer. This processor also has two versions. In Figures 1.9 (a) and (b) the topology of the new and old versions of IBM QX4 processor are shown respectively. Similar to IBM QX2, in IBM QX4, the directly implementable CNOT operations among the five-qubits in old and new version of IBM QX4 are different. Allowed CNOT operations between in five-qubits for old version are  $q[2] \rightarrow q[0]$ ,  $q[2] \rightarrow q[1]$ ,  $q[2] \rightarrow q[4]$ ,  $q[3] \rightarrow q[2]$ ,  $q[3] \rightarrow q[4]$ ,  $q[1] \rightarrow q[0]$  and those for new version are  $q[2] \rightarrow q[0]$ ,  $q[2] \rightarrow q[1]$ ,  $q[4] \rightarrow q[2]$ ,  $q[3] \rightarrow q[2]$ ,  $q[3] \rightarrow q[4]$ ,  $q[2] \rightarrow q[1]$ .

### 1.8.3 Sixteen-qubit IBM quantum computer

Figure 1.10 shows the chip layout and qubit topology of the sixteen-qubit quantum processor IBM QX5. Allowed CNOT operations among the sixteen qubits are  $q[0] \rightarrow q[1]$ ,  $q[0] \rightarrow q[2]$ ,  $q[2] \rightarrow q[3]$ ,  $q[3] \rightarrow q[14]$ ,  $q[3] \rightarrow q[4]$ ,  $q[5] \rightarrow q[4]$ ,  $q[6] \rightarrow q[11]$ ,  $q[6] \rightarrow q[7]$ ,  $q[6] \rightarrow q[5]$ ,  $q[8] \rightarrow q[7]$ ,  $q[7] \rightarrow q[10]$ ,  $q[9] \rightarrow q[8]$ ,  $q[9] \rightarrow q[10]$ ,  $q[11] \rightarrow q[10]$ ,  $q[12] \rightarrow q[13]$ ,  $q[12] \rightarrow q[11]$ ,  $q[12] \rightarrow q[5]$ ,  $q[13] \rightarrow q[14]$ ,  $q[13] \rightarrow q[4]$ ,  $q[15] \rightarrow q[14]$ ,  $q[15] \rightarrow q[2]$ ,  $q[15] \rightarrow q[0]$ . IBM has also introduced a twenty-qubit quantum processor [239] and has proposed to launch a fifty-qubit quantum processor. However, we restrict ourselves from describing those processors as those are not used in this thesis.

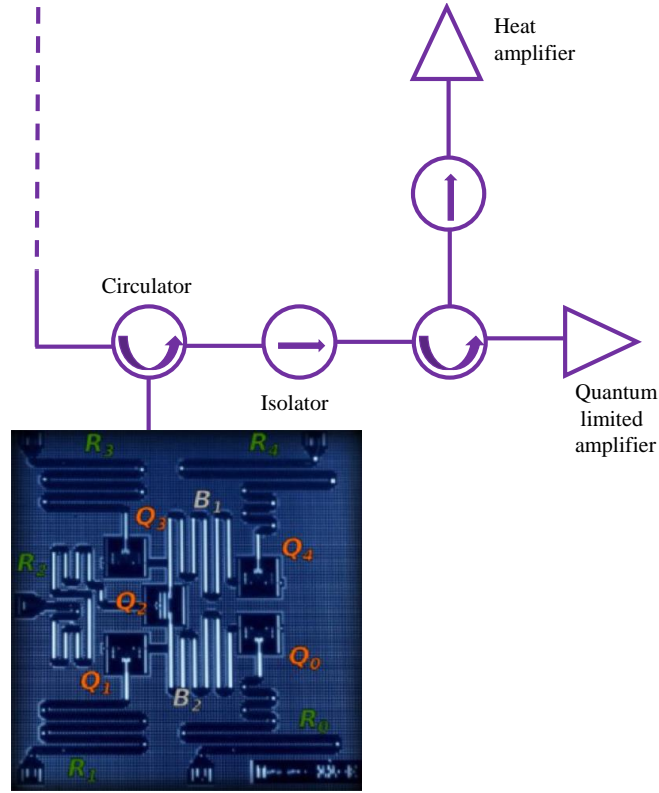


**Figure 1.8:** The architecture used in IBM five-qubit quantum computer. The upper trace in the figure helps in control and read out. The left arm is used for input, and the right arm is used for output. The lower trace is the chip layout, in which five-qubits are positioned. A dedicated coplanar waveguide resonator is used to control and read-out the individual qubits, transmission lines for the purpose are shown in dark color. The coupling between two qubits can be realized via coupled microwave resonator shown by white lines.

**Table 1.2:** Details about experimental parameters used in IBM quantum computer architecture which are available on the website. The first column is qubit index  $q$  in IBM quantum computer. The second column shows resonance frequencies  $\omega^R$  of corresponding read-out resonators. The qubit frequencies  $\omega$  are given in the third column. Anharmonicity  $\delta$ , a measure of information leakage out of the computational space, is the difference between two subsequent transition frequencies. Also,  $\chi$  and  $\kappa$  given in the fifth and sixth columns are qubit-cavity coupling strengths and coupling of the cavity to the environment for corresponding qubits.

Qubit number $q$	$\omega^R/2\pi(\text{GHz})$	$\omega/2\pi(\text{GHz})$	$\delta/2\pi(\text{MHz})$	$\chi/2\pi(\text{kHz})$	$\kappa/2\pi(\text{kHz})$
q[0]	6.530350	5.2723	-330.3	476	523
q[1]	6.481848	5.2145	-331.9	395	489
q[2]	6.436229	5.0289	-331.2	428	415
q[3]	6.579431	5.2971	-329.4	412	515
q[4]	6.530225	5.0561	-335.5	339	515

**Table 1.3:** Details about experimental parameters used in IBM quantum computer architecture which are available on the website. The first row and the first column shows qubit index  $q[i]$ . Entries of the matrix are the couplings between corresponding qubits. Last two columns depict values of longitudinal relaxation time ( $T_1$ ) and transverse relaxation time ( $T_2$ ), used in IBM quantum computer. Rest of the entries in this table have the same meaning as was described in the the previous table.

$\zeta_{ij}$ (kHz)	q[0]	q[1]	q[2]	q[3]	q[4]	$T_1$ ( $\mu s$ )	$T_2$ ( $\mu s$ )
q[0]		-43	-83			53.04 (0.64)	48.50 (2.63)
q[1]	-45		-25			63.94 (1.06)	35.07 (0.59)
q[2]	-83	-27		-127	-38	52.08 (0.58)	89.73 (1.82)
q[3]			-127		-97	51.78 (0.55)	60.93 (1.09)
q[4]			-34	-97		55.80 (0.95)	84.18 (2.41)

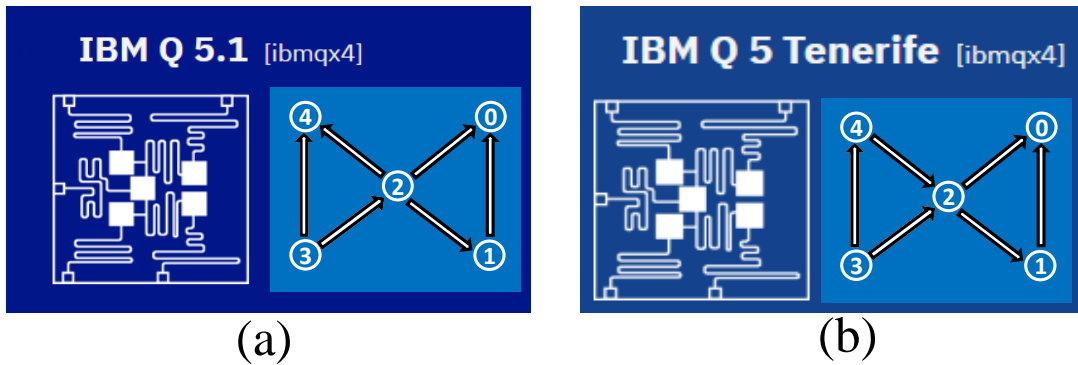


**Figure 1.9:** Figures (a) and (b) are depicting chip layout and the topology of the old and new versions of IBM QX4 processor.

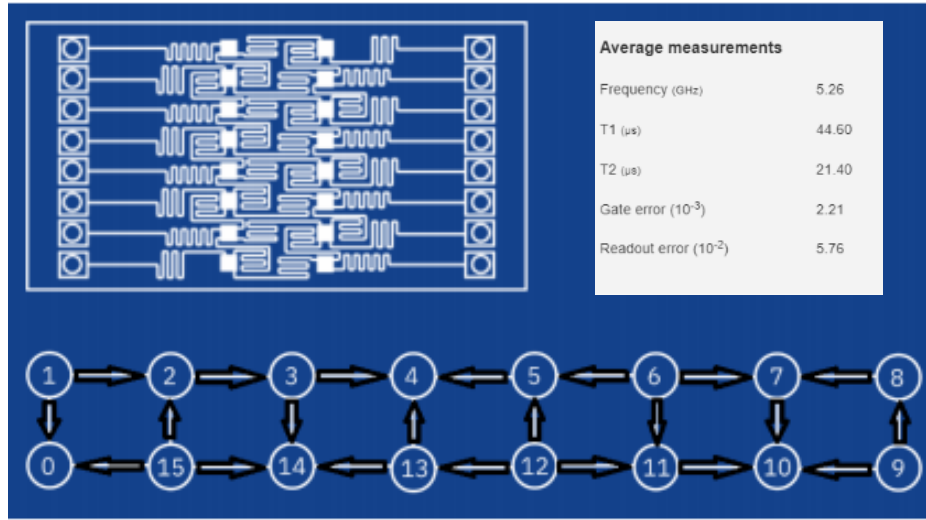


**Figure 1.10:** Chip layout and qubit topology of IBM QX5 quantum processor.

## 1.9 Basic idea of quantum state tomography (QST)

Quantum state tomography is the process of reconstructing the density matrix of a state. In the context of this thesis, to obtain the full picture, we need to reconstruct the density matrix of the teleported state using QST [216]. Till date, a large number of advanced protocols have been proposed for quantum state tomography [219, 223, 240–243]. An advanced protocol suppresses the requirement of repeated preparation of the state to be tomographed and hence allows state characterization in dynamical environment using only one experiment [244]. Quantum state tomography requires extraction of information from the experiments and the subsequent use of that information in the reconstruction process of the experimental density matrix. An experimental density matrix in the Pauli basis can be expressed as  $\rho^E = \frac{1}{2^N} \sum_{i=1}^{2^N} c_{i\dots N} \sigma_i \otimes \dots \otimes \sigma_N$ , where  $c_{i\dots N}$  can be obtained as  $\langle \sigma_i \otimes \dots \otimes \sigma_N \rangle$  with  $\sigma_{i\dots N} \in \{I, X, Y, Z\}$ . For single-qubit case the density matrix is,  $\rho = \frac{1}{2} \begin{pmatrix} 1 + \langle \sigma_Z \rangle & \langle \sigma_X \rangle - i \langle \sigma_Y \rangle \\ \langle \sigma_X \rangle + i \langle \sigma_Y \rangle & 1 - \langle \sigma_Z \rangle \end{pmatrix}$ . Availability of the expectation value  $\langle \sigma_i \rangle$  in an experiment depends on whether  $\sigma_i$  is a direct observable or an indirect observable. In the IBM architecture,  $Z$  is a direct observable hence from the experimental outcomes, i.e., available probabilities of  $|0\rangle$  and  $|1\rangle$ , the value of  $\langle Z \rangle$  can be directly calculated (without the use of any tomographic gate), while  $X$  and  $Y$  being indirect observables, calculation of  $\langle X \rangle$  and  $\langle Y \rangle$  would require the application of  $H$  and  $HS^\dagger$  gates, respectively [223]. In the present thesis, we have discussed QST in relatively more detail in Chapter 2 and 5 for two and three qubit states.

## 1.10 A brief summary of this chapter and the structure of the rest of the thesis

This thesis is focused on quantum communication protocols and in this chapter we have provided an introduction to the field of quantum communication, with an appropriate stress on its applicability in our daily life. In the beginning of this chapter, we have described the history of quantum communication and the basic concepts related to this field with a specific attention on quantum teleportation and quantum cryptography. Some quantum communication schemes which are rigorously studied in the subsequent chapters of this thesis are also discussed. A short introduction to quantum noise, QST, quantum process tomography, quantum gates and realization of quantum gates with some optical elements have also been provided in this chapter. Further, the power and limitations of the SQUID-based IBM quantum computer are discussed in this chapter.

The structure of the rest of the thesis can be summarized as follows. Chapters 2-4 are dedicated to the quantum teleportation schemes using different type of quantum resources (entangled orthogonal state and entangled nonorthogonal state) and their experimental realization using superconductivity-based IBM quantum computer. In Chapter 2, an explicit scheme (quantum circuit) is designed for the teleportation of an  $n$ -qubit quantum state. It is established that the proposed scheme requires an optimal amount of quantum resources, whereas larger amount of quantum resources have been used in a large number of recently reported teleportation schemes for the quantum states which can be viewed as special cases of the general  $n$ -qubit state considered here. A trade-off between our knowledge about the quantum state to be teleported and the amount of quantum resources required for the same is observed. A proof-of-principle experimental realization of the proposed scheme (for a two-qubit state) is also performed using five-qubit SQUID-based IBM quantum computer. The experimental results show that the state has been teleported with high fidelity. Relevance of the proposed teleportation scheme has also been discussed in the context of controlled, bidirectional, and bidirectional controlled state teleportation.

In Chapter 3 of this thesis, we explicitly show that a teleportation protocol reported by Zhao et al., [132] for the teleportation of an eight-qubit state utilizing a six-qubit state can actually be implemented by using the scheme proposed in the previous chapter. Thus, the use of six-qubit state as the teleportation channel can be circumvented. Specifically, in this chapter, we have established that there is a conceptual mistake in the work of Zhao et al., [132] and the teleportation task that they have performed can be realized using any two Bell states (i.e., without using the multi-partite entangled state used by them). Further, it is mentioned that the applicability of the observations of this Chapter is not limited to the work of Zhao et al., rather it's applicable to a large set of recent proposals for the teleportation of multi-qubit states.

Chapter 4 aims to investigate the effect of nonorthogonality of an entangled nonorthogonal

state-based quantum channel in detail in the context of the teleportation of a qubit. Specifically, average fidelity, minimum fidelity and minimum assured fidelity (MASFI) are computed for teleportation of a single-qubit state using all the Bell-type entangled nonorthogonal states known as quasi-Bell states. Using Horodecki criterion, it is shown that the teleportation scheme obtained by replacing the quantum channel (Bell state) of the usual teleportation scheme by a quasi-Bell state is optimal. Further, the performance of various quasi-Bell states as teleportation channel is compared in an ideal situation (i.e., in the absence of noise) and under different noise models (e.g., AD and PD). It is observed that the best choice of the quasi-Bell state depends on the amount of nonorthogonality, both in noisy and noiseless cases. A specific quasi-Bell state, which was found to be maximally entangled in the ideal conditions, is shown to be less efficient as a teleportation channel compared to other quasi-Bell states in particular cases when subjected to noisy channels. It has also been observed that usually the value of average fidelity falls with an increase in the number of qubits exposed to noisy channels (viz., Alice's, Bob's and to be teleported qubits), but the converse may be observed in some particular cases. Chapter 2-4 are primarily focused on a particular aspect of quantum communication, teleportation.

So, in Chapter 5, we moved our attention to a scheme for distributed quantum measurement which plays an important role in deciding which strategies/steps are to be avoided in designing schemes for quantum cryptography. The scheme for distributed quantum measurement studied here allows nondestructive or indirect Bell measurement which was proposed by Gupta et al., [245]. The scheme is experimentally realized here using the five-qubit IBM SQUID-based quantum computer. The experiment confirmed that the Bell state can be constructed and measured in a nondestructive manner with a reasonably high fidelity. A comparison of the outcomes of this study and the results obtained earlier in an NMR-based experiment (Samal et al., (2010) [246]) has also been performed. The study indicates that to make a scalable SQUID-based quantum computer, errors introduced by the gates (in the present technology used by IBM) have to be reduced considerably.

In Chapter 6, we have presented optical designs for the realization of a set of quantum cryptography schemes. There are several theoretical schemes for QKD and other quantum cryptographic tasks (e.g., schemes for secure direct quantum communication and their controlled version). However, only a few of them have yet been performed experimentally. Other schemes which have not yet been performed experimentally include, schemes for QD [2], CQD [96], Kak's three stage scheme [247–249]. This chapter aims to report optical circuits for the realization of these quantum cryptographic schemes using available optical elements, like laser, BS, PBS, HWP, and experimentally realizable quantum states like single photon states (which represents a single-qubit), two-qubit and multi qubit entangled states of light (such as GHZ-like state, W state). Finally, the thesis work is concluded in Chapter 7 with a brief discussion on the limitations of the present work and the scope for future work.

# CHAPTER 2

## DESIGN AND EXPERIMENTAL REALIZATION OF AN OPTIMAL SCHEME FOR TELEPORTATION OF AN $n$ -QUBIT QUANTUM STATE

### 2.1 Introduction

In the previous chapter, we have already introduced the concept of QT. Here, we may note that perfect QT of an arbitrary quantum state using a classical channel would require an infinite amount of classical resources. However, it is possible to teleport an arbitrary quantum state with unit fidelity using a quantum channel (a pre-shared entangled state) and a few bits of classical communication. As perfect teleportation does not have a classical analogue, schemes for quantum teleportation (QT) and their variants discussed in the previous chapter drew considerable attention of the quantum communication community. In addition to the teleportation-based schemes mentioned in Section 1.4, there exist proposals to employ teleportation in quantum repeaters to enhance the feasibility of quantum communication, and in ensuring security against an eavesdropper's attempt to encroach the private spaces of legitimate users devising trojan-horse attack [55]. This wide applicability of QT and its variants and the fact that quantum resources are costly (for example, preparation and maintenance of an  $n$ -qubit entangled state is extremely difficult for large  $n$ ) have motivated us to investigate whether the recently proposed schemes [16, 23, 38, 50–52, 63, 64, 67, 90, 93, 98, 104, 123] are using an optimal amount of quantum resources. If not, how to reduce the amount of quantum resources to be used? An effort to answer these questions has led to the present work, where we aim to propose a scheme for teleportation of an  $n$ -qubit quantum state using an optimal amount of quantum resources and to experimentally realize a particular case of the proposed scheme using five-qubit IBM quantum computer. Before we proceed to describe the findings of the present work, we would like to elaborate a bit on what makes it fascinating to work on teleportation even after almost



quarter century of its introduction.

As a natural generalization of QT schemes, protocols for teleportation of multi-qubit states have also been proposed. In 2006, Chen et al., proposed a multi-qubit generalization of the standard QT scheme [18], which enabled teleportation of multi-qubit states using a genuine multi-partite entangled channel having a general form. Chen et al.'s work also indicated that the bipartite nature of the channel is sufficient for teleportation of multi-qubit quantum states. Specifically, it was shown that QT of an arbitrary  $n$ -qubit state can be achieved by performing  $n$  rounds of Bennett et al.'s protocol [6] for QT (one for each qubit). Later, this scheme was extended to CT of an arbitrary  $n$ -qubit quantum state [59]. Along the same line, a bidirectional state teleportation and a bidirectional controlled state teleportation schemes may be designed for teleporting two arbitrary multi-qubit states, one each by Alice and Bob. Specifically, a quantum state suitable as a quantum channel for a CT (bidirectional controlled state teleportation) scheme should essentially reduce to a useful quantum channel for QT (bidirectional state teleportation) after the controller's measurement (see [95] for detail discussion). In the previous Chapter, we have already mentioned that the original QT protocol of Bennett et al., was experimentally realized by Bouwmeester et al., [137] in 1997 and later on, a number of experimental realizations of single-qubit QT has been reported [33, 68, 75, 130, 137, 138]. However, hardly any proposal for teleportation of multi-qubit quantum states have been tested experimentally because the experimental realization of those schemes would require quantum resources that are costly. This observation has further motivated us to design a general teleportation scheme that would require lesser amount of quantum resource and/or such resources that can be generated and maintained easily using available technology.

It may be noted that an optimized scheme for multi-partite QT must involve optimization of both procedure and resources. Optimization of the procedure demands use of those states as quantum channel, which can be prepared easily and are least affected by decoherence; while the optimization of resources demands that the scheme should exploit/utilize all the channel qubits that are available for performing QT. The results of Ref. [18] can be viewed as an optimization of the procedure (as Bell states can be easily prepared and are less prone to decoherence in comparison with the multi-partite entangled states). The importance of such strategies becomes evident when we try to realize QT in a quantum network designed for quantum internet [92]. Naturally, an optimized QT scheme is expected to improve the performance of such a quantum internet. Another kind of optimization has been attempted in some recent works. Specifically, efforts have been made to form teleportation channel (having lesser number of entangled qubits) suitable for the teleportation of specific types of unknown quantum states [16, 23, 38, 50–52, 63, 64, 67, 90, 93, 98, 104, 123]. For example, in [51], the three-qubit and the four-qubit unknown quantum states have been teleported using four and five-qubit cluster states, respectively. An extended list of these complex states and the corresponding channels are given in Table 2.2. In fact, some of this set of schemes has exploited the fact that some of

the probability amplitudes in the state to be teleported are zero and a QT scheme essentially transfers the unknown probability amplitudes to distant qubits. Teleportation of such states has its own significance, a trivial example that can justify its significance is the teleportation of entangled quantum states (say, a non-maximally entangled Bell-type state). We noticed that the quantum resources used in these protocols are not optimal and most of the cases involve redundant qubits. Keeping these in mind, here, we set the task for us to minimize the number of these qubits exploiting the available information regarding the mathematical structure of the quantum state to be teleported. Specifically, in what follows, we would propose an efficient and optimal (uses minimum number of Bell states as quantum channel) scheme to teleport a multi-qubit state of specific form. In what follows, it will be established that the bottleneck of our optimal scheme is the application of a unitary operation which transforms the state to be teleported from the entangled basis to the computational basis. Such a transformation allows us to render the information encoded into a smaller number of qubits. On the other hand, it increases quantum computational resources required at each node (because of the application of an extra unitary). However, it is desirable to minimize the number of qubits to be transmitted at the cost of computational resources as transmitting a rather large quantum state is much harder than computation. This is so because the former requires more resources at each step, i.e., in initialization, transmission, and measurement steps and is also prone to environmental effects. Further, it would be established that the proposed scheme is simple in nature and can be extended to corresponding CT and bidirectional controlled state teleportation schemes.

Actual relevance of an optimized scheme lies in the experimental realization of the scheme only. An interesting window for experimental realization of the schemes of quantum computation and communication in general and optimized schemes in particular has been opened up recently, when IBM provided free access to a five-qubit superconducting quantum computer by placing it in cloud [221, 235]. This has provided a platform for experimental testing of various proposals for quantum communication and computation. In the present work, we have used IBM quantum computer to experimentally realize the optimal scheme designed here. Specifically, we have successfully implemented the optimal quantum circuit designed for teleportation of a two-qubit state. The experiment performed is a proof-of-principle experiment as the receiver and the sender are not located at two distant places, but it shows successful teleportation with very high fidelity and paves the way for future realizations of the proposed scheme using optical elements.

The rest of the chapter is organized as follows. In Section 2.2, we propose a scheme for the teleportation of a multi-qubit quantum state having  $m$  unknown coefficients using optimal quantum resources. We also discuss a specific case of this scheme which corresponds to QT of a two-unknown multi-qubit quantum state using a Bell state as quantum channel. In Section 2.3, we describe optimal schemes for controlled unidirectional and bidirectional state teleportation of the quantum states. Further, in Section 2.4, an experimental realization of the proposed

scheme is reported using the five-qubit IBM quantum computer available on cloud. Finally, we conclude the chapter in Section 2.5.

## 2.2 Teleportation of an $n$ -qubit state with $m$ unknown coefficients

Consider an  $n$ -qubit quantum state to be teleported as

$$|\psi\rangle = \sum_{i=1}^m \alpha_i |x_i\rangle, \quad (2.1)$$

where  $\alpha_i$ s are the probability amplitudes ensuring normalization  $\sum_{i=1}^m |\alpha_i|^2 = 1$ . Additionally,  $x_i$ s are mutually orthogonal to each other, i.e.,  $\langle x_i | x_j \rangle = \delta_{ij} \forall (1 < i, j < m)$ . Therefore, one may note that  $x_i$ s are the elements of an  $n$ -qubit orthogonal basis iff  $m \leq 2^{(n)}$ . For example, we may consider 3-qubit quantum states  $|\xi_1\rangle = \alpha_1 |000\rangle + \alpha_2 |111\rangle$  and  $|\xi_2\rangle = \alpha_1 |000\rangle + \alpha_2 |011\rangle + \alpha_3 |100\rangle + \alpha_4 |111\rangle$ , teleportation schemes for which were proposed in Refs. [123] and [104], respectively. For both the states  $n = 3$ , but we can easily observe that  $m = 2$  for  $|\xi_1\rangle$  and  $m = 4$  for  $|\xi_2\rangle$ . In what follows, we will establish that because of this difference in the values of  $m$ , teleportation of  $|\xi_1\rangle$  would require only one Bell state, whereas that of  $|\xi_2\rangle$  would require 2 Bell states.

Here, we set the task as to teleport state  $|\psi\rangle : m \leq 2^{(n-1)}$  using optimal quantum resources (i.e., using minimum number of qubits in the multi-qubit entangled state used as quantum channel). To do so, we will transform the state to be teleported (say,  $|\psi\rangle$ ) to a quantum state of a preferred form (say,  $|\psi'\rangle$ ). Specifically, the central idea of our scheme lies in finding out a unitary  $U$ , which transforms state  $|\psi\rangle$  into  $|\psi'\rangle$ , i.e.,  $|\psi'\rangle = U|\psi\rangle$ , such that

$$|\psi'\rangle = \sum_{i=1}^m \alpha'_i |y_i\rangle. \quad (2.2)$$

Here,  $|\psi'\rangle$  is a unique  $n$ -qubit quantum state which can be reduced to an  $m$ -qubit quantum state in the computational basis  $\{y_i\}$ , after measuring the redundant qubits. Specifically, the unitary is expected to possess a one-to-one map for each element of  $\{x_i\} \rightarrow \{y_i\}$ . As shown in Figure 2.1, here we prefer  $|y_i\rangle = |0\rangle^{n-m'} \otimes |\tilde{i}\rangle$ , where  $m' = \lceil \log_2 m \rceil$  and  $\tilde{i}$  is the binary equivalent of decimal value  $i$  in an  $m'$ -bit binary string. This step transforms  $m$  elements of  $|\psi\rangle$  with non-zero projections in Eq. (2.1) to that of  $m$  elements of  $|\psi'\rangle$  in Eq. (2.2). For example, we may consider the quantum state  $|\xi_1\rangle$  or  $|\xi_2\rangle$  described above as the quantum state to be teleported. As both of these states are 3-qubit states,  $n = 3$  for both of them. However, in the expansion of  $|\xi_1\rangle$  ( $|\xi_2\rangle$ ) there are 2 (4) non-zero coefficients. Consequently,  $m = 2$  ( $m = 4$ ) and  $m' = \lceil \log_2 2 \rceil = 1$  ( $m' = \lceil \log_2 4 \rceil = 2$ ) for the quantum state  $|\xi_1\rangle$  ( $|\xi_2\rangle$ ). Therefore, the maximum advantage of

quantum resources would be obtained if the quantum state  $|\xi_1\rangle$  ( $|\xi_2\rangle$ ) is teleported using a scheme that stores two qubits (one-qubit) in a register.

However, to design the unitary able to accomplish such a task the map  $\{x_i\} \rightarrow \{y_i\}$  should exist between all the elements (both possessing either zero or non-zero projection in  $|\psi\rangle$  and  $|\psi'\rangle$ ) in both the basis. In other words, the unitary  $U$  mapping the basis elements from  $\{x_i\}$  to  $\{y_i\}$  required for the desired transformation would be

$$U = \sum_{i=1}^{2^n} |y_i\rangle\langle x_i|. \quad (2.3)$$

Being a  $2^n$  dimensional computational basis  $\{y_i\}$  is already known while state  $|\psi\rangle$  reveals only  $m$  orthogonal vectors of basis  $\{x_i\}$ . Therefore, the remaining  $(2^n - m)$  elements of basis  $\{x_i\}$  can be obtained by Gram-Schmidt procedure, such that the elements of  $\{x_i\}$  follow the completeness relation, i.e.,  $\sum_{i=1}^{2^n} |x_i\rangle\langle x_i| = \mathbb{I}$ .

The obtained quantum state  $|\psi'\rangle$  possesses the first  $n - m'$  qubits in  $|0\rangle$ , while the remaining  $m'$  qubits hold the complete information of  $|\psi\rangle$ . Therefore, our task reduces to a teleportation of an  $m'$ -qubit quantum states using an optimal amount of quantum resources. An  $m'$ -qubit quantum state can be teleported either by using at least  $2m'$ -qubit entangled state or  $m'$  Bell states, one for teleporting each qubit [18].

Preparing a multi-qubit entangled state is relatively expensive and such a state is more prone to decoherence than a two-qubit entangled state. For the reason, we prefer the second strategy and select Bell states as a quantum channel (see Figure 2.1). Once the quantum state  $|\psi'\rangle$  is reconstructed at Bob's port, he would require to perform a unitary operation  $U^\dagger$ .

For the sake of completeness of the chapter we may summarize teleportation of an arbitrary  $m'$ -qubit quantum state in the following steps:

1. The  $m'$ -qubit unknown state to be teleported (whose qubits are indexed by  $1, 2, \dots, m'$ ) and the first qubits of each  $m'$  Bell states (indexed by  $A_1, A_2, \dots, A_{m'}$ ) are with Alice and all the second qubits (indexed by  $B_1, B_2, \dots, B_{m'}$ ) are with Bob.
2. Alice performs pairwise Bell measurements on her qubits  $(i, A_i)$  and finally announces  $m'$  measurement outcomes.
3. Bob applies Pauli operations on each qubit in his possession depending upon the measurement outcome of Alice (see Table 2.1, which is adapted from Ref. [94]). At the end of this step Bob obtains the  $m'$ -qubit unknown quantum state that Alice has teleported.

Once Bob has access to the  $m'$ -qubit unknown state and knowledge of the unitary  $U$  Alice has applied, he prepares  $n - m'$  qubits in  $|0\rangle$ . Finally, he applies  $U^\dagger$  to reconstruct the unknown quantum state  $|\psi\rangle = U^\dagger|\psi'\rangle$ . Note that the unitary operation defined in Eq. (2.3) is independent of the unknown parameters of the quantum state to be teleported and exploits only the available

**Table 2.1:** Unitary applied by Bob to reconstruct the quantum state for QT. In the table, SMO is the sender's measurement outcome.

Initial state shared by Alice and Bob				
	$ \psi^+\rangle$	$ \psi^-\rangle$	$ \phi^+\rangle$	$ \phi^-\rangle$
SMO	Receiver	Receiver	Receiver	Receiver
00	$I$	$Z$	$X$	$iY$
01	$X$	$iY$	$I$	$Z$
10	$Z$	$I$	$iY$	$X$
11	$iY$	$X$	$Z$	$I$

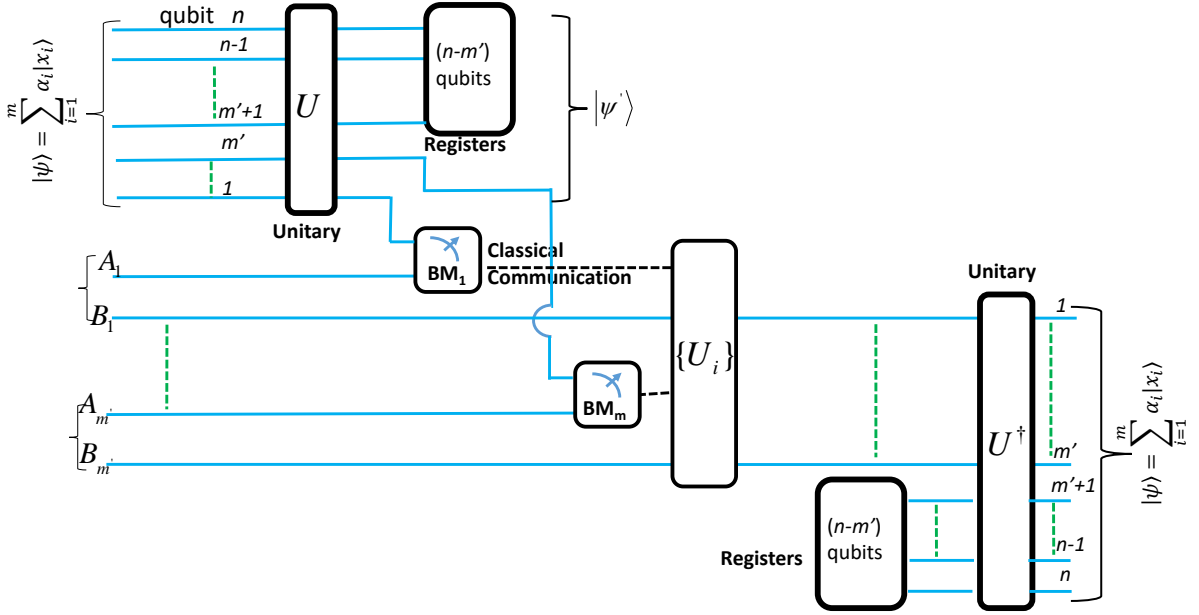


**Figure 2.1:** The circuit designed for generalized quantum teleportation of an  $n$ -qubit quantum states with  $m$  unknown coefficients. Here,  $m' = \lceil \log_2 m \rceil$  is the number of Bell states.  $U_i$  is the unitary operation applied by Bob and BM stands for Bell measurement.

knowledge of the state, i.e., the number of qubits, bases  $\{x_i\}$  and  $\{y_i\}$ , and the number of vanished coefficients.

In Table 2.2, we have given unitary operations involved in teleportation of various multi-qubit states with different number of unknowns using our scheme. Teleportation of these states using relatively fragile and expensive quantum resources have been reported in the recent past. To be specific, our technique can be used to teleport any quantum state having two unknown coefficients [16, 23, 51, 98, 123] using a single Bell state, irrespective of the number of physical qubits present in the state. In contrast, in the existing literature (cf. Columns 2 and 3 of Table 2.2) it is observed that the number of qubits used in the quantum channel increases with the increase in number of qubits to be teleported. Similarly, a quantum state having four-unknown coefficients can be teleported only using two Bell states, unlike the higher dimensional en-

tangled states used in [52, 93, 104]. This clearly establishes that our scheme allows one to circumvent the use of redundant qubits and complex entangled states that are used until now, and thus the present proposal increases the possibility of experimental realization.

### 2.2.1 Teleportation of state of type $|\psi\rangle = \alpha|x_i\rangle + \beta|x_j\rangle$

As an explicit example of the proposed scheme, consider an  $n$ -qubit state with only two unknowns, i.e.,

$$|\psi\rangle = \alpha|x_i\rangle + \beta|x_j\rangle, \quad (2.4)$$

such that,  $\langle x_i|x_j\rangle = \delta_{ij}$  and  $|\alpha|^2 + |\beta|^2 = 1$ . Here,  $x_i$  and  $x_j$  are the elements of some  $2^n$  dimensional basis set. Our task is to teleport state  $|\psi\rangle$  using optimal quantum resources (i.e., using minimum number of entangled qubits in quantum channel). As mentioned previously the minimum number of Bell states required in the quantum channel for this kind of state would be  $\lceil \log_2 2 \rceil = 1$ .

Therefore, we will transform state  $|\psi\rangle$  into  $|\psi'\rangle$ , such that  $U|\psi\rangle = |\psi'\rangle$ , such that

$$|\psi'\rangle = \alpha'|y_i\rangle + \beta'|y_j\rangle, \quad (2.5)$$

with  $\langle y_i|y_j\rangle = \delta_{ij}$  as  $y_i$  and  $y_j$  are the the elements of computational basis. For the simplest choice of  $|\psi'\rangle$ , we choose  $y_i = |0\rangle^{n-1} \otimes |0\rangle$  and  $y_j = |0\rangle^{n-1} \otimes |1\rangle$ .

Now, we will show that it is possible to teleport state  $|\psi'\rangle$  using one  $e$  bit (Bell state) and classical resource. The quantum circuit for teleporting state  $|\psi\rangle$  is given in Figure 2.2. The first part of the quantum circuit shows transformation of the state  $|\psi\rangle$  to the state  $|\psi'\rangle$  while the second part of the circuit contains standard scheme for teleporting an arbitrary single-qubit state. The third part of the circuit involves application of the unitary  $U^\dagger$  to transform the reconstructed state  $|\psi'\rangle$  into the unknown state  $|\psi\rangle$  to be teleported.

## 2.3 Controlled and bidirectional teleportation with optimal resource

Controlled teleportation of a single-qubit involves a third party (Charlie) as supervisor and hence instead of a Bell state we require tripartite entangled state as quantum channel. As mentioned in Section 2.1, many of the papers which involve multi-qubit complex states for teleportation also perform controlled teleportation using those multi-qubit complex states. Here, we

**Table 2.2:** A list of quantum states and the quantum resources used to teleport them. The number of qubits in the unknown quantum states, the unknown quantum state (i.e., the state to be teleported) and the resources used to teleport them are mentioned in the first, second and third column, respectively. Here, CS stands for cluster state and  $a_i$  represents the binary value of decimal number  $i$  expanded up to  $k$  digits. Corresponding minimum resources used to teleport that states are given in the fourth column. The unitary required to decrease the number of entangled qubits to be used as quantum channel is given in the last column.

Quantum state to be teleported	Number of qubits in the state to be teleported	Quantum state used as quantum channel and corresponding reference	Number of Bell states required in our scheme to teleport the state	Unitary to be applied by Alice
$\alpha a_0\rangle + \beta a_3\rangle$	two-qubit	four-qubit CS [23], 3-qubit W class state [16]	one	$ a_0\rangle\langle a_0  +  a_1\rangle\langle a_3  +  a_2\rangle\langle a_1  +  a_3\rangle\langle a_2 $
$\alpha a_1\rangle + \beta a_2\rangle$	two-qubit	three-qubit GHZ-like state [98]	one	$ a_0\rangle\langle a_1  +  a_1\rangle\langle a_2  +  a_2\rangle\langle a_0  +  a_3\rangle\langle a_3 $
$\alpha a_0\rangle + \beta a_7\rangle$	three-qubit	four-qubit CS [123]	one	$ a_0\rangle\langle a_0  +  a_1\rangle\langle a_7  +  a_2\rangle\langle a_1  +  a_3\rangle\langle a_2  +  a_4\rangle\langle a_3  +  a_5\rangle\langle a_4  +  a_6\rangle\langle a_5  +  a_7\rangle\langle a_6 $
$\alpha( a_0\rangle +  a_3\rangle) + \beta( a_4\rangle +  a_7\rangle)$	three-qubit	four-qubit CS [51]	one	$\frac{1}{\sqrt{2}}( a_0\rangle\langle(a_0 + a_3)  +  a_1\rangle\langle(a_4 + a_7)  +  a_2\rangle\langle(a_1 + a_2)  +  a_3\rangle\langle(a_5 + a_6)  +  a_4\rangle\langle(a_0 - a_3)  +  a_5\rangle\langle(a_4 - a_7)  +  a_6\rangle\langle(a_1 - a_2)  +  a_7\rangle\langle(a_5 - a_6) )$
$\alpha( a_0\rangle +  a_7\rangle) + \beta( a_{13}\rangle +  a_{10}\rangle)$	four-qubit	five-qubit CS [51]	one	$\frac{1}{\sqrt{2}}( a_0\rangle\langle(a_0 + a_7)  +  a_1\rangle\langle(a_{13} + a_{10})  +  a_2\rangle\langle(a_1 + a_2)  +  a_3\rangle\langle(a_3 + a_4)  +  a_4\rangle\langle(a_5 + a_6)  +  a_5\rangle\langle(a_8 + a_9)  +  a_6\rangle\langle(a_{11} + a_{12})  +  a_7\rangle\langle(a_{14} + a_{15})  +  a_8\rangle\langle(a_0 - a_7)  +  a_9\rangle\langle(a_{13} - a_{10})  +  a_{10}\rangle\langle(a_1 - a_2)  +  a_{11}\rangle\langle(a_3 - a_4)  +  a_{12}\rangle\langle(a_5 - a_6)  +  a_{13}\rangle\langle(a_8 - a_9)  +  a_{14}\rangle\langle(a_{11} - a_{12})  +  a_{15}\rangle\langle(a_{14} - a_{15}) )$

Quantum state to be teleported	Number of qubits in the state to be teleported	Quantum state used as quantum channel and corresponding reference	Number of Bell states required in our scheme to teleport the state	Unitary to be applied by Alice
$\alpha a_0\rangle + \beta a_3\rangle + \gamma a_4\rangle + \delta a_7\rangle$	three-qubit	five-qubit state [104]	two	$ a_0\rangle\langle a_0  +  a_1\rangle\langle a_3  +  a_2\rangle\langle a_4  +  a_3\rangle\langle a_7  +  a_4\rangle\langle a_1  +  a_5\rangle\langle a_2  +  a_6\rangle\langle a_5  +  a_7\rangle\langle a_6 $
$\alpha a_0\rangle + \beta a_3\rangle + \gamma a_{12}\rangle + \delta a_{15}\rangle$	four-qubit	six-qubit CS [52]	two	$ a_0\rangle\langle a_0  +  a_1\rangle\langle a_3  +  a_2\rangle\langle a_{12}  +  a_3\rangle\langle a_{15}  +  a_4\rangle\langle a_1  +  a_5\rangle\langle a_2  +  a_6\rangle\langle a_4  +  a_7\rangle\langle a_5  +  a_8\rangle\langle a_6  +  a_9\rangle\langle a_7  +  a_{10}\rangle\langle a_8  +  a_{11}\rangle\langle a_9  +  a_{12}\rangle\langle a_{10}  +  a_{13}\rangle\langle a_{11}  +  a_{14}\rangle\langle a_{13}  +  a_{15}\rangle\langle a_{14} $
$\alpha a_0\rangle + \beta a_{15}\rangle + \gamma a_{63}\rangle + \delta a_{48}\rangle$	six-qubit	six-qubit CS [93]	two	$ a_0\rangle\langle a_0  +  a_1\rangle\langle a_{15}  +  a_2\rangle\langle a_{63}  +  a_3\rangle\langle a_{48}  +  a_4\rangle\langle a_1  +  a_5\rangle\langle a_2  +  a_6\rangle\langle a_3  +  a_7\rangle\langle a_4  +  a_8\rangle\langle a_5  +  a_9\rangle\langle a_6  +  a_{10}\rangle\langle a_7  +  a_{11}\rangle\langle a_8  +  a_{12}\rangle\langle a_9  +  a_{13}\rangle\langle a_{10}  +  a_{14}\rangle\langle a_{11}  +  a_{15}\rangle\langle a_{12}  +  a_{16}\rangle\langle a_{13}  +  a_{17}\rangle\langle a_{14}  +  a_{18}\rangle\langle a_{16}  +  a_{19}\rangle\langle a_{17}  +  a_{20}\rangle\langle a_{18}  +  a_{21}\rangle\langle a_{19}  +  a_{22}\rangle\langle a_{20}  +  a_{23}\rangle\langle a_{21}  +  a_{24}\rangle\langle a_{22}  +  a_{25}\rangle\langle a_{23}  +  a_{26}\rangle\langle a_{24}  +  a_{27}\rangle\langle a_{25}  +  a_{28}\rangle\langle a_{26}  +  a_{29}\rangle\langle a_{27}  +  a_{30}\rangle\langle a_{28}  +  a_{31}\rangle\langle a_{29}  +  a_{32}\rangle\langle a_{30}  +  a_{33}\rangle\langle a_{31}  +  a_{34}\rangle\langle a_{32}  +  a_{35}\rangle\langle a_{33}  +  a_{36}\rangle\langle a_{34}  +  a_{37}\rangle\langle a_{35}  +  a_{38}\rangle\langle a_{36}  +  a_{39}\rangle\langle a_{37}  +  a_{40}\rangle\langle a_{38}  +  a_{41}\rangle\langle a_{39}  +  a_{42}\rangle\langle a_{40}  +  a_{43}\rangle\langle a_{41}  +  a_{44}\rangle\langle a_{42}  +  a_{45}\rangle\langle a_{43}  +  a_{46}\rangle\langle a_{44}  +  a_{47}\rangle\langle a_{45}  +  a_{48}\rangle\langle a_{46}  +  a_{49}\rangle\langle a_{47}  +  a_{50}\rangle\langle a_{49}  +  a_{51}\rangle\langle a_{50}  +  a_{52}\rangle\langle a_{51}  +  a_{53}\rangle\langle a_{52}  +  a_{54}\rangle\langle a_{53}  +  a_{55}\rangle\langle a_{54}  +  a_{56}\rangle\langle a_{55}  +  a_{57}\rangle\langle a_{56}  +  a_{58}\rangle\langle a_{57}  +  a_{59}\rangle\langle a_{58}  +  a_{60}\rangle\langle a_{59}  +  a_{61}\rangle\langle a_{60}  +  a_{62}\rangle\langle a_{61}  +  a_{63}\rangle\langle a_{62} $



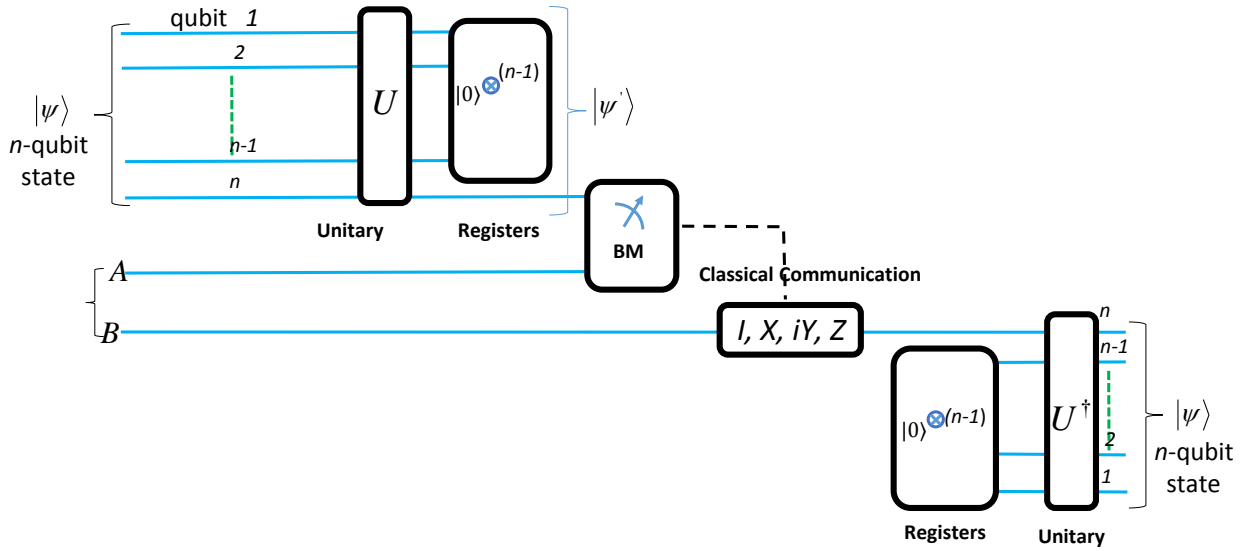


**Figure 2.2:** As an explicit example, a quantum circuit (which uses a single Bell state as quantum channel) for the teleportation of an  $n$ -qubit quantum state having two unknown coefficients is shown.

extend our scheme, for optimal QT to optimal CT. The scheme of CT using optimal resources can be explained along the same line of the QT scheme as follows.

To construct an optimal scheme, it is assumed that Charlie also knows the unitary Alice is using to reduce the size of the quantum state to be teleported. In other words, he is aware of the number of entangled qubits Alice and Bob require to perform teleportation. Suppose the reduced quantum state has  $m'$  qubits, Charlie prepares  $m'$  GHZ states and share the three qubits among Alice, Bob and himself. Charlie measures his qubit in  $\{|+\rangle, |-\rangle\}$  basis and withholds the measurement outcome. Independently, Alice and Bob perform the QT scheme with the only difference that Bob requires Charlie's measurement disclosure to reconstruct the state. Charlie announces the required classical information when he wishes Bob to reconstruct the state.

Similarly, when both Alice and Bob wish to teleport a quantum state each to Bob and Alice, respectively, under the supervision of Charlie, they perform QT schemes independently, while Charlie prepares the quantum channel in such a way that after his measurement the reduced state is the product of  $2m'$  Bell states (half of which will be used for Alice to Bob, while the remaining half for Bob to Alice communication). Charlie's disclosure of his measurement outcomes end both Alice's and Bob's ignorance regarding the quantum channel they were sharing, and they can subsequently reconstruct the unknown quantum states teleported to them (see [95] for detail). In Ref. [94], it is shown that BCST can also be accomplished solely using Bell states. Therefore, CT and BCST can also be performed using only bipartite entanglement. In the absence of the controller, a BCST scheme can be reduced to a BST scheme. Our results indicate that some of the recent schemes of CT using four-qubit cluster state [90] and quan-

tum information splitting using four and five-qubit cluster state [63, 67]; BST using three-qubit GHZ state [38]; and six-qubit cluster state [50], can also be performed with reduced amount of quantum resources (entangled states involving lesser number of qubits).

## 2.4 Experimental implementation of the proposed efficient QT scheme using IBM's real quantum processor

In Section 1.8, we have already mentioned that recently, IBM corporation has placed a five-qubit superconductivity-based quantum computer on cloud [235], and has provided its access to everyone. This initiative has enabled the interested researchers to experimentally realize various proposals for quantum information processing tasks. Interestingly, a set of superconductivity-based implementations of quantum computer that are similar to the technology used in developing IBM's five-qubit quantum computer, have already been reported [220, 221, 241]. In Section 1.8, technical aspects of the IBM quantum computer has already been reviewed briefly. In addition to what has already been told in the previous chapter, we may note that currently, the five-qubit superconductivity-based quantum computers have many limitations, like available gate library is only approximately universal, measurement of individual qubits at different time points is not allowed, limited applicability of CNOT gate, and short decoherence time [250]. Further, the real quantum computer (IBM quantum experience) available at cloud allows a user to perform an experiment using at most five-qubits. Keeping these limitations in mind, we have chosen a two-qubit two-unknown quantum state  $|\psi\rangle = \alpha(|00\rangle + |11\rangle) + \beta(|01\rangle - |10\rangle)$  :  $2(|\alpha|^2 + |\beta|^2) = 1$  as the state to be teleported.

Here, we would like to mention that implementation of a single-qubit teleportation protocol (which requires only three qubits) has already been demonstrated using IBM's quantum computer [220]. The experimental implementation of the present QT scheme is relatively complex and can be divided into four parts as shown in Figure 2.3. Part A involves preparation of state  $|\psi\rangle$  (using qubit q[0] and q[1]) and a Bell state (using qubit q[2] and q[3]). The complex circuit comprised of the quantum gates from Clifford group is shown in Figure 2.3. Here, it may be noted that the IBM quantum computer accepts quantum gates from Clifford group only. The state  $|\psi\rangle$  in this particular case is prepared with  $|\alpha|^2 = 0.375$  and  $|\beta|^2 = 0.125$ . Preparation of the desired two-qubit state by application of specific quantum gates is detailed in the following.

$$\begin{aligned}
|00\rangle &\xrightarrow{H^1, T^1} \left( \frac{|0\rangle + e^{i\frac{\pi}{4}}|1\rangle}{\sqrt{2}} \right) |0\rangle \xrightarrow{H^1, S^1} e^{i\frac{\pi}{8}} (\cos(\frac{\pi}{8})|0\rangle + \sin(\frac{\pi}{8})|1\rangle)|0\rangle \xrightarrow{T^{\dagger 1}, X^1, H^1} \\
&\sqrt{2}e^{i\frac{\pi}{8}}(\alpha|0\rangle + \beta|1\rangle)|0\rangle \xrightarrow{C^1-NOT^2} \sqrt{2}e^{i\frac{\pi}{8}}(\alpha|00\rangle + \beta|11\rangle) \xrightarrow{H^1} e^{i\frac{\pi}{8}}(\alpha(|00\rangle + |10\rangle) \\
&+ \beta(|01\rangle - |11\rangle)) \xrightarrow{C^1-NOT^2} e^{i\frac{\pi}{8}}(\alpha(|00\rangle + |11\rangle) + \beta(|01\rangle - |10\rangle)).
\end{aligned}$$

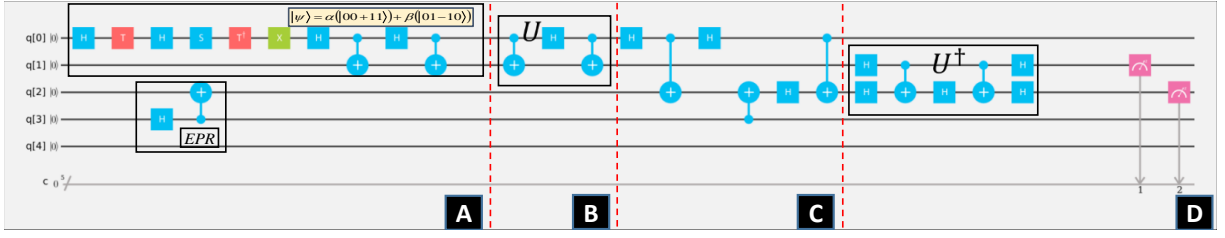


**Figure 2.3:** Teleportation circuit used for the teleportation of two-qubit unknown quantum state  $(\alpha(|00\rangle + |11\rangle) + \beta(|01\rangle - |10\rangle))$  using single Bell state as a quantum channel. This circuit which is implemented using five-qubit IBM quantum computer, is divided into four parts. In (A) part state preparation is done, where an EPR channel and a quantum state  $|\psi\rangle$  with  $|\alpha|^2 = 0.375$  and  $|\beta|^2 = 0.125$  are prepared. In (B) the decomposition of the unitary operation  $U$  which transforms  $(\alpha(|00\rangle + |11\rangle) + \beta(|01\rangle - |10\rangle))$  to  $(\alpha|00\rangle + \beta|10\rangle)$  in the computational basis is shown. In (C) teleportation of a single-qubit state is realized, and In (D)  $|\psi\rangle$  is reconstructed from the teleported single-qubit state by applying  $U^\dagger$  followed by projective measurement.

Here,  $e^{i\frac{\pi}{8}}$  is the global phase in the simulated quantum state with  $\alpha = \frac{1}{\sqrt{2}} \left( \cos \frac{\pi}{8} + e^{-i\frac{\pi}{4}} \sin \frac{\pi}{8} \right)$ , and  $\beta = \frac{1}{\sqrt{2}} \left( -\cos \frac{\pi}{8} + e^{-i\frac{\pi}{4}} \sin \frac{\pi}{8} \right)$ . We have explicitly mentioned the qubit-number on which a particular operation is to be performed by mentioning the qubit-number on the the superscript of the corresponding unitary operator.

As described in Section 2.2.1, Part B involves application of a unitary  $U = (C^2 - \text{NOT}^1) \cdot (\mathbb{I} \otimes H) \cdot (C^2 - \text{NOT}^1)$  to transform the state  $|\psi\rangle$  from the entangled basis to the computational basis and is the bottleneck of the protocol. Such a transformation allows us to render the information encoded into a smaller number of qubits (in our example it is a single-qubit) and thus it reduces the amount of resources required. Part C is dedicated to the teleportation of a single-qubit state. Here, we have used computational counterpart of teleportation [251], which can be performed when both Alice's and Bob's qubits are locally available for a two-qubit operation. Teleportation of a single-qubit state in analogy of Ref. [220] can also be performed. This part of the circuit can be divided into two sub-parts. The first one (left aligned), which includes an EPR circuit, entangles qubit q[1] to the Bell state while the second part (right aligned) disentangles Bob's qubit (q[3]) from Alice's qubits. The need of disentangling Bob's qubit from Alice's qubit is explained below. In the standard protocol for QT [6], Alice measures her qubits and announces measurement outcomes. Depending on the measurement outcome of Alice, Bob applies a unitary operation and reconstructs the unknown state. In IBM's quantum computer, simultaneous measurement of all the qubits is mandatory, which will project Bob's qubit into a mixed state. Therefore, we preferred to disentangle Bob's qubit from Alice's qubits before measurement. We would like to mention here that an optical implementation of the CNOT gate (also Bell measurement) can only work probabilistically using linear optics, while in contrast superconducting qubits allow deterministic CNOT operation. The challenges of experimental implementation of quantum teleportation using optical qubits are not addressed in the present

work. At last, in Part D, Bob applies the unitary  $U^\dagger$  followed by the projective measurement on all qubits, which reveals the state  $|\psi\rangle$  teleported to Bob's qubits. To perform a quantitative analysis of the performance of the QT scheme under consideration, we would require the density matrices of the state to be teleported and that of the teleported state. In a recent implementation of QT on IBM computer only probabilities of various outcomes were obtained [220]. However, to obtain the full picture, we need to reconstruct the density matrix of the teleported state using QST [216] which in turn requires extraction of information from the experiments and the subsequent use of that information in the reconstruction of the experimental density matrix. From the method of QST described in Section 1.9, we can easily recognize that the reconstruction of two-qubit state requires nine experiments. Using the above method we have reconstructed the teleported state (using nine rounds of experiments with 8192 runs of each experiment) as

$$\rho'' = \begin{bmatrix} 0.41 & 0.013 + 0.077i & 0.085 - 0.19i & 0.204 - 0.054i \\ 0.013 - 0.077i & 0.134 & -0.065 - 0.016i & -0.021 - 0.051i \\ 0.085 + 0.19i & -0.065 + 0.016i & 0.261 & 0.101 + 0.035i \\ 0.204 + 0.054i & -0.021 + 0.051i & 0.101 - 0.035i & 0.195 \end{bmatrix}, \quad (2.6)$$

whereas theoretically the state prepared for the teleportation is  $\rho = |\Psi\rangle\langle\Psi|$  with  $|\Psi\rangle = \{\alpha(|00\rangle + |11\rangle) + \beta(|01\rangle - |10\rangle)\}$ .

During experimental implementation the state prepared may also have some errors. Keeping this in mind, we have reconstructed the density matrix of the quantum state (which is to be teleported) generated in the experiment as

$$\rho' = \begin{bmatrix} 0.352 & -0.080 + 0.104i & 0.18 - 0.133i & 0.313 - 0.005i \\ -0.080 - 0.104i & 0.135 & -0.092 - 0.017i & -0.099 - 0.12i \\ 0.18 + 0.133i & -0.092 + 0.017i & 0.175 & 0.150 + 0.101i \\ 0.313 + 0.005i & -0.099 + 0.12i & 0.150 - 0.101i & 0.338 \end{bmatrix}. \quad (2.7)$$

Various elements of all the density matrices are shown pictorially in Figure 2.4. Finally, we would like to quantize the performance of the QT scheme using a distance-based measure, i.e. fidelity, which is defined as in Section 1.6.3. Using this, we calculated the fidelity between the theoretical state with experimentally generated state (i.e.,  $\rho^1 = \rho$  and  $\rho^2 = \rho'$ ) as 0.9221. The same calculation performed between experimentally generated and teleported state (i.e.,  $\rho^1 = \rho$  and  $\rho^2 = \rho''$ ) yields a higher value for fidelity (0.9378). Thus, the state preparation is relatively more erroneous, due to errors in gate implementation and decoherence. However, the constructed state is found to be teleported with high fidelity.

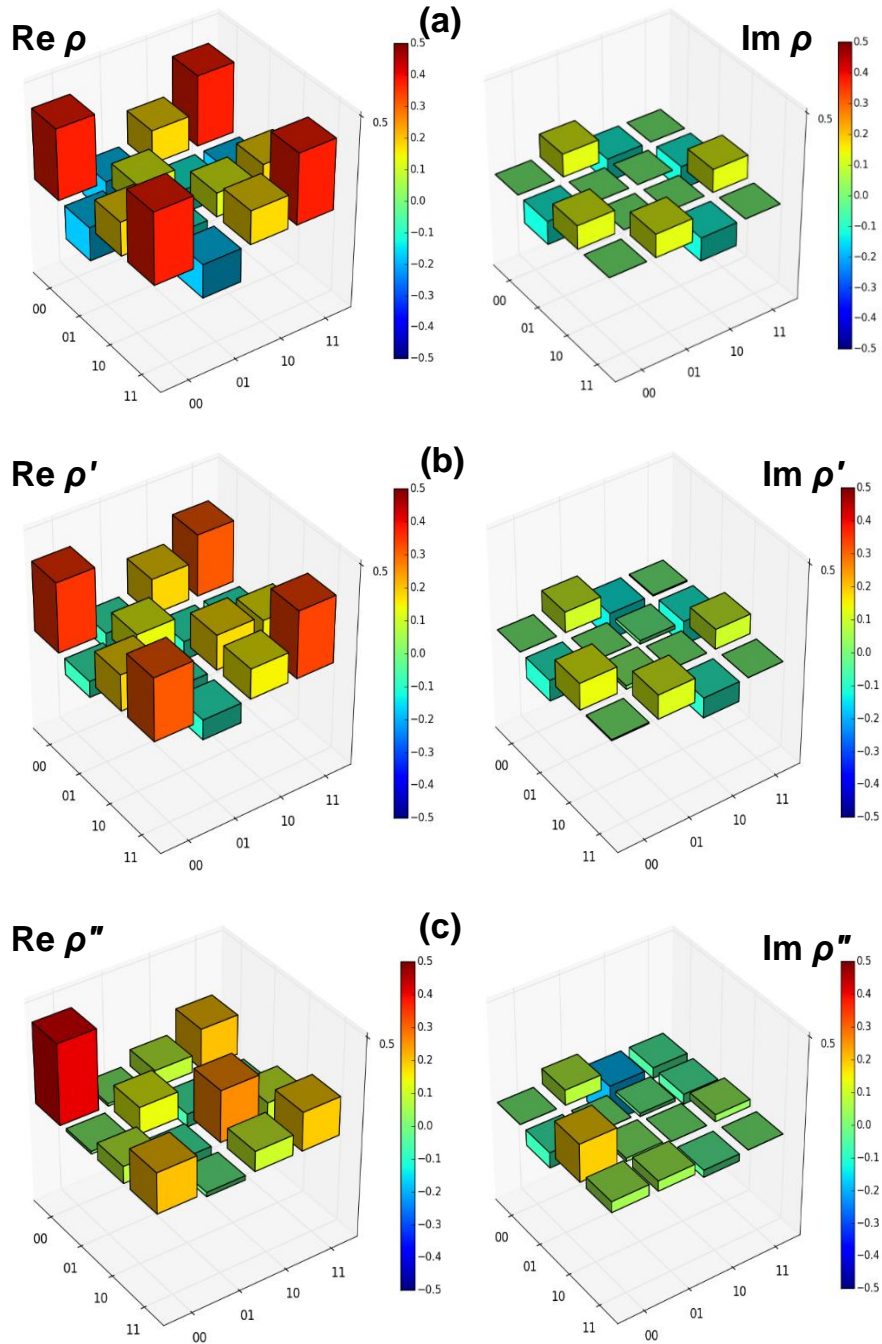


**Figure 2.4:** Graphical representation of real (Re) and imaginary (Im) parts of the density matrices of (a) the theoretical state  $\alpha(|00\rangle + |11\rangle) + \beta(|01\rangle - |10\rangle)$ , (b) the experimentally prepared state, and (c) the reconstructed state after teleportation.

## 2.5 Conclusion

Teleportation of multi-qubit states with the optimal amount of quantum resources in terms of the number of entangled qubits required in the quantum channel has been performed. Specifically, the amount of quantum resources required to teleport an unknown quantum state is found to depend (be independent of) on the number of non-zero probability amplitudes in the quantum state (the number of qubits in the state to be teleported). Also, the choice of unitary operation essentially exploits the available information regarding the quantum state, i.e., only the number of non-zero coefficients and bases  $\{x_i\}$  and  $\{y_i\}$ , and not on the values of these unknown parameters. This makes our proposal quite general in nature and manifests its wide applicability.

We have explicitly established that the complex multi-partite entangled states that are used in a large number of recent works on teleportation (cf. Table 2.2) are not required for teleportation. Extending this argument one can show that the complex multi-partite entangled states used for dense-coding in Refs. [62, 99] are not required, and the task can be performed using an optimal number of Bell states.

Further, the relevance of the present work is not restricted to QT. It is also useful in CT, BST and bidirectional controlled state teleportation schemes. The relevance of the present work also lies in the fact that the limiting cases of our scheme can perform the same task with reduced amount of quantum resources in comparison with the previously achieved counterparts. In fact, for almost all the existing works reported on teleportation of multi-qubit states with some non-zero unknowns, we have shown a clear prescription to optimize the required quantum resources.

Finally, a proof-of-principle experimental implementation of the proposed scheme is performed using the IBM quantum computer. Experimental results are rigorously analyzed. This quantitative analysis infer that the teleportation circuit implemented here is more efficient when compared with the state preparation part. This fact establishes the relevance of the proposed scheme in context of reduction of the decoherence effects on teleportation, too. As evident from the results of our four-qubit experiments, the experimental architecture provided by the IBM quantum experience facility is not sustainable to gate errors and decoherence. We believe that there exist techniques that can be used to protect coherence against gate error and decoherence. For example, IBM may use gates protected by dynamical decoupling to reduce error; alternatively, in future they may reduce error by using logic qubits instead of the physical qubits, but that would require a relatively large physical qubit register. We believe, in order to provide a reliable quantum computing architecture, incorporation of these techniques would play an important role.

We hope our attempt to optimize the resource requirement for teleportation of multi-qubit quantum states should increase the feasibility of multi-qubit quantum state teleportation performed in various quantum systems. This is also expected to impact the teleportation-based direct secure quantum communication scheme, where resources can be optimized exploiting

the form of the quantum state teleported (e.g., [45] and references therein). Along the same line, optimization of quantum resources in CT, without affecting the controller's power, will be performed and reported elsewhere.

# CHAPTER 3

## QUANTUM TELEPORTATION OF AN EIGHT-QUBIT STATE USING OPTIMAL QUANTUM RESOURCES

### 3.1 Introduction

In the previous chapter, we have already mentioned that the original protocol for quantum teleportation was designed for the teleportation of a single-qubit state using a Bell state [6]. Subsequently, many schemes have been proposed for the teleportation of multi-qubit states using various entangled states. Following the trend, recently, Zhao et al., have proposed a scheme for the teleportation of the following quantum state

$$|\varphi\rangle_{abcdefgh} = (\alpha|00000000\rangle + \beta|00100000\rangle + \gamma|11011111\rangle + \delta|11111111\rangle)_{abcdefgh}, \quad (3.1)$$

where the coefficients  $\alpha, \beta, \gamma, \delta$  are unknown and satisfies  $|\alpha|^2 + |\beta|^2 + |\gamma|^2 + |\delta|^2 = 1$  (cf. Eq. (1) of [132]). They considered this state as an eight-qubit quantum state and proposed a scheme for teleportation of this state using the following six-qubit cluster state described as

$$|\phi\rangle_{123456} = (\alpha|000000\rangle + \beta|001001\rangle + \gamma|110110\rangle + \delta|111111\rangle)_{123456}. \quad (3.2)$$

as the quantum channel (cf. Eq. (2) of [132]). The basic conceptual problem with the form of this channel is that this channel cannot be constituted as the coefficients  $\alpha, \beta, \gamma, \delta$  present in the expansion of  $|\varphi\rangle_{abcdefgh}$  are unknown. Further, Eq. (2) of [132] is not consistent with Eqs. (5)-(6) of [132] and thus with the remaining part of [132]. To stress on the more important



issues and to continue the discussion, we may consider that Zhao et al., actually intended to use

$$|\phi\rangle_{123456} = \frac{1}{2} (|000000\rangle + |001001\rangle + |110110\rangle + |111111\rangle), \quad (3.3)$$

which is consistent with Eq. (3) of [132]. However, the above mistake does not appear to be a typographical error as the same error is present in another recent work of the authors (see [131]). The more important question is whether we need Eq. (3.3) for the teleportation of  $|\phi\rangle_{abcdefgh}$ , or the task can be performed using a simpler quantum channel. This is the question, we wish to address in this chapter. Here, it is important to note that in a recent work [85], we have shown that a quantum state having  $n$  unknown coefficients can be teleported by using  $\lceil \log_2 n \rceil$  number of Bell states. Now, as there are four unknowns in  $|\phi\rangle_{abcdefgh}$ , teleportation of this state should require only two Bell states. This point can be further illustrated by noting that Zhao et al., have shown that using four CNOT gates (cf. Figure 1 of [132])  $|\phi\rangle_{abcdefgh}$  can be transformed to a state  $|\phi'\rangle_{abcdefgh} = |\chi\rangle_{abcd}|0000\rangle_{efgh}$ , where

$$|\chi\rangle_{abcd} = (\alpha|0000\rangle + \beta|0010\rangle + \gamma|1101\rangle + \delta|1111\rangle)_{abcd}, \quad (3.4)$$

and thus the actual teleportation task reduces to the teleportation of  $|\chi\rangle_{abcd}$ . Now, we can introduce a circuit which can be described as  $\text{CNOT}_{a \rightarrow d} \text{CNOT}_{a \rightarrow b} \text{SWAP}_{bc}$ , where  $\text{SWAP}_{ij}$  and  $\text{CNOT}_{i \rightarrow j}$  correspond to a gate that swaps  $i$ th and  $j$ th qubit and a CNOT that uses  $i$ th qubit as the control qubit and  $j$ th qubit as the target qubit, respectively. On application of this circuit,  $|\chi\rangle_{abcd}$  would transform to  $(\alpha|00\rangle + \beta|01\rangle + \gamma|10\rangle + \delta|11\rangle)_{ac} |00\rangle_{bd}$  as

$$\begin{aligned} \text{CNOT}_{a \rightarrow d} \text{CNOT}_{a \rightarrow b} \text{SWAP}_{bc} |\chi\rangle_{abcd} &= (\alpha|00\rangle + \beta|01\rangle + \gamma|10\rangle + \delta|11\rangle)_{ac} |00\rangle_{bd} \\ &= |\psi\rangle_{ac} |00\rangle_{bd} \end{aligned} \quad (3.5)$$

Thus, a scheme for teleportation of an arbitrary two-qubit state  $|\psi\rangle_{ac}$  will be sufficient for the teleportation of  $|\phi\rangle_{abcdefgh}$ . Such a scheme for the QT of an arbitrary two-qubit state was proposed by Rigolin in 2005 [76]. He proposed sixteen quantum channels that are capable of teleportation of the arbitrary two-qubit states and referred to those channels as generalized Bell states. However, soon after the work of Rigolin, in a comment on it, Deng [26] had shown that sixteen channels introduced by Rigolin were simply the sixteen possible product states of the 4 Bell states, and thus the work of Deng and Rigolin established the fact that the product of any two Bell states is sufficient for the teleportation of an arbitrary two-qubit state. Result of Deng and Rigolin is consistent with the more general result of ours [85], which is presented in the previous chapter and that of [9, 94, 95]. This clearly establishes that in addition to the circuit block comprise of four CNOT gates used in the work of Zhao et al., if one uses the circuit described above and well known scheme of Rigolin, then one will be able to teleport so-called an eight-qubit state  $|\phi\rangle_{abcdefgh}$  using only two Bell states. This comment could have

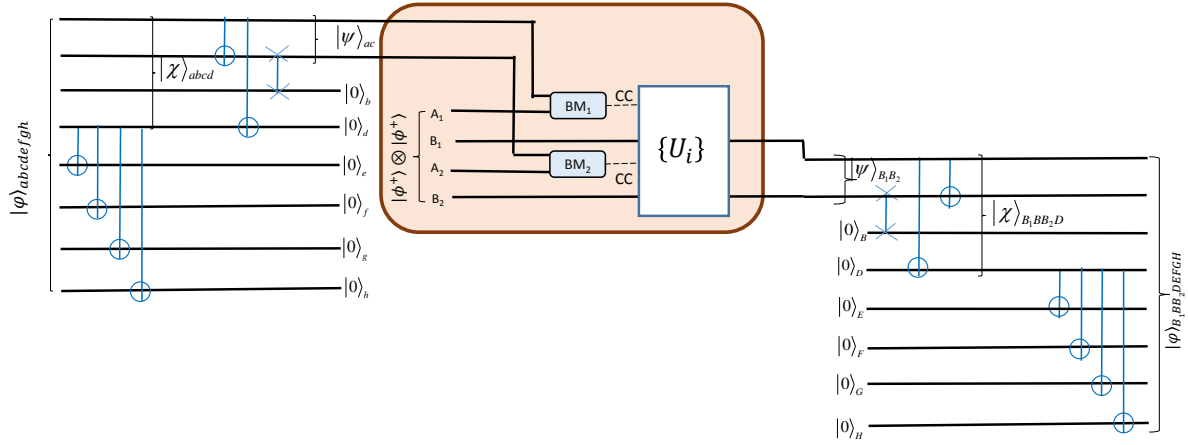


**Figure 3.1:** Teleportation circuit for the teleportation of an eight-qubit unknown quantum state (i.e., the state described by Eq. (3.1) using two Bell states (optimal amount of quantum resource). Here, BM and CC stand for Bell measurement and classical communication, respectively.  $U_i$  is the unitary operation required to reconstruct the quantum state we wish to teleport.

been concluded at this point, but for the convenience of the readers we have added the following section, where we briefly outline the complete process of teleportation of  $|\varphi\rangle_{abcdefgh}$  using two Bell states.

### 3.2 Complete teleportation process

Teleportation of  $|\varphi\rangle_{abcdefgh}$  is accomplished in three steps as illustrated in Figure 3.1. Firstly, the task of teleportation of the so called eight-qubit quantum state  $|\varphi\rangle_{abcdefgh}$  is reduced to the task of teleporting a two-qubit quantum state  $|\psi\rangle_{ac}$  by transforming  $|\varphi\rangle_{abcdefgh}$  into  $|\psi\rangle_{ac}|000000\rangle_{defgh}$ . This is done using the circuit block (comprised of six CNOT gates and one SWAP gate) shown in the left side of the complete circuit shown in Figure 3.1. The actual teleportation part is the second step which is shown in the middle block of Figure 3.1 (cf. the rectangular box in the middle of Figure 3.1). In this step, we teleport  $|\psi\rangle_{ac}$  using two Bell states as quantum channel. As an example, consider.  $|\psi^+\rangle_{A_1B_1} \otimes |\psi^+\rangle_{A_2B_2} = \frac{|00\rangle+|11\rangle}{\sqrt{2}} \otimes \frac{|00\rangle+|11\rangle}{\sqrt{2}}$  as the quantum channel. Thus, the combined state would be

$$|\Phi\rangle_{acA_1B_1A_2B_2} = |\psi\rangle_{ac} \otimes |\psi^+\rangle_{A_1B_1} \otimes |\psi^+\rangle_{A_2B_2}, \quad (3.6)$$

which can be decomposed as

$$\begin{aligned}
|\Phi\rangle_{acA_1B_1A_2B_2} &= |\psi^+\rangle_{aA_1}|\psi^+\rangle_{cA_2}I \otimes I |\psi\rangle_{B_1B_2} + |\psi^+\rangle_{aA_1}|\psi^-\rangle_{cA_2}I \otimes Z |\psi\rangle_{B_1B_2} \\
&+ |\psi^+\rangle_{aA_1}|\phi^+\rangle_{cA_2}I \otimes X |\psi\rangle_{B_1B_2} + |\psi^+\rangle_{aA_1}|\phi^-\rangle_{cA_2}I \otimes iY |\psi\rangle_{B_1B_2} \\
&+ |\psi^-\rangle_{aA_1}|\psi^+\rangle_{cA_2}Z \otimes I |\psi\rangle_{B_1B_2} + |\psi^-\rangle_{aA_1}|\psi^-\rangle_{cA_2}Z \otimes Z |\psi\rangle_{B_1B_2} \\
&+ |\psi^-\rangle_{aA_1}|\phi^+\rangle_{cA_2}Z \otimes X |\psi\rangle_{B_1B_2} + |\psi^-\rangle_{aA_1}|\phi^-\rangle_{cA_2}Z \otimes iY |\psi\rangle_{B_1B_2} \\
&+ |\phi^+\rangle_{aA_1}|\psi^+\rangle_{cA_2}X \otimes I |\psi\rangle_{B_1B_2} + |\phi^+\rangle_{aA_1}|\psi^-\rangle_{cA_2}X \otimes Z |\psi\rangle_{B_1B_2} \\
&+ |\phi^+\rangle_{aA_1}|\phi^+\rangle_{cA_2}X \otimes X |\psi\rangle_{B_1B_2} + |\phi^+\rangle_{aA_1}|\phi^-\rangle_{cA_2}X \otimes iY |\psi\rangle_{B_1B_2} \\
&+ |\phi^-\rangle_{aA_1}|\psi^+\rangle_{cA_2}iY \otimes I |\psi\rangle_{B_1B_2} + |\phi^-\rangle_{aA_1}|\psi^-\rangle_{cA_2}iY \otimes Z |\psi\rangle_{B_1B_2} \\
&+ |\phi^-\rangle_{aA_1}|\phi^+\rangle_{cA_2}iY \otimes X |\psi\rangle_{B_1B_2} + |\phi^-\rangle_{aA_1}|\phi^-\rangle_{cA_2}iY \otimes iY |\psi\rangle_{B_1B_2}.
\end{aligned} \tag{3.7}$$

Eq. (3.7) clearly shows that Alice's Bell measurement on qubits  $aA_1$  and  $cA_2$  reduces Bob's qubits  $B_1B_2$  in such a quantum state that the state  $|\psi\rangle_{B_1B_2}$  can be obtained by applying local unitary operations. The choice of the unitary operations depends on the Alice's measurement outcome (as illustrated in Eq. (3.7)). After teleporting  $|\psi\rangle$ , in the third step, the initial state to be teleported is reconstructed from  $|\psi\rangle_{B_1B_2}$  by using six ancillary qubits prepared in  $(|0\rangle^{\otimes 6})_{BDEFGH}$  and the circuit block shown in the right side of Figure 3.1. At the output of this circuit block we would obtain the so called eight-qubit state  $|\phi\rangle_{B_1BB_2DEFGH}$  that we wanted to teleport.

### 3.3 Concluding remark

Despite the existence of old results of [9, 76, 94, 95, 116] and our recent results [85], people are frequently proposing teleportation schemes [22, 53, 131] and their variants [21] using higher amount of quantum resources, although they know that the preparation and maintenance of such resources are not easy. Specially, preparation of multi-partite entanglement is difficult. Keeping that in mind, it is advisable that while designing new schemes, unnecessary use of quantum resources should be circumvented. The analysis of Zhao et al., protocol performed here, and the possible improvement shown here is only an example. It is not restricted Zhao et al., protocol only. The main idea of it is applicable to many other schemes ([21, 22, 53, 85, 131] and references therein) as their amount of quantum resources used by them are higher than the minimum required amount.

# CHAPTER 4

## TELEPORTATION OF A QUBIT USING ENTANGLED NONORTHOGONAL STATES: A COMPARATIVE STUDY

### 4.1 Introduction

In the previous chapters, we have already observed that one of the most important resources for quantum information processing is entanglement, which is essential for various tasks of quantum communication and computation. In Chapter 1, we have briefly mentioned such tasks and have also introduced the notion of entangled nonorthogonal states. In fact, in Section 1.4.1.1, interesting applications of entangled nonorthogonal states have been reviewed briefly with a focus on the entangled coherent states. In this chapter, we aim to investigate the effect of non-orthogonality of an entangled nonorthogonal state-based quantum channel in detail in the context of the teleportation of a qubit.

In the context of the studies on the applications nonorthogonal entangled states in quantum communication, the concept of minimum assured fidelity (MASFI), which was claimed to correspond to the least value of possible fidelity for any given information, was introduced by Prakash et al. [71]. Subsequently, in a series of papers ([72, 252] and references therein), they have reported MASFI for various protocols of quantum communication, and specially for the imperfect teleportation. Here, it is important to note that Adhikari et al., [141] tried to extend the domain of the standard teleportation protocol to the case of performing teleportation using entangled nonorthogonal states. To be precise, they studied teleportation of an unknown quantum state by using a specific type of entangled nonorthogonal state as the quantum channel. They also established that the amount of nonorthogonality present in the quantum channel affects the average fidelity ( $F_{ave}$ ) of teleportation. However, their work was restricted to a specific type of entangled nonorthogonal state, and neither the optimality of the scheme nor the effect of noise on it was investigated by them. In fact, in their work no effort had been made to perform

a comparative study (in terms of different measures of teleportation quality) among possible quasi-Bell states that can be used as teleportation channel. Further, the works of Prakash et al., [71, 72, 252] and others ([253, 254] and references therein) have established that in addition to  $F_{ave}$ , minimum assured fidelity (MASFI) and minimum average fidelity (MAVFI), which we refer here as minimum fidelity (MFI) can be used as measures of quality of teleportation.

Keeping these points in mind, in the present chapter, we have studied the effect of the amount of nonorthogonality on  $F_{ave}$ , MFI, and MASFI for teleportation of a qubit using different quasi-Bell states, which can be used as the quantum channel. We have compared the performance of these quasi-Bell states as teleportation channel an ideal situation (i.e., in the absence of noise) and in the presence of various types of noise (e.g., AD and PD). The relevance of the choice of these noise models has been well established in the past ([78, 79, 94] and references therein). Further, using Horodecki et al.'s relation [255] between optimal fidelity ( $F_{opt}$ ) and maximal singlet fraction ( $f$ ), it is established that the entangled nonorthogonal state-based teleportation scheme investigated in the present work, is optimal for all the cases studied here (i.e., for all the quasi-Bell states).

The remaining part of the chapter is organized as follows. In Section 4.2, we briefly describe the mathematical structure of the entangled nonorthogonal states and how to quantify the amount of entanglement present in such states using concurrence. In this section, we have restricted ourselves to very short description as most of the expressions reported here are well known. However, they are required for the sake of a self-sufficient description. The main results of the present chapter are reported in Section 4.3, where we provide expressions for MASFI,  $F_{ave}$ , and  $f$  for all the four quasi-Bell states and establish  $F_{ave} = F_{opt}$  for all the quasi-Bell states, and deterministic perfect teleportation is possible with the help of quasi-Bell states. In Section 4.4, effects of AD and PD noise on  $F_{ave}$  is discussed for various alternative situations, and finally the chapter is concluded in Section 4.5.

## 4.2 Entangled nonorthogonal states

Basic mathematical structures of standard entangled states and entangled nonorthogonal states have been provided in detail in several papers ([2, 181] and references therein). Schmidt decomposition of an arbitrary bipartite state is written as

$$|\Psi\rangle = \sum_i p_i |a_i\rangle_A \otimes |b_i\rangle_B, \quad (4.1)$$

where  $p_i$ s are the real numbers such that  $\sum_i p_i^2 = 1$ . Further,  $\{|a_i\rangle_A\}$  ( $\{|b_i\rangle_B\}$ ) is the orthonormal basis of subsystem  $A$  ( $B$ ) in Hilbert space  $H_A$  ( $H_B$ ). The state  $|\Psi\rangle$  is entangled if at least two of the  $p_i$ s are non-zero. Here, we may note that a standard bipartite entangled state can be

expressed as

$$|\psi\rangle = \mu|a\rangle_A \otimes |b\rangle_B + \nu|c\rangle_A \otimes |d\rangle_B, \quad (4.2)$$

where  $\mu$  and  $\nu$  are two complex coefficients that ensure normalization by satisfying  $|\mu|^2 + |\nu|^2 = 1$  in case of orthogonal states;  $|a\rangle$  and  $|c\rangle$  are normalized states of the first system and  $|b\rangle$  and  $|d\rangle$  are normalized states of the second system, respectively. These states of the subsystems satisfy  $\langle a|c\rangle = 0$  and  $\langle b|d\rangle = 0$  for the conventional entangled states of orthogonal states and they satisfy  $\langle a|c\rangle \neq 0$  and  $\langle b|d\rangle \neq 0$  for the entangled nonorthogonal states. Thus, an entangled state involving nonorthogonal states, which is expressed in the form of Eq. (4.2), has the property that the overlaps  $\langle a|c\rangle$  and  $\langle b|d\rangle$  are nonzero, and the normalization condition would be

$$|\mu|^2 + |\nu|^2 + \mu\nu^*\langle c|a\rangle\langle d|b\rangle + \mu^*\nu\langle a|c\rangle\langle b|d\rangle = 1. \quad (4.3)$$

Here and in what follows, for simplicity, we have omitted the subsystems mentioned in the subscript.

The two nonorthogonal states of a given system are considered to be linearly independent. They are also assumed to span a 2D subspace of the Hilbert space. We may choose an orthonormal basis  $\{|0\rangle, |1\rangle\}$  as

$$|0\rangle = |a\rangle, |1\rangle = \frac{(|c\rangle - p_1|a\rangle)}{N_1}, \quad (4.4)$$

for System A, and similarly,  $|0\rangle = |d\rangle, |1\rangle = \frac{(|b\rangle - p_2|d\rangle)}{N_2}$  for System B, where  $p_1 = \langle a|c\rangle$ ,  $p_2 = \langle d|b\rangle$ , and  $N_i = \sqrt{1 - |p_i|^2} : i \in \{1, 2\}$ . Now, we can express the nonorthogonal entangled state  $|\psi\rangle$  described by Eq. (4.2) using the orthogonal basis  $\{|0\rangle, |1\rangle\}$  as follows

$$|\psi\rangle = a'|00\rangle + b'|01\rangle + c'|10\rangle, \quad (4.5)$$

with  $a' = (\mu p_2 + \nu p_1)N_{12}$ ,  $b' = (\mu N_2)N_{12}$ ,  $c' = (\nu N_1)N_{12}$ , where the normalization constant  $N_{12}$  is given by

$$N_{12} = [|\mu|^2 + |\nu|^2 + \mu\nu^*\langle c|a\rangle\langle d|b\rangle + \mu^*\nu\langle a|c\rangle\langle b|d\rangle]^{-\frac{1}{2}}. \quad (4.6)$$

Eq. (4.5) shows that an arbitrary entangled nonorthogonal state can be considered as a state of two logical qubits. Following standard procedure, the concurrence ( $C$ ) [256, 257] of the entangled state  $|\psi\rangle$  can be obtained as [182, 185, 258]

$$C = 2|b'c'| = \frac{2|\mu||\nu|\sqrt{(1 - |\langle a|c\rangle|^2)(1 - |\langle b|d\rangle|^2)}}{|\mu|^2 + |\nu|^2 + \mu\nu^*\langle c|a\rangle\langle d|b\rangle + \mu^*\nu\langle a|c\rangle\langle b|d\rangle}. \quad (4.7)$$

For the entangled state  $|\psi\rangle$  to be maximally entangled, we must have  $C = 1$ . Fu et al., [258], showed that the state  $|\psi\rangle$  is maximally entangled state if and only if one of the following conditions is satisfied: (i)  $|\mu| = |\nu|$  for the orthogonal case, and (ii)  $\mu = \nu e^{i\theta}$  and  $\langle a|c\rangle =$

**Table 4.1:** Bell states and the corresponding quasi-Bell states. The table shows that the quasi-Bell states can be expressed in orthogonal basis and it introduces the notation used in this chapter. Here,  $|\psi^\pm\rangle = \frac{1}{\sqrt{2}}(|00\rangle \pm |11\rangle)$ ,  $|\phi^\pm\rangle = \frac{1}{\sqrt{2}}(|01\rangle \pm |10\rangle)$ ,  $\eta = \frac{2re^{i\theta}}{\sqrt{2(1+r^2)}}$ ,  $\varepsilon = \sqrt{\frac{1-r^2}{2(1+r^2)}}$ ,  $k_\pm = \frac{1 \pm r^2 e^{2i\theta}}{\sqrt{2(1 \pm r^2 \cos 2\theta)}}$ ,  $l_\pm = \frac{(\sqrt{1-r^2})re^{i\theta}}{\sqrt{2(1 \pm r^2 \cos 2\theta)}}$ ,  $m_\pm = \frac{1-r^2}{\sqrt{2(1 \pm r^2 \cos 2\theta)}}$ ,  $N_\pm = [2(1 \pm |\langle a|b\rangle|^2)]^{\frac{-1}{2}}$ , and  $M_\pm = \frac{1}{\sqrt{2(1 \pm r^2 \cos 2\theta)}}$  represent the normalization constant.

S. No.	Bell state	Corresponding quasi-Bell state (i.e., Bell-like entangled nonorthogonal state having a mathematical form analogous to the usual Bell state given in the 2nd column of the same row)	State in orthogonal basis that is equivalent to the quasi-Bell state mentioned in the 3rd column of the same row
1.	$ \psi_1\rangle =  \psi^+\rangle$	$ \psi_+\rangle = M_+( a\rangle \otimes  a\rangle +  b\rangle \otimes  b\rangle)$	$ \psi_+\rangle = k_+ 00\rangle + l_+ 01\rangle + l_+ 10\rangle + m_+ 11\rangle$
2.	$ \psi_2\rangle =  \psi^-\rangle$	$ \psi_-\rangle = M_-( a\rangle \otimes  a\rangle -  b\rangle \otimes  b\rangle)$	$ \psi_-\rangle = k_- 00\rangle - l_- 01\rangle - l_- 10\rangle - m_- 11\rangle$
3.	$ \psi_3\rangle =  \phi^+\rangle$	$ \phi_+\rangle = N_+( a\rangle \otimes  b\rangle +  b\rangle \otimes  a\rangle)$	$ \phi_+\rangle = \eta 00\rangle + \varepsilon 01\rangle + \varepsilon 10\rangle$
4.	$ \psi_4\rangle =  \phi^-\rangle$	$ \phi_-\rangle = N_-( a\rangle \otimes  b\rangle -  b\rangle \otimes  a\rangle)$	$ \phi_-\rangle = \frac{1}{\sqrt{2}}( 01\rangle -  10\rangle)$

$-\langle b|d\rangle^* e^{i\theta}$  for the nonorthogonal states, where  $\theta$  is a real parameter.

Before we investigate the teleportation capacity of the entangled nonorthogonal states, we would like to note that if we choose  $\mu = \nu$  in Eq. (4.2), then for the case of orthogonal basis, normalization condition will ensure that  $\mu = \nu = \frac{1}{\sqrt{2}}$ , and the state  $|\psi\rangle$  will reduce to a standard Bell state  $|\phi^+\rangle = \frac{1}{\sqrt{2}}(|01\rangle + |10\rangle)$ , and its analogous state under the same condition (i.e., for  $\mu = \nu$ ) in nonorthogonal basis would be  $|\phi_+\rangle = N_+(|a\rangle \otimes |b\rangle + |b\rangle \otimes |a\rangle)$ , where  $N_+$  is the normalization constant. In analogy to  $|\phi^+\rangle$  its analogous entangled nonorthogonal state is denoted as  $|\phi_+\rangle$  and referred to as quasi-Bell state [191]. Similarly, in analogy with the other three Bell states  $|\phi^-\rangle = \frac{1}{\sqrt{2}}(|01\rangle - |10\rangle)$ ,  $|\psi^+\rangle = \frac{1}{\sqrt{2}}(|00\rangle + |11\rangle)$ , and  $|\psi^-\rangle = \frac{1}{\sqrt{2}}(|00\rangle - |11\rangle)$ , we can obtain entangled nonorthogonal states denoted by  $|\phi_-\rangle$ ,  $|\psi_+\rangle$ , and  $|\psi_-\rangle$ , respectively. In addition to these notations, in what follows we also use  $|\psi^+\rangle = |\psi_1\rangle$ ,  $|\psi^-\rangle = |\psi_2\rangle$ ,  $|\phi^+\rangle = |\psi_3\rangle$ ,  $|\phi^-\rangle = |\psi_4\rangle$ . Four entangled nonorthogonal states  $\{|\psi_\pm\rangle, |\phi_\pm\rangle\}$ , which are used in this thesis, are usually referred to as quasi-Bell states [191]. They are not essentially maximally entangled, and they may be expressed in orthogonal basis (see last column of Table 4.1). Notations used in the rest of the chapter, expansion of the quasi-Bell states in orthogonal basis, etc., are summarized in Table 4.1, where we can see that  $|\psi_4\rangle = |\phi^-\rangle$  is equivalent to  $|\phi_-\rangle$ , and thus  $|\phi_-\rangle$  is always maximally entangled and can lead to perfect deterministic teleportation as can be done using usual Bell states. So  $|\phi_-\rangle$  is not a state of interest in noiseless case. Keeping this in mind, in the next section, we mainly concentrate on the properties related to the teleportation capacity of the other three quasi-Bell states. However, in Section 4.4, we would discuss the effect of noise on all four quasi-Bell states.

In what follows, we aim to perform a rigorous and comparative investigation of the suitability of using quasi-Bell states described in Table 4.1 as teleportation channel. Before we do so,

it would be apt to note that some studies [71, 72, 74, 101, 141, 252] have already reported teleportation schemes using quasi-Bell states, but those studies lack the required rigor as they could not put light on various important facets of the task. Specifically, we may note that Adhikari et al., [141] showed that it is possible to perform teleportation using  $|\phi_+\rangle$ . Interestingly, they showed that the amount of nonorthogonality present in the quantum channel affects the average fidelity ( $F_{ave}$ ) of teleportation. However, their work was restricted to the use of  $|\phi_+\rangle$  as a quantum channel for teleportation. They did not check the suitability of other quasi-Bell states as quantum channels for teleportation. Naturally, the study did not lead to a comparison between different quasi-Bell states. Further, in all realistic situations, it is impossible to circumvent the noise present in the transmission channel. However, they did not try to study the effect of noise. In fact, the optimality of the scheme was not also investigated by them. Such limitations were also present in some of the earlier works. Specifically, in Ref. [74], MASFI and MFI were calculated for non-maximally entangled quantum channels that were used to teleport an unknown state which was reconstructed by the receiver using a set of suitable unitary operations. The focus of the authors of Ref. [74] was to only obtain compact expressions of MASFI and MFI in terms of concurrence of the non-maximally entangled state in ideal (noiseless) conditions. They neither tried to compute  $F_{ave}$  and use that to quantify the quality of teleportation, and thus to obtain a comparison among various possible entangled-nonorthogonal-state-based channels, nor did they try to establish the optimality of their scheme. We have used the compact expression of MASFI obtained in Ref. [74], but for the computation of MFI we have used Pauli operations in analogy with the standard single-qubit teleportation scheme that uses Bell states; this is in contrast to the MFI result reported in Ref. [74] using optimized unitary operations. Teleportation of a coherent superposition state using one of the quasi-Bell states was performed in the past, and the decay in the amount of entanglement of the quantum channel was investigated by solving master equation [101]. The same state was teleported using another quasi-Bell state as quantum channel and considering the channel as a lossy channel in Ref. [252]. A similar study for two-mode coherent states has been performed using tripartite entangled coherent state in noiseless [71] and noisy [72] environments, too. It is relevant to note here that the focus of all these earlier works was to teleport a state in ideal or noisy environment using an entangled nonorthogonal state. However, we wish to perform a comparative study among a set of entangled nonorthogonal states (quasi-Bell states) in both these conditions, and also wish to test the optimality of such schemes.

### 4.3 Teleportation using entangled nonorthogonal state

Let us consider that an arbitrary single-qubit quantum state

$$|I\rangle = \alpha|0\rangle + \beta|1\rangle : \quad |\alpha|^2 + |\beta|^2 = 1, \quad (4.8)$$



is to be teleported using the quasi-Bell state

$$|\psi_{\pm}\rangle = N_{\pm}(|a\rangle \otimes |b\rangle \pm |b\rangle \otimes |a\rangle), \quad (4.9)$$

where the normalization constant  $N_{\pm} = [2(1 \pm |\langle a|b\rangle|^2)]^{-\frac{1}{2}}$ . These quasi-Bell states may be viewed as particular cases of Eq. (4.2) with  $|d\rangle = |a\rangle$ ,  $|c\rangle = |b\rangle$ , and  $\mu = \pm v$ . In general,  $\langle a|b\rangle$  is a complex number, and consequently, we can write

$$\langle a|b\rangle = re^{i\theta}, \quad (4.10)$$

where the real parameters  $r$  and  $\theta$ , respectively, denote the modulus and argument of the complex number  $\langle a|b\rangle$  with  $0 \leq r \leq 1$  and  $0 \leq \theta \leq 2\pi$ . As  $r = 0$  implies, orthogonal basis, we may consider this parameter as the primary measure of nonorthogonality. This is so because no value of  $\theta$  will lead to orthogonality condition. Further, for  $r \neq 0$ , we can consider  $\theta$  as a secondary measure of nonorthogonality. Now, using Eq. (4.10), and the map between orthogonal and nonorthogonal bases we may rewrite Eq. (4.4) as

$$|0\rangle = |a\rangle \text{ and } |1\rangle = \frac{[|b\rangle - \langle a|b\rangle a]}{\sqrt{1-r^2}}. \quad (4.11)$$

Thus, we have  $|a\rangle = |0\rangle$  and  $|b\rangle = \langle a|b\rangle|0\rangle + \sqrt{1-r^2}|1\rangle$ , and consequently,  $|\phi_{+}\rangle$  can now be expressed as

$$|\phi_{+}\rangle = \eta|00\rangle + \varepsilon|01\rangle + \varepsilon|10\rangle, \quad (4.12)$$

where  $\eta = \frac{2re^{i\theta}}{\sqrt{2(1+r^2)}}$  and  $\varepsilon = \sqrt{\frac{1-r^2}{2(1+r^2)}}$ . This is already noted in Table 4.1, where we have also noted that if we express  $|\phi_{-}\rangle$  in  $\{|0\rangle, |1\rangle\}$  basis, we obtain the Bell state  $|\phi_{-}\rangle = \frac{1}{\sqrt{2}}(|01\rangle - |10\rangle)$ , which is maximally entangled and naturally yields unit fidelity for teleportation. It's not surprising to obtain maximally entangled nonorthogonal states, as in [185] it has been already established that there exists a large class of bipartite entangled nonorthogonal states that are maximally entangled under certain conditions.

Using Eq. (4.7), we found the concurrence of the symmetric state  $|\phi_{+}\rangle$  as

$$C(|\phi_{+}\rangle) = \frac{1 - |\langle a|b\rangle|^2}{1 + |\langle a|b\rangle|^2} = \frac{1 - r^2}{1 + r^2}. \quad (4.13)$$

Clearly,  $|\phi_{+}\rangle$  is not maximally entangled unless  $r = |\langle a|b\rangle| = 0$ , which implies orthogonality. Thus, all quasi-Bell states of the form  $|\phi_{+}\rangle$  are non-maximally entangled. Now, if the state  $|\phi_{+}\rangle$  is used as quantum channel, then following Prakash et al., [74] we may express the MASFI for teleportation of single-qubit state (4.8) as

$$(\text{MASFI})_{\phi_{+}} = \frac{2C(|\phi_{+}\rangle)}{1+C(|\phi_{+}\rangle)} = 1 - r^2. \quad (4.14)$$

Since the value of  $r$  lies between 0 and 1, the  $(\text{MASFI})_{\phi_+}$  decreases continuously as  $r$  increases. For orthogonal state  $r=0$ , and thus,  $\text{MASFI} = 1$ . Thus, we may conclude that the quasi-Bell state  $|\phi_+\rangle$  will never lead to deterministic perfect teleportation. However, its Bell state counter part ( $r = 1$  case) leads to deterministic perfect teleportation. Here, it would be apt to note that for teleportation of a single-qubit state using  $|\phi_+\rangle$  as the quantum channel, average teleportation fidelity can be obtained as [141]

$$F_{ave,\phi_+} = \frac{3 - r^2}{3(1 + r^2)}. \quad (4.15)$$

This is obtained by computing teleportation fidelity  $F^{tel} = \sum_{i=1}^4 P_i |\langle I|\zeta_i\rangle|^2$ , where  $|I\rangle$  is the input state, and  $P_i = \text{Tr}(\langle\Omega|M_i|\Omega\rangle)$  with  $|\Omega\rangle = |I\rangle \otimes |\psi_{\text{channel}}\rangle$ , and  $M_i = |\psi_i\rangle\langle\psi_i|$  is a measurement operator in Bell basis ( $|\psi_i\rangle$ s are defined in the second column of Table 4.1), and  $|\zeta_i\rangle$  is the teleported state corresponding to  $i$ th projective measurement in Bell basis. Interestingly,  $F^{tel}$  is found to depend on the parameters of the state to be teleported (cf. Eq. (11) of Ref. [141]). Thus, if we use Bloch representation and express the state to be teleported as  $|I\rangle = \alpha|0\rangle + \beta|1\rangle = \cos\frac{\theta'}{2}|0\rangle + \exp(i\phi')\sin\frac{\theta'}{2}|1\rangle$ , then the teleportation fidelity  $F^{tel}$  will be a function of state parameters  $\theta'$  and  $\phi'$  (here  $'$  is used to distinguish the state parameter  $\theta'$  from the nonorthogonality parameter  $\theta$ ). An average fidelity is obtained by taking average over all possible states that can be teleported, i.e., by computing  $F_{ave} = \frac{1}{4\pi} \int_{\phi'=0}^{2\pi} \int_{\theta'=0}^{\pi} F^{tel}(\theta', \phi') \sin(\theta') d\theta' d\phi'$ . This definition of average fidelity is followed in [39, 141] and in this thesis. However, in the works of Prakash et al., ([71, 72, 252] and references therein),  $|\langle I|\zeta_i\rangle|^2$  was considered as fidelity and  $F^{tel}$  as average fidelity. They minimized  $F^{tel}$  over the parameters of the state to be teleported and referred to the obtained fidelity as the MAVFI. As that notation is not consistent with the definition of average fidelity used here. In what follows, we will refer to the minimum value of  $F^{tel}$  as MFI, but it would be the same as MAVFI defined by Prakash et al. Further, we would like to note that in [141] and in the present chapter, it is assumed that a standard teleportation scheme is implemented by replacing a Bell state by its partner quasi-Bell state, and as a consequence for a specific outcome of Bell measurement of Alice, Bob applies the same Pauli operator for teleportation channel  $|\psi_x\rangle$  or  $|\phi_x\rangle$  (which is a quasi-Bell state) as he used to do for the corresponding Bell state  $|\psi^x\rangle$  or  $|\phi^x\rangle$ , where  $x \in \{+, -\}$ . However, the expression of MASFI used here (see Eq. (4.14)) and derived in [74] are obtained using an optimized set of unitary (cf. discussion after Eq. (10) in Ref. [74]) and are subjected to outcome of Bell measurement of Alice, thus no conclusions should be made by comparing MASFI with MFI or  $F_{ave}$ .

From Eqs. (4.14) and (4.15), we can see that for a standard Bell state  $|\phi^+\rangle$  (i.e., when  $r = 0$ ),  $(\text{MASFI})_{\phi_+} = F_{ave} = 1$ . However, for  $r = 1$ ,  $(\text{MASFI})_{\phi_+} = 0$ , and  $F_{ave} = \frac{1}{3}$ . Thus, we conclude that for a standard Bell state both MASFI and average teleportation fidelity have the

same value. This is not surprising, as for  $r=0$  the entangled state  $|\phi_+\rangle$  becomes maximally entangled. However, for  $r \neq 0$ , this state is non-maximally entangled, and interestingly, for  $r=1$ , we obtain  $\text{MASFI} = 0$ , whereas  $F_{ave}$  is nonzero. We have already noted that no comparison of  $\text{MASFI}$  and  $F_{ave}$  obtained as above should be made as that may lead to confusing results. Here we give an example, according to [71, 74],  $\text{MASFI}$  is the least possible value of the fidelity, but for certain values of  $r$ , we can observe that  $\text{MASFI} > F_{ave}$ . For example, for  $r = 0.5$ , we obtain  $\text{MASFI} = 0.75$ , whereas  $F_{ave} = 0.733$ . Clearly, minimum found in computation of  $\text{MASFI}$ , and the average found in the computation of  $F_{ave}$  is not performed over the same data set, specifically not using the same teleportation mechanism (same unitary operations at the receiver's end).

Now we may check the optimality of the teleportation scheme by using the criterion introduced by Horodecki et al., in Ref. [255]. According to this criterion optimal average fidelity that can be obtained for a teleportation scheme which uses a bipartite entangled quantum state  $\rho$  as the quantum channel is

$$F_{opt} = \frac{2f+1}{3}, \quad (4.16)$$

where  $f$  is the maximal singlet fraction defined as

$$f = \max_i \langle \psi_i | \rho | \psi_i \rangle, \quad (4.17)$$

where  $|\psi_i\rangle$ :  $i \in \{1,2,3,4\}$  is Bell state described above and summarized in Table 4.1. As we are interested in computing  $f$  for quasi-Bell states which are pure states, we can write  $f = \max_i |\langle \psi_i | \chi \rangle|^2$ , where  $|\chi\rangle$  is a quasi-Bell state. A bit of calculation yields that maximal singlet fraction for the quasi-Bell state  $|\phi_+\rangle$  is

$$f_{\phi_+} = \frac{1-r^2}{1+r^2}. \quad (4.18)$$

Now using (4.15), (4.16) and (4.18), we can easily observe that

$$F_{opt, \phi_+} = \frac{2\left(\frac{1-r^2}{1+r^2}\right) + 1}{3} = \frac{3-r^2}{3(1+r^2)} = F_{ave}. \quad (4.19)$$

Thus, a quasi-Bell state-based teleportation scheme which is analogous to the usual teleportation scheme, but uses a quasi-Bell state  $|\phi_+\rangle$  as the quantum channel is optimal. We can also minimize  $F_{\phi_+}^{tel}(\theta', \phi')$  with respect to  $\theta'$  and  $\phi'$  to obtain

$$\text{MFI}_{\phi_+} = \frac{1-r^2}{1+r^2}, \quad (4.20)$$

which is incidentally equivalent to maximal singlet fraction in this case.

So far we have reported analytic expressions for some parameters (e.g.,  $F_{ave}$ ,  $\text{MASFI}$ , and

MFI) that can be used as measures of the quality of a teleportation scheme realized using the teleportation channel  $|\phi_+\rangle$  and have shown that the teleportation scheme obtained using  $|\phi_+\rangle$  is optimal. Among these analytic expressions,  $F_{ave,\phi_+}$  was already reported in [141]. Now, to perform a comparative study, let us consider that the teleportation is performed using one of the remaining two quasi-Bell states of our interest (i.e., using  $|\psi_+\rangle$  or  $|\psi_-\rangle$ ) described in Table 4.1) as quantum channel. In that case, we would obtain the concurrence as

$$C(|\psi_{\pm}\rangle) = 2|\pm k_{\pm}m_{\pm} - l_{\pm}^2| = \frac{1-r^2}{(1 \pm r^2 \cos 2\theta)}. \quad (4.21)$$

Clearly, in contrast to  $C|\phi_+\rangle$ , which was only  $r$  dependent, the concurrence  $C(|\psi_{\pm}\rangle)$  depends on both the parameters  $r$  and  $\theta$ . From Eq. (4.21) it is clear that at  $\theta = \frac{\pi}{2}, \frac{3\pi}{2}$  ( $\theta = 0, \pi$ ) quasi-Bell state  $|\psi_+\rangle$  ( $|\psi_-\rangle$ ) is maximally entangled, even though the states  $|a\rangle$  and  $|b\rangle$  are nonorthogonal as  $r \neq 0$ . Thus, at these points, states  $|\psi_{\pm}\rangle$  are maximally entangled. If quantum state  $|\psi_+\rangle$  is used as quantum channel, then MASFI for teleportation of an arbitrary single-qubit information state (4.8) would be

$$(\text{MASFI})_{\psi_+} = \frac{2C(|\psi_+\rangle)}{1+C(|\psi_+\rangle)} = \frac{1-r^2}{1-r^2 \sin^2 \theta}, \quad (4.22)$$

and similarly, that for quasi-Bell state  $|\psi_-\rangle$  would be

$$(\text{MASFI})_{\psi_-} = \frac{1-r^2}{1-r^2 \cos^2 \theta}. \quad (4.23)$$

Thus, the expressions for MASFI are also found to depend on both  $r$  and  $\theta$ . Clearly, at  $\theta = \frac{\pi}{2}$  and  $\frac{3\pi}{2}$ ,  $(\text{MASFI})_{\psi_+} = 1$ , and hence for these particular choices of  $\theta$ , entangled nonorthogonal state  $|\psi_+\rangle$  leads to the deterministic perfect teleportation of single-qubit information state. Clearly, for these values of  $\theta$ ,  $C(|\psi_+\rangle) = 1$ , indicating maximal entanglement. However, the entangled state is still nonorthogonal as  $r$  can take any of its allowed values. Similarly, at  $\theta = 0$  and  $\pi$ ,  $(\text{MASFI})_{\psi_-} = 1$ , and hence the entangled state  $|\psi_-\rangle$  of the nonorthogonal states  $|a\rangle$  and  $|b\rangle$  leads to deterministic perfect teleportation in these conditions. Thus, deterministic perfect teleportation is possible using quasi-Bell states  $|\phi_-\rangle$  or  $|\psi_{\pm}\rangle$  as quantum channels for teleportation, but it is not possible with  $|\phi_+\rangle$  unless it reduces to its orthogonal state counter part (i.e.,  $|\phi^+\rangle$ ). We may now compute the average fidelity for  $|\psi_{\pm}\rangle$ , by using the procedure adopted above for  $|\phi_+\rangle$  and obtain

$$F_{ave,\psi_{\pm}} = \frac{3 - 2r^2 + r^4 \mp r^2(r^2 - 3) \cos 2\theta}{3(1 \pm r^2 \cos 2\theta)}. \quad (4.24)$$

Now, we would like to compare the average fidelity expressions obtained so far for various values of nonorthogonality parameters for all the quasi-Bell states. The same is illustrated

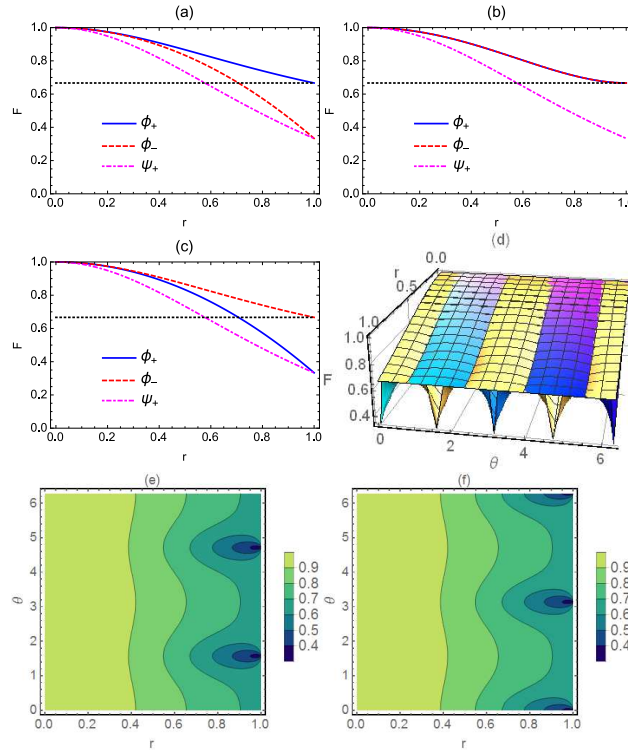


**Figure 4.1:** The dependence of the average fidelity on nonorthogonality parameters ( $r, \theta$ ) is illustrated via 2D and 3D plots. Plots (a), (b) and (c) are showing the variation of  $F$  with  $r$  for  $\theta = 0, \frac{\pi}{4},$  and  $\frac{\pi}{2}$ , respectively and in these plots the horizontal dotted black line corresponds to classical fidelity. Similarly, (d) shows the variation of  $F$  in 3D for both  $\psi_+$  and  $\psi_-$  in light (yellow) and dark (blue) colored surface plots, respectively. The same fact is illustrated using contour plots for both of these cases in (e) and (f). Note that the quantity plotted in this and the following figures is  $F_{ave}$ , which is mentioned as  $F$  in the y-axis.

in Figure 4.1. Specifically, in Figures 4.1 (a)-(c) we have shown the dependence of average fidelity on secondary nonorthogonality parameter ( $\theta$ ) using a set of plots for its variation with primary nonorthogonality parameter ( $r$ ). This establishes that the primary nonorthogonality parameter has more control over the obtained average, fidelity but a secondary parameter is also prominent enough to change the choice of quasi-Bell state to be preferred for specific value of primary nonorthogonality parameter. Thus, the amount of nonorthogonality plays a crucial role in deciding which quasi-Bell state would provide highest average fidelity for a teleportation scheme implemented using quasi-Bell state as the teleportation channel. Further, all these plots also establish that there is always a quasi-Bell state apart from  $|\phi_{-}\rangle$ , which has average fidelity more than classically achievable fidelity ( $\frac{2}{3}$ ) for all values of  $r$ . We may now further illustrate the dependence of the average fidelity on both nonorthogonality parameters via 3 D and contour plots shown in Figures 4.1 (d), (e) and (f). These plots establish that the average fidelity of  $|\psi_{+}\rangle$  state increases for the values of  $\theta$  for which  $|\psi_{-}\rangle$  decreases, and vice-versa.

We can now establish the optimality of the teleportation scheme implemented using  $|\psi_{\pm}\rangle$  by computing average fidelity and maximal singlet fraction for these channels. Specifically, computing the maximal singlet fraction using the standard procedure described above, we have obtained

$$f_{\psi_{\pm}} = \frac{2 - 2r^2 + r^4 \pm \cos 2\theta(2r^2 - r^4)}{2(1 \pm r^2 \cos 2\theta)}. \quad (4.25)$$

Using Horodecki et al., criterion (4.16), and Eq. (4.24)-(4.25), we can easily verify that  $F_{ave, \psi_{\pm}} = F_{opt, \psi_{\pm}}$ . Thus, the teleportation scheme realized using any of the quasi-Bell state are optimal. However, they are not equally efficient for a specific choice of nonorthogonality parameter as we have already seen in Figure 4.1. This motivates us to further compare the performances of these quasi-Bell states as a potential quantum channel for teleportation. For the completeness of the comparative investigation of the teleportation efficiencies of different quasi-Bell states here we would also like to report MFI that can be achieved using different quasi-Bell states. The same can be computed as above, and the computation leads to following analytic expressions of MFI for  $|\psi_{\pm}\rangle$ :

$$\text{MFI}_{\psi_{+}} = \frac{1}{2}|k_{+} + m_{+}|^2 = \frac{1-r^2(2-r^2)\sin^2\theta}{1+r^2\cos 2\theta}, \quad (4.26)$$

and

$$\text{MFI}_{\psi_{-}} = \frac{1}{2}|k_{-} + m_{-}|^2 = \frac{1-r^2(2-r^2)\cos^2\theta}{1-r^2\cos 2\theta}. \quad (4.27)$$

Interestingly, the comparative analysis performed with the expressions of MFI using their variation with various parameters led to quite similar behavior as observed for  $F_{ave}$  in Figure 4.1. Therefore, we are not reporting corresponding figures obtained for MFI.

## 4.4 Effect of noise on average fidelity

In this section, we would like to analyze and compare the average fidelity obtained for each quasi-Bell state over two well known Markovian channels, i.e., AD and PD channels. Specifically, in open quantum system formalism, a quantum state evolving under a noisy channel can be written in terms of Kraus operators as we have defined in Section 1.6 of Chapter 1.

To analyze the feasibility of quantum teleportation scheme using quasi-Bell states and to compute the average fidelity we use Eqs. (1.4) and (1.5) in Eq. (1.3). Subsequently, the effect of noise is quantified by computing "fidelity" between the quantum state which has been actually evolved under the noisy channel under consideration and the quantum state Alice wished to teleport (say  $\rho = |I\rangle\langle I|$ ). Mathematically,

$$F_k = \frac{1}{4\pi} \int_{\phi'=0}^{2\pi} \int_{\theta'=0}^{\pi} \left( \sum_{i=1}^4 P_i \langle I | \{ \rho_k(\theta', \phi') \}_i | I \rangle \right) \sin(\theta') d\theta' d\phi', \quad (4.28)$$

which is the square of the conventional fidelity expression, and  $\rho_k$  is the quantum state recovered at the Bob's port under the noisy channel  $k \in \{AD, PD\}$ . Further, details of the mathematical technique adopted here can be found in some of our group's recent works on secure [78, 79, 259] and insecure quantum communication [94, 136].

We will start with the simplest case, where we assume that only Bob's part of the quantum channel is subjected to either AD or PD noise. The assumption is justified as the quasi-Bell state used as quantum channel is prepared locally (here assumed to be prepared by Alice) and shared afterwards. During Alice to Bob transmission of an entangled qubit, it may undergo decoherence, but the probability of decoherence is much less for the other qubits that don't travel through the channel (remain with Alice). Therefore, in comparison of the Bob's qubits, the Alice's qubits or the quantum state to be teleported  $|I\rangle$ , which remain at the sender's end, are hardly affected due to noise. The effect of AD noise under similar assumptions has been analyzed for three-qubit GHZ and W states in the recent past [211]. The average fidelity for all four quasi-Bell states, when Bob's qubit is subjected to AD channel while the qubits not traveling through the channel are assumed to be unaffected due to noise, is obtained as

$$\begin{aligned} F_{AD}^{|\psi_+\rangle} &= \frac{-1}{2(3+3r^2 \cos 2\theta)} \left[ -4 + r^2 (2 + 2\sqrt{1-\eta} - 3\eta) - 2\sqrt{1-\eta} \right. \\ &\quad \left. + 2r^4(-1 + \eta) + \eta + 2r^2(-2 - \sqrt{1-\eta} + r^2\sqrt{1-\eta}) \cos 2\theta \right], \\ F_{AD}^{|\psi_-\rangle} &= \frac{1}{-6+6r^2 \cos 2\theta} \left[ -4 + r^2 (2 + 2\sqrt{1-\eta} - 3\eta) - 2\sqrt{1-\eta} \right. \\ &\quad \left. + 2r^4(-1 + \eta) + \eta - 2r^2(-2 - \sqrt{1-\eta} + r^2\sqrt{1-\eta}) \cos 2\theta \right], \\ F_{AD}^{|\phi_+\rangle} &= \frac{4+2\sqrt{1-\eta}-\eta+r^2(-2\sqrt{1-\eta}+\eta)}{6(1+r^2)}, \\ F_{AD}^{|\phi_-\rangle} &= \frac{1}{6} [(4 + 2\sqrt{1-\eta} - \eta)]. \end{aligned} \quad (4.29)$$

Here and in what follows, the subscript of fidelity  $F$  corresponds to noise model and superscript represents the choice of quasi-Bell state used as teleportation channel. Similarly, all the average fidelity expressions when Bob's qubit is subjected to PD noise can be obtained as

$$\begin{aligned}
F_{PD}^{|\psi_+\rangle} &= \frac{1}{3} \left[ 2 + \sqrt{1-\eta} + r^2 \left( -\sqrt{1-\eta} + \frac{-1+r^2}{1+r^2 \cos 2\theta} \right) \right], \\
F_{PD}^{|\psi_-\rangle} &= \frac{1}{3} \left[ 2 + \sqrt{1-\eta} - r^2 \sqrt{1-\eta} + \frac{r^2-r^4}{-1+r^2 \cos 2\theta} \right], \\
F_{PD}^{|\phi_+\rangle} &= \frac{2+\sqrt{1-\eta}-r^2\sqrt{1-\eta}}{3+3r^2}, \\
F_{PD}^{|\phi_-\rangle} &= \frac{1}{3} [2 + \sqrt{1-\eta}].
\end{aligned} \tag{4.30}$$

It is easy to observe that for  $\eta = 0$  (i.e., in the absence of noise) the average fidelity expressions listed in Eqs. (4.29) and (4.30) reduce to the average fidelity expressions corresponding to each quasi-Bell state reported in Section 4.3. This is expected and can also be used to check the accuracy of our calculation.

It would be interesting to observe the change in fidelity when we consider the effect of noise on Alice's qubit as well. Though, it remains at Alice's port until she performs measurement on it in suitable basis, but in a realistic situation Alice's qubit may also interact with its surroundings in the meantime. Further, it can be assumed that the state intended to be teleported is prepared and teleported immediately. Therefore, it is hardly affected due to noisy environment. Here, without loss of generality, we assume that the decoherence rate for both the qubits is same. Using the same mathematical formalism adopted beforehand, we have obtained the average fidelity expressions for all the quasi-Bell states when both the qubits in the quantum channel are affected by AD noise with the same decoherence rate. The expressions are

$$\begin{aligned}
F_{AD}^{|\psi_+\rangle} &= \frac{1}{3+3r^2 \cos 2\theta} [3 - 2r^2(-1+\eta)^2 + r^4(-1+\eta)^2 - 2\eta \\
&\quad + \eta^2 + r^2(3+r^2(-1+\eta) - \eta) \cos 2\theta], \\
F_{AD}^{|\psi_-\rangle} &= -\frac{1}{-3+3r^2 \cos 2\theta} [3 - 2r^2(-1+\eta)^2 + r^4(-1+\eta)^2 + (-2+\eta)\eta \\
&\quad + r^2(-3-r^2(-1+\eta) + \eta) \cos 2\theta], \\
F_{AD}^{|\phi_+\rangle} &= \frac{3-2\eta+r^2(-1+2\eta)}{3(1+r^2)}, \\
F_{AD}^{|\phi_-\rangle} &= 1 - \frac{2\eta}{3}.
\end{aligned} \tag{4.31}$$

Similarly, the average fidelity expressions when both the qubits evolve under PD channel instead of AD channel are



$$\begin{aligned}
F_{PD}^{|\psi_+\rangle} &= \frac{1}{3} \left[ 3 - \eta + r^2 \left( -1 + \eta + \frac{-1+r^2}{1+r^2 \cos 2\theta} \right) \right], \\
F_{PD}^{|\psi_-\rangle} &= \frac{1}{3} \left[ 3 + r^2(-1 + \eta) - \eta + \frac{r^2-r^4}{-1+r^2 \cos 2\theta} \right], \\
F_{PD}^{|\phi_+\rangle} &= \frac{3+r^2(-1+\eta)-\eta}{3(1+r^2)}, \\
F_{PD}^{|\phi_-\rangle} &= 1 - \frac{\eta}{3}.
\end{aligned} \tag{4.32}$$

Finally, it is worth analyzing the effect of noisy channels on the feasibility of the teleportation scheme, when even the state to be teleported is also subjected to the same noisy channel. The requirement of this discussion can be established as it takes finite time before operations to teleport the quantum state are performed. Meanwhile, the qubit gets exposed to its vicinity and this interaction may lead to decoherence. Here, for simplicity, we have considered the same noise model for the state to be teleported as for the quantum channel. We have further assumed the same rate of decoherence for all the three qubits. Under these specific conditions, when all the qubits evolve under AD channels, the average fidelity for each quasi-Bell state turns out to be

$$\begin{aligned}
F_{AD}^{|\psi_+\rangle} &= \frac{-1}{2(3+3r^2 \cos 2\theta)} \left[ -4 + r^2 (2 + 2\sqrt{1-\eta} - 3\eta) - 2\sqrt{1-\eta} + 2r^4(-1 + \eta) \right. \\
&\quad \left. + \eta + 2r^2 (-2 - \sqrt{1-\eta} + r^2\sqrt{1-\eta}) \cos 2\theta \right], \\
F_{AD}^{|\psi_-\rangle} &= \frac{1}{2(-3+3r^2 \cos 2\theta)} \left[ -2 (2 + \sqrt{1-\eta}) + \eta (3 + 2\sqrt{1-\eta} + 2(-2 + \eta)\eta) \right. \\
&\quad - 2r^2(-1 + \eta) (1 + \sqrt{1-\eta} + \eta(-3 + 2\eta)) + 2r^4(-1 + \eta)^3 \\
&\quad \left. + r^2 (4 + 2\sqrt{1-\eta} + 2\sqrt{1-\eta} (r^2(-1 + \eta) - \eta) - \eta) \cos 2\theta \right], \\
F_{AD}^{|\phi_+\rangle} &= \frac{1}{6(1+r^2)} \left[ 2 (2 + \sqrt{1-\eta}) + \eta (-3 - 2\sqrt{1-\eta} + 2\eta) \right. \\
&\quad \left. + r^2 (-2\sqrt{1-\eta} + (5 + 2\sqrt{1-\eta} - 2\eta)\eta) \right], \\
F_{AD}^{|\phi_-\rangle} &= \frac{1}{6} \left[ 4 + 2\sqrt{1-\eta} - 3\eta - 2\sqrt{1-\eta}\eta + 2\eta^2 \right].
\end{aligned} \tag{4.33}$$

Similarly, when all three qubits are subjected to PD noise with the same decoherence rate, the analytic expressions of the average fidelity are obtained as

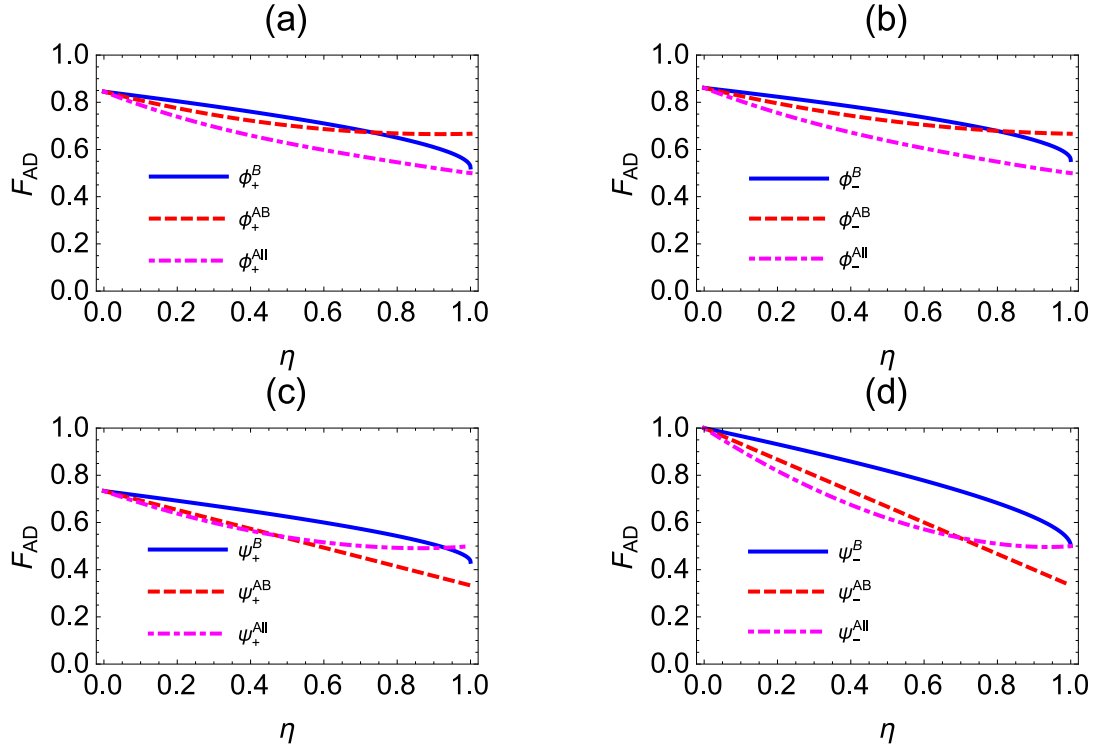


**Figure 4.2:** The dependence of the average fidelity on the number of qubits exposed to AD channels is illustrated for  $r = \frac{1}{2}$  and  $\theta = \frac{\pi}{3}$ . The choice of the initial Bell states in each case is mentioned in plot legends, where the superscript B, AB, and All corresponds to the cases when only Bob's, both Alice's and Bob's, and all three qubits were subjected to the noisy channel. The same notation is adopted in the following figures. Amplitude damping noise effect on Bob's, both Alice's and Bob's, and all three qubits (superscript B, AB, and All is mentioned in the following figures) is shown with the variation of the average fidelity ( $F_{AD}$ ) with noise parameter ( $\eta$ ) for the specific values of nonorthogonality parameters  $r = \frac{1}{2}$  and  $\theta = \frac{\pi}{3}$ .

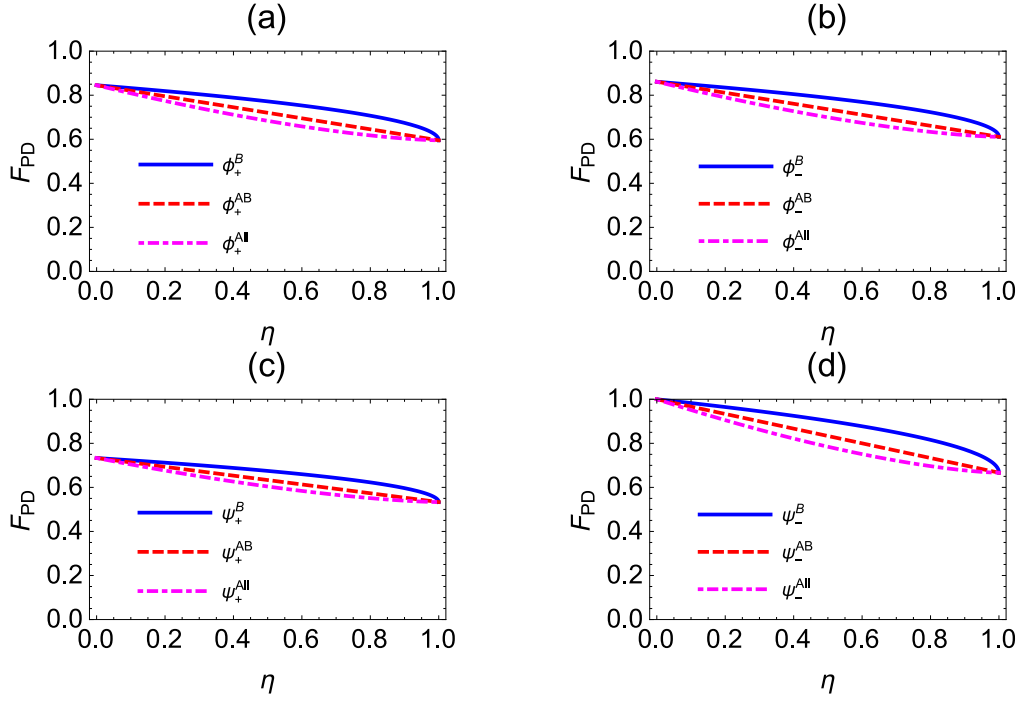


**Figure 4.3:** The effect of phase damping noise is shown for all the quasi-Bell states through the variation of the average fidelity for the specific values of  $r = \frac{1}{2}$  and  $\theta = \frac{\pi}{3}$ .

$$\begin{aligned}
F_{PD}^{|\psi_+\rangle} &= \frac{1}{(3+3r^2 \cos 2\theta)} \left[ 2 + r^4 + \sqrt{1-\eta} - \sqrt{1-\eta}\eta + r^2(-1 - \sqrt{1-\eta} + \sqrt{1-\eta}\eta) \right. \\
&\quad \left. + r^2 \left( 2 + \sqrt{1-\eta} - r^2(1-\eta)^{3/2} - \sqrt{1-\eta}\eta \right) \cos 2\theta \right], \\
F_{PD}^{|\psi_-\rangle} &= \frac{1}{3} \left[ 2 + \sqrt{1-\eta} - r^2\sqrt{1-\eta} - \sqrt{1-\eta}\eta + r^2\sqrt{1-\eta}\eta + \frac{r^2-r^4}{-1+r^2 \cos 2\theta} \right], \\
F_{PD}^{|\phi_+\rangle} &= \frac{2+\sqrt{1-\eta}+\sqrt{1-\eta}(r^2(-1+\eta)-\eta)}{3(1+r^2)}, \\
F_{PD}^{|\phi_-\rangle} &= \frac{2+(1-\eta)^{3/2}}{3}.
\end{aligned} \tag{4.34}$$

It is interesting to note that in the ideal conditions  $|\phi_-\rangle$  is the unanimous choice of quasi-Bell state to accomplish the teleportation with highest possible fidelity. However, from the expressions of fidelity obtained in Eqs. (4.29)-(4.34), it appears that it may not be the case in the presence of noise. For further analysis, it would be appropriate to observe the variation of all the fidelity expressions with various parameters. In what follows, we perform this analysis.

Figure 4.2, illustrates the dependence of the average fidelity on the number of qubits exposed to AD channel for each quasi-Bell state using Eqs. (4.29), (4.31), and (4.33). Unlike the remaining quasi-Bell states, the average fidelity for  $|\phi_-\rangle$  state starts from 1 at  $\eta = 0$ . Until a moderate value (a particular value that depends on the choice of quasi-Bell state) of decoherence rate is reached, the decay in average fidelity completely depends on the number of qubits

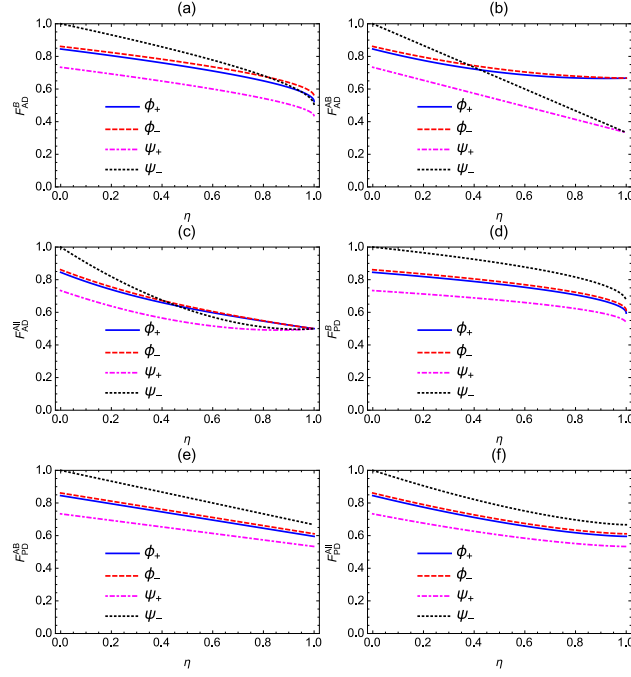


**Figure 4.4:** The variation of average fidelity is illustrated for all the possible cases by considering each quasi-Bell state as quantum channel. Average fidelity is plotted for AD ((a)-(c)) and PD ((d)-(f)) channels with  $r = \frac{1}{2}$  and  $\theta = \frac{\pi}{3}$ .

interacting with their surroundings. However, at the higher decoherence rate, this particular nature was absent. Further, Figures 4.2 (a) and (b) show that best results compared to remaining two cases can be obtained for the initial state  $|\psi_{\pm}\rangle$ , while both the channel qubits are evolving under AD noise; whereas the same case turns out to provide the worst results in case of  $|\phi_{\pm}\rangle$ . A similar study performed over PD channels instead of AD channels reveals that the decay in average fidelity solely depends on the number of qubits evolving over noisy channels (cf. Figure 4.3).

Finally, it is also worth to compare the average fidelity obtained for different quasi-Bell states when subjected to noisy environment under similar condition. This would reveal the suitable choice of initial state to be used as a quantum channel for performing teleportation. In Figure 4.4 (a), the variation of average fidelity for all the quasi-Bell states is demonstrated, while only Bob's qubit is exposed to AD noise. It establishes that although in ideal case and small decoherence rate  $|\phi_- \rangle$  state is the most suitable choice of quantum channel, which do not remain true at higher decoherence rate. While all other quasi-Bell states follow exactly the same nature for decay of average fidelity and  $|\phi_+ \rangle$  appears to be the worst choice of quantum channel. A quite similar nature can be observed for the remaining two cases over AD channels in Figures 4.4 (b) and (c). Specifically,  $|\phi_- \rangle$  remains the most suitable choice below moderate decoherence rate, while  $|\psi_{\pm} \rangle$  may be preferred for channels with high decoherence, and  $|\phi_+ \rangle$  is inevitably the worst choice.

A similar study carried out over PD channels and the obtained results are illustrated in

**Table 4.2:** The selection of the best and worst quasi-Bell state to be used as a quantum channel for quantum teleportation depends on the value of decoherence rate. A specific case ( $r = \frac{1}{2}$  and  $\theta = \frac{\pi}{3}$ ) is shown here for both AD and PD channels. The results observed for PD channel are mentioned in brackets with corresponding results for AD channel without bracket. The same notation is used in the next table, too.

Qubits exposed to noise	Decoherence rate					
	Low (below $\frac{1}{3}$ )	Moderate (between $\frac{1}{3}$ and $\frac{2}{3}$ )	High (above $\frac{2}{3}$ )			
	Best state	Worst state	Best state	Worst state	Best state	Worst state
Bob's	$ \phi_{-}\rangle ( \phi_{-}\rangle)$	$ \phi_{+}\rangle ( \phi_{+}\rangle)$	$ \phi_{-}\rangle ( \phi_{-}\rangle)$	$ \phi_{+}\rangle ( \phi_{+}\rangle)$	$ \psi_{-}\rangle ( \phi_{-}\rangle)$	$ \phi_{+}\rangle ( \phi_{+}\rangle)$
Alice's and Bob's	$ \phi_{-}\rangle ( \phi_{-}\rangle)$	$ \phi_{+}\rangle ( \phi_{+}\rangle)$	$ \psi_{-}\rangle ( \phi_{-}\rangle)$	$ \phi_{+}\rangle ( \phi_{+}\rangle)$	$ \psi_{-}\rangle ( \phi_{-}\rangle)$	$ \phi_{+}\rangle ( \phi_{+}\rangle)$
All three	$ \phi_{-}\rangle ( \phi_{-}\rangle)$	$ \phi_{+}\rangle ( \phi_{+}\rangle)$	$ \psi_{-}\rangle ( \phi_{-}\rangle)$	$ \phi_{+}\rangle ( \phi_{+}\rangle)$	$ \psi_{-}\rangle ( \phi_{-}\rangle)$	$ \phi_{+}\rangle ( \phi_{+}\rangle)$

Figures 4.4 (d) and (f). From these plots, it may be inferred that  $|\phi_{-}\rangle$  undoubtedly remains the most suitable and  $|\phi_{+}\rangle$  the worst choice of quantum channel. The investigation on the variation of the average fidelity with nonorthogonality parameters over noisy channels yields a similar nature as was observed in ideal conditions (cf. Figure 4.1). Therefore, we have not discussed it here, but a similar study can be performed in analogy with the ideal scenario.

The results obtained so far are summarized in Tables 4.2 and 4.3. In Table 4.2, we have shown that the present study may be used to select quasi-Bell state suitable as a quantum channel if the channel is characterized for noise. The table also summarizes that this choice varies with the noisy conditions (i.e., number of qubits exposed to noise and type of noise model) and decoherence rate.

The study also reveals that for each choice of quasi-Bell state, the average fidelity obtained over noisy channels falls below the classical limit for different values of decoherence rate. This fact may be used to obtain the tolerable decoherence rate for a potential quantum channel. These limits on the tolerable decoherence rates for a specific case are explicitly given in Table 4.3.

In fact, if one wishes to quantify only the effect of noise on the performance of the teleportation scheme using a nonorthogonal state quantum channel, the inner product may be taken with the teleported state in the ideal condition instead of the state to be teleported. The mathematical procedure adopted here is quite general in nature and would be appropriate to study the effect of generalized amplitude damping [78, 211], squeezed generalized amplitude damping [78, 211], bit flip [78, 136], phase flip [78, 136], and depolarizing channel [78, 136]. This discussion can further be extended to a set of non-Markovian channels [96], which will be carried out in the future and reported elsewhere.

**Table 4.3:** Even in the presence of noise, different choices of quasi-Bell states (as quantum teleportation channel) may yield fidelity higher than the maximum achievable classical fidelity in the noiseless situation ( $\frac{2}{3}$ ). Here, a specific case for  $r = \frac{1}{2}$  and  $\theta = \frac{\pi}{3}$  over both AD and PD channels is shown.

Quasi-Bell state	Qubits exposed to noise		
	Bob's	Alice's and Bob's	All three
$ \psi_+\rangle$	0.728 (0.906)	0.728 (0.692)	0.348 (0.541)
$ \psi_-\rangle$	0.803 (0.933)	0.858 (0.746)	0.372 (0.586)
$ \phi_+\rangle$	0.285 (0.505)	0.146 (0.282)	0.110 (0.206)
$ \phi_-\rangle$	0.803 (1.00)	0.490 (0.981)	0.387 (0.903)

## 4.5 Conclusion

In the present study, it has been established that all the quasi-Bell states, which are entangled nonorthogonal states may be used for quantum teleportation of a single-qubit state. However, their teleportation efficiencies are not the same, and it also depends on the nature of noise present in the quantum channel. Specifically, we have considered here four quasi-Bell states as teleportation channel, and computed average and minimum fidelity that can be obtained by replacing a Bell state quantum channel in a teleportation scheme by its nonorthogonal counterpart (i.e., corresponding quasi-Bell state). The results can be easily reduced to that obtained using usual Bell state in the limits of vanishing nonorthogonality parameter. Specifically, there are two real parameters  $r$  and  $\theta$ , considered here as primary and secondary measures of nonorthogonality.

Here,  $F_{ave}$  and MFI are used as quantitative measures of the quality of the teleportation scheme which utilizes a quasi-Bell state instead of usual Bell state as quantum channel. Therefore, during this discussion, it has been assumed that Bob performs a Pauli operation corresponding to each Bell state measurement outcome as in the standard teleportation scheme. However, we have used another quantitative measure of quality of teleportation performance, MASFI, which is computed considering an optimal unitary operation to be applied by Bob. For a few specific cases, the calculated MASFI was found to be unity. In those cases, concurrence for entangled nonorthogonal states were found to be unity, which implied maximal entanglement. However, for these sets of maximally entangled nonorthogonal states, we did not observe unit average fidelity and minimum fidelity as the unitary operations performed by Bob were not the same as was in computation of MASFI.

The performance of the teleportation scheme using entangled nonorthogonal states has also been analyzed over noisy channels. This study yield various interesting results. The quasi-Bell state  $|\phi_-\rangle$ , which was shown to be maximally entangled in an ideal situation, remains most preferred choice as quantum channel while subjected to PD noise as well. However, in AD noise, it is observed that the preferred choice of the quasi-Bell state depends on the nonorthogonality parameter and the number of qubits exposed to noisy environment. We hope

the present study will be useful for experimental realization of teleportation schemes beyond usual entangled orthogonal state regime, and will also provide a clear prescription for future research on applications of entangled nonorthogonal states.

# CHAPTER 5

## EXPERIMENTAL REALIZATION OF NONDESTRUCTIVE DISCRIMINATION OF BELL STATES USING A FIVE-QUBIT QUANTUM COMPUTER

### 5.1 Introduction

In the last three chapters, we have mostly discussed ideas related to QT. However, the domain of quantum communication is much broader, and in both quantum communication and computation, discrimination of orthogonal entangled states play a very crucial role. There exist many proposals for realizing such discrimination (see [133, 245, 260, 261] and references therein). A particularly important variant of state discrimination schemes is nondestructive discrimination of entangled states [133, 245, 260, 261], in which the state is not directly measured. The measurement is performed over some ancilla qubits/qudits coupled to entangled state and the original state remains unchanged. Proposals for such nondestructive measurements in optical quantum information processing using Kerr type nonlinearity have been discussed in Refs. [261, 262] and references therein. Such optical schemes of nondestructive discrimination are important as they are frequently used in designing entanglement concentration protocols [263]. In the same line, a scheme for generalized orthonormal qudit Bell state discrimination and an explicit quantum circuit for the task was provided in [245]. In Ref. [245], it was also established that the use of distributed measurement (i.e., nondestructive measurement where the measurement task is distributed or outsourced to ancilla qubits) have useful applications in reducing quantum communication complexity under certain conditions. The work was further generalized in [260], where the relevance of the quantum circuits for nondestructive discrimination was established in the context of quantum error correction, quantum network and distributed quantum computing. Subsequently, applications of the nondestructive discrimination of entangled states have been proposed in various other works, too. Specifically, in [43], a scheme



for two-way secure direct quantum communication, which was referred to as quantum conversation, was developed using the nondestructive discrimination scheme. In a more general scenario, Luo et al., proposed a scheme for multi-party quantum private comparison based on  $d$ -dimensional entangled states [264], where all the participants are required to perform nondestructive measurement.

These applications and the fact that the scheme proposed in [245] has been experimentally implemented for Bell state discrimination using an NMR-based three-qubit quantum computer [246], have motivated us to perform nondestructive Bell state discrimination using another experimental platform. Specifically, in this work, we aim to realize nondestructive Bell state discrimination using a five-qubit superconductivity-(SQUID)-based quantum computer [221, 235], which has been recently placed in cloud by IBM Corporation. This quantum computer was placed in the cloud in 2016. It immediately drew considerable attention of the quantum information processing community, and several quantum information tasks have already been performed using this quantum computer on cloud. Specifically, in the domain of quantum communication, properties of different quantum channels that can be used for quantum communication have been studied experimentally [265] and experimental realizations of a quantum analog of a bank cheque [222] that is claimed to work in a banking system having quantum network, and teleportation of single-qubit [220] and two-qubit quantum states using optimal resources [85], have been reported; in the field of quantum foundation, violation of multi-party Mermin inequality has been realized for 3, 4, and 5 parties [219]; an information theoretic version of uncertainty and measurement reversibility has also been implemented [266]; in the area of quantum computation, a comparison of two architectures using demonstration of an algorithm has been performed [224], and a quantum permutation algorithm [267], an algorithm for quantum summation [58] and a Deutsch-Jozsa like algorithm [268] have been implemented recently. Further, a non-abelian braiding of surface code defects [225] and a compressed simulation of the transverse field one-dimensional Ising interaction (realized as a four-qubit Ising chain that utilizes only two qubits) [223] have also been demonstrated. Thus, we can see that IBM quantum computer has already been successfully used to realize various tasks belonging to different domains of quantum information processing. However, to the best of our knowledge, IBM quantum computer is not yet used to perform nondestructive discrimination of the orthogonal entangled states, and the performance of IBM quantum computer is not yet properly compared with the performance of the quantum computers implemented using liquid NMR technology. In the present work, we aim to perform such a comparison, subject to a specific task. To be precise, we wish to compare the performance of IBM quantum computer with an NMR-based quantum computer with respect to the nondestructive discrimination of Bell states. There is another important reason for testing fundamentally important quantum circuits (in our case, quantum circuit for nondestructive discrimination of Bell states) using the IBM quantum computer and/or a similar platform- it is now understood that liquid NMR-based technology is not scalable [269],

and it will not lead to a real scalable quantum computer [269]. However, it is widely believed that a SQUID-based quantum computer can be made scalable in future [270]. In fact, an ideal quantum information processor should satisfy Di-Vincenzo's criteria [271]. One of these criteria requires the realization of a large quantum register, which is still a prime technological challenge for experimental quantum information processing [269]. A ray of hope is generated in the recent past after the introduction of the relatively new architectures, like solid-state spin systems (nitrogen vacancy centers in diamond and phosphorous vacancy centers in silicon) and superconducting-qubits based systems [272] that have the potential to become scalable. Among these technologies, owing to the scalability and functionality of superconducting-qubit registers, they have emerged as the best candidate for quantum information processing. Currently, various types of basic superconducting-qubits, namely Josephson-junction qubits, Phase qubits, Transmon qubits and Potential qubits are used [273, 274]. SQUID-based quantum information processing architectures have not only attained the popularity among the researchers, but have also led to the path for commercialization of quantum computers. Although a universal quantum computer with large qubit register is still a distant hope, large qubit registers to perform specific tasks have been devised. For example, quantum computers with register size of 512 qubits, 1000 qubits, and 2000 qubits were sold by D-Wave [275]. The machine with 51 two qubits has been deployed to tackle classification problems that are useful in image-recognition [276].

As mentioned above, the potential scalability of the SQUID-based systems has also motivated us to perform experimental realization of the Bell state discrimination circuit using a SQUID-based five-qubit quantum computer.

Rest of the chapter is organized as follows. In Section 5.2, we have described the quantum circuits (both theoretical and experimental) used here to perform Bell state discrimination and the method adopted here to perform QST. In Section 5.3, the results of the experimental realization of the circuits described in the previous section are reported and analyzed. Finally, the chapter is concluded in Section 5.4.

## **5.2 Quantum circuits and method used for nondestructive discrimination of Bell states**

We have already mentioned that in Refs. [245, 260], a quantum circuit for the nondestructive discrimination of generalized orthonormal qudit Bell states was designed by some of the present authors (cf. Figure 3 of [245] or Figure 4 of [260]). As a special case of these circuits, one can easily obtain a circuit for Bell state discrimination, as shown in Figure 5.1 (a) here and in Figure 2 of [245]. This circuit involves four-qubits, in which the measurement on the first ancilla qubit would reveal the phase information, whereas the second measurement would reveal the parity

information. Thus, to discriminate all four Bell states in a single experiment, we would require a four-qubit system, allowing non-local operations between system qubits (qubits of the Bell state) and the ancilla qubits. Apparently, this circuit should have been implemented as it is in the five-qubit IBM quantum computer, but the restriction on the application of CNOT gates, restrict us to implement this circuit as a single circuit (without causing considerable increase in the gate-count and decrease in the performance). Circumventing, the increase in circuit complexity (gate-count), initially, we have implemented the phase checking circuit and the parity checking circuit separately, as shown in Figures 5.1 (b) and (c), respectively. This is consistent with the earlier NMR-based implementation of the Bell state discrimination circuit [246], where a three-qubit quantum computer was used and naturally, parity checking part and the phase checking part was performed via 2 independent experiments. In fact, in the NMR-based implementation of the nondestructive discrimination of Bell states, an ensemble of  $^{13}\text{CHFBr}_2$  molecule was used to perform the quantum computing, as the number of independent Larmor frequency of that was 3, the quantum computer was a three-qubit one. Specifically, Samal et al., used three nuclear spins, namely  $^1\text{H}$ ,  $^{13}\text{C}$  and  $^{19}\text{F}$  of  $^{13}\text{CHFBr}_2$  which mimics a three-qubit system [246]. In their experiment, they used  $^{13}\text{C}$  as ancilla qubit and rest as system qubits. The availability of single ancilla qubit prohibited nondestructive discrimination of the Bell states in one shot. Due to the trade-off between the available quantum resources and number of experiments, they used two experiments to realize the complete protocol, one for obtaining parity information and the other one for phase information. The circuit shown in Figure 5.1 (c) is actually used for parity checking and it is easy to observe that for Bell states having even parity (i.e., for  $|\psi^\pm\rangle = \frac{|00\rangle \pm |11\rangle}{\sqrt{2}}$ ), the measurement on the ancilla qubit would yield  $|0\rangle$  and for the other two Bell states (i.e., for odd parity states  $|\phi^\pm\rangle = \frac{|01\rangle \pm |10\rangle}{\sqrt{2}}$ ) it would yield  $|1\rangle$ . In a similar fashion, the quantum circuit shown in Figure 5.1 (b) would determine the relative phase of the Bell state as the measurement on ancilla in Figure 5.1 (b) would yield  $|0\rangle$  for + states, i.e., for  $|\psi^+\rangle$  and  $|\phi^+\rangle$  and it would yield  $|1\rangle$  for – states  $|\psi^-\rangle$  and  $|\phi^-\rangle$  (see third and fourth column of Table 5.1 for more detail).

We have already mentioned that the limitations of the available quantum resources restricted Samal et al., [246] to realize the circuits shown in Figures 5.1 (b) and (c) instead of the whole circuit shown in Figure 5.1 (a) in their liquid NMR-based work.

The same situation prevailed in the subsequent work of the same group [277]. In contrast, the IBM's five-qubit quantum computer IBM QX2 is SQUID-based, and does not face scalability issues encountered by NMR-based proposals. Before reporting our experimental observations, it would be apt to briefly describe the characteristic features of the technology used in IBM quantum computer, with a focus on its architecture, control fields for manipulation and readout of qubit register, important experimental parameters, and the functioning of IBM QX2. The type of superconducting qubits used in IBM architecture are transmon qubits. Transmon qubits are charge qubits and can be designed to minimize charge noise which is a major source

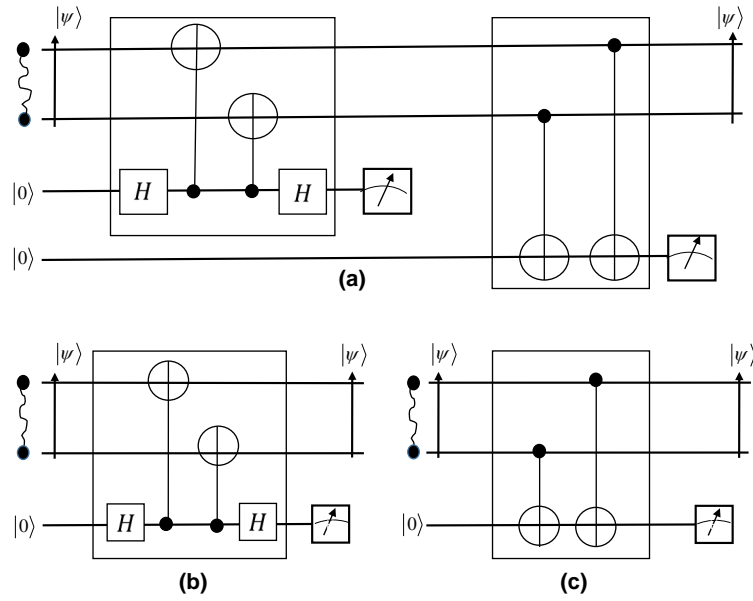
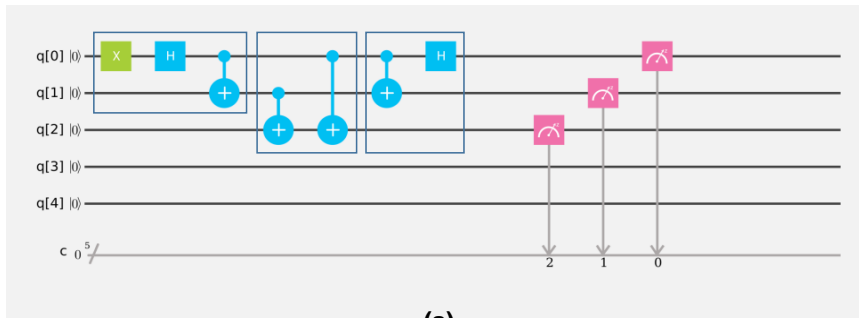
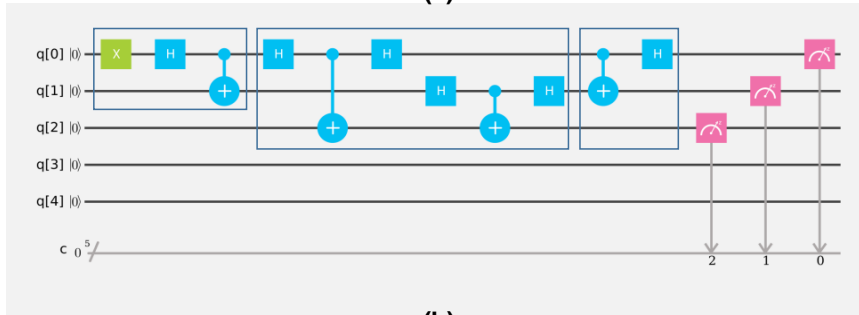


**Figure 5.1:** The circuit for nondestructive discrimination of all the four Bell states. (a) A four-qubit circuit with two system-qubits (used for Bell-state preparation) and two ancilla-qubits (subsequently used for phase detection (left block) and parity detection (right block)). Here, (b) and (c) are the divided part of (a), whereas, (b) is the phase checking circuit and (c) is the parity checking circuit.

of relaxation in charge qubits. The arrangement of five superconducting qubits (q[0], q[1], q[2], q[3], q[4]) and their control mechanism as given in [238] is already described in Section 1.8 (see Figure 1.8 and Table 1.3 for details). As evident from the Table 1.3 in IBM QX2, couplings between all pairs are not present. Absence of couplings provides restriction on the applicability of CNOT gates. In brief, it does not allow us to perform controlled operation between any two qubits, and consequently restricts us to perform the nondestructive Bell state discrimination circuit either using two independent experiments as was done in [246] (cf. Figure 1 of [246]) or using a circuit having considerably high gate-count (implementation of such a circuit will be described in the next section). Unfortunately, IBM quantum experience does not even allow us to implement the circuits shown in Figure 5.1 (b) in its actual form. We need to make some modifications to obtain equivalent circuits. In Figures 5.2 (a) and (b), we have shown the actual circuits prepared in IBM quantum computer for parity checking and phase information checking. In both the circuits, left-most box contains an EPR circuit used for preparation of the Bell state  $|\psi^-\rangle$  (similarly other states were prepared and measured). The second box from the left in Figures 5.2 (a) and (b) provide equivalent circuits for the circuits given in Figures 5.1 (c) and (b), respectively, and one can easily observe that the circuit for obtaining the phase information required decomposition for successful implementation in IBM quantum computer. In the third box, a reverse EPR circuit is inserted to establish that the measurement on ancilla does not destroy the Bell state. To obtain further information about the output states of a given

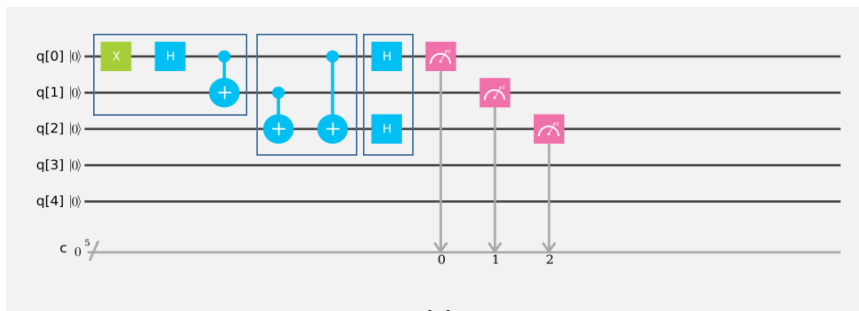


(a)

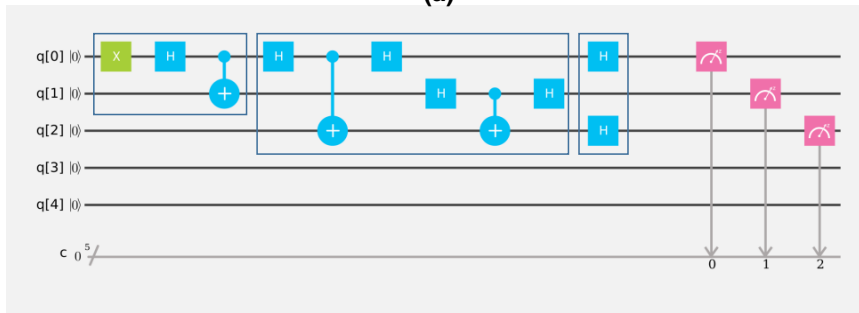


(b)

**Figure 5.2:** Experimental implementation of parity and phase checking circuits using five-qubit IBM quantum computer for the Bell state  $|\psi^-\rangle$ . Qubits q[0], q[1] are system-qubits, and q[2] mimics ancilla-qubits. Here, (a) and (b) correspond to the parity and phase checking circuits, respectively. In (a) and (b), the left block prepares desired Bell states, the middle block corresponds to a parity and phase checking circuit, respectively and the right block is used for reverse EPR circuit.



(a)



(b)

**Figure 5.3:** Experimentally implementable (a) parity and (b) phase checking circuits on IBM QX2 followed by tomography block (involves measurement in different basis). Here, configuration implements measurement in X- basis is shown.

circuit, QST is done. In Figure 5.3, we have shown a circuit that can be used to perform QST and thus to yield each element of the density matrix of the output state before measurement is performed. Specifically, in Figure 5.3, third block from the left, two hadamard gates are applied. This is operated to perform state tomography. To be precise, application of a hadamard gate transforms the measurement basis from computational basis  $\{|0\rangle, |1\rangle\}$  to diagonal basis  $\{|+\rangle, |-\rangle\}$  and thus yields  $\langle X \rangle_X$  element of the single-qubit density matrix. Here it would be apt to briefly describe the method adopted here for performing state tomography and measuring fidelity with an example. Theoretically obtained density matrix of  $|\psi^+\rangle|0\rangle$  is,

$$\rho^T = |\psi^+0\rangle\langle\psi^+0|, \quad (5.1)$$

where superscript  $T$  indicates a theoretical (ideal) density matrix. To check how nicely this state is prepared in experiment, we need to reconstruct the density matrix of the output state using QST by following the method adopted in Refs. [216, 219, 223, 240–242, 244]. Characterization of a three-qubit experimental density matrix requires extraction of information from the experiments and then using that information to reconstruct experimental density matrix. In the Pauli basis an experimental density matrix can be written as  $\rho^E = \frac{1}{8} \sum_{i,j,k} c_{ijk} \sigma_i \otimes \sigma_j \otimes \sigma_k$ , where  $c_{ijk} = \langle \sigma_i \otimes \sigma_j \otimes \sigma_k \rangle$  and  $\sigma_{ijk} = I, X, Y, Z$ , and superscript  $E$  is used to indicate experimental density matrix. Reconstruction of this  $8 \times 8$  density matrix of three-qubit state requires knowledge of 63 unknown real parameters. The evaluation of co-efficient  $c_{ijk}$  requires  $\langle \sigma_i \rangle$  where  $\sigma_i = I, X, Y, Z$  for each qubit. Since  $\langle I \rangle$  can be obtain by the experiment done on  $Z$  basis, instead of four we need only three measurement (measurement in  $X, Y$ , and  $Z$  basis) on each qubit, thus requiring total 27 measurements to tomograph each density matrix. In Chapter 1, we have already mentioned that in IBM, the only available basis for performing the measurements is  $Z$  basis. Consequently, to realize a measurement in  $X$  and  $Y$  basis we have to apply  $H$  and  $HS^\dagger$  gates, respectively prior to the  $Z$  basis measurement. Subsequently, to reconstruct the three-qubit state  $|\psi^+\rangle|0\rangle$  and to check how well the state is prepared, we have to perform 27 experiments, each of which would run 8192 times. At a later stage of the investigation, following the same strategy, we would obtain the density matrices of the retained state after measuring the ancilla qubits to discriminate the Bell states

Once  $\rho^E$  is obtained through QST, the same may be used to obtain fidelity and thus a quantitative feeling about the accuracy of the experimental implementation can be obtained. Here it would be apt to mention that the fidelity is obtained using Eq. (1.6) of Chapter 1, which described in detail in Eq. (1.6). As an example, if we consider that the desired state is  $|\psi^+0\rangle$  then  $\rho^1 = |\psi^+0\rangle\langle\psi^+0|$ , and  $\rho^2$  would be the density matrix of the state obtained experimentally by performing state tomography in a manner described above.

**Table 5.1:** Expected outcomes after parity and phase checking circuit for ancilla-Bell-state combined system for all Bell states. Expected obtained results of ancilla qubits in the same cases are also given. Column 1 illustrates Bell states to be examined. In Column 2, states of the Bell-state-ancilla composite system is shown. Outcomes of measurements on ancilla for two cases is shown in Columns 3 and 4 and outcomes of measuring composite states in the computational basis is shown in Columns 5 and 6 (from left to right).

Bell state to be discriminated/identified by nondestructive measurement	Bell-state-ancilla composite state (considered as three-qubit state as implemented in the experiment performed here)	Outcome of measurement on ancilla qubit used for parity checking	Outcome of measurement on ancilla qubit used for revealing phase information	Outcome of three-qubit measurement of parity checking circuit when the output Bell state is measured after passing through a reverse EPR circuit (cf. Figures 5.5 (a)-(d))	Outcome of three-qubit measurement of relative phase checking circuit when the output Bell state is measured after passing through a reverse EPR circuit (cf. Figures 5.5 (e)-(h))
$ \psi^+\rangle = \frac{ 00\rangle +  11\rangle}{\sqrt{2}}$	$ \psi^+\rangle 0\rangle$	$ 0\rangle$	$ 0\rangle$	$ 000\rangle$	$ 000\rangle$
$ \psi^-\rangle = \frac{ 00\rangle -  11\rangle}{\sqrt{2}}$	$ \psi^-\rangle 0\rangle$	$ 0\rangle$	$ 1\rangle$	$ 100\rangle$	$ 101\rangle$
$ \phi^+\rangle = \frac{ 01\rangle +  10\rangle}{\sqrt{2}}$	$ \phi^+\rangle 0\rangle$	$ 1\rangle$	$ 0\rangle$	$ 011\rangle$	$ 010\rangle$
$ \phi^-\rangle = \frac{ 01\rangle -  10\rangle}{\sqrt{2}}$	$ \phi^-\rangle 0\rangle$	$ 1\rangle$	$ 1\rangle$	$ 111\rangle$	$ 111\rangle$

### 5.3 Results

Initially, we prepare four Bell states (using EPR circuit, i.e., a hadamard followed by CNOT) and an ancilla in state  $|0\rangle$ . It is well known that an EPR circuit transforms input states  $|00\rangle, |01\rangle, |10\rangle, |11\rangle$  into  $|\psi^+\rangle = \frac{|00\rangle+|11\rangle}{\sqrt{2}}, |\phi^+\rangle = \frac{|01\rangle+|10\rangle}{\sqrt{2}}, |\psi^-\rangle = \frac{|00\rangle-|11\rangle}{\sqrt{2}}$  and  $|\phi^-\rangle = \frac{|01\rangle-|10\rangle}{\sqrt{2}}$ , respectively. Default initial state in IBM quantum experience is  $|0\rangle$  for each qubit line. However, the input states required by an EPR circuit to generate different Bell states can be prepared by placing NOT gate(s) in appropriate positions before the EPR circuit (see how  $|\psi^-\rangle$  is prepared in left most block of Figure 5.2 ). This is how Bell states are prepared here. To check the accuracy of the states prepared in the experiments, QST of the experimentally obtained density matrices are performed. For this purpose, we have followed the method described in the previous section. Density matrix for the experimentally obtained state corresponding to a particular case (for the expected state  $|\psi^+0\rangle$ , i.e., for  $\rho^T = \rho^1 = |\psi^+0\rangle\langle\psi^+0|$ ), is obtained as

$$\rho_{|\psi^+0\rangle}^E = \text{Re} \left[ \rho_{|\psi^+0\rangle}^E \right] + i \text{Im} \left[ \rho_{|\psi^+0\rangle}^E \right], \quad (5.2)$$

where a subscript is added to uniquely connect the experimental density matrix with the corresponding ideal state and

$$\text{Re} \left[ \rho_{|\psi^+0\rangle}^E \right] = \begin{pmatrix} 0.44 & 0.003 & 0.011 & -0.0102 & 0.006 & -0.005 & 0.365 & 0.007 \\ 0.003 & 0.002 & 0.014 & -0.005 & 0.005 & 0.005 & 0.011 & 0.001 \\ 0.011 & 0.014 & 0.074 & 0.003 & 0.005 & -0.004 & 0.006 & 0.002 \\ -0.010 & -0.005 & 0.003 & 0.002 & -0.001 & -0.005 & -0.001 & 0 \\ 0.006 & 0.005 & 0.005 & -0.005 & 0.073 & 0.001 & 0.0035 & -0.004 \\ -0.005 & 0.005 & -0.004 & -0.005 & 0.001 & 0.002 & 0.011 & -0.005 \\ 0.365 & 0.011 & 0.006 & -0.002 & 0.003 & 0.011 & 0.408 & 0.01 \\ 0.007 & 0.001 & 0.002 & 0 & -0.004 & -0.005 & 0.01 & 0.001 \end{pmatrix}, \quad (5.3)$$

and

$$\text{Im} \left[ \rho_{|\psi^+0\rangle}^E \right] = \begin{pmatrix} 0 & -0.018 & -0.024 & -0.027 & -0.034 & -0.003 & -0.030 & -0.018 \\ 0.018 & 0 & -0.003 & 0 & -0.002 & 0 & 0.021 & 0 \\ 0.024 & 0.003 & 0 & 0.018 & 0.030 & -0.002 & -0.01 & 0.006 \\ 0.027 & 0 & -0.018 & 0 & 0.004 & -0.005 & 0.0032 & 0 \\ 0.034 & 0.002 & -0.030 & -0.004 & 0 & -0.005 & -0.003 & -0.023 \\ 0.003 & 0 & 0.002 & 0.005 & 0.005 & 0 & -0.007 & 0 \\ 0.030 & -0.021 & 0.01 & -0.003 & 0.003 & 0.007 & 0 & -0.003 \\ 0.018 & 0 & -0.006 & 0 & 0.023 & 0 & 0.003 & 0 \end{pmatrix}. \quad (5.4)$$

Real part of this density matrix is illustrated in Figure 5.4 (a). Figure 5.4 also illustrates the real part of density matrices of the experimentally prepared Bell-state-ancilla composite in the other three cases. Corresponding density matrices are provided below (see Eq. (5.5)-(5.10)).



$$\text{Re} \left[ \rho_{|\psi^- \rangle}^E \right] = \begin{pmatrix} 0.476 & 0.029 & 0.029 & -0.001 & -0.007 & -0.005 & -0.375 & -0.024 \\ 0.029 & 0.003 & 0.022 & 0.001 & 0.002 & 0.0 & -0.021 & -0.003 \\ 0.029 & 0.022 & 0.066 & -0.02 & -0.015 & -0.001 & -0.012 & 0.002 \\ -0.001 & 0.001 & -0.02 & 0.001 & 0.003 & -0.001 & -0.001 & 0.0 \\ -0.007 & 0.002 & -0.015 & 0.003 & 0.058 & 0.005 & 0.018 & 0.002 \\ -0.005 & 0.0 & -0.0013 & -0.001 & 0.005 & 0.0 & 0.020 & 0.0 \\ -0.375 & -0.021 & -0.012 & -0.001 & 0.018 & 0.020 & 0.393 & 0.006 \\ -0.024 & -0.003 & 0.002 & 0.0 & 0.002 & 0.0 & 0.006 & 0.003 \end{pmatrix}, \quad (5.5)$$

$$\text{Im} \left[ \rho_{|\psi^- \rangle}^E \right] = \begin{pmatrix} 0 & -0.022 & -0.01 & -0.019 & -0.009 & 0 & -0.007 & 0.019 \\ 0.022 & 0 & 0.002 & 0.0 & -0.001 & -0.001 & -0.019 & 0.001 \\ 0.01 & -0.002 & 0 & 0.023 & -0.013 & -0.003 & -0.012 & -0.001 \\ 0.019 & 0 & -0.023 & 0 & 0.004 & 0 & -0.001 & 0 \\ 0.009 & 0.001 & 0.013 & -0.004 & 0 & -0.003 & -0.012 & -0.015 \\ 0 & 0.001 & 0.003 & 0 & 0.003 & 0.0 & -0.004 & -0.001 \\ 0.007 & 0.019 & 0.012 & 0.001 & 0.012 & 0.004 & 0 & 0.001 \\ -0.019 & -0.001 & 0.001 & 0 & 0.015 & 0.001 & -0.001 & 0 \end{pmatrix}, \quad (5.6)$$

$$\text{Re} \left[ \rho_{|\phi^+ \rangle}^E \right] = \begin{pmatrix} 0.089 & 0.007 & -0.021 & 0.004 & -0.006 & -0.004 & 0.008 & -0.002 \\ 0.007 & 0.0 & 0.016 & 0.0 & -0.002 & 0.0 & -0.001 & 0.0 \\ -0.021 & 0.016 & 0.429 & -0.001 & 0.382 & 0.024 & 0.004 & 0.002 \\ 0.004 & 0.0 & -0.001 & 0.001 & 0.02 & 0.003 & 0.002 & 0.0 \\ -0.006 & -0.002 & 0.382 & 0.02 & 0.459 & 0.024 & -0.011 & 0.008 \\ -0.004 & 0.0 & 0.024 & 0.003 & 0.024 & 0.002 & 0.015 & -0.001 \\ 0.008 & -0.001 & 0.004 & 0.002 & -0.011 & 0.015 & 0.02 & -0.017 \\ -0.002 & 0.0 & 0.002 & 0.0 & 0.008 & -0.001 & -0.017 & 0.0 \end{pmatrix}, \quad (5.7)$$

$$\text{Im} \left[ \rho_{|\phi^+ \rangle}^E \right] = \begin{pmatrix} 0 & -0.007 & -0.016 & -0.016 & -0.03 & 0.001 & 0.001 & 0.003 \\ 0.007 & 0.0 & 0.001 & 0 & 0.001 & -0.001 & -0.003 & -0.001 \\ 0.016 & -0.001 & 0 & -0.009 & -0.022 & -0.024 & -0.017 & 0.001 \\ 0.016 & 0 & 0.009 & 0 & 0.019 & 0.001 & 0.005 & 0.001 \\ 0.03 & -0.001 & 0.022 & -0.019 & 0 & -0.024 & -0.011 & -0.011 \\ -0.001 & 0.001 & 0.025 & -0.001 & 0.024 & 0 & 0.003 & -0.001 \\ -0.001 & 0.003 & 0.017 & -0.005 & 0.011 & -0.0025 & 0 & 0.013 \\ -0.003 & 0.001 & -0.001 & -0.001 & 0.011 & 0.0005 & -0.013 & 0 \end{pmatrix}, \quad (5.8)$$

$$\text{Re} \left[ \rho_{|\phi^-\rangle}^E \right] = \begin{pmatrix} 0.092 & 0.009 & -0.023 & -0.008 & 0.063 & 0.002 & 0 & -0.001 \\ 0.009 & 0.001 & 0.018 & 0 & 0.004 & 0 & 0.005 & -0.002 \\ -0.023 & 0.017 & 0.454 & 0.005 & -0.38 & -0.017 & 0.047 & -0.001 \\ -0.008 & 0 & 0.005 & 0.005 & -0.017 & -0.003 & 0.001 & 0.001 \\ 0.063 & 0.004 & -0.384 & -0.017 & 0.42 & 0.026 & -0.009 & -0.005 \\ 0.002 & 0 & -0.017 & -0.002 & 0.025 & 0.003 & 0.025 & 0 \\ 0 & 0.004 & 0.047 & 0.001 & -0.009 & 0.025 & 0.025 & -0.013 \\ -0.001 & -0.002 & -0.001 & 0.001 & -0.005 & 0 & -0.013 & 0 \end{pmatrix}, \quad (5.9)$$

and

$$\text{Im} \left[ \rho_{|\phi^-\rangle}^E \right] = \begin{pmatrix} 0 & -0.006 & -0.017 & -0.027 & -0.022 & -0.006 & -0.012 & -0.007 \\ 0.006 & 0 & -0.006 & 0 & 0.008 & -0.001 & -0.007 & -0.001 \\ 0.017 & 0.006 & 0 & 0.001 & 0.026 & 0.015 & -0.025 & 0 \\ 0.027 & 0 & -0.001 & 0 & -0.012 & 0.001 & -0.004 & 0 \\ 0.022 & -0.008 & -0.026 & 0.012 & 0 & -0.018 & -0.009 & -0.029 \\ 0.006 & 0.001 & -0.015 & -0.001 & 0.018 & 0 & -0.004 & 0.001 \\ 0.012 & 0.007 & 0.025 & 0.004 & 0.009 & 0.004 & 0 & 0.014 \\ 0.007 & 0.001 & 0 & 0 & 0.029 & -0.001 & -0.014 & 0 \end{pmatrix}. \quad (5.10)$$

Figure 5.4 clearly shows that the Bell states are prepared with reasonable amount of accuracy, but does not provide any quantitative measure of accuracy. So we have calculated the “average absolute deviation”  $\langle \Delta x \rangle$  and “maximum absolute deviation”  $\Delta x_{max}$  of the experimental density matrix from the theoretical one by using this formulae

$$\begin{aligned} \langle \Delta x \rangle &= \frac{1}{N^2} \sum_{i,j=1}^N |x_{i,j}^T - x_{i,j}^E|, \\ \Delta x_{max} &= \text{Max} |x_{i,j}^T - x_{i,j}^E|, \\ \forall i, j &\in \{1, N\}. \end{aligned} \quad (5.11)$$

where,  $x_{ij}^T$  and  $x_{ij}^E$  are the theoretical and experimental elements. Putting the values in this equation from Eq. (5.3) and Eq. (5.4) we find the “average absolute deviation” and the “maximum absolute deviation” of the Bell state  $|\psi^+\rangle|0\rangle$  which is 1.8% and 13.7%.

Similarly, we have also calculated “average absolute deviation” and “maximum absolute deviation” for other Bell states too, these values are  $|\psi^-\rangle|0\rangle$  is 1.8% and 12.5%,  $|\phi^+\rangle$  is 1.8% and 11.9% and  $|\phi^-\rangle$  is 2% and 11.8%, respectively. It may be noted that in NMR-based experiment [246], the values for “average absolute deviation” and “maximum absolute deviation” is reported as  $\sim 1\%$  and  $\sim 4\%$ , respectively. This probably indicates, that Bell states were prepared in NMR-based experiment, with higher accuracy, but the measure used there was not universal. So we also compute fidelity of the reconstructed state with respect to the desired state

and obtained following values of the fidelity for various Bell-state-ancilla composite system:  $F_{|\psi^{+0}\rangle} = 0.8890$ ,  $F_{|\psi^{-0}\rangle} = 0.8994$ ,  $F_{|\phi^{+0}\rangle} = 0.9091$ , and  $F_{|\phi^{-0}\rangle} = 0.9060$ , where  $F_{|i\rangle}$  denotes the fidelity at which the desired quantum state  $|i\rangle$  is prepared in the IBM quantum computer. The computed values of  $F_{|i\rangle}$  clearly show that the Bell-state-ancilla composite system has been prepared with reasonable accuracy in the present experiment. The values of fidelity obtained here cannot be considered very high in comparison to the fidelity with which standard quantum states are prepared in other technologies. For example, in Ref. [278] various states (including a set of phase-damped Bell states and  $X$  states belonging to the families of Werner states) were prepared with fidelity  $\geq 0.96$ , and in some cases, fidelity was as high as  $0.998 \pm 0.002$  (cf. Table 1 of Ref. [278]). Similarly, in the NMR-based implementation, some of the authors had earlier prepared states with an average fidelity of 0.99 [244, 279]. For example, quantum states  $\rho^1 = \frac{1}{2}(\sigma_z^1 + \sigma_z^2)$  and  $\rho^2 = \frac{1}{2}(\sigma_x^1 + \sigma_x^2) - \frac{1}{2}(\sigma_y^1 + \sigma_y^2) + \frac{1}{\sqrt{2}}(\sigma_z^1 + \sigma_z^2)$  were prepared with fidelities 0.997 and 0.99, respectively [244]. Before, we proceed further and continue our analysis using fidelity as a measure of figure of merit that quantify the similarity (closeness) between two quantum states, we must note that in Ref. [280], it was established that high fidelities may be achieved by pairs of quantum states with considerably different physical properties. Further, in [278], it was shown for the families of depolarized or phase-damped states that two states having high fidelity may have largely different values of discord. Thus, one needs to be extra cautious while using fidelity as a quantitative measure of closeness. However, it is very frequently used in the works related to quantum information processing in general and in particular, it has also been used in a set of works [58, 85, 268] reporting interesting results using IBM quantum experience. In this work, we also use fidelity as a quantitative measure of closeness.

After verifying that the Bell-state-ancilla composite system are prepared successfully, we perform measurements on the ancilla to perform nondestructive discrimination of the Bell state. After the measurement of ancilla, the Bell state is expected to remain unchanged, to test that a reverse EPR circuit is applied to the system qubits, and subsequently the system qubits are measured in computational basis. The reverse EPR circuit actually transforms a Bell measurement into a measurement in the computational basis. Outcomes of these measurements are shown in Figure 5.5, within the experimental error, these results are consistent with the expected theoretical results shown in Column 4 and 5 of Table 5.1. Thus, nondestructive discrimination is successfully performed in IBM quantum computer.

Figure 5.5 definitely indicates a successful implementation of nondestructive discrimination of Bell states. However, it does not reveal the whole picture. To obtain the full picture, we perform QST after implementation of parity checking circuit and phase information checking circuits. In the following, we provide experimental density matrices  $[\rho^E_{|\psi^{+0}\rangle}]$  for both the cases (phase and parity) corresponding to the ideal state  $|\psi^{+0}\rangle$  as

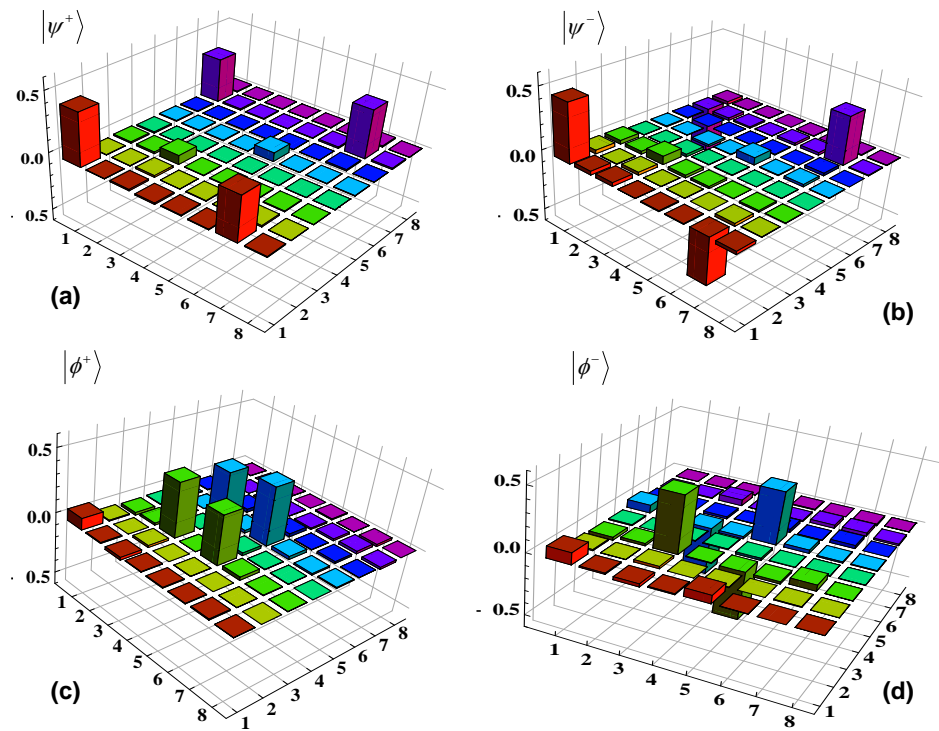


**Figure 5.4:** Reconstructed Bell states on Bell-state-ancilla composite system corresponding to ideal states (a)  $|\psi^+0\rangle$ , (b)  $|\psi^-0\rangle$ , (c)  $|\phi^+0\rangle$ , (d) and  $|\phi^-0\rangle$ . In each plot, the states  $|000\rangle, |001\rangle, |010\rangle, |011\rangle, |100\rangle, |101\rangle, |110\rangle$  and  $|111\rangle$  are labeled as 1–8 consecutively in X and Y axis.

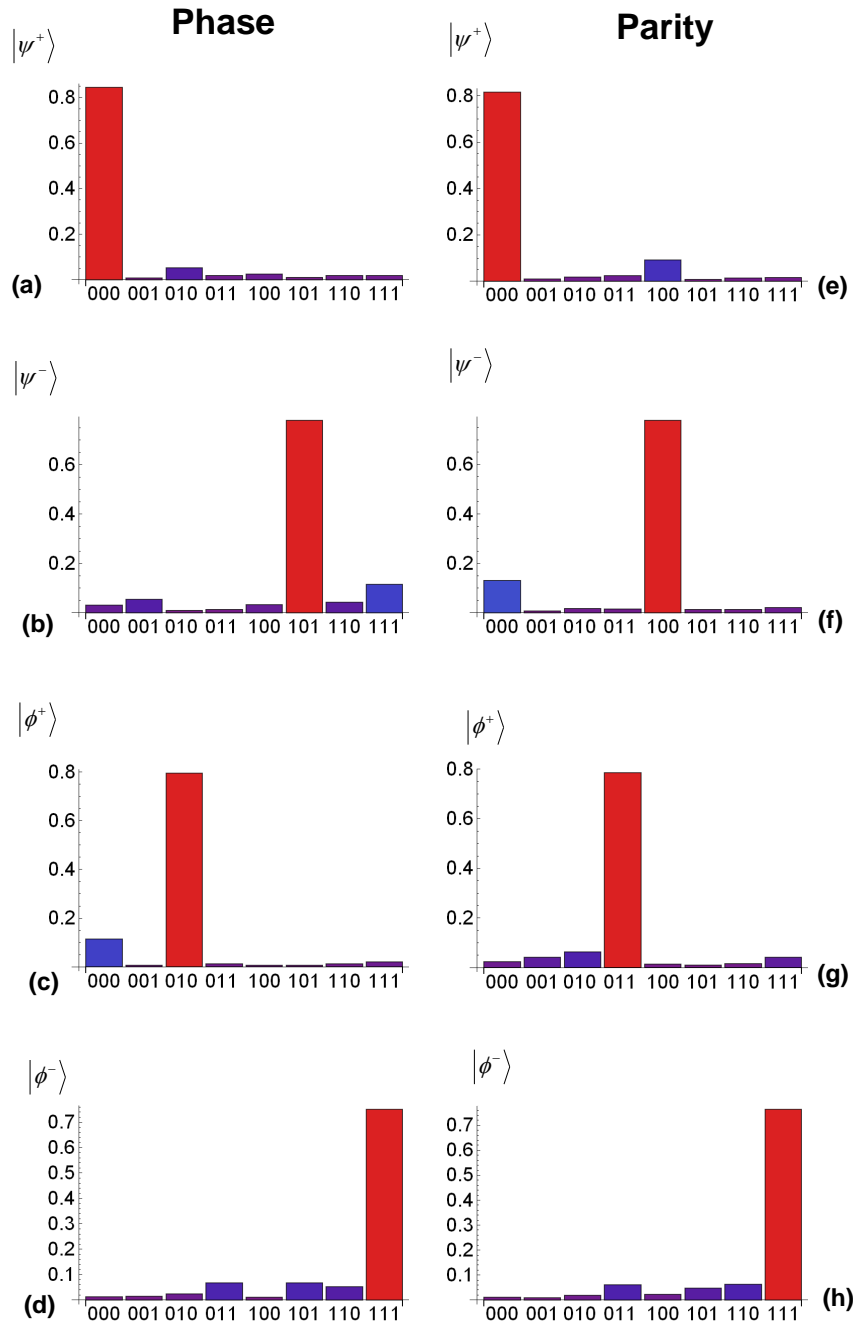


**Figure 5.5:** Experimental results obtained by implementing the circuits shown in Figure 5.2. Measurement results after implementing phase checking and parity checking circuits are shown in (a)-(d) and (e)-(h), respectively.

$$\text{Re} \left[ \rho_{|\psi^+0\rangle}^E \right]_{\text{parity}} = \begin{pmatrix} 0.462 & 0.084 & 0.011 & 0.019 & 0.016 & 0.017 & 0.34 & 0.015 \\ 0.084 & 0.005 & 0.0537 & -0.005 & 0.008 & 0.001 & 0.079 & -0.002 \\ 0.011 & 0.053 & 0.036 & -0.032 & -0.005 & 0.001 & 0.009 & 0.009 \\ 0.019 & -0.005 & -0.032 & 0.029 & -0.002 & 0.002 & 0.024 & 0.002 \\ 0.016 & 0.008 & -0.005 & -0.002 & 0.046 & 0.012 & 0.009 & 0.006 \\ 0.017 & 0.001 & 0.001 & 0.002 & 0.012 & 0.010 & 0.057 & -0.003 \\ 0.34 & 0.079 & 0.009 & 0.024 & 0.009 & 0.056 & 0.399 & 0.012 \\ 0.015 & -0.002 & 0.009 & 0.002 & 0.006 & -0.003 & 0.012 & 0.012 \end{pmatrix}, \quad (5.12)$$

$$\text{Im} \left[ \rho_{|\psi^+0\rangle}^E \right]_{\text{parity}} = \begin{pmatrix} 0 & -0.054 & -0.007 & -0.057 & -0.011 & -0.011 & -0.148 & -0.083 \\ 0.054 & 0 & 0.007 & 0.006 & -0.005 & -0.001 & 0.006 & -0.002 \\ 0.007 & -0.007 & 0 & 0.046 & -0.011 & -0.006 & -0.009 & 0.005 \\ 0.057 & -0.006 & -0.046 & 0 & 0 & 0.001 & -0.009 & -0.004 \\ 0.011 & 0.005 & 0.011 & 0 & 0 & -0.011 & -0.012 & -0.039 \\ 0.011 & 0.001 & 0.006 & -0.002 & 0.011 & 0 & -0.003 & 0.005 \\ 0.148 & -0.006 & 0.009 & 0.009 & 0.012 & 0.003 & 0 & -0.031 \\ 0.083 & 0.002 & -0.005 & 0.004 & 0.039 & -0.005 & 0.031 & 0 \end{pmatrix}, \quad (5.13)$$

$$\text{Re} \left[ \rho_{|\psi^+0\rangle}^E \right]_{\text{phase}} = \begin{pmatrix} 0.409 & 0.058 & 0.038 & 0.0437 & 0.0385 & 0.028 & 0.366 & 0.035 \\ 0.058 & 0.014 & 0.052 & -0.007 & 0.0055 & 0 & 0.0523 & 0.001 \\ 0.038 & 0.052 & 0.064 & -0.034 & 0.024 & 0.019 & 0.03 & -0.006 \\ 0.043 & -0.007 & -0.034 & 0.026 & 0.011 & -0.004 & 0.038 & -0.004 \\ 0.038 & 0.005 & 0.024 & 0.011 & 0.073 & 0.015 & 0.037 & -0.004 \\ 0.028 & 0 & 0.019 & -0.004 & 0.015 & 0.009 & 0.067 & -0.005 \\ 0.366 & 0.052 & 0.03 & 0.038 & 0.037 & 0.067 & 0.373 & 0.012 \\ 0.035 & 0.001 & -0.006 & -0.004 & -0.004 & -0.005 & 0.012 & 0.027 \end{pmatrix}, \quad (5.14)$$

and

$$\text{Im} \left[ \rho_{|\psi^+0\rangle}^E \right]_{\text{phase}} = \begin{pmatrix} 0 & -0.040 & 0.039 & -0.034 & 0.019 & 0.005 & -0.021 & -0.080 \\ 0.040 & 0 & 0.015 & 0.005 & 0.009 & 0 & 0.022 & 0.002 \\ -0.039 & -0.015 & 0 & 0.043 & -0.002 & -0.014 & -0.054 & 0.005 \\ 0.034 & -0.005 & -0.043 & 0 & 0.013 & 0.003 & -0.02 & -0.01 \\ -0.019 & -0.009 & 0.002 & -0.013 & 0 & -0.009 & -0.059 & -0.054 \\ -0.005 & 0 & 0.014 & -0.003 & 0.008 & 0 & -0.016 & 0.007 \\ 0.021 & -0.022 & 0.054 & 0.02 & 0.059 & 0.016 & 0 & -0.043 \\ 0.080 & -0.002 & -0.005 & 0.01 & 0.054 & -0.007 & 0.043 & 0 \end{pmatrix}. \quad (5.15)$$

These density matrices are obtained through QST.

The subscripts “parity” and “phase” denotes the experiment for which the experimental

density matrix is obtained via QST. Corresponding density matrices for the other Bell-state-ancilla composites are reported below (Eq. (5.16)-(5.27)).

$$\text{Re} \left[ \rho_{|\psi^{-1}\rangle}^E \right]_{phase} = \begin{pmatrix} 0.037 & 0.081 & -0.003 & -0.015 & -0.002 & 0.009 & -0.011 & -0.062 \\ 0.081 & 0.232 & 0.049 & -0.077 & 0.007 & -0.009 & -0.054 & -0.192 \\ -0.003 & 0.049 & 0.020 & -0.043 & -0.013 & -0.002 & 0.001 & 0.009 \\ -0.015 & -0.077 & -0.043 & 0.233 & 0.001 & -0.016 & 0.007 & -0.015 \\ -0.002 & 0.007 & -0.013 & 0.001 & 0.013 & 0.008 & 0.001 & 0.002 \\ 0.008 & -0.009 & -0.002 & -0.016 & 0.008 & 0.0391 & 0.048 & -0.07 \\ -0.011 & -0.054 & 0.001 & 0.007 & 0.001 & 0.048 & 0.030 & 0.018 \\ -0.062 & -0.192 & 0.009 & -0.015 & 0.002 & -0.07 & 0.018 & 0.395 \end{pmatrix}, \quad (5.16)$$

$$\text{Im} \left[ \rho_{|\psi^{-1}\rangle}^E \right]_{phase} = \begin{pmatrix} 0 & -0.085 & 0.003 & -0.062 & -0.001 & 0.009 & 0.007 & 0.075 \\ 0.085 & 0 & -0.012 & 0.052 & -0.001 & 0.023 & -0.022 & 0.03 \\ -0.003 & 0.012 & 0 & 0.040 & -0.002 & -0.006 & -0.003 & 0.004 \\ 0.062 & -0.052 & -0.040 & 0 & 0.002 & 0.006 & -0.015 & -0.051 \\ 0.001 & 0.001 & 0.002 & -0.002 & 0 & -0.011 & 0 & -0.048 \\ -0.009 & -0.023 & 0.006 & -0.006 & 0.011 & 0 & 0.016 & 0.119 \\ -0.007 & 0.021 & 0.003 & 0.015 & 0 & -0.016 & 0 & 0.016 \\ -0.075 & -0.03 & -0.004 & 0.051 & 0.048 & -0.119 & -0.016 & 0 \end{pmatrix}, \quad (5.17)$$

$$\text{Re} \left[ \rho_{|\phi^{+0}\rangle}^E \right]_{phase} = \begin{pmatrix} 0.079 & 0.013 & 0.007 & -0.008 & 0.004 & -0.0022 & 0.026 & -0.002 \\ 0.013 & 0.010 & 0.078 & -0.007 & 0.0362 & 0.002 & -0.001 & 0 \\ 0.007 & 0.078 & 0.418 & 0.001 & 0.37 & 0.0427 & -0.016 & 0.042 \\ -0.008 & -0.007 & 0.001 & 0.024 & 0.039 & -0.002 & -0.007 & 0.001 \\ 0.004 & 0.036 & 0.37 & 0.039 & 0.387 & 0.053 & 0 & 0.034 \\ -0.002 & 0.002 & 0.042 & -0.002 & 0.053 & 0.0098 & 0.041 & -0.005 \\ 0.026 & -0.001 & -0.016 & -0.007 & 0 & 0.041 & 0.046 & -0.037 \\ -0.002 & 0 & 0.042 & 0.001 & 0.034 & -0.006 & -0.037 & 0.020 \end{pmatrix}, \quad (5.18)$$

$$\text{Im} \left[ \rho_{|\phi^+0\rangle}^E \right]_{phase} = \begin{pmatrix} 0 & -0.015 & -0.065 & -0.056 & -0.055 & -0.01 & 0.002 & 0.002 \\ 0.015 & 0 & -0.023 & 0.006 & -0.021 & 0.005 & 0.007 & 0.002 \\ 0.065 & 0.023 & 0 & -0.024 & 0.002 & -0.045 & 0.045 & 0.022 \\ 0.056 & -0.005 & 0.024 & 0 & 0.064 & 0.005 & 0.002 & 0.005 \\ 0.055 & 0.021 & -0.001 & -0.064 & 0 & -0.043 & 0.056 & -0.024 \\ 0.01 & -0.005 & 0.045 & -0.005 & 0.043 & 0 & 0.006 & 0.005 \\ -0.002 & -0.007 & -0.045 & -0.002 & -0.056 & -0.006 & 0 & 0.035 \\ -0.002 & -0.005 & -0.022 & -0.004 & 0.024 & -0.005 & -0.035 & 0 \end{pmatrix}, \quad (5.19)$$

$$\text{Re} \left[ \rho_{|\phi^-1\rangle}^E \right]_{phase} = \begin{pmatrix} 0.015 & 0.014 & -0.001 & -0.010 & 0 & 0.0055 & 0.0032 & -0.013 \\ 0.014 & 0.05 & 0.048 & -0.107 & 0.020 & 0.028 & 0.011 & -0.027 \\ -0.001 & 0.048 & 0.029 & 0.022 & -0.002 & -0.045 & -0.001 & 0.008 \\ -0.010 & -0.107 & 0.022 & 0.431 & -0.058 & -0.231 & 0.006 & 0.069 \\ 0 & 0.020 & -0.002 & -0.058 & 0.032 & 0.064 & -0.002 & -0.013 \\ 0.005 & 0.028 & -0.045 & -0.231 & 0.064 & 0.23 & 0.042 & -0.091 \\ 0.0032 & 0.011 & -0.001 & 0.006 & -0.002 & 0.0422 & 0.01 & -0.037 \\ -0.013 & -0.027 & 0.008 & 0.069 & -0.013 & -0.091 & -0.037 & 0.203 \end{pmatrix}, \quad (5.20)$$

$$\text{Im} \left[ \rho_{|\phi^-1\rangle}^E \right]_{phase} = \begin{pmatrix} 0 & -0.008 & 0.0015 & -0.036 & -0.052 & -0.016 & 0.006 & -0.011 \\ 0.008 & 0 & 0.0157 & 0.14 & -0.004 & -0.094 & 0.0026 & 0.033 \\ -0.001 & -0.015 & 0 & 0.006 & -0.001 & 0.035 & -0.051 & 0.022 \\ 0.036 & -0.14 & -0.006 & 0 & -0.056 & -0.003 & -0.003 & -0.031 \\ 0.052 & 0.004 & 0.001 & 0.056 & 0 & -0.08 & 0.001 & -0.048 \\ 0.016 & 0.094 & -0.035 & 0.003 & 0.08 & 0 & -0.004 & 0.026 \\ -0.006 & -0.002 & 0.051 & 0.002 & -0.001 & 0.004 & 0 & 0.035 \\ 0.011 & -0.033 & -0.022 & 0.031 & 0.048 & -0.026 & -0.035 & 0 \end{pmatrix}, \quad (5.21)$$

$$\text{Re} \left[ \rho_{|\psi^-0\rangle}^E \right]_{parity} = \begin{pmatrix} 0.462 & 0.085 & 0.016 & 0.013 & 0.010 & -0.012 & -0.334 & -0.017 \\ 0.085 & 0.003 & 0.052 & -0.004 & 0.006 & 0 & -0.0776 & -0.003 \\ 0.016 & 0.052 & 0.030 & -0.031 & 0.007 & 0.0018 & 0.01 & 0.001 \\ 0.013 & -0.004 & -0.031 & 0.029 & 0.010 & -0.007 & -0.0295 & 0.003 \\ 0.010 & 0.006 & 0.007 & 0.011 & 0.048 & 0.011 & 0.0105 & 0.004 \\ -0.012 & 0 & 0.001 & -0.007 & 0.011 & 0.009 & 0.0522 & -0.005 \\ -0.334 & -0.077 & 0.01 & -0.029 & 0.010 & 0.052 & 0.4008 & 0.016 \\ -0.017 & -0.003 & 0.001 & 0.003 & 0.004 & -0.005 & 0.0165 & 0.012 \end{pmatrix}, \quad (5.22)$$



$$\text{Im} \left[ \rho_{|\psi^{-0}\rangle}^E \right]_{parity} = \begin{pmatrix} 0 & -0.051 & -0.020 & -0.066 & -0.011 & 0 & 0.158 & 0.071 \\ 0.051 & 0 & 0.003 & 0.01 & 0.001 & 0 & -0.010 & 0 \\ 0.020 & -0.003 & 0 & 0.048 & -0.01 & -0.006 & -0.009 & -0.002 \\ 0.066 & -0.01 & -0.048 & 0 & 0.006 & -0.001 & 0.006 & -0.005 \\ 0.011 & -0.001 & 0.01 & -0.006 & 0 & -0.011 & -0.018 & -0.041 \\ 0 & 0 & 0.006 & 0.001 & 0.011 & 0 & -0.004 & 0.003 \\ -0.158 & 0.010 & 0.009 & -0.006 & 0.018 & 0.004 & 0 & -0.027 \\ -0.071 & 0 & 0.002 & 0.005 & 0.041 & -0.003 & 0.027 & 0 \end{pmatrix}, \quad (5.23)$$

$$\text{Re} \left[ \rho_{|\phi^{+1}\rangle}^E \right]_{parity} = \begin{pmatrix} 0.05 & 0.020 & -0.002 & -0.017 & -0.002 & -0.020 & 0.007 & -0.005 \\ 0.020 & 0.046 & 0.054 & -0.093 & 0.002 & 0.003 & 0.005 & -0.005 \\ -0.002 & 0.054 & 0.021 & -0.021 & 0.006 & 0.026 & 0.003 & -0.014 \\ -0.017 & -0.093 & -0.021 & 0.427 & 0.092 & 0.189 & -0.018 & 0.019 \\ -0.002 & 0.002 & 0.006 & 0.092 & 0.03 & 0.102 & -0.003 & -0.004 \\ -0.020 & 0.003 & 0.026 & 0.189 & 0.102 & 0.239 & 0.0282 & -0.067 \\ 0.007 & 0.005 & 0.003 & -0.018 & -0.003 & 0.028 & 0.029 & -0.026 \\ -0.005 & -0.005 & -0.014 & 0.019 & -0.004 & -0.067 & -0.026 & 0.158 \end{pmatrix}, \quad (5.24)$$

$$\text{Im} \left[ \rho_{|\phi^{+1}\rangle}^E \right]_{parity} = \begin{pmatrix} 0 & -0.011 & 0.004 & -0.054 & -0.001 & -0.002 & -0.002 & -0.013 \\ 0.011 & 0 & 0.004 & 0.091 & 0.006 & -0.008 & -0.005 & 0.038 \\ -0.004 & -0.004 & 0 & 0 & -0.003 & -0.044 & -0.002 & 0.007 \\ 0.054 & -0.091 & 0 & 0 & 0.055 & -0.032 & 0.013 & -0.019 \\ 0.001 & -0.006 & 0.003 & -0.055 & 0 & -0.066 & 0.004 & -0.04 \\ 0.002 & 0.008 & 0.044 & 0.032 & 0.066 & 0 & 0.007 & 0.076 \\ 0.002 & 0.005 & 0.002 & -0.013 & -0.004 & -0.007 & 0 & 0.034 \\ 0.013 & -0.038 & -0.007 & 0.019 & 0.04 & -0.076 & -0.034 & 0 \end{pmatrix}, \quad (5.25)$$

$$\text{Re} \left[ \rho_{|\phi^{-1}\rangle}^E \right]_{parity} = \begin{pmatrix} 0.028 & 0.015 & 0.002 & -0.032 & 0.006 & 0.024 & -0.005 & -0.004 \\ 0.015 & 0.049 & 0.058 & -0.094 & 0.01 & 0.006 & 0.007 & 0.006 \\ 0.002 & 0.058 & 0.015 & -0.022 & -0.005 & -0.019 & -0.005 & 0.002 \\ -0.032 & -0.094 & -0.022 & 0.439 & -0.083 & -0.226 & 0.022 & 0.019 \\ 0.006 & 0.01 & -0.005 & -0.083 & 0.026 & 0.108 & -0.002 & -0.003 \\ 0.024 & 0.006 & -0.019 & -0.226 & 0.108 & 0.256 & 0.022 & -0.072 \\ -0.005 & 0.007 & -0.005 & 0.022 & -0.002 & 0.022 & 0.022 & -0.029 \\ -0.004 & 0.006 & 0.002 & 0.019 & -0.003 & -0.072 & -0.029 & 0.165 \end{pmatrix}, \quad (5.26)$$

and

$$\text{Im} \left[ \rho_{|\phi^{-1}\rangle}^E \right]_{\text{parity}} = \begin{pmatrix} 0 & -0.007 & 0.001 & -0.052 & 0.003 & 0.002 & 0.002 & 0 \\ 0.007 & 0 & 0.006 & 0.097 & 0.002 & -0.003 & 0.007 & 0.016 \\ -0.001 & -0.006 & 0 & 0.004 & 0.007 & 0.037 & -0.005 & 0.007 \\ 0.052 & -0.097 & -0.004 & 0 & -0.044 & -0.007 & -0.003 & -0.01 \\ -0.003 & -0.002 & -0.007 & 0.044 & 0 & -0.055 & -0.002 & -0.028 \\ -0.002 & 0.003 & -0.037 & 0.007 & 0.055 & 0 & 0.018 & 0.071 \\ -0.002 & -0.007 & 0.005 & 0.003 & 0.002 & -0.08 & 0 & 0.032 \\ 0 & -0.015 & -0.007 & 0.01 & 0.028 & -0.071 & -0.032 & 0 \end{pmatrix}. \quad (5.27)$$

Real part of the density matrices obtained through the parity checking and phase information checking circuits are shown in Figure 5.6. The results illustrated through these plots clearly show that the Bell state discrimination has been realized appropriately. Further, the obtained density matrices allows us to quantitatively establish this fact through the computation of fidelity, and analogy of Figure 5.6 with Figure 6 of Ref. [246] allows us to compare the NMR-based results with the SQUID-based results. However, the nonavailability of the exact density matrices for the NMR-based results, restricts us from a quantitative comparison. The obtained fidelities for the realization of phase and parity information checking circuits are given below. The corresponding cases can be identified by superscript phase and parity.  $F_{|\psi^{+0}\rangle}^{\text{phase}}=0.8707$ ,  $F_{|\psi^{-1}\rangle}^{\text{phase}}=0.7114$ ,  $F_{|\phi^{+0}\rangle}^{\text{phase}}=0.8794$ ,  $F_{|\phi^{-1}\rangle}^{\text{phase}}=0.7493$ ,  $F_{|\psi^{+0}\rangle}^{\text{parity}}=0.8751$ ,  $F_{|\psi^{-0}\rangle}^{\text{parity}}=0.8751$ ,  $F_{|\phi^{+1}\rangle}^{\text{parity}}=0.7224$ , and  $F_{|\phi^{-1}\rangle}^{\text{parity}}=0.7576$ , here the ideal state is given in subscript and superscript "phase" and "parity" corresponds to phase discrimination and parity discrimination realized by phase checking circuit in Figure 5.3 (a) and parity checking circuit in Figure 5.3 (b). Obtained fidelities are reasonably good, but to make a SQUID-based scalable quantum computer, it is necessary to considerably improve the quality of quantum gates. Specifically, we can see that the fidelities of the constructed Bell states were much higher than the fidelities obtained after phase information or parity information of the given Bell state is obtained through the distributed measurement. Clearly, increase in the circuit complexity has resulted in the reduction of fidelity. To illustrate this point, we would now report implementation of the circuit shown in Figure 5.1 (a), i.e., implementation of a four-qubit circuit for nondestructive discrimination of Bell state, where phase information and parity information will be revealed in a single experiment. A four-qubit quantum circuit corresponding to the circuit shown in Figure 5.1 (a) with initial Bell state  $|\psi^{+}\rangle$  is implemented using IBM quantum computer and the same is shown in Figure 5.7 (a), where we have used a circuit theorem shown in Figure 5.7 (b). Although, the circuit and the corresponding results shown here are for  $|\psi^{+}\rangle$ , but we have performed experiments for all possible Bell states and have obtained similar results (which are not illustrated here). Due to the restrictions provided by the IBM computer, the left (right) CNOT gate shown in LHS of Figure 5.7 (b) is implemented using the gates shown in the left

(right) rectangular box shown in RHS of Figure 5.7 (b). In fact, the right most rectangular box actually swaps qubits 2 and 3, apply a CNOT with control at first qubit and target at the second qubit and again swaps qubit 2 and 3. The use of the circuit identity Figure 5.7 (b), allows us to implement the circuit shown in Figure 5.1 (a), but it causes 10 fold increase in gate count (from 2 CNOT gates to a total of 20 gates) for the parity checking circuit. As a consequence of the increase in gate count, the success probability of the experiment reduces considerably, and that can be seen easily by comparing the outcome of the real experiment illustrated in Figure 5.7 (c) with the outcome of the simulation (expected state in the ideal noise-less situation) shown in Figure 5.7 (d). This comparison in general and the outcome observed in Figure 5.7 (c), clearly illustrate that until now the technology used in IBM quantum computer is not good enough for the realization of complex quantum circuits. This fact is also reflected in the low fidelity (as low as 47.64) reported in Ref. [58] in the context of a quantum circuit (having gate count of 11) that implements quantum summation (cf. Figure 6 (d) of [58]). A relatively low value of fidelity (57.03) for a circuit implementing Deutsch-Jozsa algorithm (having a gate count of 18) has also been reported in [268] (cf. Figure 7 of Ref. [268])<sup>1</sup>. However, we cannot be conclusive about the fidelity reported in [268] as the definition of fidelity used there (cf. the definition of fidelity given above Eq. (23) of [268] is  $F(\rho^E, \rho^T) = Tr\sqrt{\rho^E \rho^T \rho^E}$  which is not consistent with the standard definition of fidelity ( $F(\rho^E, \rho^T) = Tr\sqrt{\sqrt{\rho^E} \rho^T \sqrt{\rho^E}}$ ) which is used here. In a similar manner, nothing conclusive can be obtained from the extremely high fidelity values reported in [265]. This is so because, the procedure followed to obtain the fidelity was not described in [265] and extremely high fidelity were even reported when the experimental results were found to considerably mismatch with the theoretically expected results (cf. Figure 3 of [265]). In contrast, in this work a clear prescription for computation of fidelity has been provided and fidelity is computed rigorously. We hope this would help others to compute fidelity for various circuits implemented using IBM quantum experience. The fact that most of the gates implemented in IBM quantum experience introduce more error in comparison to the error introduced by the same gates implemented using some of the other technologies used in quantum computing leads to relatively low fidelity. To illustrate this, one would require to perform quantum process tomography and obtain gate fidelity, average purity, and entangling capability (where it is applicable) and these quantities reflecting gate performance are to be computed for arbitrary input states [281]. In [223], an effort has been made to obtain gate fidelities for the quantum gates used in IBM quantum experience. However, the obtained results don't provide us the desired gate fidelity as they are obtained only for input state  $|0\rangle$  or  $|00\rangle$ , and as QST was performed instead of quantum process tomography. We will further elaborate this point in a

---

<sup>1</sup>Gate count (number of elementary quantum gates) is not an excellent measure for circuit cost here as the error introduced by different gates are different and even the error introduced by the same gate placed in different qubit lines are different. However, reduction of fidelity with this idealized circuit cost (gate count) provides us a qualitative feeling about the problems that may restrict the scalability of the technology used in IBM quantum experience.

future work.

## 5.4 Conclusion

We have already noted that nondestructive discrimination of Bell states have wide applicability. Ranging from quantum error correction to measurement-based quantum computation, and quantum communication in a network to distributed quantum computing. Keeping that in mind, here, we report an experimental realization of a scheme for nondestructive Bell state discrimination. Due to the limitations of the available quantum resources (IBM quantum computer being a five-qubit quantum computer with few restrictions) this study is restricted to the discrimination of Bell states only, but our earlier theoretical proposal is valid in general for discrimination of generalized orthonormal qudit Bell states. We hope that the work reported in this chapter will be generalized in the near future and will be used for the experimental discrimination of more complex entangled states. Further, as the work provides a clean prescription for using IBM quantum experience to experimentally realize quantum circuits that may form building blocks of a real quantum computer, a similar approach may be used to realize a set of other important circuits. Finally, the comparison with the NMR-based technology, reveals that this SQUID-based quantum computer's performance is comparable to that of the NMR-based quantum computer as far as the discrimination of Bell states is concerned. As the detail of the density matrix obtained (through QST) in earlier works [246, 277] was not available, fidelity of NMR-based realization earlier and the SQUID-based realization reported here could not be compared. However, the fidelity computed for the states prepared and retained after the nondestructive discrimination operation is reasonably high and that indicate the accuracy of the IBM quantum computer. Further, it is observed that all the density matrices produced here through the state tomography are mixed state (i.e., for all of them  $Tr(\rho^2) < 1$ ). This puts little light on the nature of noise present in the channel and/or the errors introduced by the gates used. However, it can exclude certain possibilities. For example, it excludes the possibility that the combined effect of noise/error present in the circuit can be viewed as bit flip and/or phase flip error as such errors would have kept the state as pure. More on characterization of noise present in IBM quantum experience will be discussed elsewhere.

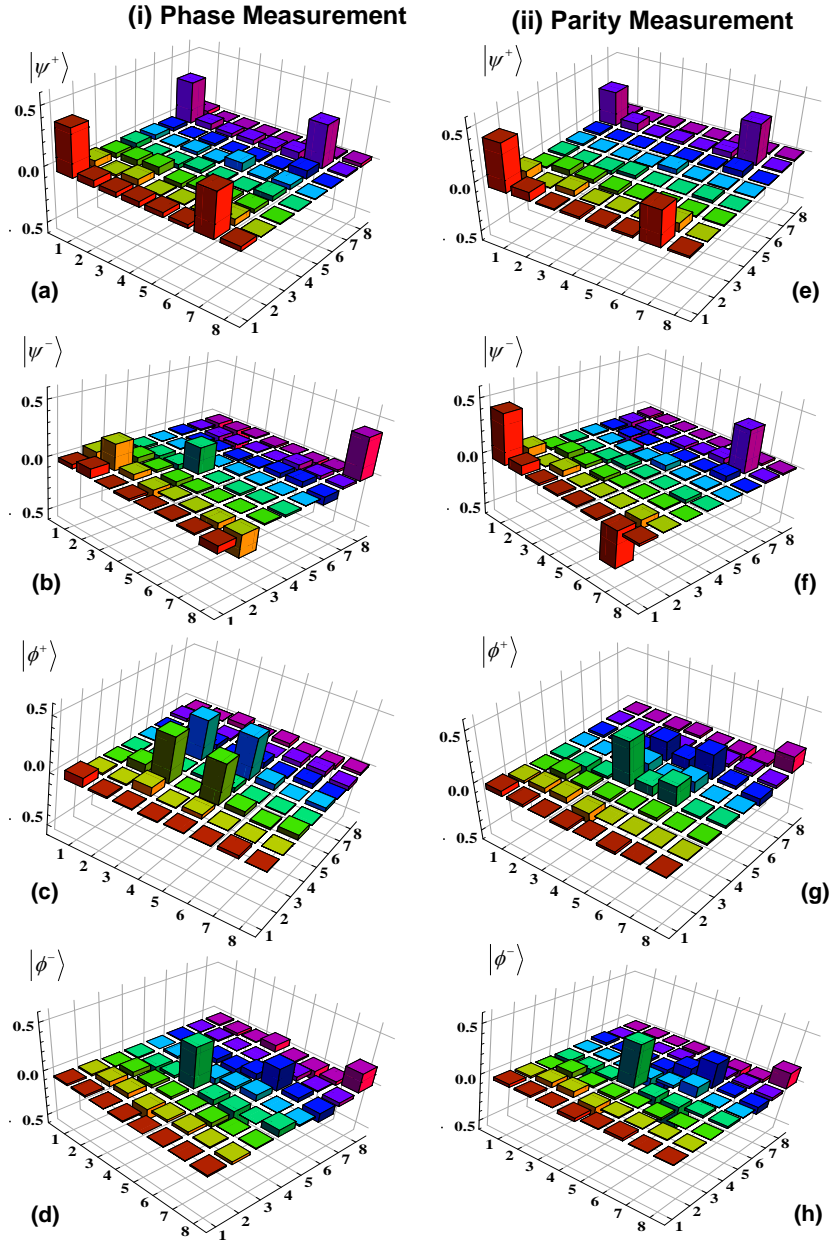
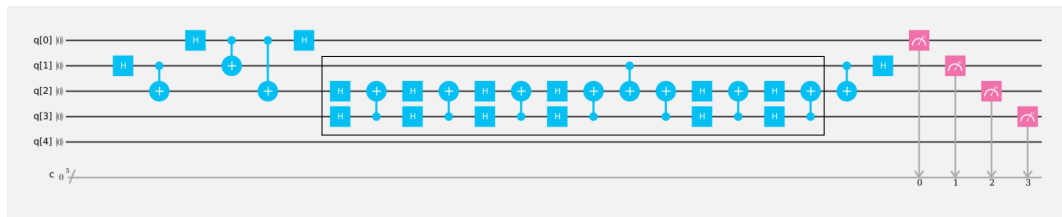
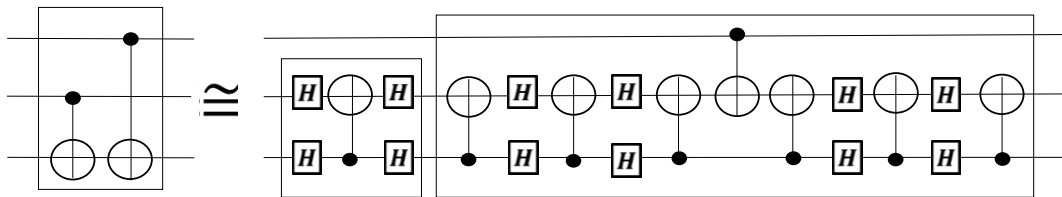


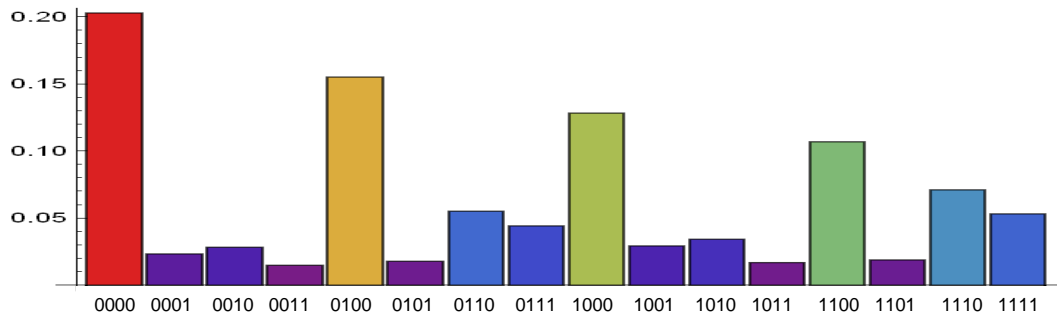
**Figure 5.6:** Reconstructed density matrices of various states of Bell-state-ancilla composite system obtained after the implementation of phase and parity checking circuits shown in Figure 5.3. The first column (a)-(d) illustrates the density matrices corresponding to ideal quantum states  $|\psi^+0\rangle$ ,  $|\psi^-1\rangle$ ,  $|\phi^+0\rangle$ , and  $|\phi^-1\rangle$ , respectively. The density matrices in the second column correspond to ideal states (e)-(h)  $|\psi^+0\rangle$ ,  $|\psi^-0\rangle$ ,  $|\phi^+1\rangle$ , and  $|\phi^-1\rangle$ , respectively.



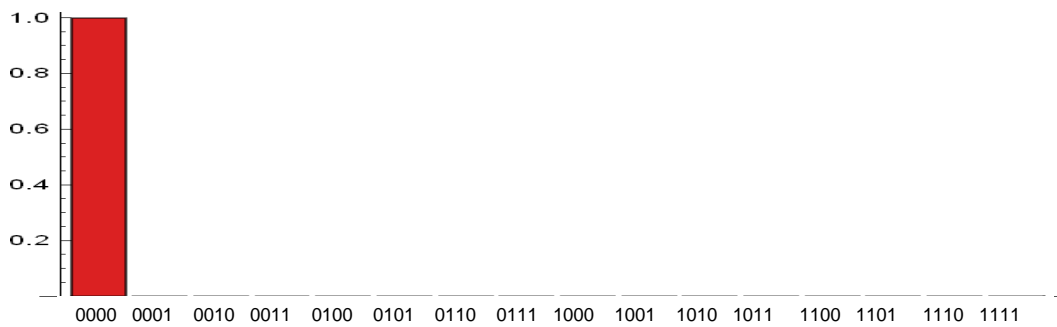
(a)



(b)



(c)



(d)

**Figure 5.7:** (a) For the Bell state  $|\psi^+\rangle$ , actual implementation of the combined (phase and parity checking) four-qubit quantum circuit shown in Figure 5.1 a using five-qubit IBM quantum computer. (b) To circumvent the constraints of IBM quantum computer, the implemented circuit utilizes this circuit identity. (c) Probability of various measurement outcomes obtained in actual quantum computer after running the circuit 8192 times. (d) Simulated outcome after running the circuit on IBM simulator. This outcome coincides exactly with the expected theoretical value, but the experimental outcome shown in (c) is found to deviate considerably from it.

# CHAPTER 6

## OPTICAL DESIGNS FOR THE REALIZATION OF A SET OF SCHEMES FOR QUANTUM CRYPTOGRAPHY

### 6.1 Introduction

In the previous chapters, we have proposed and analyzed a set of protocols for insecure quantum communication with entangled orthogonal and entangled nonorthogonal state based quantum channels. Specifically, schemes for QT have been studied and their performance has been analyzed over Markovian channels. Above studies have motivated us to look at the most fascinating and useful aspect of the quantum communication, i.e., quantum cryptography, where various secure communication tasks can be performed with unconditional security. In Chapter 1, we have already mentioned that the first unconditionally secure protocol for QKD (BB84 protocol) was proposed by Bennett and Brassard in 1984 [3]. Since then it has been strongly established that the quantum cryptography can provide unconditional security, which is a clear advantage over its classical counterparts [282, 283]. Because of this advantage, various schemes of QKD and other cryptographic tasks have been proposed (we have already mentioned about many of them in Chapter 1). Some of them have also been realized experimentally [151, 154, 163, 284, 285]. Interestingly, the quantum resources and the experimental techniques used in these successful experiments are not the same. To stress on this particular point, we may note that the QKD entered into the experimental era with the pioneering experimental work of Bennett et al., in 1992 [286]. In this work, randomly prepared polarization states of single photons were used, but as there does not exist any on demand single photon source, they used faint laser beams as approximate single photon source. If such a source is used, to circumvent photon number splitting (PNS) attack, it expected that decoy qubits are to be used. In 1992 work of Bennett et al., no decoy qubit was used. However, in later experiments, decoy states are frequently used. For example, in 2006, Zhao et al., had realized a decoy state based QKD protocol [287] using

the acousto-optic modulators (AOMs) to achieve polarization insensitive modulation. In the absence of on demand single photon sources, various strategies have been used to realize single photon based QKD schemes, like BB88 and B92. Some of the experimentalists used weak coherent pulse (WCP) as an approximate single photon source [284, 288–295]. Others used heralded single photon source [296, 297]. In the 27 years, a continuous progress has been observed in the experimental QKD. It started from the experimental realization of a single photon based QKD scheme using WCP, but as time passes many other facets of QKD have been experimentally realized. For example, in one hand MDI-QKD has been realized using untrusted source [298, 299], and heralded single photon source [149, 300]. On the other hand, soon it was realized that continuous variable QKD can be used to circumvent the need of single photon sources and thus to avoid several attacks. Naturally, some of the continuous variable QKD schemes have been realized in the recent past [301–303]. Beyond this, to address the concerns of the end users, over the time the devices used have become portable (say, a silicon photonic transmitter is designed for polarization-encoded QKD [304, 305], and chip-based QKD systems have been realized [306]); QKD has been realized using erroneous source [294]; key generation rate over noisy channel has been increased (e.g., in [307], a key generation rate of 1.3 Gbit/s was achieved over a 10-dB-loss channel); distance over which a key can be securely distributed has been increased, for example, in [308] QKD is performed over 421 km in optical fiber and in the last 2-3 years couple of QKD experiments have been performed using satellites [152, 153] - the one which needs special mention is the quantum communication between the ground stations located at China and Austria at distance of 7600 kilometers [153]. Furthermore, various commercial products like Clavis 2 and Clavis 3 of ID Quantique [177] and MagiQ QPN of MagiQ [178] have also been marketed.

From the discussion above it seems that the experimental QKD is now a matured area. However, the same is not true for other aspects of quantum cryptography, i.e., for the schemes beyond QKD (e.g., schemes for QD, QSDC, DSQC, CQD). Only a handful of experiments have yet been performed. Specifically, QSDC has been realized with entangled photons [151, 154], and single photons [163]. On top of that, quantum secret sharing has also been demonstrated [309, 310] and extended to multiparty scenario as well [311]. However, our discussion is focused on direct communication schemes and quantum secret sharing is beyond the scope of the present chapter.

The above status of the experimental works have motivated us to investigate possibilities of experimental realization of quantum cryptographic schemes, such as QD [2, 65], CQD [94], Kak's three stage scheme inspired direct communication scheme [247], controlled DSQC with entanglement swapping [312] which have not been experimentally realized so far. In the process, to design optical schemes for the realization of these schemes, we have realized that the implementation requires some modifications of the original schemes. Keeping this point in mind, in the following sections of this chapter, we have modified the original schemes which



remains operationally equivalent to the original scheme/without compromising with the security and have designed optical circuits for the above mentioned quantum cryptographic schemes, which are based on single photon, two-qubit and multi-qubit entangled states (such as GHZ-like state, W state) using available optical elements, like laser, BS, PBS, HWP.

The rest of the chapter is organized as follows. In Section 6.2, we have presented the designs of optical circuits for various quantum cryptographic tasks. Each circuit and the protocol it implements are also described in the section. Finally, the Chapter is concluded in Section 6.3.

## 6.2 Quantum cryptographic protocols

In the previous section and in Chapter 1, we have already mentioned that there exist unconditionally secure protocols for various quantum communication tasks and a good number of experiments have been done. However, until the recent past, experimental works on secure quantum communication were restricted to the experimental realizations of different protocols of QKD. Only recently (in 2016), a protocol of QSDC was realized experimentally by Hu et al. [163]. Specifically, Hu et al., realized DL04 protocol [313] using single-photon frequency coding. This pioneering work was a kind of proof-of-principle table-top experiment. In this work, the requirement of quantum memory was circumvented by delaying the photonic qubits in the fiber coils. However, soon after Hu et al.'s pioneering work, Zhang et al., [151] reported another experimental realization of QSDC protocol through a table top experiment. Zhang et al.'s experiment was fundamentally different from Hu et al.'s experiment in two aspects- firstly Zhang et al., used entangled states and secondly they used quantum memories based on atomic ensembles. Almost immediately after the Zhang et al.'s experiment, Zhu et al., reported experimental realization of a QSDC scheme over a relatively longer distance in 2017 [154]. With these three experiments, experimental quantum cryptography arrived at a stage beyond QKD, where a set of schemes of two-party one-way secure direct communication can be experimentally realized using the available technologies. However, there exist many multi-party schemes of secure direct quantum communication, some of which are also two-way schemes. For example, any scheme for QD would require two-way communication, whereas any scheme of controlled quantum communication involves at least three parties (say, a scheme for CQD). No such protocol has yet been realized experimentally. In what follows, we will see that many of these protocols can be realized experimentally using the existing technology. However, to do so, some of the protocols would require some modifications, which are needed for experimental realizations. In this chapter, we would concentrate on such suitably modified protocols, and the optical circuits which can be used to experimentally realize those schemes. The optical designs proposed here can also be used for experimental implementation of some other DSQC, for instance, MDI-QSDC scheme using two-qubit entanglement and single photon source as well as Bell measurement to accomplish required teleportation [314].

In the following section, we will briefly describe a protocol of CQD and how to implement that using the existing optical technology. To do so, we will be very precise and restrict ourselves from the detailed discussion of the protocols or their security proof as those are available elsewhere and those are not of the interest of the present thesis. Specifically, we will briefly describe a protocol in a few steps which are essential. We will also provide a clear schematic diagram of the optical setup that can be used to realize the protocol, and will provide a step-wise description of the working of the setup. The same strategy will be followed in describing the other protocols, too.

## 6.2.1 Controlled quantum dialogue

To begin with, we may note that CQD is a three party scheme. In this scheme, Alice and Bob want to exchange their secret messages simultaneously to each other with the help of a third party Charlie (controller). In what follows, we will first summarize a set of CQD schemes of our interest [94, 96] and the bottleneck present in the implementation of the theoretical schemes. After that we will explicitly show that it's possible to design optical circuits to experimentally realize CQD with entangled photons and single photon (in more than one way).

### 6.2.1.1 CQD with single photons

CQD scheme based on single-qubit is summarized in the following steps:

**CQDS\_1:** Charlie prepares a random string of single qubits prepared in one of four states  $|0\rangle$ ,  $|1\rangle$ ,  $|+\rangle$  and  $|-\rangle$ .

**CQDS\_2:** Charlie sends the string to Alice.

**CQDS\_3:** After Alice confirms that she has received the string she randomly measures half of the qubits either in  $\{|0\rangle, |1\rangle\}$  or  $\{|+\rangle, |-\rangle\}$  basis and announces her measurement basis and results with corresponding position for checking the eavesdropping. Then Charlie compares the Alice's measurement result with that of state preparation by using classical communication (CC) in all the cases where they have chosen the same basis<sup>1</sup>.

**CQDS\_4:** Alice encodes her message on the one-half of the remaining qubits by using Pauli operations  $I$  or  $iY$  to encode 0 or 1, respectively.

**CQDS\_5:** Alice sends the message encoded and decoy qubits to Bob.

---

<sup>1</sup>Throughout this chapter, transmission of qubits is performed along the same line after concatenation of a randomly prepared string of decoy qubits followed by permutation of qubits in the enlarged string. Subsequently, the error estimation on the transmitted decoy qubits provides an upper bound of the errors introduced during transmission on the remaining message qubits, which can be solely attributed to the disturbance caused due to an eavesdropping attempt for the sake of simplicity and attaining utmost security. The choice of decoy qubits could be the single-qubit states used in BB84 protocol or entangled states (see [79] for a detailed discussion).

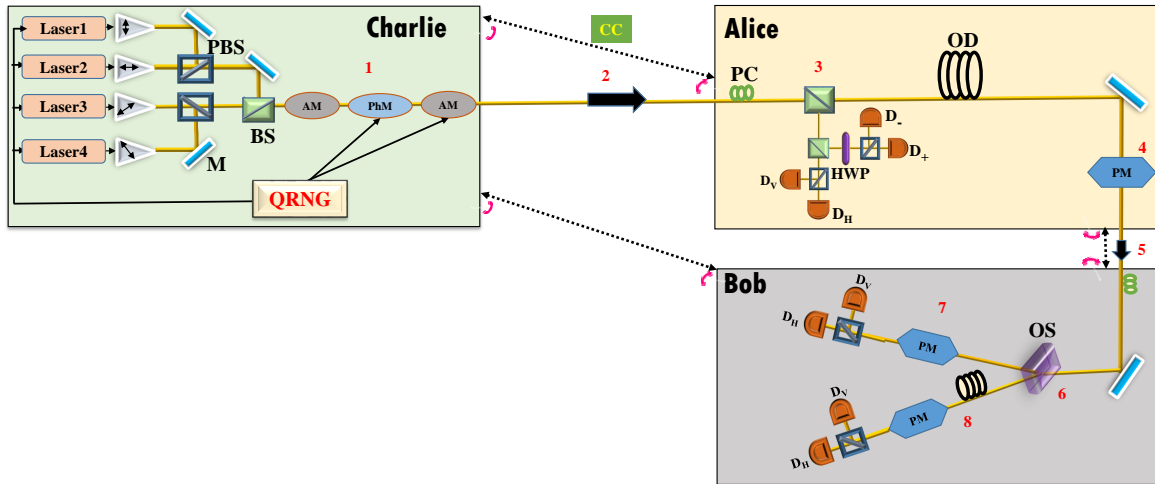


**Figure 6.1:** Schematic diagram for CQD scheme based on polarization qubit. Four lasers are used to prepare the polarization states of photons. In the proposed optical design, BS stands for symmetric (50:50) beam splitter, PBS is polarizing BS, M is mirror, AM is amplitude modulator, PhM is phase modulator, QRNG is quantum random number generator, PC is polarization controller, HWP is half wave plate, OD is optical delay, PM is polarization modulator, OS is optical switch,  $D_i$  represents the detector; whereas  $D_H$  and  $D_V$  correspond to detectors used for measurements in horizontal and vertical basis and similarly  $D_+$  and  $D_-$  correspond to measurements in the diagonal basis; and CC is classical communication.

**CQDS\_6:** Bob receives the encoded photons (along with the remaining half to be used as decoy qubits).

**CQDS\_7:** To ensure the absence of Eve, Alice discloses the positions of the decoy qubits and Charlie announces corresponding choice of basis.

**CQDS\_8:** Now, Bob encodes his message on the same qubits as used by Alice to encode his message. Charlie announces the basis information for the message encoded qubits when he wishes the task to be accomplished. After knowing the basis of the initial state from Charlie, Bob measures the corresponding qubits in that basis and announces the measurement outcome. Using the measurement outcome both Alice and Bob can decode each other's messages.

The aforementioned CQD scheme has not yet been realized experimentally due to unavailability of quantum memory, difficulty in building on demand single photon sources, and limitation in performing the scheme over scalable distance due to the complexity of the task. However, there is a silver lining that the CQD protocol using single photons can be realized using the existing technology, such as using frequency encoding. To stress on this point a schematic diagram of the optical setup that can be used to realize the above protocol using polarization qubits is illustrated in Fig. 6.1 and in what follows, the same is elaborated in a few steps.

## Optical design for CQD protocol using single photons (polarization qubits)

**CQDS-Op\_1:** Charlie uses four lasers to generate the polarization state of the photons and two PBS, three mirrors, one symmetric (50:50) BS, two AM, one PhM, to generate the random string of single photons in one of the four polarization states  $|H\rangle$ ,  $|V\rangle$ ,  $\frac{|H\rangle+|V\rangle}{\sqrt{2}}$  and  $\frac{|H\rangle-|V\rangle}{\sqrt{2}}$ . Whereas, the first AM is used to generate the decoy photons, the second AM is used to control the intensity of light and the global phase of each photon is modulated by PhM [292]. This is not the unique method for the preparation of polarization qubit, which can also be generated by heralding one outputs of the SPDC outputs.

**CQDS-Op\_2:** Charlie sends the string of single photons to Alice through optical fiber, open-air, through satellite, or under-water in case of maritime cryptography.

**CQDS-Op\_3:** Alice receives the string of photons and randomly selects one-half of the incoming photons using a BS to check any eavesdropping attempt. She randomly measures all the reflected photons either in  $\{|H\rangle, |V\rangle\}$  or  $\left\{\frac{|H\rangle+|V\rangle}{\sqrt{2}}, \frac{|H\rangle-|V\rangle}{\sqrt{2}}\right\}$  basis (again using a BS) and announces her measurement basis and results with corresponding position for checking the eavesdropping. Then Charlie compares Alice's measurement result with that of state preparation. While the eavesdropping checking between Charlie and Alice, she uses an optical delay (serving as a quantum memory) for the rest of the photons. Suppose Charlie prepares the photon from laser1, i.e., in state  $|V\rangle$  then detector  $D_V$  is expected click in the ideal case, but if the detector  $D_H$  clicks, then it will be registered as bit error. However, if the detectors  $D_+$  or  $D_-$  clicks then these cases will be discarded.

**CQDS-Op\_4:** Alice encodes her message on one-half of the transmitted photons by using a PM or a set of a half-wave plate sandwiched between two quarter-wave plates.

**CQDS-Op\_5:** Alice sends encoded and decoy photons to Bob.

**CQDS-Op\_6:** Bob receives the encoded photons along with the decoy photons and keeps the received photons in an optical delay. Subsequently, Alice discloses the positions of the decoy qubits and Bob passes the string of photons through an optical switch which sends the encoded photons and decoy photons on different paths.

**CQDS-Op\_7:** To ensure the absence of Eve, Bob chooses the basis of the decoy qubits by using a PM and measures them to compute the error rate. They proceed if the errors are below threshold.

**CQDS-Op\_8:** Bob encodes his message using a PM on the same photons used by Alice to encode his message. Subsequently, Charlie reveals the basis information of state preparation. After knowing the basis choice of the initial state from Charlie, he measures the message encoded photons using two single photon detectors and a PM to choose the basis

of the states to be measured and announces his result. In fact, Bob can perform the same task using only one PM if he delays his encoding till Charlie reveals the basis information. From the measurement outcomes both Alice and Bob will be able to decode each other's messages.

### **6.2.1.2 Kak's three-stage scheme inspired five-stage scheme of CQD with single photons**

A three stage QKD scheme proposed in the past [247] was shown recently able to perform direct communication. Here, we propose a three-stage scheme inspired CQD protocol, which can be viewed as a five-stage protocol of CQD. The protocol is summarized in the following steps:

**CQD-K\_1:** Charlie prepares a string of single qubits in the computational basis. Subsequently, he applies random unitary operators on each qubit and keeps the corresponding information with himself.

**CQD-K\_2:** Same as **CQDS\_2**.

**CQD-K\_3:** After Alice confirms that she has received the qubits she measures one-half of the received qubits to check eavesdropping chosen by Charlie, who also disclose corresponding rotation operator and the initial state.

**CQD-K\_4:** Alice applies a random rotation operator on all the qubits.

**CQD-K\_5:** Same as **CQDS\_5**.

**CQD-K\_6:** Same as **CQD-K\_3**, here Bob measures one-half of the received qubits with the help of information of rotation operators by Charlie and Alice as well as the initial state revealed by Charlie.

**CQD-K\_7:** Same as **CQD-K\_4**, but Bob applies his rotation operator.

**CQD-K\_8:** Bob sends all the qubits to Charlie.

**CQD-K\_9:** After Charlie confirms that he has received the qubits he measures one half of the received qubits to check eavesdropping with the help of Alice's, Bob's, and his own rotation operators.

**CQD-K\_10:** Charlie applies an inverse of his rotation operator applied in **CQD-K\_1**.

**CQD-K\_11:** Same as **CQDS\_2**.

**CQD-K\_12:** Same as **CQD-KS\_3**, but here Alice requires information of the rotation operator from Bob.

**CQD-K\_13:** Alice applies inverse of the rotation operator applied in **CQD-K\_4**. Subsequently, she also encodes her message on one-half of the remaining qubits using Pauli operations  $I$  or  $X$  to send 0 or 1, respectively.

**CQD-K\_14:** Same as **CQDS\_5**.

**CQD-K\_15:** Same as **CQD-KS\_6**, but Bob needs only his rotation operator.

**CQD-K\_16:** Bob applies inverse of his rotation operator and encodes his message on all the qubits. He subsequently measures the transformed qubits in the computational basis and announces the measurement outcome. Finally, Charlie reveals the initial state when he wishes them to accomplish the task. With the help of the initial and final states both Alice and Bob can decode each other's messages.

To complete two rounds, first for locking and second for unlocking, between three parties the qubits should travel five times through the lossy transmission channel which sets limitations on the experimental implementation of the present scheme. However, to remain consistent with the theme of the present work, where reduction of complex quantum cryptographic tasks to obtain the solutions of simpler secure communication tasks, we now discuss the optically implementable scheme. In principle, the protocol described here can also be realized using available optical elements and a schematic diagram for that is shown in Figure 6.2, and the same is described below in a few steps.

### **Optical design for five-stage scheme using single photons**

**CQD-Op-K\_1:** Charlie prepares a random string of horizontal and vertical polarized single photons and uses  $PM_C$  to rotate the polarization of light randomly.

**CQD-Op-K\_2:** Same as **CQDS-Op\_2**.

**CQD-Op-K\_3:** Same as **CQDS-Op\_3**, but here Charlie informs the decoy qubits by revealing the positions and corresponding random unitary operation using which Alice measures the photons in the computational basis with the help of optical switch, polarization modulator and single photon detectors. They proceed only if fewer than the threshold bit-flip errors are observed.

**CQD-Op-K\_4:** Alice applies a random rotation on the rest of the qubits using  $PM_A$ .

**CQD-Op-K\_5:** Same as **CQDS-Op\_5**.

**CQD-Op-K\_6:** Same as **CQD-Op-K\_3**, here Alice and Bob perform eavesdropping checking with the help of Charlie.

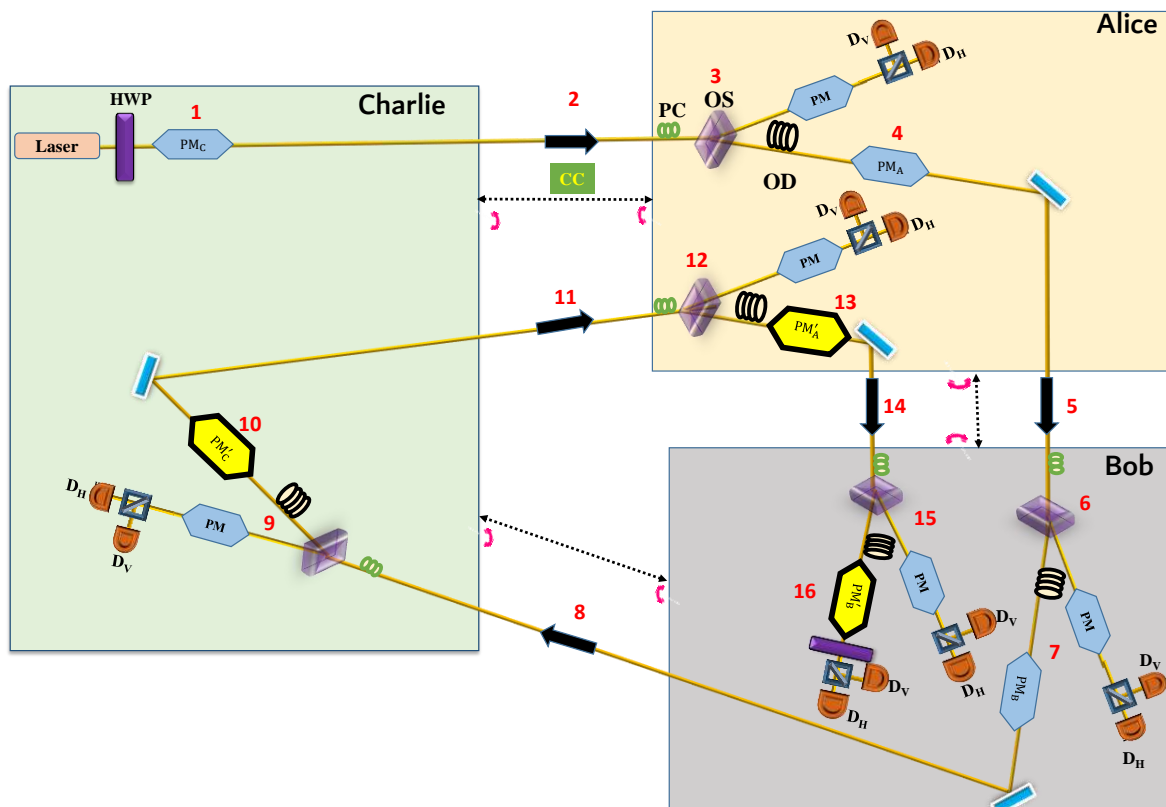


**Figure 6.2:** A proposed optical implementation using polarization qubit of the CQD scheme inspired from the three stage scheme. Laser is used to prepare the photons. In the all lab's,  $PM_{A,B,C}$  is polarization modulator used to implement a rotation operator, and  $PM'_{A,B,C}$  performs corresponding inverse rotation operator.

**CQD-Op-K\_7:** Same as **CQD-Op-K\_4**, but Bob applies the random operation.

**CQD-Op-K\_8:** Bob sends all the qubits to Charlie.

**CQD-Op-K\_9:** Same as **CQD-Op-K\_3**, here Charlie needs assistance of both Alice and Bob to perform eavesdropping checking.

**CQD-Op-K\_10:** Charlie applies the inverse of his rotation operator  $PM'_C$ .

**CQD-Op-K\_11-12:** Same as **CQDS-Op\_2-3**.

**CQD-Op-K\_13:** Alice applies an inverse operation of her rotation operator using  $PM'_A$ . She also encodes her message in this step.

**CQD-Op-K\_14-15:** Same as **CQDS-Op\_5-6**.

**CQD-Op-K\_16:** Bob applies his inverse rotation operator  $PM'_B$  and encodes his message. Then he measures the polarization of the transformed qubits and announces the result. When Charlie wishes them to complete the task, he reveals the initial choice of polarization of his qubit.

So far, we have discussed schemes of CQD using single photons. Extending the idea, in what follows, we will discuss the CQD scheme using entangled states and subsequently discuss the optical implementation of such scheme.

### 6.2.1.3 CQD protocol with entangled photons

CQD scheme based on entangled qubits is summarized in the following steps:

**CQDE\_1:** Charlie prepares a string of three qubit GHZ-like state  $|\psi\rangle = |\psi^+0\rangle + |\psi^-1\rangle$ . He uses first and second qubit as a travel qubit and third qubit as a home qubit.

**CQDE\_2:** Charlie keeps all the third qubits and sends the strings of first and second qubits to Alice and Bob, respectively after inserting some decoy qubits in each string.

**CQDE\_3:** Same as **CQDS\_3**, but here both Alice and Bob perform eavesdropping checking on the strings received from Charlie.

**CQDE\_4:** Same as **CQDS\_4**, but Alice can use dense coding and encode 2 bits of message using all four Pauli operations.

**CQDE\_5:** Same as **CQDS\_5**, but here Alice randomly inserts freshly prepared decoy qubits before sending message encoded qubits to Bob.

**CQDE\_6:** Same as **CQDS\_6**.



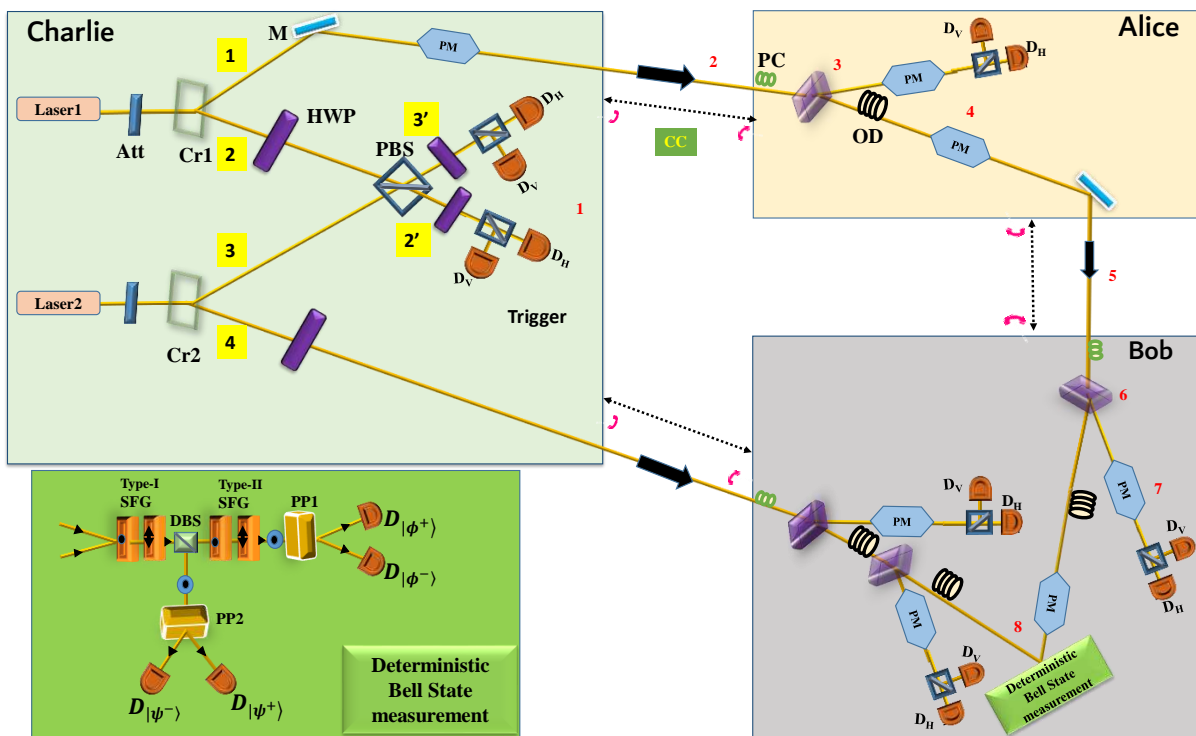


**Figure 6.3:** Optical design of the CQD scheme with a complete Bell state measurement (BSM). In Charlie's lab Cr is a nonlinear crystal which is used to generate the entangled photon. Sum frequency generation (SFG) type-I and type-II are nonlinear interactions, which are used to perform the BSM. DBS is dichroic BS and PP1 and PP2 are  $45^\circ$  projector. Attenuator (Att) is used to control the intensity of light so that a single Bell pair can be generated. This can also be controlled by changing the pump power. BSM is shown in the box.

**CQDE\_7:** Same as **CQDS\_7**, but Charlie need not disclose anything.

**CQDE\_8:** Now, Bob encodes his message on the same qubits which qubits were used by Alice to encode his message. Subsequently, Bob performs the Bell measurement on the messages encoded string and the string received from Charlie. Then he announces the measurement results. Now, Alice and Bob decode the message with the help of Charlie's measurement results of the third qubits.

The CQD protocol using entangled photons described above can be realized using optical elements. A schematic diagram for that is shown in Figure 6.3, which is described briefly below in a few steps.

### Optical design for CQD protocol using entangled photons

**CQDE-Op\_1:** Charlie uses two lasers and two non-linear crystals (Cr1 and Cr2) to generate the two pair of Bell states with the help of SPDC process.

$$|\psi\rangle_1 = \left( \frac{|HH\rangle + |VV\rangle}{\sqrt{2}} \right)_{12} \otimes \left( \frac{|HH\rangle + |VV\rangle}{\sqrt{2}} \right)_{34},$$

where  $H$  and  $V$  represent the horizontal and vertical polarizations, respectively.

Now,  $2^{nd}$  and  $4^{th}$  photon passes through the HWP ( $2\theta = 45^0$ ) and the state becomes

$$\begin{aligned} |\psi\rangle_2 &= \left( \frac{|H+\rangle + |V-\rangle}{\sqrt{2}} \right)_{12} \otimes \left( \frac{|H+\rangle + |V-\rangle}{\sqrt{2}} \right)_{34}, \\ &= \frac{1}{2} (|H+H+\rangle + |H+V-\rangle + |V-H+\rangle + |V-V-\rangle)_{1234}, \end{aligned} \quad (6.1)$$

where diagonal polarization states are represented by  $|\pm\rangle = \frac{|H\rangle \pm |V\rangle}{\sqrt{2}}$ . Subsequently, the  $2^{nd}$  and  $4^{th}$  photon pass through the PBS (which transmits the horizontal photon and reflect the vertical photon). The postselected state after passing through PBS such that only one photon will be in each output path can be written as after renormalization

$$|\psi\rangle_3 = \frac{1}{2} (|HHH+\rangle + |HVV-\rangle + |VHH+\rangle - |VVV-\rangle)_{12'3'4}.$$

Then photon  $2'$  passes through a HWP ( $2\theta = 45^0$ ) and state transforms as

$$\begin{aligned} |\psi\rangle_4 &= \frac{1}{2} (|+\rangle_{2'} (|HH+\rangle + |HV-\rangle + |VH+\rangle - |VV-\rangle)_{13'4} \\ &\quad + |-\rangle_{2'} (|HH+\rangle - |HV-\rangle + |VH+\rangle + |VV-\rangle)_{13'4}) \\ |\psi\rangle_4 &= \frac{1}{2} (|+\rangle_{2'} (|+H+\rangle + |-V-\rangle)_{13'4} + |-\rangle_{2'} (|+H+\rangle - |-V-\rangle)_{13'4}) \\ &= \frac{1}{2} (|+\rangle_{2'} (|+\rangle_{3'} |\psi^+\rangle_{14} + |-\rangle_{3'} |\phi^+\rangle_{14}) + |-\rangle_{2'} (|+\rangle_{3'} |\phi^+\rangle_{14} + |-\rangle_{3'} |\psi^+\rangle_{14})) \\ &= \frac{1}{2} (|+\rangle_{2'} (|\Phi_1\rangle) + |-\rangle_{2'} (|\Phi_2\rangle)) \end{aligned} \quad (6.2)$$

From the obtained state one can clearly see that if Charlie measures qubit  $2'$  and announces the measurement outcome, depending upon which all the parties can decide which channel they are sharing. Otherwise, if Charlie measures  $|+\rangle$ , then he will get  $|+\rangle_{3'}|\psi^+\rangle_{14} + |-\rangle|\phi^+\rangle_{14}$ , no need to apply any gate, i.e., identity, if he measures  $|-\rangle$ , then he will get  $|+\rangle_{3'}|\phi^+\rangle_{14} + |-\rangle|\psi^+\rangle_{14}$ , he need to apply NOT gate by using on 1 or 4, then the state will be  $|+\rangle_{3'}|\psi^+\rangle_{14} + |-\rangle|\phi^+\rangle_{14}$ . Also note that  $|\Phi_i\rangle$  are the unitary equivalent of the state prepared in **CQDE\_1**. The experimental preparation of three-qubit states using this approach can be found in Ref. [125].

**CQDE-Op\_2:** Charlie sends corresponding photons 1 and 4 to Alice and Bob, respectively.

**CQDE-Op\_3:** Both Alice and Bob receive the photons and choose the same set of photons using an optical switch to check their correlations with Charlie to check the eavesdropping. Bob keeps her photons in an optical delay. Here, it is worth mentioning that Alice and Bob can also use BS for this task, but that will reduce qubit efficiency as the cases where one of them has measured entangled state, but not other will be discarded.

**CQDE-Op\_4:** Same as **CQDS-Op\_4**, but Alice uses dense coding as well.

**CQDE-Op\_5-6:** Same as **CQDS-Op\_5-6**.

**CQDE-Op\_7:** Same as **CQDS-Op\_7**, but Charlie has to reveal the measurement outcome for the corresponding decoy qubits.

**CQDE-Op\_8:** Same as **CQDS-Op\_8**, but Bob encode his 2 bits of message on each photon by using PM on the same photons used by Alice. After that, Bob performs Bell measurement [315] and announces the measurement outcome. Similarly, Charlie measures his qubit in the diagonal basis and announces the measurement result when he wishes Alice and Bob to decode the messages. There are schemes for probabilistic Bell measurement, but is not desirable in the implementation of direct communication schemes as it is prone to loss in encoded message. The drawback of deterministic BSM is small efficiency due to involvement of nonlinear optics in its implementation.

## 6.2.2 Controlled direct secure quantum communication

Another controlled communication scheme where DSQC from Alice to Bob is controlled by a controller. Specifically, Alice can directly transmits the message in a secure manner to Bob with the help of controller. Controller controls the channel between Alice and Bob.

### 6.2.2.1 CDSQC with single photons

The CQD schemes discussed in the previous section can be reduced to CDSQC schemes if Bob does not encode his message in the last step. Additionally, he need not to announce the measurement outcome as he is not sending message to Alice in this task.

### 6.2.2.2 CDSQC with entangled photons

The entangled states based CQD scheme can also be reduced analogous to single photon based scheme to obtain a CDSQC scheme. Here, we have presented another entangled state based CDSQC 6.4 with entanglement swapping, where message encoded qubits are not accessible to Eve as those qubits don't travel through the channel.

### 6.2.2.3 CDSQC with entanglement swapping

CDSQC with entanglement swapping is summarized in the following steps:

**CDSQC\_1:** Charlie prepares a four qubit entangled state

$$|\psi\rangle = \frac{1}{2} (|+\rangle_{2'} (|0\rangle_{3'} |\psi^+\rangle_{14} + |1\rangle_{3'} |\phi^+\rangle_{14}) + |-\rangle_{2'} (|0\rangle_{3'} |\phi^+\rangle_{14} + |1\rangle_{3'} |\psi^+\rangle_{14})), \quad (6.3)$$

where qubit  $2'$  corresponds to Charlie, qubits 1 and 4 for Alice and  $3'$  for Bob.

**CDSQC\_2:** Same as **CQDE\_2**.

**CDSQC\_3:** Same as **CQDE\_3**.

**CDSQC\_4:** Alice prepares  $|\psi^+\rangle_{A_1A_2}$  to encode her secret information. Specifically, she encodes 1 (0) by applying a  $X$  ( $I$ ) gate on one of the qubits of the Bell state. Thus, the combined state becomes

$$\begin{aligned} |\psi'\rangle = & \frac{1}{2\sqrt{2}} (|\psi^+\rangle_{A_1A_2} |+\rangle_{2'} (|0\rangle_{3'} |\psi^+\rangle_{14} + |1\rangle_{3'} |\phi^+\rangle_{14}) \\ & + |\psi^+\rangle_{A_1A_2} |-\rangle_{2'} (|0\rangle_{3'} |\phi^+\rangle_{14} + |1\rangle_{3'} |\psi^+\rangle_{14})) \end{aligned} \quad (6.4)$$

**CDSQC\_5:** Alice measures qubits  $A_1$  and 1 as well as  $A_2$  and 4 in the Bell basis, while Bob and Charlie can measure his qubits in the computational basis and diagonal basis, respectively. Subsequently, Alice and Charlie announce their measurement outcomes, which should reveal Alice's message to Bob.

To illustrate this point we can write the state before Alice's and Bob's measurements while

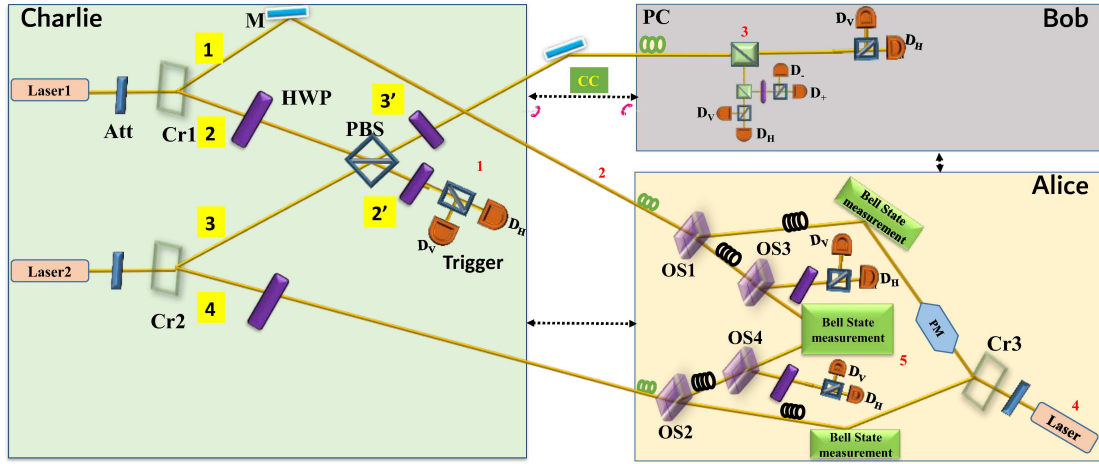


**Figure 6.4:** Schematic optical design of controlled direct secure quantum communication with entanglement swapping.

Charlie's measurement result is  $|+\rangle$  when Alice encodes 0.

$$\begin{aligned}
 |\psi'\rangle &= \frac{1}{2\sqrt{2}} (\{|\psi^+\rangle_{A_11}|\psi^+\rangle_{A_24} + |\phi^+\rangle_{A_11}|\phi^+\rangle_{A_24} + |\phi^-\rangle_{A_11}|\phi^-\rangle_{A_24} + |\psi^-\rangle_{A_11}|\psi^-\rangle_{A_24}\} |0\rangle_{3'} \\
 &+ \{|\psi^+\rangle_{A_11}|\phi^+\rangle_{A_24} + |\psi^-\rangle_{A_11}|\phi^-\rangle_{A_24} + |\phi^+\rangle_{A_11}|\psi^+\rangle_{A_24} + |\phi^-\rangle_{A_11}|\psi^-\rangle_{A_24}\} |1\rangle_{3'}). \quad (6.5)
 \end{aligned}$$

Similarly, if Charlie's measurement result is  $|-\rangle$  and Alice encodes 1

$$\begin{aligned}
 |\psi'\rangle &= \frac{1}{2\sqrt{2}} (\{|\psi^+\rangle_{A_11}|\phi^+\rangle_{A_24} + |\phi^+\rangle_{A_11}|\psi^+\rangle_{A_24} - |\phi^-\rangle_{A_11}|\psi^-\rangle_{A_24} - |\psi^-\rangle_{A_11}|\phi^-\rangle_{A_24}\} |1\rangle_{3'} \\
 &+ \{|\psi^+\rangle_{A_11}|\psi^+\rangle_{A_24} - |\psi^-\rangle_{A_11}|\psi^-\rangle_{A_24} + |\phi^+\rangle_{A_11}|\phi^+\rangle_{A_24} - |\phi^-\rangle_{A_11}|\phi^-\rangle_{A_24}\} |0\rangle_{3'}). \quad (6.6)
 \end{aligned}$$

Similarly, if Charlie's measurement result is  $|+\rangle$  and Alice encodes 1

$$\begin{aligned}
 |\psi'\rangle &= \frac{1}{2\sqrt{2}} (\{|\psi^+\rangle_{A_11}|\psi^+\rangle_{A_24} - |\psi^-\rangle_{A_11}|\psi^-\rangle_{A_24} + |\phi^+\rangle_{A_11}|\phi^+\rangle_{A_24} - |\phi^-\rangle_{A_11}|\phi^-\rangle_{A_24}\} |1\rangle_{3'} \\
 &+ \{|\psi^+\rangle_{A_11}|\phi^+\rangle_{A_24} - |\psi^-\rangle_{A_11}|\phi^-\rangle_{A_24} + |\phi^+\rangle_{A_11}|\psi^+\rangle_{A_24} - |\phi^-\rangle_{A_11}|\psi^-\rangle_{A_24}\} |0\rangle_{3'}). \quad (6.7)
 \end{aligned}$$

and if Charlie's measurement result is  $|-\rangle$  and Alice encodes 0

$$\begin{aligned}
 |\psi'\rangle &= \frac{1}{2\sqrt{2}} (\{|\psi^+\rangle_{A_11}|\phi^+\rangle_{A_24} + |\psi^-\rangle_{A_11}|\phi^-\rangle_{A_24} + |\phi^+\rangle_{A_11}|\psi^+\rangle_{A_24} + |\phi^-\rangle_{A_11}|\psi^-\rangle_{A_24}\} |0\rangle_{3'} \\
 &+ \{|\psi^+\rangle_{A_11}|\psi^+\rangle_{A_24} + |\psi^-\rangle_{A_11}|\psi^-\rangle_{A_24} + |\phi^+\rangle_{A_11}|\phi^+\rangle_{A_24} + |\phi^-\rangle_{A_11}|\phi^-\rangle_{A_24}\} |1\rangle_{3'}). \quad (6.8)
 \end{aligned}$$

## Optical design for CDSQC protocol with entanglement swapping using single photons:

**CDSQC-Op\_1:** Same as **CQDE-Op\_1**. The four qubit state is

$$|\psi\rangle = \frac{1}{2} (|+\rangle_{2'} (|+\rangle_{3'} |\psi^+\rangle_{14} + |-\rangle_{3'} |\phi^+\rangle_{14}) + |-\rangle_{2'} (|+\rangle_{3'} |\phi^+\rangle_{14} + |-\rangle_{3'} |\psi^+\rangle_{14})).$$

**CDSQC-Op\_2:** Charlie sends corresponding photons 3' after passing through HWP to Bob and photons 1 and 4 Alice without any operation.

**CDSQC-Op\_3:** Bob randomly selects the photons by using BS from the received photons to check the eavesdropping and measures the photons by using single photon detectors. Same will be happen from Alice's side, but, Alice's photons will pass through two optical switches OS 1 and OS 2 to choose the decoy qubits. After that, she chooses a set of qubits (corresponding to computational basis measurement by Bob) using optical switches OS 3 and OS 4 to measure the received photons in Bell basis, while she performs single-qubit measurements on the rest of the qubits (corresponding to diagonal basis measurement by Bob) to check eavesdropping.

**CDSQC-Op\_4:** Alice prepares entangled state  $|\psi^+\rangle_{A_1A_2}$  to encode her secret information. Specifically, she applies a PM on one of the qubits of the Bell state to encode "1" and does nothing to send "0". Therefore, the combined state of Alice and Bob before her encoding is

$$\begin{aligned} |\psi'\rangle &= \frac{1}{2\sqrt{2}} (|\psi^+\rangle_{A_1A_2} |+\rangle_{2'} (|0\rangle_{3'} |\psi^+\rangle_{14} + |1\rangle_{3'} |\phi^+\rangle_{14}) \\ &+ |\psi^+\rangle_{A_1A_2} |-\rangle_{2'} (|0\rangle_{3'} |\phi^+\rangle_{14} + |1\rangle_{3'} |\psi^+\rangle_{14})) \end{aligned}$$

**CDSQC-Op\_5:** Alice measures qubits  $A_1$  and 1 as well as  $A_2$  and 2 in Bell basis, while Bob can measure his qubits in the computational basis by using SPD. Subsequently, she announces her measurement outcomes, which should reveal her message to Bob and Charlie measure his qubit in diagonal basis.

### 6.2.3 Quantum Dialogue

Quantum dialogue (QD) is a two party scheme, whereas Alice and Bob as two parties wish to communicate their secret messages simultaneously to each other. Quantum dialogue can be reduced from the CQD as shown in [96]. Therefore, we have presented the feasibility of QD with single photons and entangled photons. Here, we briefly discuss the changes to be made in the CQD scheme to obtain the corresponding QD scheme.

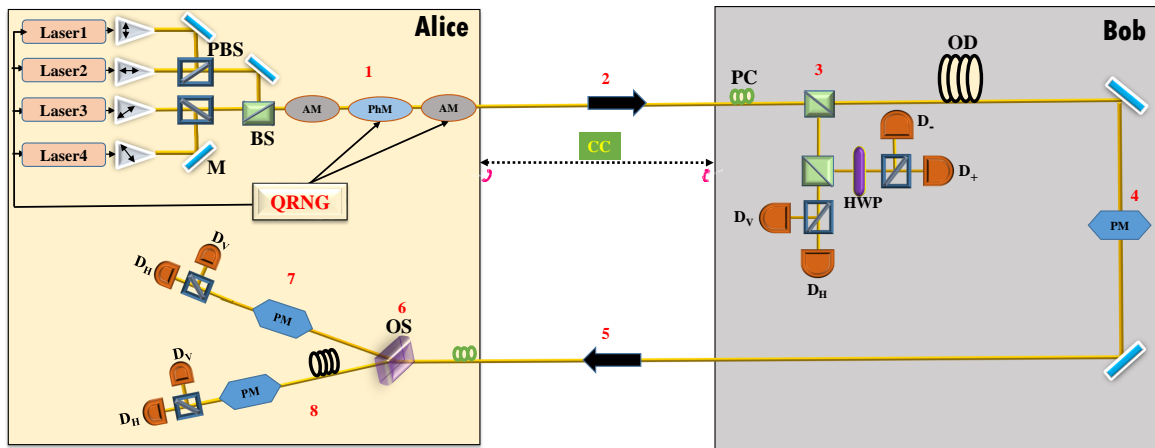


**Figure 6.5:** The proposed optical diagram using linear optics of the QD scheme which is based on single photons.

### 6.2.3.1 QD with single photons

QD protocol is summarized in the following steps:

**QD\_1:** Same as **CQDS\_1**, but here Alice prepares the string.

**QD\_2:** Alice sends the string to Bob as in **CQDS\_2**. In the following steps up to **CQD\_8** is same as **CQD\_8**, but the difference is only here, Alice plays a role of Bob and Bob plays a role of Alice.

**QD\_3:** Same as **CQDS\_3**, but Alice and Bob perform eavesdropping checking.

**QD\_4-7:** Same as **CQDS\_4-7**.

**QD\_8:** Same as **CQDS\_8**, while Alice prepares the initial string, so she knows the basis used for its preparation. Therefore, in the end, Alice announces both initially prepared state and final states on measurement. Without loss of generality the initial state can be assumed public knowledge.

The above summarized QD protocol using single photons can be realized by optical elements and the optical circuit for that is illustrated in Figure 6.5, and the same is explained below in steps.

#### Optical design for QD protocol using single photons:

**QD-Op\_1:** Same as **CQDS-Op\_1**, but here Alice prepares the string.

**QD-Op\_2:** Alice sends it to Bob. In the following steps up to **QD-Op\_8** is same as **CQDS-Op\_8**, but the difference is only here, Alice plays a role of Bob and Bob plays a role of Alice.

**QD-Op\_3-7:** Same as **CQDS-Op\_3-7**.

**QD-Op\_8:** Same as **CQDS-Op\_8**, while Alice prepares the initial string, so she knows the basis of string.

Similarly, the rest of the QD schemes using single photon and entangled states can be reduced from corresponding CQD schemes. Therefore, here we avoid such repetition and mention only briefly for the sake of completeness.

#### **6.2.4 Quantum secure direct communication/Direct secure quantum communication**

In quantum secure direct communication scheme, messages are transmitted directly in a deterministic and secure manner from Alice to Bob. A QSDC scheme can be viewed as a quantum dialogue, but the difference is only here that one party is restricted to encode the identity only. Similarly, a DSQC scheme can be deduced from a QSDC or CDSQC scheme where the receiver does not encode his/her message and requires an additional 1 bit of classical communication from the sender to decode the message.

#### **6.2.5 Quantum key agreement**

The proposed optical designs can also be used to reduce QKA schemes. Specifically, in quantum key agreement, all parties take part in the key generation process and none can control the key solely. A QKA scheme has been proposed in the recent past using a modified version of QSDC/DSQC scheme [316] which can be realized experimentally using present optical designs. Precisely, using QSDC scheme, one party sends his/her raw to another party in a secure manner, while the other party publicly announces his/her key and the final key is combined from both raw keys. Therefore, the optical designs can be used for secure transmission of the first parties raw key.

#### **6.2.6 Quantum key distribution**

The optical designs can be used to describe prepare-and-measure QKD schemes, too. Specifically, decoy qubit based QKD [317, 318] can be visualized from **CQDS-Op\_1-3** if Charlie (Bob) is the sender (receiver) and they share a quantum key by the end of this scheme. Similarly, the entangled state based CQD can be used to describe BBM scheme [319].



## 6.3 Conclusions

In this chapter, we have provided optical circuits for various quantum cryptographic schemes (CQD, CDSQC with entanglement swapping, QD, Kak's three stage scheme, etc.) with single photons, entangled photon (GHZ-like) and also modified version of Kak's protocol. Interestingly, most of the designed optical circuits can be realized using both optical fiber based and open air based architectures. Being a theoretical physics group, we could not realize these optical circuits in the laboratory, but others having laboratory facility are expected to find the work reported here as interesting enough to perform experiments to realize the optical circuits designed in this chapter.

# CHAPTER 7

## CONCLUSIONS AND SCOPE FOR FUTURE WORK

This concluding chapter aims to briefly summarize the results obtained in this thesis work and it also aims to provide some insights in to the scope of future works. Before we start summarizing the results, we may note that the domain of quantum communication is rapidly growing. Several schemes for quantum communication to perform various cryptographic and non-cryptographic tasks (e.g., QT and its variants, QKD, QSDC, dense coding) have been introduced and critically analyzed in the recent past. Many of them have also been experimentally analyzed. Realizing the importance of this rapidly growing field, we have tried to contribute something to this field through this thesis work.

Among various facets of quantum communication, quantum teleportation deserves specific attention as it leads to many other schemes for quantum communication (see Section 1.4). Motivated by this fact, a major part of the present thesis work is dedicated to the study of quantum teleportation schemes. In addition, in this thesis we have also worked on another extremely important facet of quantum communication- quantum cryptography. Here, we may note that in this thesis, we have designed two schemes for quantum communication, but the focus of the thesis is not to design new protocols, rather it aims to address the following question: Which quantum resources are essential/sufficient for implementing a particular quantum communication task? In what follows, we briefly summarize the results obtained in this work in an effort to answer the above question.

### 7.1 Conclusions and a brief summary of the work

This thesis is entitled, “Design and analysis of communication protocols using quantum resources”. As the title suggests, this thesis work focused on quantum communication has two aspects-(a) designing and (b) analysis. In what follows, we will first summarize the outcome of the works done in the designing part and subsequently we will summarize the outcome of the

analysis done in this thesis work.

**Designing:** In the designing part, this work introduces two schemes for teleportation- (i) an entangled orthogonal state-based scheme that allows us to teleport multi-qubit quantum states with the optimal quantum resources and (ii) an entangled nonorthogonal states-based scheme. Further, relevant circuits are designed for the experimental realization of the first scheme by using IBM's five-qubit quantum processor (IBMQX2). Quantum circuits for the implementation of nondestructive discrimination of Bell states using IBM quantum processor are also designed. In Chapter 6, optical designs for the realization of a set of schemes for quantum cryptography have also been provided. We may briefly summarize designing part of this thesis work under the following points:

1. **Quantum teleportation scheme:** The major part of this thesis is dedicated to the quantum teleportation schemes (entangled orthogonal-based and entangled nonorthogonal state-based). As we mentioned in Chapter 2, a large number of quantum teleportation protocols of multi-qubit quantum states have been proposed in the recent past. Most of them are found to use multi-qubit entangled orthogonal states which are very difficult to produce and maintain (cf. Table 2.2). Motivated by this fact, in the second chapter of this thesis, we have tried to design an entangled orthogonal state-based quantum teleportation scheme that can teleport a multi-qubit quantum state using minimum amount of quantum resource, i.e., the minimum number of Bell states. Specifically, it has been shown that the amount of quantum resources required to teleport an unknown quantum state depends only on the number of non-zero probability amplitudes present in the quantum state to be teleported and is independent of the number of qubits in the state to be teleported. We have explicitly established that the complex multi-partite entangled states that are used in a large number of recent works on teleportation (cf. Table 2.2) are not essential for teleportation as there exists a minimum number of Bell states that can be used as a quantum channel to teleport a multi-qubit state of specific form in an optimal and efficient manner. This scheme has also been discussed in the context of dense coding and variants of QT, such as CT and BST. In Chapter 3, we have elaborated on a specific quantum teleportation scheme, which can be viewed as a particular case of the scheme proposed in Chapter 2. Usually, standard entangled states, which are inseparable states of orthogonal states, are used to realize schemes for teleportation and its variants (as is done in Chapters 2-3). However, entangled nonorthogonal states do exist, and they may be used to implement some of the teleportation-based protocols [141]. Specifically, entangled coherent states [100] and Schrödinger cat states prepared using SU(2) coherent states [187] are the typical examples of entangled nonorthogonal states. In the fourth chapter of this thesis, we have designed a teleportation scheme which can be realized using entangled nonorthogonal states. Specifically, we have considered here four quasi-Bell states (Bell-type entangled nonorthogonal states) as teleportation channel for the teleportation of a

single-qubit state, and computed average and minimum fidelity that can be obtained by replacing a Bell state quantum channel in a teleportation scheme by its nonorthogonal counterpart (i.e., corresponding quasi-Bell state).

2. **Experimental realization:** In this thesis work, to experimentally realize the quantum communication schemes, we have used a recently introduced experimental platform (superconductivity IBM quantum computer) that can be accessed through the cloud based services. Specifically, in Chapter 2, a proof-of-principle experimental realization of our proposed optimal quantum teleportation scheme has been reported. For the same, we have designed a quantum circuit on the IBM quantum computer for teleportation of two-qubit quantum state using maximally entangled orthogonal state, i.e., Bell state. Further, in Chapter 5, we have discussed discrimination of orthogonal entangled states, which plays a very crucial role in quantum information processing. There exist many proposals for realizing such discrimination ([245, 260] and references therein). A particularly important variant of state discrimination schemes is nondestructive discrimination of entangled states [260–262], in which the state is not directly measured. Specifically, we have realized nondestructive Bell state discrimination using a five-qubit superconductivity-(SQUID)-based quantum computer [221, 235], which has been recently placed in cloud by IBM Corporation. We have designed Clifford+T circuits for nondestructive discrimination of Bell states in accordance with the restrictions imposed by the particular architecture of the IBM quantum processor.
3. **Optical Implementation:** We have also looked at some aspects of quantum cryptography. Quantum cryptography in general and QKD in particular have drawn considerable attention of the scientific community, because of its relevance in our day-to-day life to defense, banking to inter-Government communication. Naturally, several protocols of quantum communication have been proposed, but only a few of those quantum cryptographic schemes have yet been realized experimentally. This fact motivated us to investigate whether it's possible to realize hitherto unrealized schemes of quantum cryptography using the available technology (i.e., using the devices available in a modern optical laboratory and quantum states that can be prepared in a lab). A designing effort has been made in this direction, and optical circuits for the realization of various quantum cryptographic tasks (including QD, CQD, Kak's three stage scheme modified QD, controlled DSQC with entanglement swapping) have been designed. Optical designs are provided for fiber-based implementation as well as open-air implementation of the schemes of quantum cryptography. Being a theoretical physics group, we could not experimentally implement these optical circuits, but we hope other groups will realize these circuits soon.

**Analysis:** The analysis part of the thesis is also performed in Chapters 2-6. Specifically, in the designed second scheme of QT, i.e., Chapter 4, the effect of noise is studied to reveal that in

a noisy environment the performance of all the quasi-Bell states are not equivalent. Further, using the IBM quantum computer, experimentally nondestructive discrimination of Bell states is performed and the results are analyzed to compare them with those of an earlier experiment done using NMR. The relevance of this experiment is discussed in the context of quantum cryptography. Benefits of the schemes and circuits designed here are also quantitatively analyzed by theoretically computing average fidelity, minimum fidelity and minimum assured fidelity in the presence of noise and also by obtaining the fidelity of the experimentally generated quantum states with the help of QST. We have briefly summarized analysis part of this thesis work in the following points:

1. **Quantum teleportation scheme:** The performance of the teleportation scheme using entangled nonorthogonal states has been analyzed over noisy channels in Chapter 4 of the present thesis. Specifically, the effect of PD and AD noise were studied to reveal that the quasi-Bell state  $|\phi_{-}\rangle$ , which was shown to be maximally entangled in an ideal situation, remains the most preferred choice as quantum channel while subjected to PD noise. However, in the presence of damping effects due to interaction with an ambient environment (i.e., in AD noise), the choice of the quasi-Bell state is found to depend on the nonorthogonality parameter and the number of qubits exposed to noisy environment. We have investigated the performance of the standard teleportation scheme using  $F_{ave}$  and MFI as quantitative measures of the quality of the teleportation scheme by considering a quasi-Bell state instead of usual Bell state as quantum channel.
2. **Experimental realization:** In 2010, nondestructive Bell state discrimination scheme has been experimentally implemented using an NMR-based three-qubit quantum computer [246] which have motivated us to perform nondestructive Bell state discrimination using another experimental platform. So in Chapter 5, we have realized this scheme experimentally using IBM quantum computer and also analyzed the results of experimentally nondestructive discrimination of Bell states to compare with NMR results. The analysis of the results obtained using IBM quantum processors have also revealed that the present technology needs much improvement to achieve the desired scalability. This is so because the gate fidelity of the individual gates realized here is relatively low compared to the same obtained in NMR and a few other more matured technologies. Consequently, state fidelity of the output of a more complex circuit would be low.

We may now conclude this section as well as this thesis by restressing on the main findings of the thesis by listing them here below

1. The quantum teleportation scheme is generalized to design a new scheme capable of teleportation of multi-qubit quantum states with optimal amount of quantum resources. Specifically, our scheme allows teleportation of a multi-qubit quantum state by using the

minimum number of Bell states. Thus, it circumvents the need for complex multi-partite entangled quantum states as a teleportation channel.

2. It's established that the amount of quantum resources required to teleport an unknown quantum state depends only on the number of nonzero probability amplitudes present in the quantum state and is independent of the number of qubits in the state to be teleported.
3. The idea behind the designing of the above mentioned generalized scheme for QT is found to be relevant in the context of designing corresponding schemes for CT, BST and BCST, too.
4. In Chapter 4, it's observed that if we convert  $|\phi_{-}\rangle$  quasi-Bell state in orthogonal basis  $\{|0\rangle, |1\rangle\}$ , we obtain the maximally entangled Bell state  $|\phi^{-}\rangle = \frac{1}{\sqrt{2}}(|01\rangle + |10\rangle)$ . Naturally, this state is found to be the best choice (among quasi-Bell states) as a teleportation channel.
5. It's observed that the amount of nonorthogonality plays a crucial role in deciding which quasi-Bell state would provide highest average fidelity for a teleportation scheme implemented using a quasi-Bell state as the teleportation channel.
6. The quasi-Bell state  $|\phi_{-}\rangle$  which was shown to be maximally entangled in an ideal situation, is found to remain the most preferred choice as quantum channel while subjected to PD noise as well.
7. With appropriate analysis, it's established that the existing IBM quantum computers are scalable. To construct a larger and useful quantum computer IBM has to considerably reduce the gate-error rate. The finding is supported by both quantum state tomography and quantum process tomography, Further, a comparison of results obtained using IBM quantum computers with the corresponding results obtained using NMR-based quantum computers is found to reveal that NMR results are better as far as the state fidelity and gate fidelity are concerned.
8. It's shown that the optical implementation of the other quantum cryptographic schemes which have not yet been performed experimentally is possible with available technology. Relevant optical circuits have been designed so that the interested experimental groups can implement them.

## 7.2 Limitations of the present work and scope for future work

In this thesis, we have studied the effect of Markovian noise only. In future, the effect of non-Markovian noise can also be studied. It may be further hoped that the optimal scheme for teleportation reported in Chapter 2 will find its application in designing various other optimal schemes of quantum communication as many schemes of quantum communications can be viewed as the variant of teleportation.

This thesis work was initially, planned to be theoretical. However, as IBM provided free access to its five-qubit quantum computer, we have also performed some experiments using IBM quantum processors. These experiments were only proof-of principle experiments as the architecture of IBM restricted us to keep Alice and Bob in the same place. This is a limitation of the present work. However, optical experiments will not have such a restriction. Keeping this fact in mind, in Chapter 6 we have provided a set of optical circuits for various quantum cryptographic tasks. Interestingly, most of the designed optical circuits can be realized using both optical fiber based and open air based architectures. Being a theoretical physics group, we could not realize these optical circuits in the laboratory. However, we hope that the teleportation schemes presented in Chapters 2 and 3 as well as the optical designs presented in Chapter 6 will be experimentally realized optically in the near future.

## References

- [1] Wiesner S., “*Conjugate coding*”, ACM Sigact News, vol. 15, pp. 78–88, 1983.
- [2] Pathak A., *Elements of quantum computation and quantum communication*, CRC Press, 2013.
- [3] Bennett C.H., Brassard G., “*Quantum cryptography: public key distribution and coin tossing*”, *International Conference on Computer System and Signal Processing, IEEE, 1984*, pp. 175–179, 1984.
- [4] Ekert A.K., “*Quantum cryptography based on Bell’s theorem*”, *Physical Review Letters*, vol. 67, p. 661, 1991.
- [5] Bennett C.H., Wiesner S.J., “*Communication via one-and two-particle operators on Einstein-Podolsky-Rosen states*”, *Physical Review Letters*, vol. 69, p. 2881, 1992.
- [6] Bennett C.H., Brassard G., Crépeau C., Jozsa R., Peres A., Wootters W.K., “*Teleporting an unknown quantum state via dual classical and Einstein-Podolsky-Rosen channels*”, *Physical Review Letters*, vol. 70, p. 1895, 1993.
- [7] Acín A., Brunner N., Gisin N., Massar S., Pironio S., Scarani V., “*Device-independent security of quantum cryptography against collective attacks*”, *Physical Review Letters*, vol. 98, p. 230501, 2007.
- [8] Zheng S.B., “*Splitting quantum information via W states*”, *Physical Review A*, vol. 74, p. 054303, 2006.
- [9] Pathak A., Banerjee A., “*Efficient quantum circuits for perfect and controlled teleportation of n-qubit non-maximally entangled states of generalized Bell-type*”, *International Journal of Quantum Information*, vol. 9, pp. 389–403, 2011.
- [10] Wang X.W., Xia L.X., Wang Z.Y., Zhang D.Y., “*Hierarchical quantum-information splitting*”, *Optics Communications*, vol. 283, pp. 1196–1199, 2010.
- [11] Shukla C., Pathak A., “*Hierarchical quantum communication*”, *Physics Letters A*, vol. 377, pp. 1337–1344, 2013.



- [12] Hillery M., Bužek V., Berthiaume A., “*Quantum secret sharing*”, *Physical Review A*, vol. 59, p. 1829, 1999.
- [13] Shukla C., Pathak A., “*Orthogonal-state-based deterministic secure quantum communication without actual transmission of the message qubits*”, *Quantum Information Processing*, vol. 13, pp. 2099–2113, 2014.
- [14] Pati A.K., “*Minimum classical bit for remote preparation and measurement of a qubit*”, *Physical Review A*, vol. 63, p. 014302, 2000.
- [15] Sharma V., Shukla C., Banerjee S., Pathak A., “*Controlled bidirectional remote state preparation in noisy environment: a generalized view*”, *Quantum Information Processing*, vol. 14, pp. 3441–3464, 2015.
- [16] Cao Z.L., Song W., “*Teleportation of a two-particle entangled state via W class states*”, *Physica A: Statistical Mechanics and its Applications*, vol. 347, pp. 177–183, 2005.
- [17] Cao T.B., Nguyen B.A., “*Deterministic controlled bidirectional remote state preparation*”, *Advances in Natural Sciences: Nanoscience and Nanotechnology*, vol. 5, p. 015003, 2013.
- [18] Chen P.X., Zhu S.Y., Guo G.C., “*General form of genuine multipartite entanglement quantum channels for teleportation*”, *Physical Review A*, vol. 74, p. 032324, 2006.
- [19] Chen X.B., Zhang N., Lin S., Wen Q.Y., Zhu F.C., “*Quantum circuits for controlled teleportation of two-particle entanglement via a W state*”, *Optics Communications*, vol. 281, pp. 2331–2335, 2008.
- [20] Choudhury B.S., Dhara A., “*Teleportation protocol of three-qubit state using four-qubit quantum channels*”, *International Journal of Theoretical Physics*, vol. 55, pp. 3393–3399, 2016.
- [21] Choudhury B.S., Samanta S., “*Asymmetric bidirectional  $3 \leftrightarrow 2$  qubit teleportation protocol between Alice and Bob via 9-qubit cluster state*”, *International Journal of Theoretical Physics*, vol. 56, pp. 3285–3296, 2017.
- [22] Choudhury B.S., Dhara A., Samanta S., “*Teleportation of five-qubit state using six-qubit state*”, *Physics of Particles and Nuclei Letters*, vol. 14, pp. 644–646, 2017.
- [23] Da-Chuang L., Zhuo-Liang C., “*Teleportation of two-particle entangled state via cluster state*”, *Communications in Theoretical Physics*, vol. 47, p. 464, 2007.
- [24] Dai H.Y., Chen P.X., Li C.Z., “*Probabilistic teleportation of an arbitrary two-particle state by a partially entangled three-particle GHZ state and W state*”, *Optics communications*, vol. 231, pp. 281–287, 2004.

- [25] Deng F.G., Long G.L., Liu X.S., “*Two-step quantum direct communication protocol using the Einstein-Podolsky-Rosen pair block*”, *Physical Review A*, vol. 68, p. 042317, 2003.
- [26] Deng F.G., “*Comment on "quantum teleportation of an arbitrary two-qubit state and its relation to multipartite entanglement"*”, *Physical Review A*, vol. 72, p. 036301, 2005.
- [27] Dong L., Xiu X.M., Gao Y.J., Chi F., “*A controlled quantum dialogue protocol in the network using entanglement swapping*”, *Optics Communications*, vol. 281, pp. 6135–6138, 2008.
- [28] Dong L., Xiu X.M., Gao Y.J., Ren Y.P., Liu H.W., “*Controlled three-party communication using GHZ-like state and imperfect Bell-state measurement*”, *Optics Communications*, vol. 284, pp. 905–908, 2011.
- [29] Duan Y.J., Zha X.W., “*Bidirectional quantum controlled teleportation via a six-qubit entangled state*”, *International Journal of Theoretical Physics*, vol. 53, pp. 3780–3786, 2014.
- [30] Fang X., Zhu X., Feng M., Mao X., Du F., “*Experimental implementation of dense coding using nuclear magnetic resonance*”, *Physical Review A*, vol. 61, p. 022307, 2000.
- [31] Fang J., Lin Y., Zhu S., Chen X., “*Probabilistic teleportation of a three-particle state via three pairs of entangled particles*”, *Physical Review A*, vol. 67, p. 014305, 2003.
- [32] Fu H.Z., Tian X.L., Hu Y., “*A general method of selecting quantum channel for bidirectional quantum teleportation*”, *International Journal of Theoretical Physics*, vol. 53, pp. 1840–1847, 2014.
- [33] Furusawa A., Sørensen J.L., Braunstein S.L., Fuchs C.A., Kimble H.J., Polzik E.S., “*Unconditional quantum teleportation*”, *Science*, vol. 282, pp. 706–709, 1998.
- [34] Gorbachev V., Trubilko A., “*Quantum teleportation of an Einstein-Podolsky-Rosen pair using an entangled three-particle state*”, *Journal of Experimental and Theoretical Physics*, vol. 91, pp. 894–898, 2000.
- [35] Guan X.W., Chen X.B., Wang L.C., Yang Y.X., “*Joint remote preparation of an arbitrary two-qubit state in noisy environments*”, *International Journal of Theoretical Physics*, vol. 53, pp. 2236–2245, 2014.
- [36] Hao J.C., Li C.F., Guo G.C., “*Controlled dense coding using the Greenberger-Horne-Zeilinger state*”, *Physical Review A*, vol. 63, p. 054301, 2001.

- [37] Hassanpour S., Houshmand M., “*Efficient controlled quantum secure direct communication based on GHZ-like states*”, *Quantum Information Processing*, vol. 14, pp. 739–753, 2015.
- [38] Hassanpour S., Houshmand M., “*Bidirectional teleportation of a pure EPR state by using GHZ states*”, *Quantum Information Processing*, vol. 15, pp. 905–912, 2016.
- [39] Henderson L., Hardy L., Vedral V., “*Two-state teleportation*”, *Physical Review A*, vol. 61, p. 062306, 2000.
- [40] Hong L., “*Probabilistic teleportation of the three-particle entangled state via entanglement swapping*”, *Chinese Physics Letters*, vol. 18, p. 1004, 2001.
- [41] Huang Z., Zhang C., Situ H., “*Performance analysis of simultaneous dense coding protocol under decoherence*”, *Quantum Information Processing*, vol. 16, p. 227, 2017.
- [42] Huelga S.F., Vaccaro J.A., Chefles A., Plenio M.B., “*Quantum remote control: teleportation of unitary operations*”, *Physical Review A*, vol. 63, p. 042303, 2001.
- [43] Jain S., Muralidharan S., Panigrahi P.K., “*Secure quantum conversation through non-destructive discrimination of highly entangled multipartite states*”, *Europhys. Lett.*, vol. 87, p. 60008, 2009.
- [44] Joo J., Park Y.J., Oh S., Kim J., “*Quantum teleportation via a W state*”, *New Journal of Physics*, vol. 5, p. 136, 2003.
- [45] Joy D., Surendran S.P., et al., “*Efficient deterministic secure quantum communication protocols using multipartite entangled states*”, *Quantum Information Processing*, vol. 16, p. 157, 2017.
- [46] Karlsson A., Bourennane M., “*Quantum teleportation using three-particle entanglement*”, *Physical Review A*, vol. 58, p. 4394, 1998.
- [47] Li X., Pan Q., Jing J., Zhang J., Xie C., Peng K., “*Quantum dense coding exploiting a bright Einstein-Podolsky-Rosen beam*”, *Physical Review Letters*, vol. 88, p. 047904, 2002.
- [48] Li L., Qiu D., “*The states of W-class as shared resources for perfect teleportation and superdense coding*”, *Journal of Physics A: Mathematical and Theoretical*, vol. 40, p. 10871, 2007.
- [49] Li Y.h., Li X.l., Sang M.h., Nie Y.y., Wang Z.s., “*Bidirectional controlled quantum teleportation and secure direct communication using five-qubit entangled state*”, *Quantum Information Processing*, vol. 12, pp. 3835–3844, 2013.

- [50] Li Y.h., Nie L.p., Li X.l., Sang M.h., “*Asymmetric bidirectional controlled teleportation by using six-qubit cluster state*”, International Journal of Theoretical Physics, vol. 55, pp. 3008–3016, 2016.
- [51] Li Y.h., Li X.l., Nie L.p., Sang M.h., “*Quantum teleportation of three and four-qubit state using multi-qubit cluster states*”, International Journal of Theoretical Physics, vol. 55, pp. 1820–1823, 2016.
- [52] Li Y.h., Sang M.h., Wang X.p., Nie Y.y., “*Quantum teleportation of a four-qubit state by using six-qubit cluster state*”, International Journal of Theoretical Physics, vol. 55, pp. 3547–3550, 2016.
- [53] Li M., Zhao N., Chen N., Zhu C.h., Pei C.x., “*Quantum teleportation of five-qubit state*”, International Journal of Theoretical Physics, vol. 56, pp. 2710–2715, 2017.
- [54] Liu X., Long G., Tong D., Li F., “*General scheme for superdense coding between multiparties*”, Physical Review A, vol. 65, p. 022304, 2002.
- [55] Lo H.K., Chau H.F., “*Unconditional security of quantum key distribution over arbitrarily long distances*”, Science, vol. 283, pp. 2050–2056, 1999.
- [56] Lütkenhaus N., Calsamiglia J., Suominen K.A., “*Bell measurements for teleportation*”, Physical Review A, vol. 59, p. 3295, 1999.
- [57] Ma X.S., Herbst T., Scheidl T., Wang D., Kropatschek S., Naylor W., Wittmann B., Mech A., Kofler J., Anisimova E., et al., “*Quantum teleportation over 143 kilometres using active feed-forward*”, Nature, vol. 489, p. 269, 2012.
- [58] Majumder A., Mohapatra S., Kumar A., “*Experimental realization of secure multiparty quantum summation using five-qubit IBM quantum computer on cloud*”, arXiv preprint arXiv:1707.07460, 2017.
- [59] Man Z.X., Xia Y.J., An N.B., “*Genuine multiqubit entanglement and controlled teleportation*”, Physical Review A, vol. 75, p. 052306, 2007.
- [60] Mattle K., Weinfurter H., Kwiat P.G., Zeilinger A., “*Dense coding in experimental quantum communication*”, Physical Review Letters, vol. 76, p. 4656, 1996.
- [61] Mozes S., Oppenheim J., Reznik B., “*Deterministic dense coding with partially entangled states*”, Physical Review A, vol. 71, p. 012311, 2005.
- [62] Muralidharan S., Panigrahi P.K., “*Perfect teleportation, quantum-state sharing, and superdense coding through a genuinely entangled five-qubit state*”, Physical Review A, vol. 77, p. 032321, 2008.

- [63] Muralidharan S., Panigrahi P.K., “*Quantum-information splitting using multipartite cluster states*”, *Physical Review A*, vol. 78, p. 062333, 2008.
- [64] Nandi K., Mazumdar C., “*Quantum teleportation of a two qubit state using GHZ-like state*”, *International Journal of Theoretical Physics*, vol. 53, pp. 1322–1324, 2014.
- [65] Nguyen B.A., “*Quantum dialogue*”, *Physics Letters A*, vol. 328, pp. 6–10, 2004.
- [66] Nie Y.Y., Hong Z.H., Huang Y.B., Yi X.J., Li S.S., “*Non-maximally entangled controlled teleportation using four particles cluster states*”, *International Journal of Theoretical Physics*, vol. 48, pp. 1485–1490, 2009.
- [67] Nie Y.Y., Li Y.H., Liu J.C., Sang M.H., “*Quantum information splitting of an arbitrary three-qubit state by using two four-qubit cluster states*”, *Quantum Information Processing*, vol. 10, pp. 297–305, 2011.
- [68] Nielsen M.A., Knill E., Laflamme R., “*Complete quantum teleportation using nuclear magnetic resonance*”, *Nature*, vol. 396, pp. 52–55, 1998.
- [69] Pati A., Parashar P., Agrawal P., “*Probabilistic superdense coding*”, *Physical Review A*, vol. 72, p. 012329, 2005.
- [70] Pati A.K., Agrawal P., “*Probabilistic teleportation of a qudit*”, *Physics Letters A*, vol. 371, pp. 185–189, 2007.
- [71] Prakash H., Chandra N., Prakash R., et al., “*Improving the teleportation of entangled coherent states*”, *Physical Review A*, vol. 75, p. 044305, 2007.
- [72] Prakash H., Chandra N., Prakash R., Shivani, “*Effect of decoherence on fidelity in teleportation of entangled coherent states*”, *International Journal of Quantum Information*, vol. 6, pp. 1077–1092, 2008.
- [73] Prakash H., Mishra M.K., “*Increasing average fidelity by using non-maximally entangled resource in teleportation of superposed coherent states*”, arXiv preprint arXiv:1107.2533, 2011.
- [74] Prakash H., Verma V., “*Minimum assured fidelity and minimum average fidelity in quantum teleportation of single qubit using non-maximally entangled states*”, *Quantum Information Processing*, vol. 11, pp. 1951–1959, 2012.
- [75] Riebe M., Häffner H., Roos C., Hänsel W., Benhelm J., Lancaster G., Körber T., Becher C., Schmidt-Kaler F., James D., et al., “*Deterministic quantum teleportation with atoms*”, *Nature*, vol. 429, pp. 734–737, 2004.

- [76] Rigolin G., “*Quantum teleportation of an arbitrary two-qubit state and its relation to multipartite entanglement*”, *Physical Review A*, vol. 71, p. 032303, 2005.
- [77] Sang M.h., “*Bidirectional quantum controlled teleportation by using a seven-qubit entangled state*”, *International Journal of Theoretical Physics*, vol. 55, pp. 380–383, 2016.
- [78] Sharma V., Thapliyal K., Pathak A., Banerjee S., “*A comparative study of protocols for secure quantum communication under noisy environment: single-qubit-based protocols versus entangled-state-based protocols*”, *Quantum Information Processing*, vol. 15, pp. 4681–4710, 2016.
- [79] Sharma R.D., Thapliyal K., Pathak A., Pan A.K., De A., “*Which verification qubits perform best for secure communication in noisy channel?*”, *Quantum Information Processing*, vol. 15, pp. 1703–1718, 2016.
- [80] Shi B.S., Jiang Y.K., Guo G.C., “*Probabilistic teleportation of two-particle entangled state*”, *Physics Letters A*, vol. 268, pp. 161–164, 2000.
- [81] Shukla C., Banerjee A., Pathak A., “*Bidirectional controlled teleportation by using 5-qubit states: a generalized view*”, *International Journal of Theoretical Physics*, vol. 52, pp. 3790–3796, 2013.
- [82] Shukla C., Kothari V., Banerjee A., Pathak A., “*On the group-theoretic structure of a class of quantum dialogue protocols*”, *Physics Letters A*, vol. 377, pp. 518–527, 2013.
- [83] Shukla C., Banerjee A., Pathak A., “*Improved protocols of secure quantum communication using W states*”, *International Journal of Theoretical Physics*, vol. 52, pp. 1914–1924, 2013.
- [84] Sisodia M., Verma V., Thapliyal K., Pathak A., “*Teleportation of a qubit using entangled non-orthogonal states: a comparative study*”, *Quantum Information Processing*, vol. 16, p. 76, 2017, doi:10.1007/s11128-017-1526-x.
- [85] Sisodia M., Shukla A., Thapliyal K., Pathak A., “*Design and experimental realization of an optimal scheme for teleportation of an n-qubit quantum state*”, *Quantum Information Processing*, vol. 16, p. 292, 2017.
- [86] Sisodia M., Pathak A., “*Comment on "quantum teleportation of eight-qubit state via six-qubit cluster state"*”, *International Journal of Theoretical Physics*, vol. 57, pp. 2213–2217, 2018.
- [87] Situ H., Qiu D., “*Simultaneous dense coding*”, *Journal of Physics A: Mathematical and Theoretical*, vol. 43, p. 055301, 2010.

- [88] Situ H., “*Controlled simultaneous teleportation and dense coding*”, International Journal of Theoretical Physics, vol. 53, pp. 1003–1009, 2014.
- [89] Situ H., Qiu D., Mateus P., Paunković N., “*Secure  $n$ -dimensional simultaneous dense coding and applications*”, International Journal of Quantum Information, vol. 13, p. 1550051, 2015.
- [90] Song-Song L., Yi-You N., Zhi-Hui H., Xiao-Jie Y., Yi-Bin H., “*Controlled teleportation using four-particle cluster state*”, Communications in Theoretical Physics, vol. 50, p. 633, 2008.
- [91] Srinatha N., Omkar S., Srikanth R., Banerjee S., Pathak A., “*The quantum cryptographic switch*”, Quantum Information Processing, vol. 13, pp. 59–70, 2014.
- [92] Sun Q.C., Mao Y.L., Chen S.J., Zhang W., Jiang Y.F., Zhang Y.B., Zhang W.J., Miki S., Yamashita T., Terai H., et al., “*Quantum teleportation with independent sources and prior entanglement distribution over a network*”, Nature Photonics, vol. 10, pp. 671–675, 2016.
- [93] Tan X., Zhang X., Song T., “*Deterministic quantum teleportation of a particular six-qubit state using six-qubit cluster state*”, International Journal of Theoretical Physics, vol. 55, pp. 155–160, 2016.
- [94] Thapliyal K., Pathak A., “*Applications of quantum cryptographic switch: various tasks related to controlled quantum communication can be performed using Bell states and permutation of particles*”, Quantum Information Processing, vol. 14, pp. 2599–2616, 2015.
- [95] Thapliyal K., Verma A., Pathak A., “*A general method for selecting quantum channel for bidirectional controlled state teleportation and other schemes of controlled quantum communication*”, Quantum Information Processing, vol. 14, pp. 4601–4614, 2015.
- [96] Thapliyal K., Pathak A., Banerjee S., “*Quantum cryptography over non-markovian channels*”, Quantum Information Processing, vol. 16, p. 115, 2017.
- [97] Ting G., Feng-Li Y., Zhi-Xi W., “*Controlled quantum teleportation and secure direct communication*”, Chinese Physics, vol. 14, p. 893, 2005.
- [98] Tsai C.W., Hwang T., “*Teleportation of a pure EPR state via GHZ-like state*”, International Journal of Theoretical Physics, vol. 49, pp. 1969–1975, 2010.
- [99] Tsai C., Hsieh C., Hwang T., “*Dense coding using cluster states and its application on deterministic secure quantum communication*”, The European Physical Journal D, vol. 61, pp. 779–783, 2011.

- [100] van Enk S.J., Hirota O., “*Entangled coherent states: teleportation and decoherence*”, *Physical Review A*, vol. 64, p. 022313, 2001.
- [101] van Enk S., “*Quantum-information processing for a coherent superposition state via a mixed entangled coherent channel*”, *Physical Review A*, vol. 64, p. 022313, 2001.
- [102] Wang J.W., Shu L., “*Bidirectional quantum controlled teleportation of qudit state via partially entangled GHZ-type states*”, *International Journal of Modern Physics B*, vol. 29, p. 1550122, 2015.
- [103] Weedbrook C., Lance A.M., Bowen W.P., Symul T., Ralph T.C., Lam P.K., “*Quantum cryptography without switching*”, *Physical Review Letters*, vol. 93, p. 170504, 2004.
- [104] Wei Z.H., Zha X.W., Yu Y., “*Comment on “teleportation protocol of three-qubit state using four-qubit quantum channels”*”, *International Journal of Theoretical Physics*, vol. 55, pp. 4687–4692, 2016.
- [105] Xi-Han L., Fu-Guo D., Hong-Yu Z., “*Controlled teleportation of an arbitrary multi-qudit state in a general form with  $d$ -dimensional Greenberger–Horne–Zeilinger states*”, *Chinese Physics Letters*, vol. 24, p. 1151, 2007.
- [106] Xia Y., Fu C.B., Zhang S., Hong S.K., Yeon K.H., Um C.I., “*Quantum dialogue by using the GHZ state*”, *Journal of the Korean Physical Society*, vol. 48, pp. 24–27, 2006.
- [107] Xia Y., Song J., Song H.S., Wang B.Y., “*Generalized teleportation of a  $d$ -level  $n$ -particle GHZ state with one pair of entangled particles as the quantum channel*”, *International Journal of Theoretical Physics*, vol. 47, pp. 2835–2840, 2008.
- [108] Xia Y., Song J., Lu P.M., Song H.S., “*Teleportation of an  $n$ -photon Greenberger-Horne-Zeilinger (GHZ) polarization-entangled state using linear optical elements*”, *JOSA B*, vol. 27, pp. A1–A6, 2010.
- [109] Xiao-Ming X., Li D., Ya-Jun G., Feng C., “*Controlled quantum teleportation of a one-particle unknown state via a three-particle entangled state*”, *Communications in Theoretical Physics*, vol. 48, p. 261, 2007.
- [110] Xin-Wei Z., Hai-Yang S., Gang-Long M., “*Bidirectional swapping quantum controlled teleportation based on maximally entangled five-qubit state*”, arXiv preprint arXiv:1006.0052, 2010.
- [111] Xiu L., Hong-Cai L., “*Probabilistic teleportation of an arbitrary three-particle state*”, *Chinese Physics*, vol. 14, p. 1724, 2005.



- [112] Ya-Hong W., He-Shan S., Chang-Shui Y., “*Faithful controlled teleportation of an arbitrary unknown two-atom state via special W-states and qed cavity*”, *Communications in Theoretical Physics*, vol. 49, p. 1199, 2008.
- [113] Yadav P., Srikanth R., Pathak A., “*Two-step orthogonal-state-based protocol of quantum secure direct communication with the help of order-rearrangement technique*”, *Quantum Information Processing*, vol. 13, pp. 2731–2743, 2014.
- [114] Yan F., Zhang X., “*A scheme for secure direct communication using EPR pairs and teleportation*”, *The European Physical Journal B-Condensed Matter and Complex Systems*, vol. 41, pp. 75–78, 2004.
- [115] Yan A., “*Bidirectional controlled teleportation via six-qubit cluster state*”, *International Journal of Theoretical Physics*, vol. 52, pp. 3870–3873, 2013.
- [116] Yang C.P., Guo G.C., “*Multiparticle generalization of teleportation*”, *Chinese Physics Letters*, vol. 17, p. 162, 2000.
- [117] Yang C.P., Chu S.I., Han S., “*Efficient many-party controlled teleportation of multiqubit quantum information via entanglement*”, *Physical Review A*, vol. 70, p. 022329, 2004.
- [118] Yang K., Huang L., Yang W., Song F., “*Quantum teleportation via GHZ-like state*”, *International Journal of Theoretical Physics*, vol. 48, pp. 516–521, 2009.
- [119] Yeo Y., “*Quantum teleportation using three-particle entanglement*”, arXiv preprint quant-ph/0302030, 2003.
- [120] Yeo Y., Chua W.K., “*Teleportation and dense coding with genuine multipartite entanglement*”, *Physical Review Letters*, vol. 96, p. 060502, 2006.
- [121] Yin J., Ren J.G., Lu H., Cao Y., Yong H.L., Wu Y.P., Liu C., Liao S.K., Zhou F., Jiang Y., et al., “*Quantum teleportation and entanglement distribution over 100-kilometre free-space channels*”, *Nature*, vol. 488, p. 185, 2012.
- [122] Yong-Jian G., Yi-Zhuang Z., Guang-Can G., “*Probabilistic teleportation of an arbitrary two-particle state*”, *Chinese Physics Letters*, vol. 18, p. 1543, 2001.
- [123] Yu L.Z., “*Teleportation of an unknown three-particle entangled state via a cluster state*”, *Advanced Materials Research*, vol. 734, pp. 3022–3025, Trans Tech Publ, 2013.
- [124] Zha X.W., Zou Z.C., Qi J.X., Song H.Y., “*Bidirectional quantum controlled teleportation via five-qubit cluster state*”, *International Journal of Theoretical Physics*, vol. 52, pp. 1740–1744, 2013.

- [125] Zhang Q., Goebel A., Wagenknecht C., Chen Y.A., Zhao B., Yang T., Mair A., Schmiedmayer J., Pan J.W., “*Experimental quantum teleportation of a two-qubit composite system*”, *Nature Physics*, vol. 2, p. 678, 2006.
- [126] Zhang Z., Liu Y., Wang D., “*Perfect teleportation of arbitrary  $n$ -qudit states using different quantum channels*”, *Physics Letters A*, vol. 372, pp. 28–32, 2007.
- [127] Zhang Q.Y., Zhan Y.B., Zhang L.L., Ma P.C., “*Schemes for splitting quantum information via tripartite entangled states*”, *International Journal of Theoretical Physics*, vol. 48, pp. 3331–3338, 2009.
- [128] Zhang Y.L., Wang Y.N., Xiao X.R., Jing L., Mu L.Z., Korepin V., Fan H., “*Quantum network teleportation for quantum information distribution and concentration*”, *Physical Review A*, vol. 87, p. 022302, 2013.
- [129] Zhang C., Situ H., Li Q., He G.P., “*Efficient simultaneous dense coding and teleportation with two-photon four-qubit cluster states*”, *International Journal of Quantum Information*, vol. 14, p. 1650023, 2016.
- [130] Zhao Z., Chen Y.A., Zhang A.N., Yang T., Briegel H.J., Pan J.W., “*Experimental demonstration of five-photon entanglement and open-destination teleportation*”, *Nature*, vol. 430, pp. 54–58, 2004.
- [131] Zhao N., Li M., Chen N., Pei C.x., “*An efficient quantum teleportation of six-qubit state via an eight-qubit cluster state*”, *Canadian Journal of Physics*, vol. 96, pp. 650–653, 2017.
- [132] Zhao N., Li M., Chen N., Zhu C.h., Pei C.x., “*Quantum teleportation of eight-qubit state via six-qubit cluster state*”, *International Journal of Theoretical Physics*, vol. 57, pp. 516–522, 2018.
- [133] Zheng C., Gu Y., Li W., Wang Z., Zhang J., “*Complete distributed hyper-entangled-Bell-state analysis and quantum super dense coding*”, *International Journal of Theoretical Physics*, vol. 55, pp. 1019–1027, 2016.
- [134] Zhou J., Hou G., Wu S., Zhang Y., “*Controlled quantum teleportation*”, arXiv preprint quant-ph/0006030, 2000.
- [135] Zhou P., Li X.H., Deng F.G., Zhou H.Y., “*Multiparty-controlled teleportation of an arbitrary  $m$ -qudit state with a pure entangled quantum channel*”, *Journal of Physics A: Mathematical and Theoretical*, vol. 40, p. 13121, 2007.
- [136] Shukla C., Thapliyal K., Pathak A., “*Hierarchical joint remote state preparation in noisy environment*”, *Quantum Information Processing*, vol. 16, p. 205, 2017.

- [137] Bouwmeester D., Pan J.W., Mattle K., Eibl M., Weinfurter H., Zeilinger A., “*Experimental quantum teleportation*”, *Nature*, vol. 390, pp. 575–579, 1997.
- [138] Barrett M., Chiaverini J., Schaetz T., Britton J., Itano W., Jost J., Knill E., Langer C., Leibfried D., Ozeri R., et al., “*Deterministic quantum teleportation of atomic qubits*”, *Nature*, vol. 429, pp. 737–739, 2004.
- [139] Huang Y.F., Ren X.F., Zhang Y.S., Duan L.M., Guo G.C., “*Experimental teleportation of a quantum controlled-NOT gate*”, *Physical Review Letters*, vol. 93, p. 240501, 2004.
- [140] Jin X.M., Ren J.G., Yang B., Yi Z.H., Zhou F., Xu X.F., Wang S.K., Yang D., Hu Y.F., Jiang S., et al., “*Experimental free-space quantum teleportation*”, *Nature photonics*, vol. 4, p. 376, 2010.
- [141] Adhikari S., Majumdar A., Home D., Pan A., Joshi P., “*Quantum teleportation using non-orthogonal entangled channels*”, *Physica Scripta*, vol. 85, p. 045001, 2012.
- [142] Bennett C.H., “*Quantum cryptography using any two nonorthogonal states*”, *Physical Review Letters*, vol. 68, p. 3121, 1992.
- [143] Boström K., Felbinger T., “*Deterministic secure direct communication using entanglement*”, *Physical Review Letters*, vol. 89, p. 187902, 2002.
- [144] Lucamarini M., Mancini S., “*Secure deterministic communication without entanglement*”, *Physical Review Letters*, vol. 94, p. 140501, 2005.
- [145] Noh T.G., et al., “*Counterfactual quantum cryptography*”, *Physical Review Letters*, vol. 103, p. 230501, 2009.
- [146] Brida G., Cavanna A., Degiovanni I.P., Genovese M., Traina P., “*Experimental realization of counterfactual quantum cryptography*”, *Laser Physics Letters*, vol. 9, p. 247, 2012.
- [147] Liu Y., Ju L., Liang X.L., Tang S.B., Tu G.L.S., Zhou L., Peng C.Z., Chen K., Chen T.Y., Chen Z.B., et al., “*Experimental demonstration of counterfactual quantum communication*”, *Physical Review Letters*, vol. 109, p. 030501, 2012.
- [148] Ren M., Wu G., Wu E., Zeng H., “*Experimental demonstration of counterfactual quantum key distribution*”, *Laser Physics*, vol. 21, pp. 755–760, 2011.
- [149] Zhou Y.y., Zhou X.j., Su B.b., “*A measurement-device-independent quantum key distribution protocol with a heralded single photon source*”, *Optoelectronics Letters*, vol. 12, pp. 148–151, 2016.

- [150] Zhou Z.R., Sheng Y.B., Niu P.H., Yin L.G., Long G.L., “*Measurement-device-independent quantum secure direct communication*”, arXiv preprint arXiv:1805.07228, 2018.
- [151] Zhang W., Ding D.S., Sheng Y.B., Zhou L., Shi B.S., Guo G.C., “*Quantum secure direct communication with quantum memory*”, *Physical Review Letters*, vol. 118, p. 220501, 2017.
- [152] Khan I., Heim B., Neuzner A., Marquardt C., “*Satellite-based QKD*”, *Optics and Photonics News*, vol. 29, pp. 26–33, 2018.
- [153] Liao S.K., Cai W.Q., Handsteiner J., Liu B., Yin J., Zhang L., Rauch D., Fink M., Ren J.G., Liu W.Y., et al., “*Satellite-relayed intercontinental quantum network*”, *Physical Review Letters*, vol. 120, p. 030501, 2018.
- [154] Zhu F., Zhang W., Sheng Y., Huang Y., “*Experimental long-distance quantum secure direct communication*”, *Science Bulletin*, vol. 62, pp. 1519–1524, 2017.
- [155] Krawec W.O., “*Security proof of a semi-quantum key distribution protocol*”, *2015 IEEE International Symposium on Information Theory (ISIT)*, pp. 686–690, IEEE, 2015.
- [156] Yu K.F., Yang C.W., Liao C.H., Hwang T., “*Authenticated semi-quantum key distribution protocol using Bell states*”, *Quantum Information Processing*, vol. 13, pp. 1457–1465, 2014.
- [157] Sun Y., Wen Q.Y., “*Counterfactual quantum key distribution with high efficiency*”, *Physical Review A*, vol. 82, p. 052318, 2010.
- [158] Salih H., “*Tripartite counterfactual quantum cryptography*”, *Physical Review A*, vol. 90, p. 012333, 2014.
- [159] Gisin N., Pironio S., Sangouard N., “*Proposal for implementing device-independent quantum key distribution based on a heralded qubit amplifier*”, *Physical Review Letters*, vol. 105, p. 070501, 2010.
- [160] Lim C.C.W., Portmann C., Tomamichel M., Renner R., Gisin N., “*Device-independent quantum key distribution with local Bell test*”, *Physical Review X*, vol. 3, p. 031006, 2013.
- [161] Pironio S., Acin A., Brunner N., Gisin N., Massar S., Scarani V., “*Device-independent quantum key distribution secure against collective attacks*”, *New Journal of Physics*, vol. 11, p. 045021, 2009.

- [162] Shenoy-Hejamadi A., Pathak A., Radhakrishna S., “*Quantum cryptography: key distribution and beyond*”, *Quanta*, vol. 6, pp. 1–47, 2017.
- [163] Hu J.Y., Yu B., Jing M.Y., Xiao L.T., Jia S.T., Qin G.Q., Long G.L., “*Experimental quantum secure direct communication with single photons*”, *Light: Science & Applications*, vol. 5, p. e16144, 2016.
- [164] Hillery M., Ziman M., Bužek V., Bieliková M., “*Towards quantum-based privacy and voting*”, *Physics Letters A*, vol. 349, pp. 75–81, 2006.
- [165] Vaccaro J.A., Spring J., Chefles A., “*Quantum protocols for anonymous voting and surveying*”, *Physical Review A*, vol. 75, p. 012333, 2007.
- [166] WEN X.j., CAI X.j., “*Secure quantum voting protocol*”, *Journal of Shandong University (Natural Science)*, p. 4, 2011.
- [167] Jiang L., He G., Nie D., Xiong J., Zeng G., “*Quantum anonymous voting for continuous variables*”, *Physical Review A*, vol. 85, p. 042309, 2012.
- [168] Bao N., Halpern N.Y., “*Quantum voting and violation of arrow’s impossibility theorem*”, *Physical Review A*, vol. 95, p. 062306, 2017.
- [169] Xue P., Zhang X., “*A simple quantum voting scheme with multi-qubit entanglement*”, *Scientific reports*, vol. 7, p. 7586, 2017.
- [170] Thapliyal K., Sharma R.D., Pathak A., “*Protocols for quantum binary voting*”, *International Journal of Quantum Information*, vol. 15, p. 1750007, 2017.
- [171] Thapliyal K., Sharma R.D., Pathak A., “*Analysis and improvement of tian-zhang-li voting protocol based on controlled quantum teleportation*”, arXiv preprint arXiv:1602.00791, 2016.
- [172] Hogg T., Harsha P., Chen K.Y., “*Quantum auctions*”, *International Journal of Quantum Information*, vol. 5, pp. 751–780, 2007.
- [173] Piotrowski E.W., Śładkowski J., “*Quantum auctions: Facts and myths*”, *Physica A: Statistical Mechanics and its Applications*, vol. 387, pp. 3949–3953, 2008.
- [174] Qin S.J., Gao F., Wen Q.Y., Meng L.M., Zhu F.C., “*Cryptanalysis and improvement of a secure quantum sealed-bid auction*”, *Optics Communications*, vol. 282, pp. 4014–4016, 2009.
- [175] Zhao Z., Naseri M., Zheng Y., “*Secure quantum sealed-bid auction with post-confirmation*”, *Optics Communications*, vol. 283, pp. 3194–3197, 2010.

- [176] Sharma R.D., Thapliyal K., Pathak A., “*Quantum sealed-bid auction using a modified scheme for multiparty circular quantum key agreement*”, *Quantum Information Processing*, vol. 16, p. 169, 2017.
- [177] “*Id quantique home page*”, <http://www.idquantique.com/>.
- [178] “*Magiq home page*”, <https://www.magiqtech.com/solutions/network-security/>.
- [179] Gruska J., *Quantum computing*, vol. 2005, McGraw-Hill London, 1999.
- [180] Mishra S., Shukla C., Pathak A., Srikanth R., Venugopalan A., “*An integrated hierarchical dynamic quantum secret sharing protocol*”, *International Journal of Theoretical Physics*, vol. 54, pp. 3143–3154, 2015.
- [181] Sanders B.C., “*Entangled coherent states*”, *Physical Review A*, vol. 45, p. 6811, 1992.
- [182] Mann A., Sanders B., Munro W., “*Bell’s inequality for an entanglement of nonorthogonal states*”, *Physical Review A*, vol. 51, p. 989, 1995.
- [183] Peres A., “*Unperformed experiments have no results*”, *American Journal of Physics*, vol. 46, pp. 745–747, 1978.
- [184] Mann A., Revzen M., Schleich W., “*Unique Bell state*”, *Physical Review A*, vol. 46, p. 5363, 1992.
- [185] Wang X., “*Bipartite entangled non-orthogonal states*”, *Journal of Physics A: Mathematical and General*, vol. 35, p. 165, 2001.
- [186] Mishra M.K., Prakash H., “*Teleportation of a two-mode entangled coherent state encoded with two-qubit information*”, *Journal of Physics B: Atomic, Molecular and Optical Physics*, vol. 43, p. 185501, 2010.
- [187] Wang X., Sanders B.C., Pan S.h., “*Entangled coherent states for systems with  $su(2)$  and  $su(1, 1)$  symmetries*”, *Journal of Physics A: Mathematical and General*, vol. 33, p. 7451, 2000.
- [188] Prakash H., Chandra N., Prakash R., Shivani, “*Swapping between two pairs of nonorthogonal entangled coherent states*”, *International Journal of Modern Physics B*, vol. 23, pp. 2083–2092, 2009.
- [189] Kumar S.A., Prakash H., Chandra N., Prakash R., “*Noise in swapping between two pairs of non-orthogonal entangled coherent states*”, *Modern Physics Letters B*, vol. 27, p. 1350017, 2013.

- [190] Dong L., Wang J.X., Xiu X.M., Li D., Gao Y.J., Yi X., “A *continuous variable quantum key distribution protocol based on entanglement swapping of quasi-Bell entangled coherent states*”, International Journal of Theoretical Physics, vol. 53, pp. 3173–3190, 2014.
- [191] Hirota O., Van Enk S.J., Nakamura K., Sohma M., Kato K., “*Entangled nonorthogonal states and their decoherence properties*”, arXiv preprint quant-ph/0101096, 2001.
- [192] de Souza D.D., Vidiella-Barranco A., “*Quantum phase estimation with squeezed quasi-Bell states*”, arXiv preprint arXiv:1609.00370, 2016.
- [193] Vernam. G.S., “*Secret signaling system*”, U. S. Patent 1,310,719., 1919.
- [194] Goldenberg L., Vaidman L., “*Quantum cryptography based on orthogonal states*”, Physical Review Letters, vol. 75, p. 1239, 1995.
- [195] Long G.L., Deng F.g., Wang C., Li X.h., Wen K., Wang W.y., “*Quantum secure direct communication and deterministic secure quantum communication*”, Frontiers of Physics in China, vol. 2, pp. 251–272, 2007.
- [196] Hai-Jing C., He-Shan S., “*Quantum secure direct communication with  $W$  state*”, Chinese Physics Letters, vol. 23, p. 290, 2006.
- [197] Zhu A.D., Xia Y., Fan Q.B., Zhang S., “*Secure direct communication based on secret transmitting order of particles*”, Physical Review A, vol. 73, p. 022338, 2006.
- [198] Hwang T., Hwang C., Tsai C., “*Quantum key distribution protocol using dense coding of three-qubit  $W$  state*”, The European Physical Journal D, vol. 61, pp. 785–790, 2011.
- [199] Zhong-Xiao M., Zhan-Jun Z., Yong L., “*Deterministic secure direct communication by using swapping quantum entanglement and local unitary operations*”, Chinese Physics Letters, vol. 22, p. 18, 2005.
- [200] Long G.L., Liu X.S., “*Theoretically efficient high-capacity quantum-key-distribution scheme*”, Physical Review A, vol. 65, p. 032302, 2002.
- [201] Braunstein S.L., Kimble H.J., “*Dense coding for continuous variables*”, *Quantum Information with Continuous Variables*, pp. 95–103, Springer, 2000.
- [202] Man Z.X., Zhang Z.J., Li Y., “*Quantum dialogue revisited*”, Chinese Physics Letters, vol. 22, pp. 22–24, 2005.
- [203] An N.B., “*Secure dialogue without a prior key distribution*”, Journal of the Korean Physical Society, vol. 47, p. 562, 2005.

- [204] Tan Y.g., Cai Q.y., “*Classical correlation in quantum dialogue*”, International Journal of Quantum Information, vol. 6, pp. 325–329, 2008.
- [205] Gao G., “*Two quantum dialogue protocols without information leakage*”, Optics communications, vol. 283, pp. 2288–2293, 2010.
- [206] Li D., Xiao-Ming X., Ya-Jun G., Feng C., “*Quantum dialogue protocol using a class of three-photon W states*”, Communications in Theoretical Physics, vol. 52, p. 853, 2009.
- [207] Banerjee S., “*Open quantum systems*”, 2018.
- [208] McMahan D., *Quantum computing explained*, John Wiley & Sons, 2007.
- [209] Nielsen M.A., Chuang I.L., “*Quantum computation and quantum information*”, 2000.
- [210] Huang J.H., Zhu S.Y., “*Necessary and sufficient conditions for the entanglement sudden death under amplitude damping and phase damping*”, Physical Review A, vol. 76, p. 062322, 2007.
- [211] Thapliyal K., Banerjee S., Pathak A., Omkar S., Ravishankar V., “*Quasiprobability distributions in open quantum systems: spin-qubit systems*”, Annals of Physics, vol. 362, pp. 261–286, 2015.
- [212] Kim Y.S., Lee J.C., Kwon O., Kim Y.H., “*Protecting entanglement from decoherence using weak measurement and quantum measurement reversal*”, Nature Physics, vol. 8, p. 117, 2012.
- [213] Turchette Q., Myatt C., King B., Sackett C., Kielpinski D., Itano W., Monroe C., Wineland D., “*Decoherence and decay of motional quantum states of a trapped atom coupled to engineered reservoirs*”, Physical Review A, vol. 62, p. 053807, 2000.
- [214] Myatt C.J., King B.E., Turchette Q.A., Sackett C.A., Kielpinski D., Itano W.M., Monroe C., Wineland D.J., “*Decoherence of quantum superpositions through coupling to engineered reservoirs*”, Nature, vol. 403, p. 269, 2000.
- [215] Marques B., Matoso A., Pimenta W., Gutiérrez-Esparza A., Santos M., Pádua S., “*Experimental simulation of decoherence in photonics qudits*”, Scientific reports, vol. 5, p. 16049, 2015.
- [216] Chuang I.L., Gershenfeld N., Kubinec M.G., Leung D.W., “*Bulk quantum computation with nuclear magnetic resonance: theory and experiment*”, Proceedings of the Royal Society of London A: Mathematical, Physical and Engineering Sciences, vol. 454, pp. 447–467, The Royal Society, 1998.



- [217] Jozsa R., “*Fidelity for mixed quantum states*”, *Journal of modern optics*, vol. 41, pp. 2315–2323, 1994.
- [218] Landauer R., “*Irreversibility and heat generation in the computing process*”, *IBM journal of research and development*, vol. 5, pp. 183–191, 1961.
- [219] Alsina D., Latorre J.I., “*Experimental test of Mermin inequalities on a five-qubit quantum computer*”, *Physical Review A*, vol. 94, p. 012314, 2016.
- [220] Fedortchenko S., “*A quantum teleportation experiment for undergraduate students*”, arXiv preprint arXiv:1607.02398, 2016.
- [221] Devitt S.J., “*Performing quantum computing experiments in the cloud*”, *Physical Review A*, vol. 94, p. 032329, 2016.
- [222] Behera B.K., Banerjee A., Panigrahi P.K., “*Experimental realization of quantum cheque using a five-qubit quantum computer*”, *Quantum Information Processing*, vol. 16, p. 312, 2017.
- [223] Hebenstreit M., Alsina D., Latorre J., Kraus B., “*Compressed quantum computation using a remote five-qubit quantum computer*”, *Physical Review A*, vol. 95, p. 052339, 2017.
- [224] Linke N.M., Maslov D., Roetteler M., Debnath S., Figgatt C., Landsman K.A., Wright K., Monroe C., “*Experimental comparison of two quantum computing architectures*”, *Proceedings of the National Academy of Sciences*, p. 201618020, 2017.
- [225] Wootton J.R., “*Demonstrating non-abelian braiding of surface code defects in a five qubit experiment*”, *Quantum Science and Technology*, vol. 2, p. 015006, 2017.
- [226] Ghosh D., Agarwal P., Pandey P., Behera B.K., Panigrahi P.K., “*Automated error correction in IBM quantum computer and explicit generalization*”, *Quantum Information Processing*, vol. 17, p. 153, 2018.
- [227] Singh R.K., Panda B., Behera B.K., Panigrahi P.K., “*Demonstration of a general fault-tolerant quantum error detection code for  $(2n+1)$ -qubit entangled state on IBM 16-qubit quantum computer*”, arXiv preprint arXiv:1807.02883, 2018.
- [228] Hegade N.N., Behera B.K., Panigrahi P.K., “*Experimental demonstration of quantum tunneling in IBM quantum computer*”, arXiv preprint arXiv:1712.07326, 2017.
- [229] Behera B.K., Reza T., Gupta A., Panigrahi P.K., “*Designing quantum router in IBM quantum computer*”, arXiv preprint arXiv:1803.06530, 2018.

- [230] Dash A., Sarmah D., Behera B.K., Panigrahi P.K., “*Exact search algorithm to factorize large biprimes and a triprime on IBM quantum computer*”, arXiv preprint arXiv:1805.10478, 2018.
- [231] Behera B.K., Panigrahi P.K., et al., “*A simulational model for witnessing quantum effects of gravity using IBM quantum computer*”, arXiv preprint arXiv:1806.10229, 2018.
- [232] Kapil M., Behera B.K., Panigrahi P.K., “*Quantum simulation of klein gordon equation and observation of klein paradox in IBM quantum computer*”, arXiv preprint arXiv:1807.00521, 2018.
- [233] Malik G.R., Singh R.P., Behera B.K., Panigrahi P.K., “*First experimental demonstration of multi-particle quantum tunneling in IBM quantum computer*”, 2019.
- [234] Pathak A., “*Experimental quantum mechanics in the class room: testing basic ideas of quantum mechanics and quantum computing using IBM quantum computer*”, arXiv preprint arXiv:1805.06275, 2018.
- [235] “*IBM quantum computing platform*”, "<http://research.ibm.com/ibm-q/qx/>", 2016. Online accessed 04-May-2016.
- [236] Steffen M., DiVincenzo D.P., Chow J.M., Theis T.N., Ketchen M.B., “*Quantum computing: an IBM perspective*”, IBM Journal of Research and Development, vol. 55, pp. 13–1, 2011.
- [237] Malkoc O., “*Quantum computation with superconducting qubits.*”, Quantum, 2013.
- [238] “*Architecture used in 5-qubit quantum computer*”, "<https://github.com/IBM/qiskit-qx-info/blob/master/backends/IBMQx2/README.md>", 2017.
- [239] “*IBM q experience*”, "e. <https://quantumexperience.ng.bluemix.net/qx/devices>", 2017. Online accessed 27-December-2017.
- [240] James D.F., Kwiat P.G., Munro W.J., White A.G., “*Measurement of qubits*”, Physical Review A, vol. 64, p. 052312, 2001.
- [241] Rundle R., Tilma T., Samson J., Everitt M., “*Quantum state reconstruction made easy: a direct method for tomography*”, Physical Review A, vol. 96, p. 022117, 2017.
- [242] Filipp S., Maurer P., Leek P., Baur M., Bianchetti R., Fink J., Göppl M., Steffen L., Gambetta J., Blais A., et al., “*Two-qubit state tomography using a joint dispersive readout*”, Physical Review Letters, vol. 102, p. 200402, 2009.
- [243] Schmied R., “*Quantum state tomography of a single qubit: comparison of methods*”, Journal of Modern Optics, vol. 63, pp. 1744–1758, 2016.

- [244] Shukla A., Rao K.R.K., Mahesh T., “*Ancilla-assisted quantum state tomography in multi-qubit registers*”, *Physical Review A*, vol. 87, p. 062317, 2013.
- [245] Panigrahi P.K., Gupta M., Pathak A., Srikanth R., “*Circuits for distributing quantum measurement*”, *AIP Conference Proceedings*, vol. 864, pp. 197–207, 2006.
- [246] Samal J.R., Gupta M., Panigrahi P., Kumar A., “*Non-destructive discrimination of Bell states by NMR using a single ancilla qubit*”, *Journal of Physics B: Atomic, Molecular and Optical Physics*, vol. 43, p. 095508, 2010.
- [247] Kak S., “*A three-stage quantum cryptography protocol*”, *Foundations of Physics Letters*, vol. 19, pp. 293–296, 2006.
- [248] Mandal S., Macdonald G., El Rifai M., Puneekar N., Zamani F., Chen Y., Kak S., Verma P.K., Huck R.C., Sluss J., “*Multi-photon implementation of three-stage quantum cryptography protocol*”, *Information Networking (ICOIN), 2013 International Conference on*, pp. 6–11, IEEE, 2013.
- [249] Thapliyal K., Pathak A., “*Kak’s three-stage protocol of secure quantum communication revisited: hitherto unknown strengths and weaknesses of the protocol*”, *Quantum Information Processing*, vol. 17, p. 229, 2018.
- [250] “*Various parameters of IBM quantum computer*”, “<https://quantumexperience.ng.bluemix.net/qx/editor>”, 2016. Online accessed 04-May-2016.
- [251] Adami C., Cerf N.J., “*Quantum computation with linear optics*”, *Quantum Computing and Quantum Communications*, pp. 391–401, Springer, 1999.
- [252] Prakash H., Chandra N., Prakash R., et al., “*Effect of decoherence on fidelity in teleportation using entangled coherent states*”, *Journal of Physics B: Atomic, Molecular and Optical Physics*, vol. 40, p. 1613, 2007.
- [253] Oh S., Lee S., Lee H.w., “*Fidelity of quantum teleportation through noisy channels*”, *Physical Review A*, vol. 66, p. 022316, 2002.
- [254] D’Ariano G., Presti P.L., Sacchi M., “*Bell measurements and observables*”, *Physics Letters A*, vol. 272, pp. 32–38, 2000.
- [255] Horodecki M., Horodecki P., Horodecki R., “*General teleportation channel, singlet fraction, and quasidistillation*”, *Physical Review A*, vol. 60, p. 1888, 1999.
- [256] Hill S., Wootters W.K., “*Entanglement of a pair of quantum bits*”, *Physical Review Letters*, vol. 78, p. 5022, 1997.

- [257] Wootters W.K., “*Entanglement of formation of an arbitrary state of two qubits*”, Physical Review Letters, vol. 80, p. 2245, 1998.
- [258] Fu H., Wang X., Solomon A.I., “*Maximal entanglement of nonorthogonal states: classification*”, Physics Letters A, vol. 291, pp. 73–76, 2001.
- [259] Banerjee A., Shukla C., Thapliyal K., Pathak A., Panigrahi P.K., “*Asymmetric quantum dialogue in noisy environment*”, Quantum Information Processing, vol. 16, p. 49, 2017.
- [260] Gupta M., Pathak A., Srikanth R., Panigrahi P.K., “*General circuits for indirecting and distributing measurement in quantum computation*”, International Journal of Quantum Information, vol. 5, pp. 627–640, 2007.
- [261] Wang X.W., Zhang D.Y., Tang S.Q., Xie L.J., “*Nondestructive Greenberger-Horne-Zeilinger-state analyzer*”, Quantum Information Processing, vol. 12, pp. 1065–1075, 2013.
- [262] Li J., Shi B.S., Jiang Y.K., Fan X.F., Guo G.C., “*A non-destructive discrimination scheme on 2n-partite GHZ bases*”, Journal of Physics B: Atomic, Molecular and Optical Physics, vol. 33, p. 3215, 2000.
- [263] Banerjee A., Shukla C., Pathak A., “*Maximal entanglement concentration for a set of (n+ 1)-qubit states*”, Quantum Information Processing, vol. 14, pp. 4523–4536, 2015.
- [264] Luo Q.b., Yang G.w., She K., Niu W.n., Wang Y.q., “*Multi-party quantum private comparison protocol based on d-dimensional entangled states*”, Quantum Information Processing, vol. 13, pp. 2343–2352, 2014.
- [265] Wei S.J., Xin T., Long G.L., “*Efficient universal quantum channel simulation in IBM’s cloud quantum computer*”, SCIENCE CHINA Physics, Mechanics and Astronomy, vol. 61, p. 070311, 2018.
- [266] Berta M., Wehner S., Wilde M.M., “*Entropic uncertainty and measurement reversibility*”, New Journal of Physics, vol. 18, p. 073004, 2016.
- [267] Yalçinkaya İ., Gedik Z., “*Optimization and experimental realization of the quantum permutation algorithm*”, Physical Review A, vol. 96, p. 062339, 2017.
- [268] Gangopadhyay S., Behera B.K., Panigrahi P.K., et al., “*Generalization and demonstration of an entanglement-based Deutsch–Jozsa-like algorithm using a 5-qubit quantum computer*”, Quantum Information Processing, vol. 17, p. 160, 2018.
- [269] Jones J.A., “*Quantum computing and nuclear magnetic resonance*”, PhysChemComm, vol. 4, pp. 49–56, 2001.

- [270] Paauw F., Fedorov A., Harmans C.M., Mooij J., “*Tuning the gap of a superconducting flux qubit*”, *Physical Review Letters*, vol. 102, p. 090501, 2009.
- [271] DiVincenzo D.P., “*Topics in quantum computers*”, *Mesoscopic electron transport*, pp. 657–677, Springer, 1997.
- [272] Cottet A., *Implementation of a quantum bit in a superconducting circuit*, Ph.D. thesis, PhD Thesis, Université Paris 6, 2002.
- [273] Clarke J., Wilhelm F.K., “*Superconducting quantum bits*”, *Nature*, vol. 453, pp. 1031–1042, 2008.
- [274] Wendin G., Shumeiko V., “*Quantum bits with josephson junctions*”, *Low Temperature Physics*, vol. 33, pp. 724–744, 2007.
- [275] “*D-wave news*”, <https://www.dwavesys.com/news/press-releases>, 2017.
- [276] “*Quantum computer passes speed test*”, <http://blogs.nature.com/news/2013/05/quantum-computer-passes-speed-test.html/>, 2017.
- [277] Manu V., Kumar A., Home D., Kar G., Majumdar A.S., “*Non-destructive discrimination of arbitrary set of orthogonal quantum states by NMR using quantum phase estimation*”, *AIP Conference Proceedings*, vol. 1384, pp. 229–240, AIP, 2011.
- [278] Benedetti C., Shurupov A.P., Paris M.G.A., Brida G., Genovese M., “*Experimental estimation of quantum discord for a polarization qubit and the use of fidelity to assess quantum correlations*”, *Physical Review A*, vol. 87, p. 052136, 2013.
- [279] Joshi S., Shukla A., Katiyar H., Hazra A., Mahesh T., “*Estimating franck-condon factors using an NMR quantum processor*”, *Physical Review A*, vol. 90, p. 022303, 2014.
- [280] Bina M., Mandarino A., Olivares S., Paris M.G.A., “*Drawbacks of the use of fidelity to assess quantum resources*”, *Physical Review A*, vol. 89, p. 012305, 2014.
- [281] O’Brien J.L., Pryde G., Gilchrist A., James D., Langford N.K., Ralph T., White A., “*Quantum process tomography of a controlled-NOT gate*”, *Physical Review Letters*, vol. 93, p. 080502, 2004.
- [282] Shor P.W., Preskill J., “*Simple proof of security of the BB84 quantum key distribution protocol*”, *Physical Review Letters*, vol. 85, p. 441, 2000.
- [283] Renner R., “*Security of quantum key distribution*”, *International Journal of Quantum Information*, vol. 6, pp. 1–127, 2008.

- [284] Duplinskiy A., Ustimchik V., Kanapin A., Kurochkin V., Kurochkin Y., “*Low loss QKD optical scheme for fast polarization encoding*”, *Optics Express*, vol. 25, pp. 28886–28897, 2017.
- [285] Mavromatis A., Ntavou F., Salas E.H., Kanellos G.T., Nejabati R., Simeonidou D., “*Experimental demonstration of quantum key distribution (QKD) for energy-efficient software-defined internet of things*”, *2018 European Conference on Optical Communication (ECOC)*, pp. 1–3, IEEE, 2018.
- [286] Bennett C.H., Bessette F., Brassard G., Salvail L., Smolin J., “*Experimental quantum cryptography*”, *Journal of cryptology*, vol. 5, pp. 3–28, 1992.
- [287] Zhao Y., Qi B., Ma X., Lo H.K., Qian L., “*Experimental quantum key distribution with decoy states*”, *Physical Review Letters*, vol. 96, p. 070502, 2006.
- [288] Diamanti E., Lo H.K., Qi B., Yuan Z., “*Practical challenges in quantum key distribution*”, *npj Quantum Information*, vol. 2, p. 16025, 2016.
- [289] Kiktenko E.O., Pozhar N.O., Duplinskiy A.V., Kanapin A.A., Sokolov A.S., Vorobey S.S., Miller A.V., Ustimchik V.E., Anufriev M.N., Trushechkin A., et al., “*Demonstration of a quantum key distribution network in urban fibre-optic communication lines*”, *Quantum Electronics*, vol. 47, p. 798, 2017.
- [290] Koashi M., “*Efficient quantum key distribution with practical sources and detectors*”, arXiv preprint quant-ph/0609180, 2006.
- [291] Korzh B., Lim C.C.W., Houlmann R., Gisin N., Li M.J., Nolan D., Sanguinetti B., Thew R., Zbinden H., “*Provably secure and practical quantum key distribution over 307 km of optical fibre*”, *Nature Photonics*, vol. 9, p. 163, 2015.
- [292] Lo H.K., Curty M., Tamaki K., “*Secure quantum key distribution*”, *Nature Photonics*, vol. 8, p. 595, 2014.
- [293] Wang J., Qin X., Jiang Y., Wang X., Chen L., Zhao F., Wei Z., Zhang Z., “*Experimental demonstration of polarization encoding quantum key distribution system based on intrinsically stable polarization-modulated units*”, *Optics express*, vol. 24, pp. 8302–8309, 2016.
- [294] Xu F., Wei K., Sajeed S., Kaiser S., Sun S., Tang Z., Qian L., Makarov V., Lo H.K., “*Experimental quantum key distribution with source flaws*”, *Physical Review A*, vol. 92, p. 032305, 2015.

- [295] Gleim A., Egorov V., Nazarov Y.V., Smirnov S., Chistyakov V., Bannik O., Anisimov A., Kynev S., Ivanova A., Collins R., et al., “*Secure polarization-independent subcarrier quantum key distribution in optical fiber channel using BB84 protocol with a strong reference*”, *Optics express*, vol. 24, pp. 2619–2633, 2016.
- [296] Soujaeff A., Nishioka T., Hasegawa T., Takeuchi S., Tsurumaru T., Sasaki K., Matsui M., “*Quantum key distribution at 1550 nm using a pulse heralded single photon source*”, *Optics express*, vol. 15, pp. 726–734, 2007.
- [297] Wang Q., Chen W., Xavier G., Swillo M., Zhang T., Sauge S., Tengner M., Han Z.F., Guo G.C., Karlsson A., “*Experimental decoy-state quantum key distribution with a sub-poissionian heralded single-photon source*”, *Physical Review Letters*, vol. 100, p. 090501, 2008.
- [298] Liu C.Q., Zhu C.H., Wang L.H., Zhang L.X., Pei C.X., “*Polarization-encoding-based measurement-device-independent quantum key distribution with a single untrusted source*”, *Chinese Physics Letters*, vol. 33, p. 100301, 2016.
- [299] Lo H.K., Curty M., Qi B., “*Measurement-device-independent quantum key distribution*”, *Physical review letters*, vol. 108, p. 130503, 2012.
- [300] Zhang C.H., Zhang C.M., Guo G.C., Wang Q., “*Biased three-intensity decoy-state scheme on the measurement-device-independent quantum key distribution using heralded single-photon sources*”, *Optics express*, vol. 26, pp. 4219–4229, 2018.
- [301] Grosshans F., Grangier P., “*Continuous variable quantum cryptography using coherent states*”, *Physical Review Letters*, vol. 88, p. 057902, 2002.
- [302] Gottesman D., Preskill J., “*Secure quantum key distribution using squeezed states*”, *Physical Review A*, vol. 63, pp. Art–No, 2001.
- [303] Ralph T.C., “*Continuous variable quantum cryptography*”, *Physical Review A*, vol. 61, p. 010303, 1999.
- [304] Ma C., Sacher W.D., Tang Z., Mikkelsen J.C., Yang Y., Xu F., Thiessen T., Lo H.K., Poon J.K., “*Silicon photonic transmitter for polarization-encoded quantum key distribution*”, *Optica*, vol. 3, pp. 1274–1278, 2016.
- [305] Ding Y., Bacco D., Dalgaard K., Cai X., Zhou X., Rottwitt K., Oxenløwe L.K., “*High-dimensional quantum key distribution based on multicore fiber using silicon photonic integrated circuits*”, *npj Quantum Information*, vol. 3, p. 25, 2017.

- [306] Sibson P., Erven C., Godfrey M., Miki S., Yamashita T., Fujiwara M., Sasaki M., Terai H., Tanner M.G., Natarajan C.M., et al., “*Chip-based quantum key distribution*”, *Nature communications*, vol. 8, p. 13984, 2017.
- [307] Zhang Z., Chen C., Zhuang Q., Heyes J.E., Wong F.N., Shapiro J.H., “*Experimental quantum key distribution at 1.3 gbit/s secret-key rate over a 10-db-loss channel*”, *CLEO: QELS\_Fundamental Science*, pp. FTu3G–5, Optical Society of America, 2018.
- [308] Boaron A., Boso G., Rusca D., Vulliez C., Autebert C., Caloz M., Perrenoud M., Gras G., Bussièrès F., Li M.J., et al., “*Secure quantum key distribution over 421 km of optical fiber*”, *Physical Review Letters*, vol. 121, p. 190502, 2018.
- [309] Hai-Qiang M., Ke-Jin W., Jian-Hui Y., “*Experimental single qubit quantum secret sharing in a fiber network configuration*”, *Optics letters*, vol. 38, pp. 4494–4497, 2013.
- [310] Schmid C., Trojek P., Bourennane M., Kurtsiefer C., Żukowski M., Weinfurter H., “*Experimental single qubit quantum secret sharing*”, *Physical Review Letters*, vol. 95, p. 230505, 2005.
- [311] Smania M., Elhassan A.M., Tavakoli A., Bourennane M., “*Experimental quantum multi-party communication protocols*”, *Npj Quantum Information*, vol. 2, p. 16010, 2016.
- [312] Pathak A., “*Efficient protocols for unidirectional and bidirectional controlled deterministic secure quantum communication: different alternative approaches*”, *Quantum Information Processing*, vol. 14, pp. 2195–2210, 2015.
- [313] Deng F.G., Long G.L., “*Secure direct communication with a quantum one-time pad*”, *Physical Review A*, vol. 69, p. 052319, 2004.
- [314] Niu P.H., Zhou Z.R., Lin Z.S., Sheng Y.B., Yin L.G., Long G.L., “*Measurement-device-independent quantum communication without encryption*”, *Science Bulletin*, vol. 63, pp. 1345–1350, 2018.
- [315] Kim Y.H., Kulik S.P., Shih Y., “*Quantum teleportation of a polarization state with a complete Bell state measurement*”, *Physical Review Letters*, vol. 86, p. 1370, 2001.
- [316] Shukla C., Alam N., Pathak A., “*Protocols of quantum key agreement solely using Bell states and Bell measurement*”, *Quantum Information Processing*, vol. 13, pp. 2391–2405, 2014.
- [317] Lo H.K., Ma X., Chen K., “*Decoy state quantum key distribution*”, *Physical Review Letters*, vol. 94, p. 230504, 2005.



- [318] Rosenberg D., Harrington J.W., Rice P.R., Hiskett P.A., Peterson C.G., Hughes R.J., Lita A.E., Nam S.W., Nordholt J.E., “*Long-distance decoy-state quantum key distribution in optical fiber*”, Physical Review Letters, vol. 98, p. 010503, 2007.
- [319] Bennett C.H., Brassard G., Mermin N.D., “*Quantum cryptography without Bell’s theorem*”, Physical Review Letters, vol. 68, p. 557, 1992.

## LIST OF PUBLICATIONS DURING Ph.D. THESIS WORK

### *Publications in International Journals*

1. **Sisodia M.**, Verma V., Thapliyal K., Pathak A., “*Teleportation of a qubit using entangled nonorthogonal states: a comparative study*”, Quantum Information Processing, vol. 16, p. 76, 2017. (**Thomson Reuters I.F.** = 2.283, **h index** = 38, **h5-index** = 38, **Published by** Springer New York, **Indexed in** SCI and SCOPUS).
2. **Sisodia M.**, Shukla A., Thapliyal K., Pathak A., “*Design and experimental realization of an optimal scheme for teleportation of an n-qubit quantum state*”, Quantum Information Processing, vol. 16, p. 292, 2017. (**Thomson Reuters I.F.** = 2.283, **h index** =38, **h5-index** = 38, **Published by** Springer New York, **Indexed in** SCI and SCOPUS).
3. **Sisodia M.**, Shukla A., Pathak A., “*Experimental realization of nondestructive discrimination of Bell states using a five-qubit quantum computer*”, Physics Letters A, vol. 381, pp. 3860-3874, 2017. (**Thomson Reuters I.F.** = 1.863, **h index** = 153, **h5-index** =41, **Published by** Elsevier Netherlands, **Indexed in** SCI and SCOPUS).
4. **Sisodia M.**, Pathak A., “*Comment on “Quantum Teleportation of Eight-Qubit State via Six-Qubit Cluster State”*”, International Journal of Theoretical Physics, vol. 57, pp. 2213-2217, 2018. (**Thomson Reuters I.F.** = 1.121, **h index** =51, **h5-index** =30, **Published by** Springer New York, **Indexed in** SCI and SCOPUS).
5. **Sisodia M.**, Thapliyal K., Pathak A., “*Optical designs for a set of quantum cryptographic protocols*”, Communicated, 2019.

### *Communicated to International Journals and not included in the thesis*

1. Shukla A., **Sisodia M.**, Pathak A., “*Complete characterization of the single-qubit quantum gates used in the IBM quantum processors*”, arXiv:1805.07185, 2018.
2. **Sisodia M.**, Shukla A., de Almeida A.A., Dueck G.W ., Pathak A., “*Circuit optimization for IBM processors: a way to get higher fidelity and higher values of nonclassicality witnesses*”, arXiv:1812.11602, 2018.

3. **Sisodia M.**, Shukla C., Long G-L, “*Linear optics based entanglement concentration protocols for Cluster-type entangled coherent state*”, Quantum Information Processing, vol. 18, p. 253, 2019.

*Communicated to International Conference and not included in the thesis*

1. **Sisodia M.** “*An improved scheme of quantum teleportation for four-qubit state*”, Communicated, 2019.

### **Extended abstracts and short papers in International/National conferences**

1. Sisodia, M., Shukla, A., Thapliyal K., Pathak, A., “*Scheme for teleporting a multi-qubit state using optimal resource*” Book of Abstract, Young Quantum-2017, Harish-Chandra Research Institute, Allahabad, February 27- March 1, (2017).
2. Sisodia, M., Shukla, A., Pathak, A., “*Our experience with the IBM quantum experience: The story of successful achievements and failures due to the limitations of the IBM quantum computers*” Book of Abstract, Quantum Frontiers and Fundamentals-2018, Raman Research Institute, Bengaluru, April 30- May 4, (2018) pp. 99-102.
3. Sisodia, M., Shukla, A., Thapliyal K., Pathak, A., “*Optical designs for a set of quantum cryptographic protocols*” Book of Abstract, Student Conference On Optics and Photonics-2018, Physical Research Laboratory, Ahmedabad, October 4-6, (2018) pp. 47-48.
4. Sisodia, M., Shukla, A., Pathak, A., “*What reduces the accuracy of the IBM quantum computers: An answer from the perspective of quantum process tomography*” Book of Abstract, Quantum Information Processing and Applications (QIPA-2018), Harish-Chandra Research Institute, Allahabad, December 2-8, (2018).
5. Sisodia, M. “*Comment on Improving the Teleportation Scheme of Five-Qubit State with a Seven-Qubit Quantum Channel*” Book of Abstract, International Conference on Photonics, Metamaterials and Plasmonics-2019, Jaypee Institute of Information Technology, Noida, February 14-16, (2019) p. 74.